The Institute for Solid State Physics
The University of Tokyo

Activity Report 2013

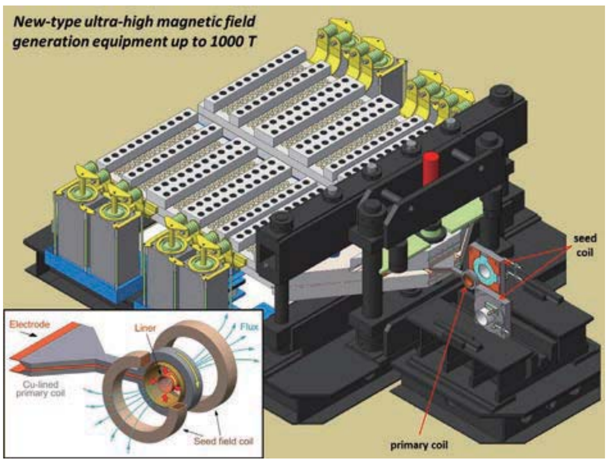

ISSP

ISSP

Activity Report 2013

Contents

Pages

Preface

We are pleased to present the annual ISSP Activity Report for the academic year 2013. ISSP (Institute for Solid State Physics) was established in 1957 as a joint-use research institution attached to the University of Tokyo. Since then both in-house research and collaboration with external users have been essential elements of the activities of ISSP.

The research at ISSP has been pursued along two major directions. Synthesis of new materials and nano-structures in search for novel phenomena and functions using advanced and original techniques is at the core of modern condensed matter science. Such activities are being conducted by relatively small independent groups at ISSP and their collaborators. At the same time, importance of large experimental and computational facilities in materials science has been rapidly increasing in recent years. An important mission of ISSP is active participation in the development and operation of some of those large facilities that are difficult to maintain for typical university faculties. Notable achievements in this direction are summarized below.

(1) ISSP has been operating supercomputers dedicated to materials science. In addition, the Center of Computational Materials Science launched in 2011 provides technical supports to facilitate use of massively parallel computational resources such as the K-computer. (2) The International MegaGauss Science Laboratory continues to develop both the destructive ultrahigh magnetic field by electromagnetic compression aimed at 1000 tesla and the non-destructive long-pulse magnetic field by a flywheel generator. (3) ISSP has been providing the users access to advanced spectroscopy using quantum beams such as neutrons and synchrotron light sources. Although it is a pity for the neutron scattering society that the JRR-3 reactor at Tokai has been still shut down after the earthquake in 2011, the pulse spectrometer at J-PARC is now in operation. The latest development is the opening of the new Laser and Synchrotron Research Center in 2012, which is aimed at making a new frontier of advanced spectroscopy by combining laser, synchrotron, and X-FEL light sources in ultraviolet and soft X-ray region.

June, 2014

Masashi Takigawa
Director
Institute for Solid State Physics
The University of Tokyo

Research Highlights

---Division of New Materials Science----------------

Multiband Superconductivity with Unexpected Deficiency of Nodal Quasiparticles in $CeCu_2Si_2$

Sakakibara Group

The gap symmetry of unconventional superconductors has attracted much attention of scientific community because it is closely related to the exotic pairing mechanism. $CeCu_2Si_2$ (T_c ~ 0.6 K) is a historically important compound that made a breakthrough in the field of superconductivity; in 1979, exotic superconductivity was discovered for the first time in this strongly-correlated heavy-electron system [1]. Until quite recently, its gap symmetry was believed to be a nodal *d*-wave pairing mediated by spin fluctuations [2]. The presence of line nodes had been suggested from the power-law temperature dependence of various physical quantities, such as the NMR relaxation rate $1/T_1$ [3] and the specific heat, both of which were measured in the intermediate temperature region above 0.1 K. Recent interest has been focused on the location of line nodes: whether the gap symmetry is $d_{x^2-y^2}$ or d_{xy} type [4,5].

To elucidate the gap symmetry of $CeCu_2Si_2$, we performed specific-heat measurements at low temperatures down to 40 mK using a high-quality single crystal (*S*-type)[6]. Quite unexpectedly, the zero-field specific heat C_e exhibits exponential temperature dependence below 80 mK (Fig. 1(a)), reminiscent of full-gap superconductivity. In addition, we provide thermodynamic evidence for nodeless superconductivity that the low-temperature specific heat is proportional to the magnetic field at low fields for all field orientations and does not change with the *c*-plane field rotation. We found that the temperature dependence of the zero-field C_e/T including the linear behavior in the intermediate-*T* region can be reproduced on the basis of a phenomenological two-gap model within the conventional BCS framework using two BCS gaps, $\Delta_1 = 1.76k_BT_c$ and $\Delta_2 = 0.7k_BT_c$, whose weights are 65% and 35% of the total density of states, respectively (Fig. 1(b)). We also found anomalous behaviors in the field variations of the specific heat as well as the magnetization at low temperatures in the high-field regime (Fig. 1(c)), which can be interpreted as a strong Pauli paramagnetic effect occurring in a multiband superconductor. All the present results match with the prediction of multiband superconductivity in the absence of nodal quasiparticles.

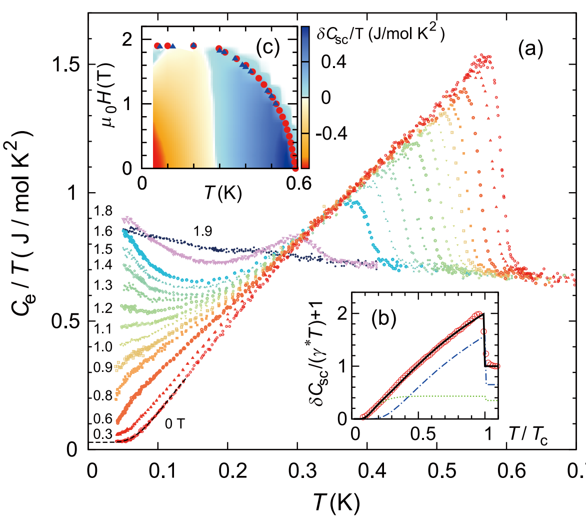

Fig. 1. (a) Temperature dependence of the electronic specific heat of $CeCu_2Si_2$ divided by temperature, C_e/T, for *H* // [100]. (b) Temperature dependence of C_e/T at zero field, where the *T*-dependent normal-state contribution is subtracted. The solid line is a best fit to the two-gap BCS model. (c) Field-temperature phase diagram for *H* // [100] and a contour plot of the superconducting contribution to C_e/T. Anomalous behavior that can be ascribed to the Pauli paramagnetic effect is clearly seen in the high-field and low-temperature region below 0.1 K.

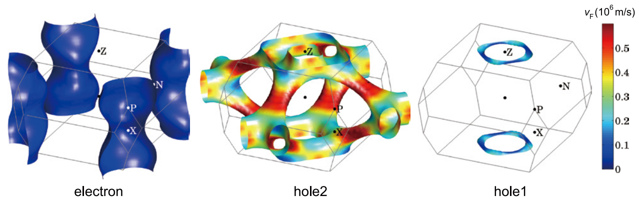

Fig. 2. The calculated Fermi surfaces of $CeCu_2Si_2$ colored by the magnitude of the Fermi velocity v_F.

One may suspect that line nodes might exist in the gap on light-mass bands, since the specific heat measurement mainly probes the heavy-mass band. To get an insight into the band structure of $CeCu_2Si_2$, we have performed first-principles calculations by the LDA+*U* method. As shown in Fig. 2, $CeCu_2Si_2$ has a flat electron band around the *X* point with the heaviest mass and two hole bands around the *Z* point. In this Fermi-surface topology, the deficiency of nodal quasiparticles requires the negligibly small effective mass of the two light-mass bands, which contradicts the multiband feature detected from the specific-heat measurement. This leads to a conclusion that the pairing symmetry of $CeCu_2Si_2$ is not the anticipated *d*-wave state, but the multiband full-gap state, including an unconventional *s*-wave such as *s*±-wave, a conventional *s*-wave, or a fully-gapped *d*+*id* state. These findings would open a new door into electron pairing in $CeCu_2Si_2$ and help understand the pairing mechanism of exotic superconductors.

References

[1] F. Steglich *et al*., Phys. Rev. Lett. **43**, 1892 (1979).
[2] O. Stockert *et al*., Nat. Phys. **7**, 119 (2011).
[3] Y. Kitaoka *et al*., J. Phys. Soc. Jpn. **55**, 723 (1986).
[4] H. A. Vieyra *et al*., Phys. Rev. Lett. **106**, 207001 (2011).
[5] I. Eremin *et al*., Phys. Rev. Lett. **101**, 187001 (2008).
[6] S. Kittaka *et al*., Phys. Rev. Lett. **112**, 067002 (2014).

Authors

S. Kittaka, Y. Aoki, Y. Shimura, T. Sakakibara, S. Seiro[a], C. Geibel[a], F. Steglich[a], H. Ikeda[b], K. Machida[c]
[a]Max-Planck-Institute for Chemical Physics of Solids
[b]Kyoto University
[c]Okayama University

Gapless Quantum Spin Liquid State in a Purely Organic Spin-1/2 Triangular Lattice κ-H_3(Cat-EDT-TTF)$_2$

Mori Group

A quantum spin-liquid (QSL) state is an exotic ground state where interacting spins continue to fluctuate without any formation of long-range magnetic order (LRMO) even at a sufficiently low temperature. A variety of QSL states have been theoretically predicted, but nevertheless, a systematic understanding of the elementary excitation from the experiments remains an arduous challenge. This is mainly because of the rareness of the experimental candidates, which are still restricted to the several spin-frustrated lattices, such as triangular, kagome, and hyperkagome lattices. Recently, Mori group has discovered gapless quantum spin liquid state in a purely organic spin-1/2 triangular lattice κ-H_3(Cat-EDT-TTF)$_2$ (abbreviated as κ-H)[1,2]. In this article, the results of SQUID and torque magnetometry suggesting the QSL state with gapless magnetic excitations in purely organic single-component molecular Mott insulator, κ-H, have been demonstrated [3].

Samples were prepared by the electrochemical oxidation of H_2Cat-EDT-TTF molecules in the presence of a base [1, 2]. A characteristic structural feature of this material is that, in a 2D layer, two face-to-face (H_2Cat-EDT-TTF)$^{0.5+}$ molecules form a strongly dimerized molecular unit, as shown in Fig. 1(a). Because of the strong dimerization, a dimerized unit can be treated as one site, resulting in an effective spin 1/2 per site. As schematically illustrated in Fig. 1(b), each spin is arranged on the triangular mesh with the anisotropy parameter t'/t ~ 1.48 at T = 50 K, where t and t' are the hopping integrals around the sides of rhomboids and along one diagonal, respectively. It is specific that this Mott insulator contains only conducting layers linked by hydrogen bonds without anion layers (Fig. 1(c)), namely purely organic single-component quantum spin liquid crystal.

Firstly, we measured the static magnetic susceptibility at 1 T employing a magnetic property measurement system (Quantum Design) in the temperature region from 2 to 300 K

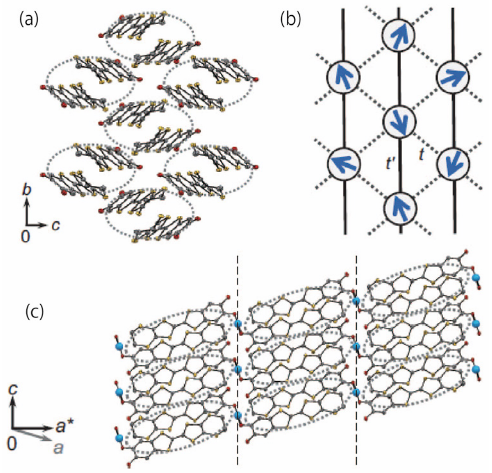

Fig. 1. (a) Molecular arrangement in a two-dimensional layer (b-c plane) of κ-H_3(Cat-EDT-TTF)$_2$. The dotted ellipsoids denote the strongly dimerized molecules. (b) A schematic of the anisotropic triangular lattice with transfer integrals t' and t. The closed circles and the arrows on them represent the sites of the triangular lattice composed of the dimerized molecules and the S = 1/2 spins, respectively. (c) The interlayer packing structure viewed in the a-c plane. The adjacent layers are connected by hydrogen bonds. The dotted ellipsoids represent dimerized molecules similar to those described in (a).

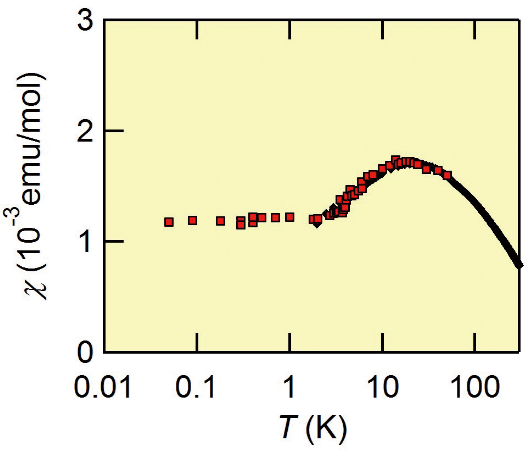

Fig. 2. Magnetic susceptibility as a function of temperature $\chi(T)$ on a semilogarithmic plot. The black diamonds denote the result of the SQUID measurement at 1 T. The red squares represent $\chi(T)$ estimated from the torque at 10 T for a–b rotation. The susceptibility $\chi(T)$ for the a–b rotation is normalized to χ(50 K) from the SQUID measurement. The $\chi(T)$ is nearly independent of temperature below T ~ 3 K, possibly being attributed to the Pauli paramagnetic contribution and suggesting the presence of gapless magnetic excitations in the QSL state.

using poly-crystalline samples of ~16 mg (Fig. 2). The entire temperature dependence of χ is roughly described by the S = 1/2 Heisenberg antiferromagnetic model of an isotropic triangular lattice, with an antiferromagnetic exchange-coupling constant J/k_B ~ 80–100 K. To shed light on the magnetic properties at lower temperatures, we measured the magnetic torque. As the magnetic torque only detects the anisotropic susceptibility in principle, the isotropic contribution from impurity spins is naturally eliminated, providing us with the intrinsic low temperature magnetic properties. For our system, it should be noted that sinusoidal behavior with two-fold periodicity is observed up to H = 17 T and down to T = 50 mK. Moreover, the observed amplitude of the sinusoidal torque curve is precisely proportional to the square of the magnetic field. These observations indicate that the system remains paramagnetic even at T = 50 mK. The above argument about the torque together with the susceptibility $\chi(T)$ reveals that spin frustration on the triangular lattice strongly suppresses the formation of long-range antiferromagnetic order even at $J/kB\,/\,T$ ~ 10^3, suggesting the development of the QSL state as the ground state. Secondly, we focus on the excitation spectrum of the QSL state. In Fig. 2, $\chi(T)$ from torque magnetometry is normalized using χ determined from the SQUID measurement. What is notable in Fig. 2 is that $\chi(T)$ is nearly independent of temperature below T ~ 3 K, possibly being attributed to the Pauli paramagnetic contribution. This suggests the presence of gapless magnetic excitations in the QSL state.

In conclusion, we report the results of SQUID and torque magnetometry of an organic spin-1/2 triangular-lattice κ-H_3(Cat-EDT-TTF)$_2$. Despite antiferromagnetic exchange coupling at 80–100 K, we observed no sign of antiferromagnetic order down to 50 mK owing to spin frustration on the triangular lattice. In addition, we found nearly temperature-independent susceptibility below 3 K associated with Pauli paramagnetism. These observations suggest the development of gapless quantum spin liquid as the ground state. On the basis of a comparative discussion, we point out that the gapless quantum spin liquid states in organic systems share a possible mechanism, namely the formation of a band with a Fermi surface possibly attributed to spinons.

References

[1] H. Kamo, A. Ueda, T. Isono, K. Takahashi, and H. Mori, Tetrahedron Lett. **53**, 4385 (2012).
[2] T. Isono, H. Kamo, A. Ueda, K. Takahashi, A. Nakao, R. Kumai, H. Nakao, K. Kobayashi, Y. Murakami, and H. Mori, Nature Commun. **4**, 1344 (2013).
[3] T. Isono, H. Kamo, A. Ueda, K.Takahashi, M. Kimata, H. Tajima, S. Tsuchiya, T. Terashima, S. Uji, and H. Mori, Phys. Rev. Lett. **112**, 177201 (2014).

Authors

T. Isono, H. Kamo, A. Ueda, K. Takahashi[a], M. Kimata, H. Tajima, S. Tsuchiya[b], T. Terashima[b], S. Uji[b], and H. Mori
[a]Kobe University
[b]National Institute for Materials Science

Quantum Criticality in a Metallic Spin Liquid System $Pr_2Ir_2O_7$

Nakatsuji Group

At finite temperatures, electronic magnetic moments in magnetic materials are thermally fluctuating and one may have magnetic phase transitions accompanied by critical thermal fluctuations. This transition temperature can be lowered by controlling external parameters like pressure and magnetic field. In temperature near absolute zero, thermal fluctuations will be reduced, allowing quantum fluctuations to take effect. When the quantum fluctuations are strong enough, one may have a phase transition at absolute zero, namely quantum phase transition. In the vicinity of the quantum phase transition point, anomalous magnetic and metallic behaviors may be observed, such as high-T_c superconductivity in the cuprates and iron pnictides, and unconventional superconductivity in the heavy fermion systems. These phenomena are stemmed from the anomalous metallic state around the quantum critical point.

Intensive studies on quantum critical phenomena have been done on the groups of compounds so called heavy fermion systems. It is well known that the tuning of the external parameters by applying pressure or magnetic field suppresses the magnetic order down to absolute zero, leading to the emergence of quantum criticality along with the evolution of exotic phase such as anomalous superconductors. Here we have revealed the existence of quantum criticality in a metallic spin liquid system $Pr_2Ir_2O_7$, which may provide a key insight on the mechanism of large spontaneous anomalous Hall effect observed in its spin liquid state [1-4]. In this material, Pr ions form the pyrochlore structure, where the vertices of the corner sharing network of tetrahedra are occupied by Pr ions' Ising type spins, and the ferromagnetic interaction between them causes geometrically frustrated

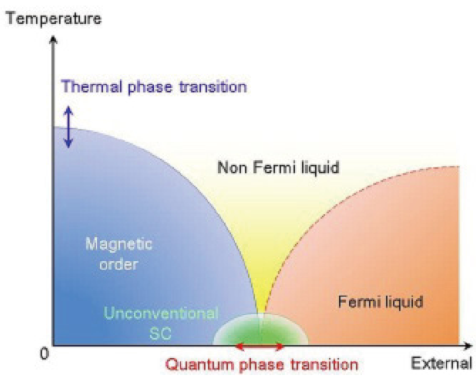

Fig. 1. Schematic phase diagram of temperature (T) vs. external parameters in strongly correlated electron systems.

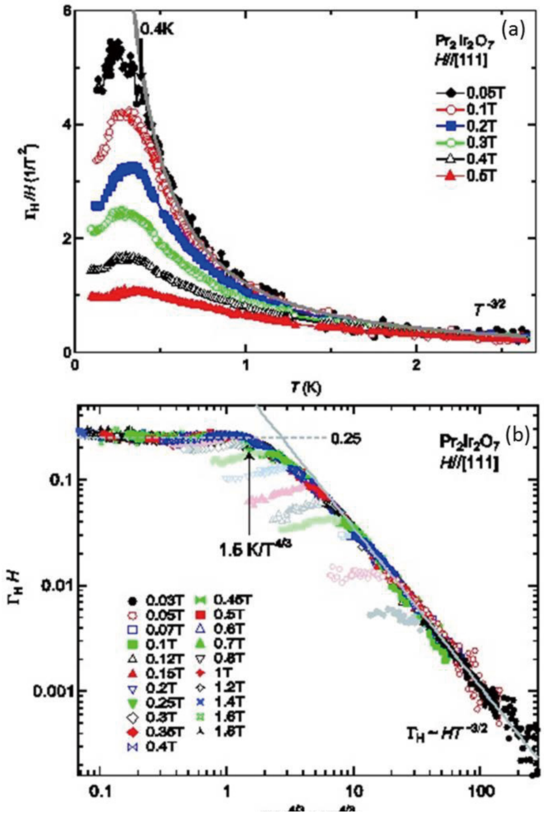

Fig. 2. (a) Temperature dependence of the magnetic Grüneisen ratio Γ_H of $Pr_2Ir_2O_7$. The divergent behavior of Γ_H appears with decreasing of a magnetic field. (b) Critical scaling of the magnetic Grüneisen ratio Γ_H for $Pr_2Ir_2O_7$. This analysis evidences a zero-field quantum critical point in the material.

spin ice state. As a result, the ground state is considered to be spin liquid, having no dipolar magnetic order. In addition, the spontaneous Hall effect appears in this spin liquid phase, suggesting the emergence of a chiral spin liquid state which has finite spin chirality.

In this study, we performed the precise magnetocaloric effect measurements on $Pr_2Ir_2O_7$ [1]. The magnetic Grüneisen ratio, which measures the change of temperature with magnetic field under adiabatic conditions, generally is known to diverge at the quantum critical point, and thus this physical quantity is very sensitive to the existence of quantum criticality.

The results show the divergence of magnetic Grüneisen ratio, indicating the existence of quantum criticality. In addition, the critical scaling which examines the position of a quantum critical point, suggests that $Pr_2Ir_2O_7$ has a quantum critical point at zero magnetic field. Therefore, this system is located at a zero-field quantum critical point without tuning of any external parameter.

In summary, we have found the zero-field quantum criticality in $Pr_2Ir_2O_7$ as indicated by the divergent Grüneisen ratio and zero-field quantum critical point. All these results suggest that the chiral spin liquid phase accompanied with the spontaneous Hall effect emerges under the influence of the quantum criticality led by geometrical frustration. This supports the manifestation of novel type of "quantum critical spin liquid" states. Our study highlights the spin ice as the parent state of the chiral spin liquid state, inducing the spontaneous Hall effects and many other intriguing quantum magnetic phenomena as represented by coherent propagation of monopoles. Our findings of quantum criticality which emerges in a spin liquid state of a highly frustrated metal require further studies, both experimental and theoretical, on the group of frustrated metals.

References
[1] S. Nakatsuji *et al*., Phys. Rev. Lett. **96**, 087204 (2006).
[2] Y. Machida, S. Nakatsuji, Y. Maeno, T. Tayama, T. Sakakibara, and S. Onoda, Phys. Rev. Lett. **98**, 057203 (2007).
[3] L. Balicas, S. Nakatsuji, Y. Machida, and S. Onoda, Phys. Rev. Lett. **106**, 217204 (2011).
[4] Y. Machida, S. Nakatsuji, S. Onoda, T. Tayama and T. Sakakibara, Nature **463**, 210 (2010).
[5] Y. Tokiwa, J. J. Ishikawa, S. Nakatsuji, and P. Gegenwart, Nat. Mater. **13**, 356 (2014).

Authors
Y. Tokiwa[a], J. J. Ishikawa, S. Nakatsuji, and P. Gegenwart[a]
[a]University of Augsburg

Superconductivity in Anti-Post-Perovskite Vanadium Compound

Ohgushi Group

Superconductivity, which is a quantum state induced by spontaneous gauge symmetry breaking, frequently emerges in quasi-two-dimensional materials. The typical examples are high-critical-temperature cuprate with the layered-perovskite (pv) structure, and other examples include a ruthenate Sr_2RuO_4, boride MgB_2, hafnium nitride chloride, cobaltate Na_xCoO_2•yH_2O, an intercalated graphite C_6Ca, and iron-based pnictides and chalcogenides. Hence, the layered character of the host crystal structures is widely believed to be essential in producing superconductivity. This provides an important hint for exploring new superconducting materials. Recently, the post-perovskite (ppv) structural transition of $MgSiO_3$ was discovered under extremely high-pressure (~120 GPa), and captures great interests because the ppv $MgSiO_3$ is considered to be the main constitute of the Earth's lowermost mantle, D" layer [1]. The ppv structure has a peculiar two-dimensional character, and is expected to be a good platform for superconductivity. However, up to now, no superconductivity has been observed in isostructural materials.

We here report the discovery of superconductivity in the anti-post-perovskite (anti-ppv) compounds [2]. We focused on the vanadium compound V_3PN with an anti-ppv structure, where the anion and cation positions are reversed with respect to the ppv structure. We then demonstrated that the compound exhibits superconductivity below 4.2 K (Fig. 1). This is the first report of superconductivity in an isostructural compound. Even though the critical temperature is limited to low temperatures at present, it should be possible to increase the critical temperature by optimizing chemical composition. Indeed, the critical temperature reaches the maximum value of 5.6 K in a slightly N-deficient compound, V_3PN_x with x = 0.9. This discovery stimulates further explorations of new superconducting materials with ppv and anti-ppv structures.

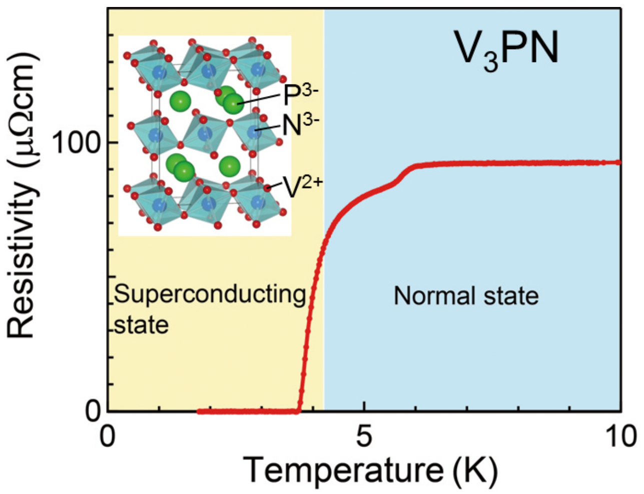

Fig. 1. The resistivity of an anti-post-perovskite compound V_3PN. The resistivity drops to zero at low temperature, indicating the onset of superconductivity. The inset shows the crystal structure.

References
[1] M. Murakami, K. Hirose, K. Kawamura, N. Sata, and Y. Ohishi, Science **304**, 855 (2004).
[2] B. Wang and K. Ohgushi, Scientific Reports **3**, 3381 (2013).

Authors
B. Wang and K. Ohgushi

---Division of Condensed Matter Theory------------

Quantum Phase Transitions of the Hubbard Model on the 1/5-Depleted Square Lattice

Ueda Group

Quantum phase transition is one of the central issues of the present-day condensed matter physics. One of the routes to approach quantum criticality is to introduce geometrical frustration. Another way is to deplete lattice sites periodically, leading to weaker connectivity. A typical example is depletion from the triangular lattice: One can obtain the honeycomb lattice by the 1/3-depletion and the kagome lattice by the 1/4-depletion. It is interesting to note that the tight-binding models on the depleted lattices often show peculiar dispersions like flat bands and/or Dirac cones.

In the present study [1, 2, 3] we investigate Hubbard model on the 1/5-depleted square lattice, Fig. 1. Although the lattice structure looks very artificial, this structure can be found in nature in CaV_4O_9 or $K_{0.8}Fe_{1.6}Se_2$. The unit cell of this lattice contains four sites and thus the energy band structure of the non-interacting system has four bands. At the symmetric point where $t_1 = t_2$ the lowest band and the third one touch at the Γ point, forming a Dirac cone. The second lowest band intersects the apex of the Dirac cone. Therefore this characteristic dispersion is relevant to quantum phase transitions of the Hubbard model on this lattice at quarter filling [1, 2]. With the Coulomb interaction the ground state phase diagram obtained by the mean field theory changes from the non-magneteic insulating phase to the paramagnetic metallic phase, then to an antiferromagnetic metallic phase, and finally to an antiferromagnetic insulating phase, as the ratio t_2/t_1 is increased. Since the Dirac cone is embedded in threefold degenerate electronic states the effective theory around the Γ point is SU(3) Dirac electrons. The rich phase diagram of the Hubbard model is understood by using this effective theory.

The quantum phase transitions at half-filling are also very interesting [3]. It has been known that the Heisenberg model, which is the effective Hamiltonian in the strong correlation limit, shows two quantum phase transitions, one from the dimer singlet phase to the insulating phase with the antiferromagnetic long range order and then onto the plaquette singlet phase. We have looked at the quantum phase transitions of the Hubbard model as a function of Coulomb interaction

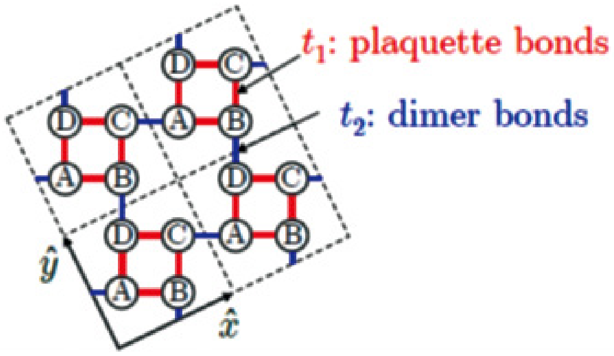

Fig. 1. The 1/5-depleted square lattice. One can define either the unique plaquette covering or the dimer covering. We consider the Hubbard model on this lattice with different hopping matrix elements for the plaquette bonds or the dimer bonds.

under the assumption of paramagnetic states. The nature of the metal-insulator transition is different depending on the ratio of t_2/t_1. On the dimer side, it is shown by applying the cluster dynamical mean field theory that the metal-insulator transition is continuous. This continuous Mott transition is characterized as a Lifshitz transition driven by the Coulomb interaction.

References

[1] Y. Yamashita, M. Tomura, Y. Yanagi, and K. Ueda, Phys. Rev. B **88** 195104 (2013).
[2] Y. Yamashita, M. Tomura, Y. Yanagi, and K. Ueda, JPS Proceedings, SCES2013.
[3] Y. Yanagi and K. Ueda, JPS Proceedings, SCES2013.

Authors
Y. Yamashita[a], M. Tomura, Y. Yanagi[b], and K. Ueda
[a]Nihon University
[b]Tokyo University of Science

Structural Evolution of 1D Spectral Function from Low- to High-Energy Limits

Takada Group

The concept of spin-charge separation plays a central role in describing low-energy physics near Fermi points in a one-dimensional (1D) interacting electron gas, a typical example of the spin-1/2 Luttinger liquid (LL). This concept may be confirmed in real materials by various experiments, including the recent high-resolution angular resolved photoemission spectroscopy in which the one-electron spectral function $A(p,\omega)$ can be directly measured in the wide range of momentum p and energy ω.

If p is not restricted to the region near the Fermi momentum p_F, the linear spectrum approximation, usually adopted in the LL theory, is not sufficient in appropriately obtaining $A(p,\omega)$. In fact, the effect of the nonlinear spectrum on $A(p,\omega)$ has been intensively studied in recent years. According to those studies on integrable systems, $A(p,\omega)$ has singularities for arbitrary p in proportion to $|\omega-\varepsilon_\nu(p)|^{-\mu_\nu(p)}$ with ν=s and c, where $\varepsilon_s(p)$ and $\varepsilon_c(p)$ are energies of spin and charge collective excitations, respectively. In the usual LL theory, the exponent $\mu_\nu(p)$ is independent of p, but the nonlinearity in the electron dispersion makes it depend on p. Since the edge of support of $A(p,\omega)$ is located at $\omega=\varepsilon_s(p)$, $\mu_s(p)$ determines the power of the threshold singularity in $A(p,\omega)$ and its actual value has been given from the finite-size spectrum obtained by the Bethe-ansatz method. For nonintegrable systems, this threshold singularity remains intact, but the singularity at $\omega=\varepsilon_c(p)$ is smeared into a broad peak.

In those preceding works, only the singularities at $\omega=\varepsilon_s(p)$ and $\omega=\varepsilon_c(p)$ are discussed on the belief that the electron nature will not sustain in the spin-charge separated system. For p far away from p_F, however, the effect of interactions becomes so weak that we would naively expect that the nature of an injected electron to measure $A(p,\omega)$ manifests itself as a main peak in $A(p,\omega)$. Then a natural question arises: ***Does an electron-like excitation mode actually exist in the 1D interacting electron gas for p much larger than p_F?*** If yes, a related and more intriguing question is: ***How does the electron-like mode reconcile with the physics of spin-charge separation for p near p_F?***

In pursuit of answers to those questions, we have carefully studied the 1D one-electron Green's function $G(p,t)$ in momentum space and time and found that for $p\sim p_F$, its long-time asymptotic form is composed of ***three*** independent modes of power-law decay [1]. Two of them correspond to well-known spinon and (anti)holon excitations, but the rest describes the mode of an electron-like particle (***pseudoelectron***) which may be regarded as an electron dressed with a "cloud" of low-lying spin and charge collective excitations. This pseudoelectron does not appear as a main structure in $A(p,\omega)$ for $p\sim p_F$ and never leads to a finite jump in the momentum distribution function $n(p)$. As p goes away from p_F, the pseudoelectron structure gets broader, but with the further increase of p, it becomes less broad and eventually for $p\gg p_F$, it evolves as a main and divergent peak in $A(p,\omega)$ by swallowing the antiholon mode. Concomitantly, its dispersion relation approaches the one of a free electron, allowing us to regard the pseudoelectron as a free electron, but actually it is not quite, nor the Landau's quasiparticle, basically because this excitation is accompanied by power-law decay. Those results clarify the generic feature of $A(p,\omega)$ in a 1D metal and answer the aforementioned two questions.

As an illustration of the overall behavior of $A(p>p_F,\omega)$ with the change of p and ω, we adopt the Yang-Gaudin model in the weak-coupling region in order to explicitly compute $A(p,\omega)$. In Fig. 1, the obtained result is displayed with increasing p from p_F to show its complete structural evolution in the 1D weakly-interacting electron gas with the quadratic dispersion ξ_p ($=p^2/2m-p_F^2/2m$). Since we focus on the region of ω in the very vicinity of ξ_p, only the pseudoelectron mode appears as a singular structure in $A(p,\omega)$ in Fig. 1.

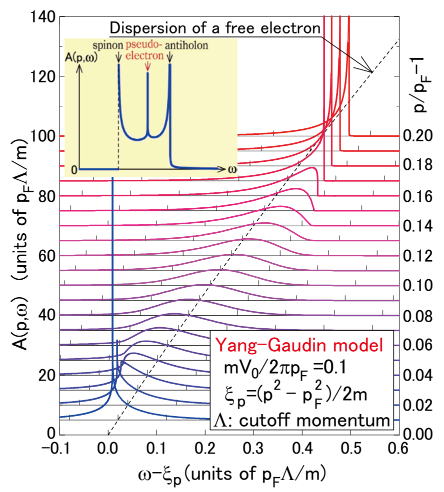

Fig. 1. Structural change of the pseudoelectron peak in the one-electron spectral function $A(p,\omega)$ for the Luttinger liquid (Yang-Gaudin model). Inset: The entire structure of the spectral function near the Fermi point.

The pseudoelectron introduced here very much resembles a quasiparticle in higher-dimensional Fermi-liquid systems, although it is not quite the same, reflecting the specialty of 1D physics. We hope that this concept of a pesudoelectron will be confirmed in the future through experiment and/or large-scale numerical calculation with deliberately-chosen parameters so as to avoid its overdamping regime.

Reference

[1] H. Maebashi and Y. Takada, Phys. Rev. B 89, 201109 (R) (2014).

Authors
H. Maebashi and Y. Takada

Particle Statistics, Frustration, and Ground-State Energy

Oshikawa Group

Quantum statistics of identical particles is one of the most fascinating aspects of quantum mechanics. The wavefunction does not change when two identical bosons are exchanged, while it acquires a negative sign when two identical fermions are exchanged. This fundamental distinction leads to various differences in physical properties between a system of many bosons and that of many fermions. For example, fermions obey Pauli exclusion principle, which forbids more than one particles to occupy the same single-particle state. In contrast, any number of bosons can occupy the same single-particle state, concerning the quantum statistics. In fact, at sufficiently low temperatures, a macroscopic number of bosons may occupy the same single-particle state. This is the celebrated Bose-Einstein Condensation, which has been directly observed in ultracold atoms.

Let us consider two systems with the "identical" Hamiltonian, but the one consists of many bosons and the other consists of many fermions. By "identical" Hamiltonian we mean the single-particle eigenstates and their energy eigenvalues are identical. Our question is: which system has the lower ground-state energy, the one of bosons or that of fermions? It might appear a trivial question, since in the ground state all the bosons will occupy the lowest-energy single-particle eigenstate, while most of the fermions will occupy higher energy single-particle eigenstates because of the Pauli exclusion principle. Then the ground-state energy of fermions would be always higher than that of bosons. However, this simple argument is only valid when there is no interaction. When there is an interaction between the particles, as is the case in realistic systems, the Bose-Einstein Condensation is not perfect. Thus the comparison is a nontrivial question in the presence of interaction.

We first proved [1] a theorem which states: even in the presence of interaction, bosons have a lower ground-state energy if all the hopping amplitudes are positive. This theorem can be understood in terms of frustration among quantal phases; if all the hopping amplitudes are positive, there is no such frustration in the system of bosons while fermions are subject to frustration due to their quantum statistics. We can violate the assumption of the theorem by introducing negative and/or complex hopping amplitudes. This makes it possible that the inequality between the ground-state energies to be reversed. This again can be understood in terms of frustration introduced among hoppings. In fact, we succeeded in constructing several concrete examples, in which the ground-state energy of fermions is lower than that of corresponding bosons [1]. This includes a rigorous proof on the delta-chain case, for which the reversal was reported earlier on small clusters [2].

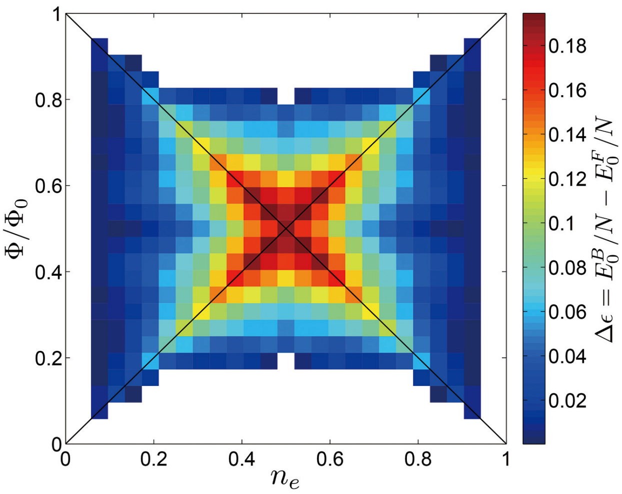

Fig. 1. Comparison of the ground-state energies of fermions and hard-core bosons on the square lattice of 26 sites. The horizontal axis is the number of particles ne per site, and the vertical axis is the flux per plaquette Φ in unit of the flux quantum Φ_0. The ground-state energy of fermions is lower than that of bosons in the colored region, and the difference is most significant in the red-colored region, where $n_e = \Phi/\Phi_0$ or an equivalent relation approximately holds.

References

[1] W. Nie, H. Katsura, and M. Oshikawa, Phys. Rev. Lett. **111**, 100402 (2013).
[2] S. D. Huber and E. Altman, Phys. Rev. B **82**, 184502 (2010).

Authors
W. Nie, H. Katsura[a], and M. Oshikawa
[a]Gakushuin University

K-computer Simulation for Electrochemical Energy Conversion

Sugino Group

Energy flows through matters in various forms and controlling the energy flow is an important subject of interdisciplinary material research. The energy flow dynamics is complex but is particularly rich near the interface, where the energy carrier (particle or field) switches from one to another. The electrochemical interface offers a field for converting an *ionic flow* to the *electronic flow*, and this conversion process is used as the principle of a battery. The corresponding basic process is the electron-transfer reaction dynamics, which has now attracted renewed attention not only from electrochemistry but also from many other fields. In this context, this group is intended to describe the dynamics, with the help of the K-computer power, unambiguously within the first-principles molecular dynamics (FPMD) scheme. A simulation team was organized from research groups of Osaka/Tohoku/Nagoya University and national laboratories (AIST and NIMS). The joint simulation team has recently made progress toward the goal.

The team modeled the system using a metal slab, a solution slab, and the dielectric continuum slab as shown in Fig. 1. This model, called the effective screening medium (ESM) model, was originally developed by the present group in 2006 [1] but was recently improved to enable a precise

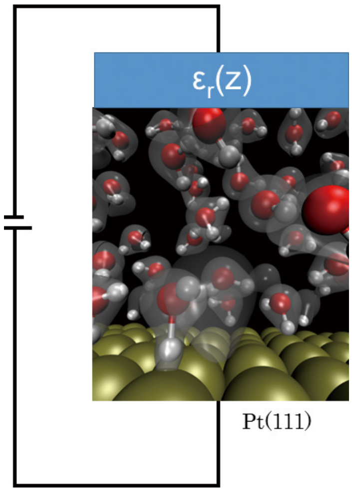

Fig. 1. The ESM modeling of the electrochemical interface. The model consists of the electrode slab (Pt(111) in the present case), solution slab (liquid water plus a hydronium ion) and the dielectric continuum. The continuum is characterized by the dielectric constant. The bias potential is controlled with the potentiostat scheme [2].

control of the bias potential [2,3]. By this technique one can describe a subtle imbalance of chemical equilibrium between the electrons and the ions, essential for studying an electrochemical process. This algorithm was implemented to an FPMD code, called STATE-senri, which had been highly parallelized for K-computer.

One of the first target of this new FPMD scheme was to investigate how the solvent fluctuation would affect the catalytic activity. The solvent fluctuation causes the bias potential to fluctuate, whereby assisting the catalytic reaction to occur. The fluctuation is small for the bulk catalysts but is increasingly enhanced as the catalyst is reduced in size. By combining the simulation with the classical Marcus theory, the exchange current for the reaction, which is a measure of catalytic activity, was found to be enhance by 15 when the size of nano-particle is reduced to 3 nm in diameter [4]. This enhancement factor is indeed a large value which is comparable to (or larger than) that achievable with the nano-shell method, i.e., a technique to enhance the activity by alloying the subsurface Pt. The fluctuation effect has not been seriously studied so far, but the present calculation suggests further room for enhancing the catalytic activity by controlling the structure of the interface.

This group has been performing a large number of first-principles simulations, with or without the ESM, and the results have accumulated. With those data, this group has reconsidered how the reduction of an oxygen molecule would occur, which is the central issue of electrochemistry and many efforts have been devoted. When the simulation results were analyzed together with recently available experimental results, it was found that some of the reaction pathways can be excluded and accordingly narrowed down the possibilities [5]. It was then concluded that the reaction proceeds mainly through a pathway called the associative pathway in the steady state, while the other one, called the dissociative pathway, is chosen prior to steady state. This analysis emphasizes importance of the dynamical effect in discussing the dominant mechanism.

More extensive simulations are now conducted in K-computer. The team is preparing further for the coming exa-flops supercomputers to establish a microscopic theory of electrochemical energy conversion.

References

[1] M. Otani and O. Sugino, Phys. Rev. B **73**, 115407 (2006).
[2] N. Bonnet, T. Morishita, O. Sugino, and M. Otani, Phys. Rev. Lett. **109**, 266101 (2012).
[3] I. Hamada, O. Sugino, N. Bonnet, and M. Otani, Phys. Rev. B **88**, 155427 (2013).
[4] N. Bonnet, O. Sugino, and M. Otani, J. Chem. Phys. **140**, 044703 (2014).
[5] N. Bonnet, O. Sugino, and M. Otani, to be published in J. Phys. Chem. C.

Authors

O. Sugino[b], N. Bonnet[b], I. Hamada[a], M. Otani[a], T. Ikeshoji[a], Y. Morikawa[b], K. Inagaki[b], H. Kizaki[b], K. Akagi[c], M. Araidai[d]
[a]Advanced Industrial Science and Technology
[b]Osaka University
[c]Tohoku University
[d]Nagoya University

Kondo Signature in Heat Transfer via a Local Two-State System

Kato Group

Heat and electric transport have several similarities as well as dissimilarities. Fourier's law in heat transport corresponds to Ohm's law in electric transport, and these laws are commonly categorized as diffusive transport. Ballistic transport leads to the quantization of conductance in electric as well as heat transport. The conductance quantum was measured in mesoscopic electric conduction in 1988, and much later, the version of heat transport was also measured [1]. Recently, the concept of thermal diode has also been discussed, and an experiment has been conducted for demonstrating this [2]. Recent progress in transport studies strongly indicates that heat transport analogue exists for many categories of electric transport.

We have studied the Kondo effect in heat transport via a local two-state system [3]. We consider a two-state system coupled to phonon environments. The two-state system is, for example, obtained from truncation from a symmetric double-well system with a small tunneling matrix element Δ. The present system is described by the spin-boson Hamiltonian with Ohmic dissipation. The cut-off energy of the phonon bath and the dimensionless system-environment coupling are denoted with ω_c and α, respectively. It is known that the spin-boson model can be mapped onto the Kondo model with anisotropic exchange coupling. In order to

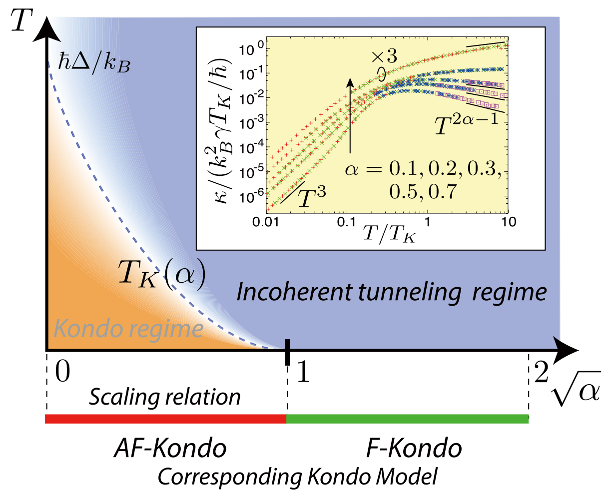

Fig. 1. (Main panel) Two different regimes expected in the spin-boson model. (Inset) The thermal conductance calculated by the quantum Monte Carlo method is shown as a function of the temperature.

study the Kondo-like effect in the phonon systems, we have derived the exact formula of thermal conductance, and have evaluated it by the quantum Monte Carlo method.

Summary of the results is shown in Fig. 1. The main figure shows the Kondo regime and the incoherent tunneling regime in the space of temperature T versus dimensionless coupling strength α. At the bottom of the main figure, mapping onto corresponding anisotropic Kondo model is shown: the antiferromagnetic Kondo (AF-Kondo) and the ferromagnetic Kondo (F-Kondo) region are respectively mapped onto the region of $0<\alpha<1$ and $1<\alpha<4$ in the spin-boson Hamiltonian. Heat transport via the Kondo effect is realized in the Kondo regime (the orange region).

In the inset of the figure, we show temperature dependence of the thermal conductance κ calculated by the quantum Monte Carlo method. Different legends in the graph denote with different ratios of Δ/ω_c. As seen in the figure, the data for a fixed α fall onto one curve by appropriate scaling of the temperature and the thermal conductance with the Kondo temperature T_K. This behavior is characteristic of the Kondo effect. Below the Kondo temperature, conductance follows the universal temperature dependence proportional to T^3. The obtained thermal conductance is much larger than the one expected from stochastic transition of the two-state system [4]. This is a manifestation of strong correlation between system and reservoirs, which is analogous to the Kondo effect in electric transport. On the other hand, at temperatures higher than the Kondo temperature T_K, the thermal conductance becomes proportional to $T^{2\alpha-1}$. This behavior is understood by a simple approximation based on the Fermi's golden rule. We note that the thermal conductance is always proportional to $T^{2\alpha-1}$ for $\alpha>1$ since the Kondo temperature is zero.

In summary, we have investigated the Kondo effect in thermal transport via a local two-state system, by utilizing the spin-boson model with ohmic dissipation. We hope that our study motivates further research on low-energy heat transfer via local systems. Other types of dissipation (superohmic/subohmic dissipation) and far-from-equilibrium effect will be intriguing subjects in this direction.

References

[1] B. J. Wees *et al.*, Phys. Rev. Lett. **60**, 848 (1988); K. Schwab *et al.*, Nature (London) **404**, 974 (2000); H.-Y. Chiu *et al.*, Phys. Rev. Lett. **95**, 226101 (2005).

[2] N. Li, J. Ren, L. Wang, G. Zhang, P. Hänggi, and B. Li, Rev. Mod. Phys. **84**, 1045 (2012); C. W. Chang, D. Okawa, A. Majumdar, and A. Zettl, Science **314**, 1121 (2006).

[3] K. Saito and T. Kato, Phys. Rev. Lett. **111**, 214301 (2013).

[4] T. Ruokola and T. Ojanen, Phys. Rev. B **83**, 045417 (2011).

Authors

K. Saito[a] and T. Kato

[a]Keio University

---Division of Nanoscale Science---------------------------

Nature of Spin Polarization in a Quantum Point Contact

Katsumoto Group

Creation of spin current in quantum structures of non-magnetic materials is a key technique in semiconductor spin-electronics (spintronics). The use of spin-orbit interaction (SOI) and quantum point contact (QPC) structure is a promising candidate. So called Rashba-type SOI

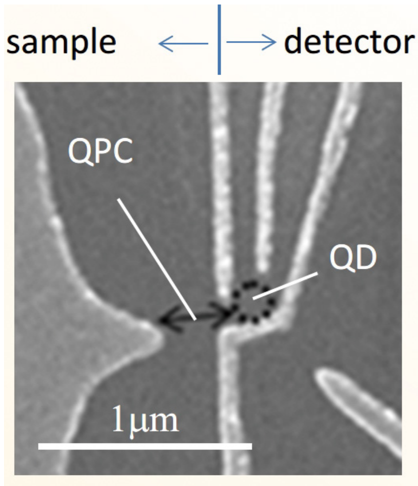

Fig. 1. Scanning electron micrograph of the gate configuration for the sample. The gray regions are metallic Schottky gates.

splits electronic spin states according to the direction of momentum. Electronic states in a QPC structure are a set of one-dimensional bands with discrete edges due to quantization transverse to the one-dimensional motion. As a result, ordinary conductance of a QPC is quantized with the unit of $2e^2/h$, which is called conductance quantum. There are a number of experimental reports on the anomalous quantization of conductance at a half conductance quantum, i.e. e^2/h, which phenomenon, called 0.5 conductance plateau has been attributed to the result of perfect spin polarization [1] though direct evidence was not obtained. Such a high spin polarization was also predicted on the 1.0 plateau (i.e. $2e^2/h$) [2] but due to the lack of detection method, there have been no experimental confirmation.

We have developed a new technique for the detection of spin-polarization with time-domain spin blockade. For that the two-electron tunneling process from the target device to a quantum dot (QD) is used. When the process is to a single orbital level, the probability is suppressed while it is not for the tunneling into two orbital levels. Hence the degree of suppression has a direct relationship to the spin-polarization in the target with the spin-relaxation time in the QD as a parameter.

As the base system, two-dimensional electron gas (2DEG) in an (In, Ga)As quantum well was adopted. The sample consists of a QPC with a side-coupled QD with another QPC for the remote charge detection (Fig. 1). The conductance of the QPC as a function of the gate voltage shown in Fig. 2 clearly exhibits 0.5 anomalous plateau struc-

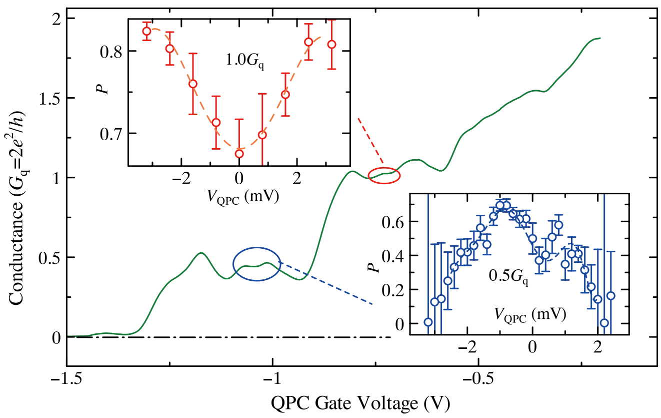

Fig. 2. QPC conductance as a function of the gate voltage. The unit is the quantum conductance $G_q=2e^2/h$. The insets show bias voltage (V_{QPC}) dependence of spin-polarization of 0.5 G_q and 1.0 G_q plateaus respectively.

ture in addition to the ordinary quantized plateau at $2e^2/h$. Spin-polarization measured with the QD detector is shown as a function of the QPC bias voltage V_{QPC} in the insets of Fig. 2, both for 0.5 and 1.0 plateaus. Here the definition of spin-polarization P is $P = (N_u–N_d) / (N_u+N_d)$, where N_u and N_d correspond to the concentration of up-spin electrons and down-spin electrons respectively. At zero-bias voltage, P is high on 0.5 plateau while it decreases with increasing V_{QPC}. The differential conductance of the QPC, on the contrary, increases with V_{QPC} indicating that the mechanism of the spin-polarization is a kind of spin-filtering, which cuts the flow of spin-down electrons. On the other hand at 1.0 plateau, P gradually increases with V_{QPC}, indicating that the mechanism here is spin-rotation, which turns up the down spin of electrons. There is a small dip structure in P near the zero-bias at 0.5 plateau, which reflects the formation of the Kondo cloud. As just described we have demonstrated the powerfulness of the present method and revealed the mechanisms of spin-polarization in a QPC with Rashba-type SOI.

References
[1] P. Debray *et al.*, Nature Nanotechnology **4**, 759 (2009).
[2] M. Eto, T. Hayashi, and Y. Kurotani, J. Phys. Soc. Jpn. **74**, 1934 (2005).
[3] M. Kohda *et al.*, Nature Communications **3**, 1082 (2012).

Authors
S. Katsumoto, S.W. Kim, T. Nakamura, and Y. Hashimoto

Spin Injection into a Superconducting Niobium

Otani Group

Spintronics is a spin counterpart of electronics and its potentiality for future applications as well as for novel physics has boosted a number of researches in recent years. Among diverse materials, superconductors are promising for their distinct properties of spin transport; because of a superconducting energy gap, spins are mediated by quasiparticles and it is theoretically predicted that the spin relaxation time (τ_s) is enhanced owing to the reduced group velocity of quasiparticles. However, previous experimental studies are not conclusive due to the problems of device structures. Thus, for both basic physics and applications, it is highly desirable to estimate τ_s in superconductors *correctly* without spurious effects. In this work [1], we aimed at injecting a

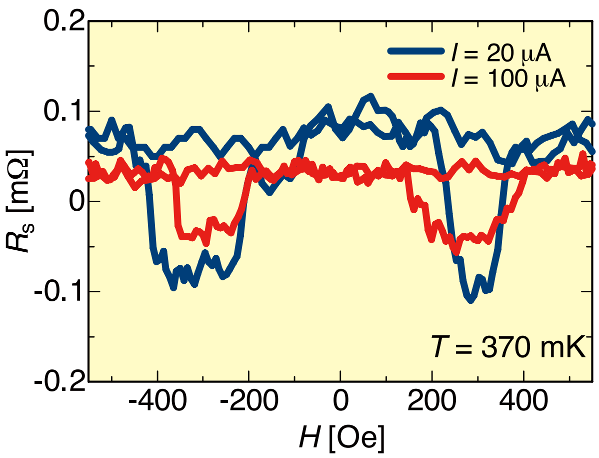

Fig. 1. NLSV signals R_s measured at 370 mK (< T_C) with two different currents I = 20 μA (red) and 100 μA (blue).

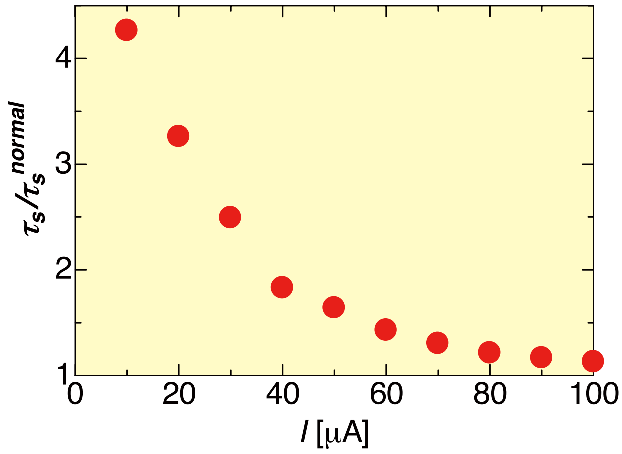

Fig. 2. The relation between τ_s and I. τ_s is normalized by that in the normal state (τ_s^{normal} = 2.3 × 10^{-13} s). As I decreases, τ_s dramatically increases.

pure spin current into superconductors with a large spin-orbit (SO) interaction and estimating τ_s appropriately. Through the use of such superconductors, we can expect more complex phenomena for further studies where superconductivity, magnetism and SO interaction are closely coupled.

We fabricated a typical lateral spin valve structure with a superconductor Nb, consisting of two ferromagnetic Permalloy ($Ni_{81}Fe_{19}$; Py) wires bridged by a nonmagnetic Cu wire and a Nb wire inserted below the Cu bridge in between the two Py wires. By flowing a charge current (I) from one of the Py wires to the Cu, a pure spin current is generated in the Cu bridge and partly absorbed into the Nb due to its large SO interaction. The pure spin current can be detected by the other Py wire, and the detected nonlocal spin valve (NLSV) signal is reduced when the spin absorption occurs. In our study we performed spin absorption measurements both above and below the critical temperature of Nb (T_C = 5.5 K).

In Fig. 1, we show a result of the spin absorption measurements taken at 370 mK, much lower than T_C. The NLSV signal shown here is normalized by I. Above T_C, it is independent of I (not shown here), as expected for normal metals. Far below T_C, on the other hand, the NLSV signal obviously increases as I decreases, indicating the suppression of the spin absorption at the Nb wire. In order to evaluate the amount of the pure spin current absorbed from Cu into Nb, we calculated the density of states of the superconducting Nb using the Usadel equation where the superconducting proximity effect between Cu and Nb is taken into account. In the Usadel equation, τ_s of the superconducting Nb is treated as a free parameter. With this parameter, we can reproduce the NLSV signal for each I, and simultaneously obtain τ_s. The obtained data are shown in Fig. 2. τ_s is clearly enhanced with decreasing I. To know the relation between I and temperature, we also measured the interface resistance between Cu and Nb as functions of I and temperature, and found that the effective temperature (T) at the interface is increased by I. These results clearly demonstrate the enhancement of τ_s in a superconductor with decreasing T consistent with the theoretical prediction [2].

References
[1] T. Wakamura, N. Hasegawa, K. Ohnishi, Y. Niimi, and Y. Otani, Phys. Rev. Lett. **112**, 036602 (2014).
[2] T. Yamashita, S. Takahashi, H. Imamura, and S. Maekawa, Phys. Rev. B **65**, 172509 (2002).

Authors
T. Wakamura, N. Hasegawa, Y. Niimi, and Y. Otani

One-dimensional Fermi Surface is Stabilized on Ge Surface Even at Low Temperature

Komori group

In solid-state physics, we learn that electrons in one-dimensional metals undergo metal-to-insulator transition induced by the Peierls instability due to electron-phonon interaction or exhibit a Luttinger liquid behavior due to electron-electron interaction with decreasing temperature. Atomic nanowires formed on semiconductor surfaces offer an opportunity to investigate such intriguing phenomena of one-dimensional metals. So far, however, their manifestations are largely disturbed by the presence of defects in the nanowires. Highly-ordered atomic nanowires at surfaces are thus essential not only for clarifying if they exhibit the Peierls instability or a Luttinger liquid behavior, but also for understanding universal nature of one-dimensional electronic systems. On the Ge(001) surface, defect- and kink-free Pt-induced atomic nanowires (Pt/Ge(001) NWs) can be formed, and are very suitable for the study of one-dimensional electrons. [1,2,3] We have investigated the ground-state electronic properties of Pt/Ge(001) NWs at the Fermi level (E_F) *in situ* by angle-resolved photoelectron spectroscopy at 6 K, a sufficiently lower temperature than its structural phase transition at 80 K, using single-domain samples shown in Fig. 1.

Figure 2(a) shows the Fermi-surface mapping at 6 K. Two metallic surface bands labeled S_1 and S_2 are clearly identified. The Fermi surface of S_1 consists of straight lines in the k_y direction, indicating that the S_1 band disperses only in the nanowire direction. It is therefore an ideal one-dimensional metallic state which is decoupled from neighboring electronic systems. As shown in Fig. 2(b,c), it exhibits a steep dispersion and clearly crosses E_F in the substrate bulk band gap. Obviously, there is no gap opening at E_F. Thus, the S_1 band does not directly contribute to the structural phase transition at 80 K and is stable against the Peierls instability if it exists. The electron-phonon interaction could not be strong enough to induce any structural transition with the nesting vector for S_1 by the Peierls instability scheme. In order to examine a Luttinger liquid behavior, the energy distribution curve of S_1 was analyzed as shown in Fig. 2(d). The observed spectral shape agrees with the normal Fermi-Dirac-type distribution function without any indication of the power-law behavior predicted for a Luttinger liquid. These novel results provide not only a valuable contribution to the phenomenology of nanowires/semiconductor systems but also a major advance for understanding the intriguing physics of the one-dimensional electrons on solid surfaces.

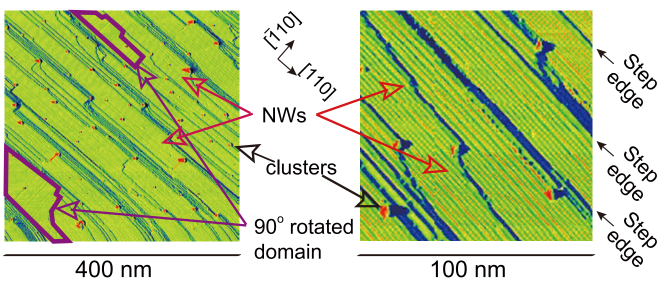

Fig. 1. STM images of Pt/Ge(001) nanowires (NW) on a vicinal Ge(001) substrate. The substrate was tilted toward the [$\bar{1}$10] direction by 2°. Most of wide terraces are covered by the nanowires parallel to the step edges. The areas surrounded by purple lines in (left) represent minority domains. In both images, the bias voltage is 1.5 V and the tunneling current 0.5 nA.

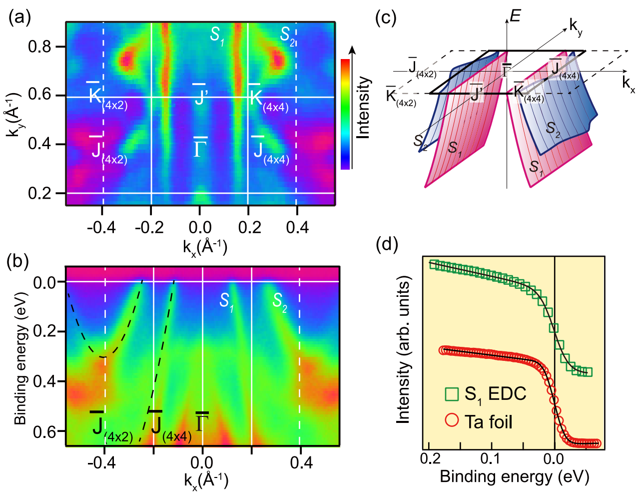

Fig. 2. (a) Constant energy ARPES intensity map at E_F of Pt/Ge(001) NWs with single-domain samples formed on the vicinal Ge(001) substrate. The photoelectron intensity is represented by color scale. (b) ARPES image taken along $\bar{\Gamma}\bar{J}$. Dashed curves represent the band structures of S_1 and S_2, which were fitted to the data. (c) Schematic illustration of the S_1 and S_2 bands. (d) Integrated energy distribution curve of S_1 near E_F over k_y in the surface Brillouin zone is compared with the results of a Ta foil.

References

[1] Gürlu *et al.*, Appl. Phys. Lett. **83**, 4610 (2003).
[2] I. Mochizuki *et al.*, Phys. Rev. B **85**, 245438 (2012).
[3] K. Yaji *et al.*, Phys. Rev. B **87**, 241413(R) (2013).

Authors

K. Yaji, I. Mochizuki[a], S. Kim, Y. Takeichi[a], A. Harasawa, Y. Ohtsubo[b], P. Le Fèvre[b], F. Bertran[b], A. Taleb-Ibrahimi[b], A. Kakizaki, and F. Komori

[a]High Energy Accelerator Research Organization
[b]Synchrotron SOLEIL

Fabrication, Spectroscopic Characterization and Transport Properties of Aromatic Monolayers Covalently bonded to Si(111)

Yoshinobu Group

Fabrication of self-assembled monolayers (SAMs) of organic molecules on semiconductor surfaces is one of the central issues in surface science and device chemistry because of its ability to impart renewed functionalities on the surfaces. Since well-ordered and dense organic SAMs can be fabricated without severe reaction conditions and expensive equipment, organic SAMs on a semiconductor have become attractive materials that are easily accessible model systems for both fundamental scientific research and development of practical molecular devices. Among various semiconductor–organic interface structures, Si-organic molecule systems are promising candidates for future applications because of the actual proven performance of Si in today's electronics.

In this study [1], SAMs composed of aromatic molecules with different anchor groups were fabricated on the Si(111) surfaces by wet chemical reactions. We investigated the bonding structures and transport properties by spectroscopic and electrical measurements, respectively. By using simple

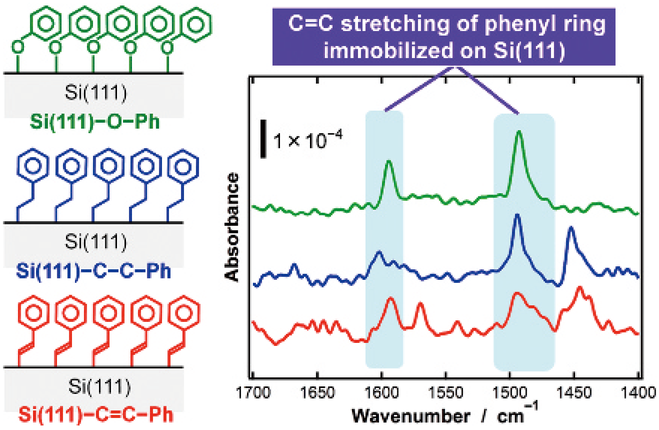

Fig. 1. (left) Schematic representations of the aromatic monolayers on Si(111) in this study [Si(111)–O–Ph (green), Si(111)–C–C–Ph (blue), and Si(111)–C=C–Ph (red)]. (right) Transmission FT-IR spectra of these Si(111)-aromatic SAMs measured at an incident angle of 60°. Copyright © 2013 American Chemical Society.

aromatic molecules (phenol, styrene, and phenylacetylene) as initial precursors, we successfully fabricated aromatic SAMs covalently bonded to Si(111) surfaces through different anchor structures (Si–O–, Si–CH_2–CH_2–, and Si–CH=CH–). Transmission infrared spectra clearly indicate that the phenyl rings in the SAMs are oriented almost perpendicular to the Si surfaces. High-resolution X-ray photoelectron spectra using synchrotron radiation (KEK-PF BL13) reveal that the aromatic molecules attach to the Si surface with the surface coverage of ~ 0.5. These experimental results lead to a conclusion that the aromatic SAMs form densely packed monolayers on Si(111) using the present wet chemical methods. Judging from the current density–voltage measurements of Hg/aromatic SAM–Si(111) sandwiched structures, the "Si(111)–O–Ph" (SAM by using phenol) system shows higher conductivity compared with the long-chain alkyl SAM on Si(111).

Reference

[1] Y. Harada, T. Koitaya, K. Mukai, S. Yoshimoto, and J. Yoshinobu, J. Phys. Chem. C **117**, 7497 (2013).

Authors

Y. Harada, T. Koitaya, K. Mukai, S. Yoshimoto, and J. Yoshinobu

Visualization of "Reflectionless Tunneling" in the Superconducting Proximity Effect

Hasegawa and Kato Groups

When a superconducting material is brought into contact with a normal metal, superconducting properties penetrate into the metal. The phenomenon called proximity effect has been utilized to induce the pair correlation into various materials, including topological insulators to realize elucidating Majorana fermions.

The propagation of the proximity effect depends on the distribution of scattering centers in the normal metal, as you may expext. But curiously, it is enhanced by the presence of elastic scatters. The proximity effect is caused by the Andreev reflection at the super/normal interface, where injected electrons from the normal metal is retro-reflected as a hole whose phase is conjugated with that of the electron. Elastic scatters redirect reflected electrons/holes toward the interface, making a loop in their trajectories with the interface. Because of constructive quantum interference due to the phase conjugation, the looped trajectories enhance the probability of the Andreev reflection and consequently proximity effect. As the Andreev-reflected quasiparticles can tunnel though the interface without reflection, the enhancement is called reflectionless tunneling.

Using scanning tunneling microscopy (STM), we studied the proximity effect and the roles of the atomic-scale defects in real-space with nano-meter scale spatial resolution. The measurement was performed at 2.15 K in ultrahigh vacuum. The proximity effect was characterized via tunneling spectroscopy of a gap formed by the pair correlation at the Fermi energy. The investigated super/normal interface was formed *in situ* by creating superconducting Pb islands on a Pb-induced two-dimensional (2D) normal metal formed on a Si substrate. In Fig. 1, a topographic STM image (left) and a mapping of the corresponding conductance at the bottom of the gap, that is, zero bias conductance (ZBC) mapping (right), are shown.

In the ZBC mapping, all Pb islands are colored green, which indicates zero ZBC and good superconductivity there, and the normal metal far from the Pb islands is colored yellow, indicating no gap there. The area surrounding the Pb islands has the color of blue to red, implying a gap formation by the proximity effect. The gap propagates from the superconducting Pb islands and decays into the normal metal with the coherence length ξ of 40 nm. It is found from the mapping that the proximity effect strongly depends on the atomic structure of the interface; it is strong at the place where a Pd island is directly sitting on the 2D layer, and

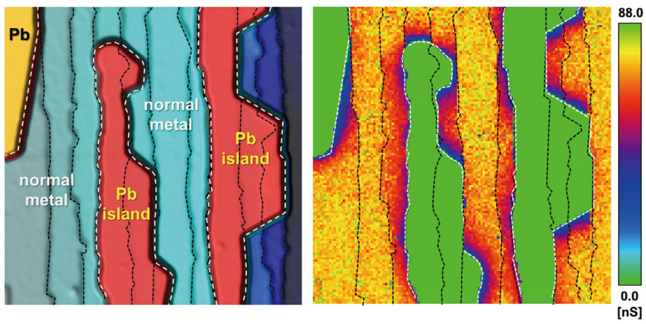

Fig. 1. (left) STM image of Pb islands on a Pb-induced two-dimensional normal metal formed on a Si substrate (1.0 μm square). The edges of the Pb islands and the steps of the normal metal layer are highlighted with white and black dotted lines, respectively. (right) The zero-bias conductance (ZBC) color map of the same area as in the topographic image.

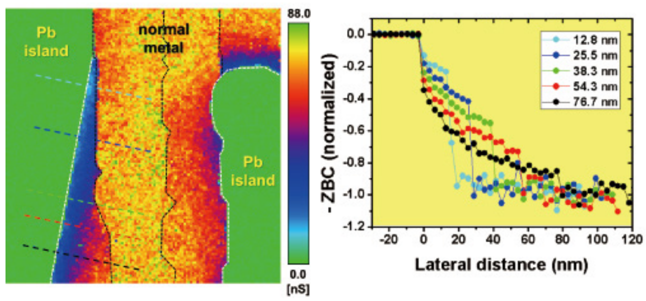

Fig. 2. (left) 400 nm × 400 nm ZBC color map taken on a confined area surrounded by the Pb island and a step edge of the normal metal layer. (right) Normalized negative ZBC profiles across the super/normal interface and the step edges measured along the colored lines drawn in the topographic image. The length written for each plot is the terrace width measured along the corresponding line.

basically no gap formation is observed at the edge of the island that coincides with the downward step of the 2D layer. The observed structural dependence can be explained by the variation of the conductivity at the super/normal interface.

We also found that the surface steps severely block the propagation, which indicate they behave as a strong potential barrier or an elastic scatter for the two-dimensional electrons. In order to find the role of the steps on the proximity effect, we investigated an area where the step is very close to the super/normal interface shown in Fig. 2 (the upper left of Fig. 1). In the wedged area whose terrace width ranges from almost 0 to 2ξ we observed the enhancement of the gap and found that deeper gap is formed on narrower terrace, as demonstrated in the right panel of Fig. 2, which shows ZBC profiles for various width terraces. Because of the real-space and cross-sectional observation, we can probe ZBC throughout the system while eliminating unwanted effects of structural defects at the super/normal interface and in the normal metal. The observed enhancement is overall consistent with the reflectionless tunneling. The dependence of the enhancement on the terrace width is, however, not explained quantitatively with the calculation based on the Usadel equation, a quasi-classical Green's function formalization. Some phenomena that are not considered in the calculation are probably involved in the enhancement of the proximity effect.

References

[1] H. Kim, S.-Z. Lin, M. J. Graf, T. Kato, and Y. Hasegawa, arXiv:1401.2602

Authors
H. Kim, S.-Z. Lin[a], M. J. Graf[a], T. Kato, and Y. Hasegawa
[a]Los Alamos National Laboratory

Ferromagnetic Josephson Junctions

Lippmaa Group

Ferromagnetism and superconductivity are generally incompatible because in conventional superconductors Cooper pairs are formed by two electrons with opposite spins, while in ferromagnets, exchange interactions align the spins parallel to each other. In our recent work, we study the possibility of a long-range supercurrent surviving in highly spin-selective materials, such as half-metals in spin filter tunnel junctions. In particular, our interest is in determining the role of magnetic disorder in promoting a spin-triplet supercurrent in a superconducting tunnel junction with a ferromagnetic insulator barrier.

The tunnel junctions (Fig. 1a) were grown by pulsed laser deposition and consisted of superconducting $La_{1.85}Sr_{0.15}CuO_4$ (LSCO) and Au/Nb/Au electrodes at the bottom and the top of the device. The gold layers were used as oxygen diffusion barriers but were superconducting due to the proximity effect. The tunnel barrier material was $Pr_{0.8}Ca_{0.2}Mn_{0.9}Sc_{0.1}O_3$ (PCMSO), which is a weakly ferromagnetic insulator. The PCMSO layer was doped with Ca to obtain the ferromagnetic insulating phase, while partial Mn substitution by Sc was used to tune the coercivity of the barrier layer and to introduce intentional magnetic disorder. An array of lithographically patterned junctions can be seen in Fig. 1b.

The tunnel junctions showed characteristic step-like

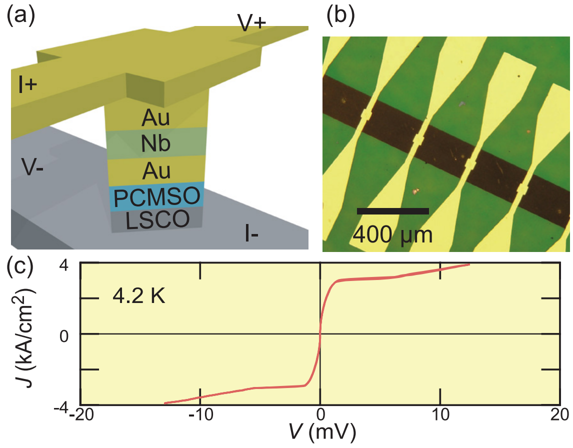

Fig. 1. (a) Schematic view of the $La_{1.85}Sr_{0.15}CuO_4$ (LSCO) / $Pr_{0.8}Ca_{0.2}Mn_{0.9}Sc_{0.1}O_3$ (PCMSO) / Au / Nb / Au junction. (b) Image of a patterned junction array. (c) Current-voltage characteristic of a junction at 4.2 K.

current-voltage characteristics below 6.9 K (Fig. 1c), limited by the superconducting transition temperature of the Au/Nb top electrode. Differential conductance spectra of the junctions showed three characteristic peaks that correspond to various quasi-particle tunneling maxima, as illustrated in Fig. 2. The spectra measured at various temperatures yielded the expected gap values for LSCO (8 to 14 meV) and Au/Nb (1.25 meV) above 4.5 K. Below this temperature, an anomalous increase of the gap energies was observed. This gap energy change was visible as an increase of the normalized critical current, $I_C R_N$ of the devices. Since the contribution of a direct leak between the *s*-wave Nb/Au top electrode and the *d*-wave LSCO bottom electrode is unlikely, we consider the possibility of scattering from magnetic disorder induced in the PCMSO barrier by the Sc doping. Magnetic disorder at a c-axis-oriented cuprate superconductor and a ferromagnet may give rise to spin-triplet supercurrent, effectively increasing the junction critical current.

The devices developed in this work allow us to probe the role of magnetic disorder at superconductor – ferromagnet interfaces, since it is possible to adjust the disorder by suitable level of Sc doping in PCMSO, while the junction characteristics can be probed as a function of an external magnetic field. Our future interest is to discern if singlet

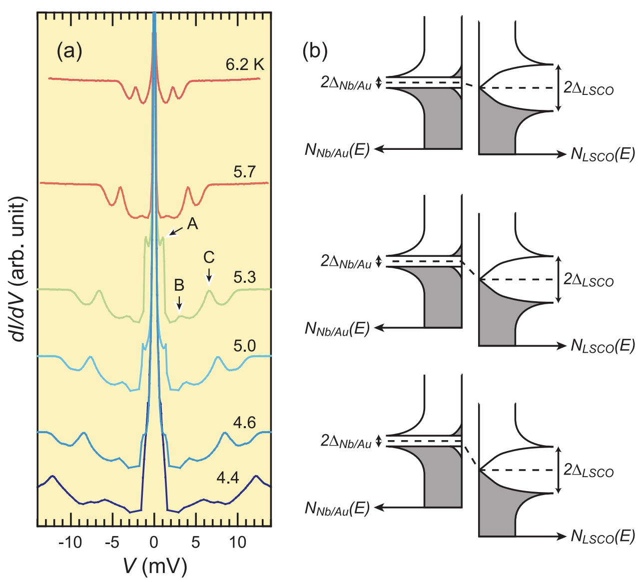

Fig. 2. (a) Differential tunneling spectra at various temperatures and (b) proposed band diagrams explaining the origins of the three peaks, A (top), B (middle), and C (bottom) in the tunneling spectra.

pairs may be stabilized by local antiferromagnetism in the barrier or if scattering into spin-triplet Cooper pairs dominates.

Athors
T. Harada[a], M. Matvejeff[b], R.Takahashi, and M. Lippmaa
[a]Max Planck Institute for Solid State Research
[b]Aalto University

Possible Kondo Physics Near a Metal-Insulator Crossover in the A-site Ordered Perovskite $CaCu_3Ir_4O_{12}$

Uwatoko Group

The interplay between localized and itinerant electrons is at the heart of many intriguing phenomena such as the heavy-fermion behavior and the unconventional superconductivity associated with a magnetic quantum critical point [1]. The archetype systems for studying such interplay are concentrated on the 4*f*/5*f*-based intermetallic compounds, which can be effectively described as a Kondo lattice consisting of a dense periodic array of f electrons interacting with the conduction-band electrons [2]. Here, we reported the realization of an analog d-electron Kondo lattice in a novel *A*-site-ordered perovskite $CaCu_3Ir_4O_{12}$, which can be synthesized only under high-pressure conditions, *e.g.* at 9 GPa and 1250 °C [3].

As shown in Fig. 1(b), the *A*-site-ordered perovskite $CaCu_3B_4O_{12}$ can accommodate the Cu^{2+} and the transition-metal B^{4+} ions, respectively, in the square-planar CuO_4 and octahedral BO_6 units, in which the *d* electrons can be coupled by strong covalent mixing with shared O^{2-} ions. Depending on the B^{4+} ions, the Cu^{2+} 3*d* electrons can be tuned to be either localized or itinerant. A plot of Cu-O versus *B*-O bond length in Fig. 1(a) illustrated that the Cu^{2+} 3*d* electronic states in $CaCu_3Ir_4O_{12}$ is located right at the itinerant-to-localized boundary. In consistent with this observation, the magnetic susceptibility of $CaCu_3Ir_4O_{12}$ shown in Fig. 1(b) demonstrated a crossover from the high-temperature Curie-Weiss (CW) behavior to a low-temperature enhanced Pauli paramagnetism.

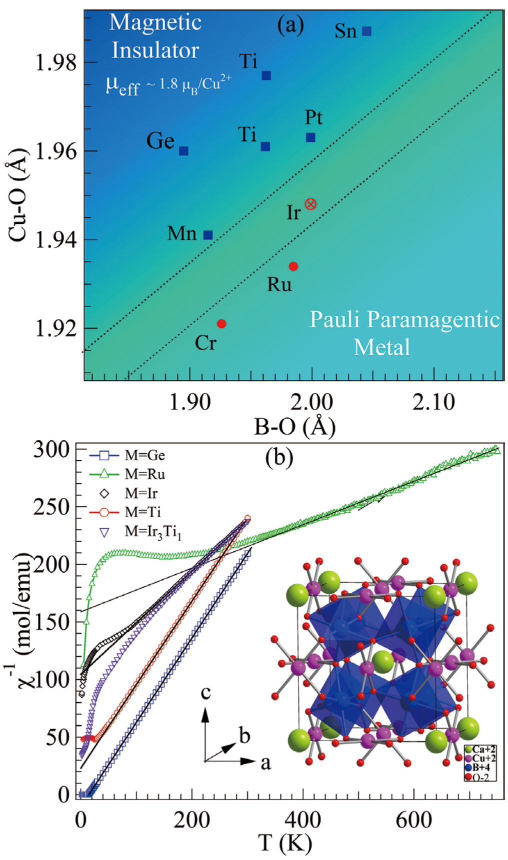

Fig. 1. (a) The Cu-O bond length in the coplanar CuO_4 versus *B*-O bond length in the octahedral BO_6 for *A*-site ordered perovskites $CaCu_3B_4O_{12}$; (b) The inverse magnetic susceptibility of several $CaCu_3B_4O_{12}$ perovskites; inset: schematic crystal structure of the *A*-site ordered perovskite.

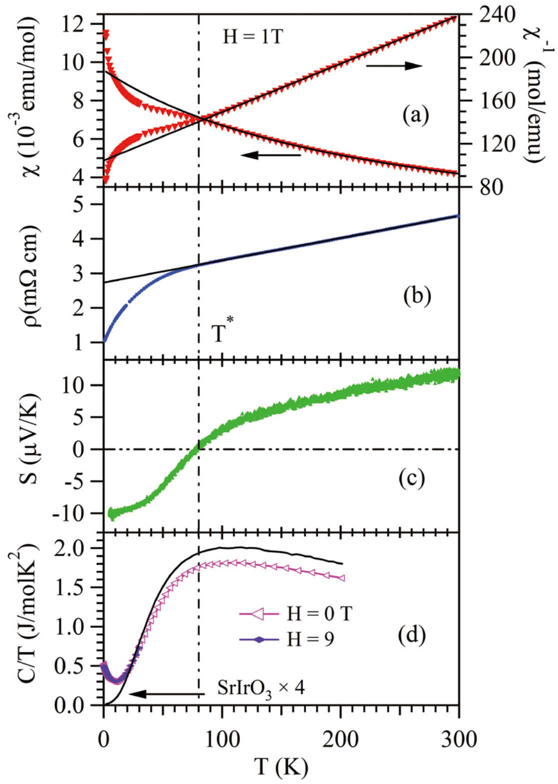

Fig. 2. Temperature dependence of (a) magnetic susceptibility $\chi(T)$ and its inverse χ^{-1}(T) measured under H = 1 T after zero-field cooling, (b) resistivity $\rho(T)$ under H = 0 T, (c) thermopower S(T), and (d) specific heat $C(T)$ under H = 0 and 9 T.

Figure 2 summarizes the physical properties of $CaCu_3Ir_4O_{12}$. The $\chi(T)$ measured at H = 1 T shows no signature of a magnetic ordering transition down to 1.8 K, but a clear deviation from the CW law below $T^* \approx$ 80 K. The susceptibility anomaly below T^* is echoed in $\rho(T)$, and also in the thermoelectric power $S(T)$. Above T^*, $\rho(T)$ follows a perfect linear T-dependence; below T^*, $\rho(T)$ exhibits a strong downward trend with no sign of a curvature change down to 0.5 K, strongly suggestive of non-Fermi-liquid behavior. Significantly, $S(T)$ also behaves anomalously, changing sign at T^* and remaining large as T approaches zero. The large thermoelectric power at low temperatures signals strongly energy-dependent quasiparticle properties. The absence of a corresponding anomaly in the specific heat $C(T)$ rules out the possibility of a second-order phase transition at T^*. Interestingly, C/T of $CaCu_3Ir_4O_{12}$ exhibits a remarkable enhancement below ~ 20 K. The absence of a corresponding enhancement in the closely related $SrIrO_3$ perovskite, which is a Pauli paramagnetic metal, indicates that this low-temperature anomaly must be associated with the Cu^{2+} 3*d* electrons or with interactions between Cu:3*d* and Ir:5*d*.

The presence of a characteristic temperature at T^* = 80

K is reminiscent of the low-temperature behavior in typical heavy-Fermion materials, and is suggestive of Kondo-like hybridization between primarily localized Cu^{2+} 3*d* electrons and the itinerant Ir 5*d* electrons below T^*. In this picture, electrons on the two sublattices are weakly coupled above T^*. The initial reduction in $\chi(T)$ relative to the extrapolated $T > T^*$ CW fit, may signal the onset of hybridization of Cu electrons with the itinerant Ir^{4+} 5*d* electrons. The quick drop of $\rho(T)$ and the sign crossover of $S(T)$ at T^* appear to confirm the emergence of a hybridization between more localized electrons on Cu and more itinerant electrons on Ir. The incorporation of the Cu^{2+} 3*d* electrons into the itinerant bands would not only enhance the density of states, but also reduce the scattering from local magnetic moments. Further evidence for the coherent incorporation of Cu local moments in the Ir bands can be found in the specific-heat measurement, leading to a strong enhanced electronic specific-heat coefficient γ = 173 mJ/mol K^2 for $CaCu_3Ir_4O_{12}$. Our results demonstrated that the *A*-site-ordered perovskites can host a broad spectrum of interesting phenomena that deserve further explorations.

References

[1] O. Stockert and F. Steglich, Annu. Res. Condens. Matter. Phys. **2**, 79 (2011).
[2] Y.-F. Yang, and D. Pines, PNAS **109**, E3060 (2012).
[3] J.-G. Cheng, J.-S. Zhou, Y.-F. Yang, H. D. Zhou, K. Matsubayashi, Y. Uwatoko, A. MacDonald, and J. B. Goodenough, Phys. Rev. Lett. **111**, 176403 (2013).

Authors

J.-G. Cheng, K. Matsubayashi, Y. Uwatoko, J.-S. Zhou[a], A. MacDonald[a], J. B. Goodenough[a], Y.-F. Yang[b], H. D. Zhou[c]
[a]University of Texas at Austin
[b]Institute of Physics Chinese Academy of Sciences
[c]University of Tennessee

Stability of Quantum Hall Ferromagnetic Phase under High Magnetic Fields in the Organic Dirac Fermion System

Osada Group

A layered organic conductor α-(BEDT-TTF)$_2$I$_3$ under high pressure (>1.5 GPa) is a multilayer Dirac fermion system, in which 2D massless Dirac fermion layers stack with weak interlayer coupling, and the Fermi level is fixed at the Dirac point. Such an undoped 2D Dirac fermion system shows the $\nu = 0$ quantum Hall (QH) effect at sufficiently high magnetic fields resulting from the spontaneous symmetry breaking (SSB) of four-fold (spin and valley) degeneracy of the singular $n = 0$ Landau level. Generally, two kinds of the $\nu = 0$ QH state are possible in the Dirac systems (Fig. 1): One is the QH ferromagnet (QHF) state with the metallic helical edge state consisting of a pair of $n = 0$ QH chiral edge states with opposite spin and chirality. The other is the QH insulator (QHI) state with no edge state and some real-space structure. In this way, the high-field ground state is one of the key issues of the physics of the Dirac fermion system.

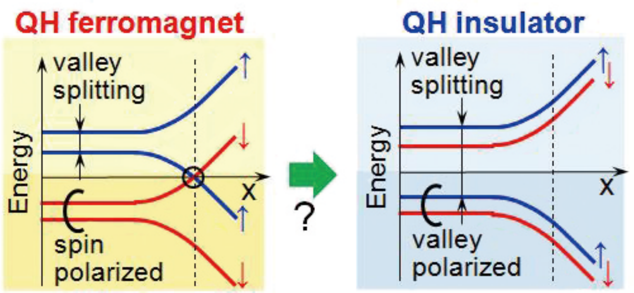

Fig. 1. Schematic energy dispersion of QH edge states in the QHF (left) and QHI (right) states. If the valley splitting becomes larger than the spin splitting in high magnetic fields, the QHF-QHI transition might occur. The helical edge channel (indicated by a circle) in the QHF phase disappears at the QHI phase.

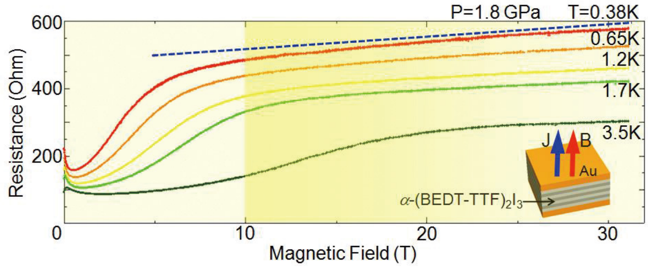

Fig. 2. High-field interlayer magnetoresistance of 2D organic Dirac fermion system α-(BEDT-TTF)$_2$I$_3$. No sign of the QHF-QHI transition was observed.

In graphene, the typical 2D Dirac fermion system, the high-field ground state (the $\nu = 0$ QH state) is believed to be the QHI phase. In contrast, in α-(BEDT-TTF)$_2$I$_3$, the high-field ground state is considered to be the QHF phase. Its interlayer magnetoresistance shows anomalous saturation at high fields. We illustrated that this saturation resistance is scaled not by the sectional area of sample crystals but by sample perimeter. This fact directly means that the metallic surface transport is dominant in the saturating region, and it strongly suggests that the QHF phase with the metallic helical edge state is realized. However, recently, Kanoda *et al.* observed the fine structures of the NMR lineshape at higher fields (B > 15 T), which suggests the appearance of some real-space structure accompanied by the QHI. Their result shows the possibility of transition from the QHF to the QHI in higher field region.

To confirm this possibility experimentally, we performed high-field transport measurement up to 31 T using the National High Magnetic Field Laboratory at Tallahassee, USA. Since no surface transport exists in the QHI phase, rapid increase of the interlayer resistance can be expected at the QHF-QHI transition. As shown in Fig. 2, the interlayer resistance shows increase reflecting the activated bulk transport at low fields, and it switches to weak increase at higher fields up to 31 T. This saturation is caused by the surface transport via helical edge state. We can see no anomaly in the saturating region, especially around 15 T. This result means that the QHF state survives up to 31 T with no QHF-QHI transition suggested by the NMR study.

The pure QHF phase is spatially uniform state. To explain the NMR result, it might be necessary to consider the mixture of spin and valley degree of freedom.

Authors

T. Osada, M. Sato, T. Konoike, and K. Uchida

Parallelizable Multi-Worm Algorithm

Kawashima Group

Massively parallel computations open the door to many otherwise intractable problems in condensed matter physics, in particular, quantum many-body problems. Recent high-performance computers, symbolized by K-computer in Kobe, rely on a large number, as many as a million, of processors (or more precisely "cores"). Therefore, we must split the computational tasks into many bits and assigning each to one of the numerous processors. This is by no means a trivial thing to do. Often we must significantly alter algorithms to split the task in an efficient way. In other words, we must develop new parallelizable algorithms. The quantum Monte Carlo method with the worm update algorithm [1, 2] has a broad range of applicability and is one of the standard tools to treat quantum many-body problems. However, in this algorithm, update of configurations is realized via the motion of a single-point object in the whole space-time (or the lattice), making it hard to split the task.

Based on the directed-loop algorithm [2], one of the variants of the worm algorithm, we proposed a parallelizable worm algorithm, which we named the parallelizable multi-worm algorithm (PMWA). In PMWA, multiple worms are introduced by an artificial source field η and the space-time is decomposed into many domains, as illustrated in Fig. 1. Each domain is assined to a processor and typically contains 10-100 worms. We estimate physical observables by extrapolation to the $\eta = 0$ imit. Introducing multiple worms requires a different procedure from the conventional worm algorithm so as to satisfy the detailed balance condition. The migration of the worms over the domain boundaries is effectively realized through communications between domains so that the ergodicity condition is satisfied. The PMWA is applicable to the soft-core Bosons and the quantum spins as the conventional worm algorithm.

We applied the PMWA to the extended Hard-core Bose-Hubbard model on square lattice defined by

$$H = -t\sum_{\langle ij\rangle} b_i^{+} b_j + V\sum_{\langle ij\rangle} n_i n_j - \mu\sum_i n_i - \eta\sum_i (b_i^{+} + b_i)$$

where b_i is the annihilation operator at site i, t is the hopping energy, V is the nearest neighbor repulsion, and μ is the chemical potential. We established the extrapolation procedure to obtain physical quantities in the $\eta = 0$ limit. Then, we confirmed that the extrapolated PMWA result agreed with the result obtained by the conventional DLA algorithm. Figure 2(a) shows the order parameter of the Bose-Einstein condensate $Q \equiv \langle b \rangle$ as a function of η. Here we carried out simulations of the size of $L \times L \times \beta$ = 10,240×10,240×16 using 3,200 processing cores, where L is the system's linear dimension and β is the inverse temperature. This size exceeds the maximum reachable size of the conventional worm algorithm. To evaluate the parallelization efficiency of the algorithm, we measured the standard error as a function of the number of domains N. We found a very weak N-dependence for the relaxation time in the simulation with fixed number of the Monte Carlo steps (Fig. 2(b)). In addition, in comparison with the conventional DLA results, PMWA results show better accuracy in fixed wall-clock time with N>8 (Fig. 2(c)), and the difference increases as the system becomes larger.

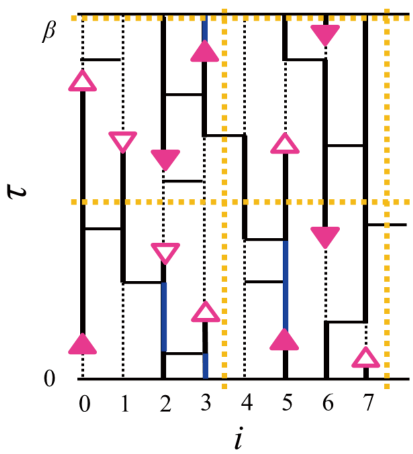

Fig. 1. Worms and worldlines in PMWA. The yellow dashed lines are the domain boundaries.

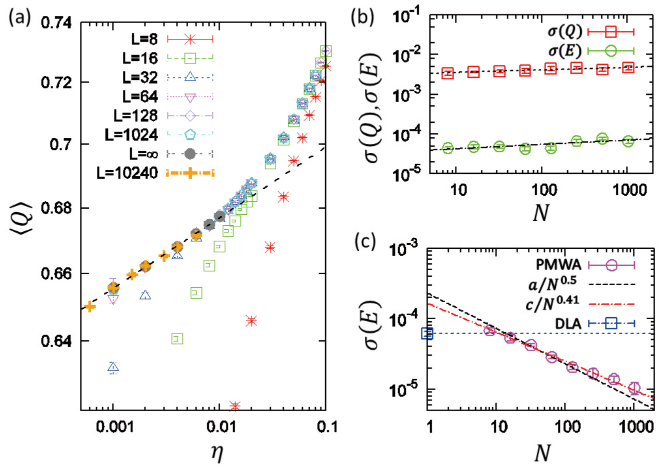

Fig. 2. (a) The order parameter of the Bose-Einstein condensate as a function of η;. (b) The standard error as a function of the number of domains with the fixed number of Monte Carlo steps. (c) The standard error as a function of the number of domains with the computational time (wall-clock time) being fixed.

References

[1] N. Prokof'ev, B. Svistunov, and I. Tupitsyn, Sov. Phys. JETP **87**, 310 (1998) etc.

[2] O. F. Syljuasen and A. W. Sandvik, Phys. Rev. E **66**, 046701 (2012).

[3] A. Masaki-Kato, T. Suzuki, K. Harada, S. Todo, and N. Kawashima, arXiv:1307.0328 (2013), to be published in Phys. Rev. Lett. (2014).

Authors
A. Masaki-Kato, T. Suzuki[a], K. Harada[b], S. Todo, and N. Kawashima
[a]University of Hyogo
[b]Kyoto University

---Neutron Science Laboratory----------------

Dynamic Light Scattering Microscope: Accessing Opaque Samples with High Spatial Resolution

Shibayama Group

Dynamic light scattering (DLS) is a technique for obtaining the size distribution of particles in solution. However, it cannot be applied to opaque samples. There are two types of opaque samples. One is a black sample, which is a strong light-absorbing material such as ink. In this case, scattered light is completely absorbed by the sample itself and one cannot obtain the signal. The other type is milky samples, which are strong light-scattering materials such as milk. In this case, multiple scattering is inevitable. In addition to this, poor spatial resolution sometimes also becomes a problem. There is a growing demand to investi-

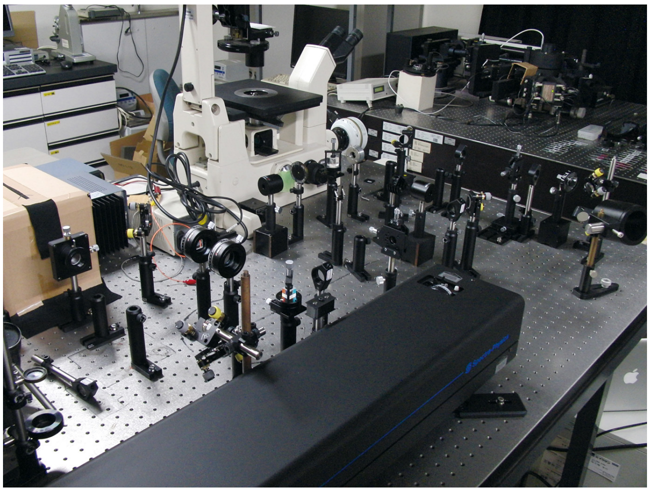

Fig. 1. Photograph of the dynamic light scattering microscope.

gate the dynamic behavior of samples with a higher spatial resolution. One such example is a tracking of material transportation in biological cells. To realize such applications, the spatial resolution needs to be near the diffraction limit. Here, we propose a new DLS technique, "DLS microscope" that mitigates the above-mentioned disadvantages (Fig. 1) [1]. The proposed DLS microscope obtains signals with a backscattering geometry. This enables us to measure opaque samples with high spatial resolution.

By using the DLS microscope, we measured the size distribution of opaque samples such as polystyrene latex and Chinese ink with changing their concentrations. Figure 2 shows the results for the polystyrene latex suspension and Chinese ink. In the case of polystyrene latex suspension, the data show the monodisperse nature. The calculated diameter shows good agreement with the nominal diameter (100 nm). Since the result for the polystyrene latex suspension shows peaks at almost the same position in all concentrations, we can conclude that the polystyrene latex suspension shows no morphology change through varying the concentration. This is consistent with the following molecular interpretation: each particle has a negative charge on the surface, and the particles repel each other keeping their form unchanged and showing Brownian motion. This result corresponds to the result obtained by using diffusing wave spectroscopy [2]. In contrast, the result for Chinese ink seems to show that the average particle size increases and the size distribution broadens at higher concentrations. However, as Chinese ink is a protective colloidal solution, the particles are considered not to aggregate. One of the possible explanations for our result is the existence of attractive interactions between colloidal particles. In other words, colloidal particles show collective motion rather than Brownian motion at higher concentrations. This consideration is supported by the fact that the viscosity of neat ink is approximately five times higher than that of water. Taking advantage of its high spatial resolution, this technique can also be readily applied to other media such as biological cells and gels.

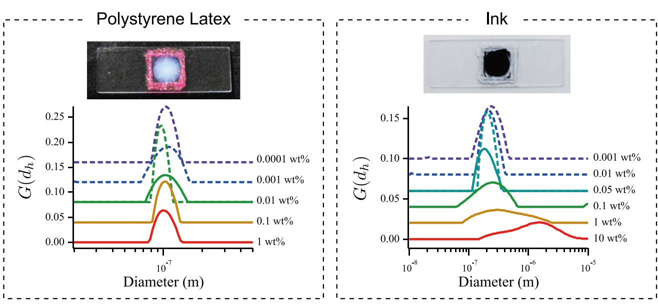

Fig. 2. (Left side) Concentration dependence of the size distribution of a polystyrene latex suspension. The nominal diameter of the polystyrene latex particles is 100 nm. The 1 - 0.01 wt%, as measured by the DLS microscope, is represented by the solid lines. The 0.01 - 0.0001 wt%, as measured by the typical DLS system, is represented by the dashed lines. (Right side) Concentration dependence of the size distribution of Chinese ink. The 10 - 0.05 wt%, as measured by the DLS microscope, is represented by the solid lines. The 0.05 - 0.001 wt%, as measured by the typical DLS system, is represented by the dashed lines.

References

[1] T. Hiroi and M. Shibayama, Opt. Express. **21**, 20260 (2013).
[2] P. Navabpour *et al.*, Colloid Polym. Sci. **283**, 1025 (2005).

Authors
T. Hiroi and M. Shibayama

Magnetic Relaxation in a Tb-based Single Molecule Magnet

Yamamuro Group

A single-molecule magnet (SMM) is a metal complex that behaves as an individual nanomagnet. Each molecule, containing several metal centers with unpaired electrons, possesses a giant resultant spin. Given that the giant spin exhibits easy-axis anisotropy ($D < 0$), the magnetization reversal between the ground states with $S_z = +/-S$ is hindered by the potential barrier of DS_z^2. The traditional research subjects have been SMMs containing multiple transition metal atoms such as Mn, Fe, and Ni, while the current mainstream is shifting to lanthanide SMMs. Owing to a large contribution of angular momentum, lanthanide complexes can become SMMs containing only one or two magnetic ions. One of the central issues in lanthanide SMMs is the quantum tunneling mechanism for the magnetization reversal. In most cases, the tunneling occurs between ground states (pure tunneling process) and/or excited states (thermally assisted tunneling process). The origins of the tunneling have not been fully understood yet.

We have investigated the spin dynamics of Tb-Cu dinuclear SMM by means of neutron scattering techniques. The chemical formula of the sample is $TbCuC_{19}D_{20}N_3O_{16}$ and its molecular structure is schematically shown in the

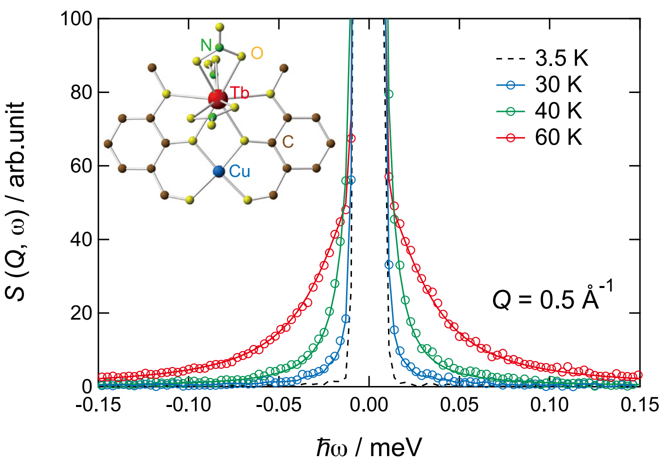

Fig. 1. Dynamic structure factors of TbCu-SMM. The data at 3.5 K represent the resolution function. The other data are fitted to the combination of delta and Lorentz functions. The inset shows the molecular structure of TbCu-SMM.

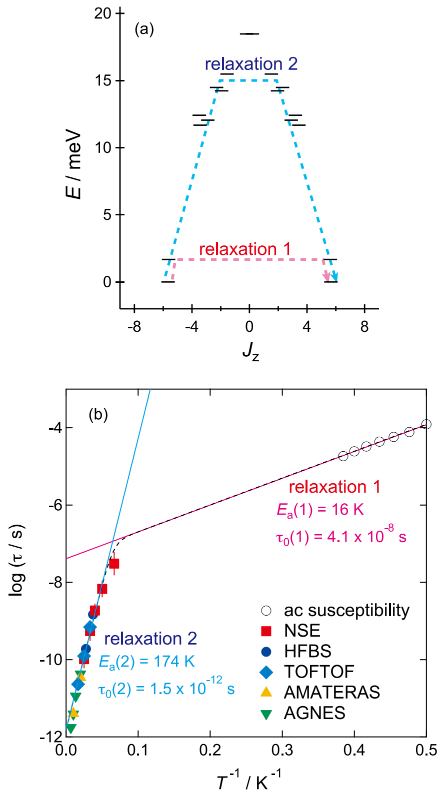

Fig. 2. (a) Calculated energy diagram as a function of z-component of the total angular momentum of Tb ion. Dashed lines represent possible relaxation processes. (b) Arrhenius plot of the relaxation times observed on the five spectrometers. The results from the ac susceptibility measurements are also shown.

inset of Fig.1. In order to reduce the contribution from the strong incoherent scattering of H atoms, the sample was fully deuterated. Only two magnetic ions, Tb^{3+}(J = 6) and Cu^{2+}(S = 1/2), are involved in a molecule. Following inelastic neutron scattering studies to determine the energy scheme [1], we investigated the magnetic relaxation by means of quasielastic neutron scattering (QENS) experiments using various spectrometers with different energy resolutions; AGNES (ΔE = 49 μeV) at JRR-3, AMATERAS (ΔE = 120 μeV) at J-PARC, TOFTOF (ΔE = 8 μeV) at FRM II (Germany), HFBS (ΔE = 0.8 μeV) and neutron spin-echo NSE (Fourier time, $0.007 < t < 12$ ns) at NCNR (USA) [2]. The use of five spectrometers enables us to investigate relaxations over a wide time range between 1 ps and 100 ns.

Figure 1 shows the dynamic structure factors of Tb-Cu SMM at Q = 0.5Å^{-1} taken on the TOFTOF spectrometer. Clearly, QENS broadening was observed above 30 K. The QENS spectra were well fitted to the combination of delta and Lorentz functions. The linewidth of the Lorentzian, Γ(Q), exhibits no pronounced Q-dependence, indicating that the relaxation is of a local origin. The relaxation times were obtained from the relation $\tau = 1/\Gamma$. In Fig. 2(b), we show the Arrhenius plot of relaxation times estimated from the QENS together with those from the ac magnetic susceptibility measurements. This provides a clear evidence of the existence of two distinct relaxation processes. We designate the slower relaxation as the relaxation 1 and the faster one as relaxation 2. Both relaxation processes follow the Arrhenius relation $\tau = \tau_0 \exp(\Delta E_a/k_B T)$. As for the relaxation 1, the activation energy E_a and prefactor τ_0 are estimated to be 16.0 K and 4.1×10^{-8} s, respectively. It should be emphasized that E_a corresponds to the excitation energy of 1.7 meV observed in the INS study [1]. We have calculated an energy diagram as a function of the z-component of the total angular momentum of the Tb ion, J_z (see Fig. 2(a)), assuming the spin Hamiltonian including ligand field anisotropy, exchange interaction between Tb^{3+} and Cu^{2+}, and hyperfine interaction. The excitation of 1.7 meV is the transition between the ground and the first excited states. We thus conclude that the magnetization reversal occurs through quantum tunneling between the pairs of degenerated excited states at 1.7 meV. This is called thermally activated tunneling process, in other words the Orbach mechanism of spin-lattice relaxation. On the other hand, the relaxation 2 detected by QENS has quite different E_a and τ_0; $E_a(2)$ = 174 K and $\tau_0(2) = 1.5 \times 10^{-12}$ s. The relaxation 2 is also of the Debye type and gets activated upon heating according to the Arrhenius law. The simplest scenario for the origin of the relaxation 2 is that the relaxation 2 takes place through the tunneling between higher excited states. The activation energy of 174 K (= 15 meV) roughly corresponds to the higher energy level as seen in the energy diagram in Fig. 2(a).

This is the first successful QENS work to observe magnetic relaxation in SMM. The use of QENS can open a new window into the study of relaxation processes in the class of SMMs.

References

[1] M. Kofu, O. Yamamuro, T. Kajiwara, Y. Yoshimura, M. Nakano, K. Nakajima, S. Ohira-Kawamura, T. Kikuchi, and Y. Inamura, Phys. Rev. B **88**, 064405 (2013).
[2] M. Kofu, T. Kajiwara, J. S. Gardner, G. G. Simeoni, M. Tyagi, A. Faraone, K. Nakajima, S. Ohira-Kawamura, M. Nakano, and O. Yamamuro, Chem. Phys. **427**, 147 (2013).

Authors
M. Kofu, T. Kajiwara[a], G. G. Simeoni[b], and O. Yamamuro
[a]Nara Women's University
[b]Technical University of Munich

Nano-magnetism in Relaxor Magnet $LuFeCoO_4$

Masuda Group

Dielectric property exhibiting an enhanced permittivity in wide temperature range is known as relaxor ferroelectricity and it has attracted great interest in the field of basic and applied physics. In the relaxor system Polar Nanoregions (PNRs), where coherent polarizations in nano-scale domains are randomly oriented in the bulk crystal, play important role. So far disordered perovskite oxides such as $Pb(Mg_{1/3}Nb_{2/3})O_3$, $Pb(Sc_{1/2}Ta_{1/2})O_3$, etc., have been extensively studied [1] and all of them are purely dielectric and non-magnetic. Here natural question arises: what would happen if the relaxor system contains magnetic ions? One of our group members answered to the question in his pioneering work on a relaxor magnet, $2/3BiFeO_3$-$1/3BaTiO_3$ [2]; appearance of a new type of nano-magnetism where superparamagnetic moments are induced limitedly inside the PNRs. For further understanding of relaxor magnets we study a new compound $LuFeCoO_4$ by combination of bulk properties measurements and neutron diffraction technique. Our study reveals the relationship between PNRs and magnetic correlation, and establishes the magnetic and dielectric phase diagrams of the relaxor magnet as shown in Fig. 1(a) [3].

$LuFeCoO_4$ is a two-dimensional (2D) triangular spin

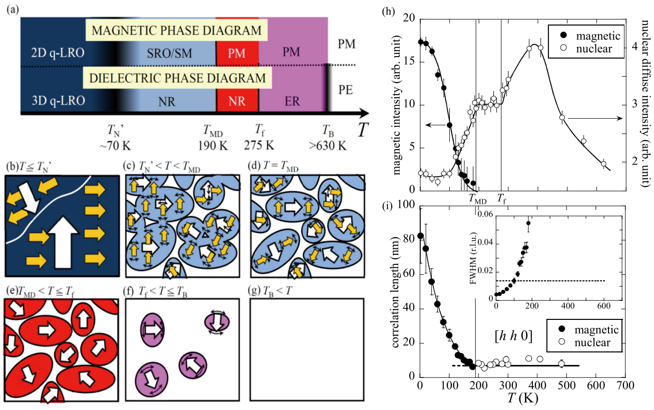

Fig. 1. (a) Magnetic phase diagram (upper panel) and dielectric phase diagram (lower panel). PM, SM, NR, ER, and PE mean paramagnetism, superparamagnetism, nonergodic relaxor, ergodic relaxor, and paraelectric, respectively. (b)-(g) The relationship between PNR and magnetic correlation at various temperatures. White arrows are electric polarization and yellow arrow are weak-ferromagnetic moments. (h) Temperature dependence of magnetic and nuclear diffuse intensities. (i) The temperature dependencies of magnetic and nuclear correlations.

system where Fe^{3+} and Co^{2+} ions are randomly positioned on the vertices of the triangles. Temperature dependence of the permittivity constant showed a typical behavior of a conventional relaxor. The result suggested the existence of PNRs and it is supported by neutron diffuse scattering. Magnetic susceptibility showed a weak-ferromagnetic component and magnetization showed superparamagnetic behavior at T < 190 K. With further decreasing the temperature the susceptibility showed a well-defined anomaly at 70 K and the magnetization showed hysteretic behavior at the base temperature, indicating a realization of magnetic order with a weak-ferromagnetic component.

The nuclear scattering results at T > 190 K in Fig. 1(h) show typical behavior of relaxor systems. At 190 K < T < 275 K, the PNRs are freezed and static. With decreasing the temperature at T = 190 K the nuclear diffuse intensity begins to decrease and simultaneously the magnetic peak appears. These results mean that the size of the PNRs increases and, synchronizedly, magnetic correlation develops. The magnetic correlation length at 190 K is 7 nm and it is the same as that of nuclear scattering as shown in Fig. 1(i).

Based on the bulk property measurements and neutron diffraction experiments, we propose a superparamagnetic model that a weak ferromagnetic correlation is, in the temperature range of 190 K < T, developed in the crystallographic c plane inside the PNRs as schematized in Fig. 1(d). Outside the PNRs the nuclear correlation is incoherent and so is the magnetic correlation. Spin moments in the PNRs behave as superparamagnetic moments and those outside the PNRs do as conventional paramagnetic spins. At the temperature T_{MD} ~ 190 K the magnetic correlation achieves long-ranged inside the PNRs. With decreasing the temperature the domain size of PNR increases and consequently the accompanied magnetic domain increases as described in Fig. 1(c). At the $T_{N'}$ = 70 K a magnetic correlation in 2D and dielectric correlation in 3D are both in quasi-long-range order as schematized in Fig. 1(b). Meanwhile at $T \geq T_{MD}$ the magnetic order is absent as shown in Figs. 1(e)-(g). The proposed model consistently explains both bulk properties and neutron scattering results.

References

[1] A.A. Bokov and Z.-G. Ye, J. Mater. Sci. **41**, 31 (2006).
[2] M. Soda *et al.*, J. Phys. Soc. Jpn. **80**, 043705 (2011).
[3] M. Soda *et al.*, submitted to Phys Rev. B.

3D Liner Imploding Process in the Electro-Magnetic Flux Compression

Takeyama Group

The electromagnetic flux compression (EMFC) technique in ISSP has been established to generate magnetic fields up to 730 T [1], which is the world strongest magnetic field in an indoor experiment. There, a metallic cylinder called the "liner" is subjected to the inductive electromagnetic force from a primary coil, and the initial magnetic field (~4 T) is compressed by an imploding liner within a few microseconds before the magnet destruction. Owing to the high reproducibility in its operation of the EMFC technique, solid-state physics experiments are nowadays available in ultra-high magnetic fields of up to 700 T at room temperature and up to 600 T at temperatures as low as 5 K. For solid-state physics experiments performed under ultra-high magnetic fields, the particularly important issues are (a) high precision of the magnetic field intensity, (b) the spatial uniformity of the magnetic field, and (c) appropriate bore at a peak magnetic field. For issue (a), the magnetic field intensity was recently verified to have a precision of 3 % up to 500 T, by calibrating with the Faraday rotation measurement on optical glasses [2]. For issues (b) and (c), detailed knowledge of dynamical magnetic-flux compression processes is required, for which computer simulation can be a powerful tool. Thus, we clarified the relationship between the liner's imploding process and the spatiotemporal distribution of the magnetic field intensity, by comparing with the simulation [3].

In Fig. 1(a), the solid curve is the magnetic field intensity curve (hereafter termed as the B-t curve) at z = 0. We adopted the liner of 50 mm length (L_{lin}, illustrated in the inset) and of 1.5 mm thickness. A multi-probe with an eight pick-up coils were set along the magnetic field axis (defined as the z-axis) at the center of the imploding liner, and the spatial distribution of the magnetic field intensity was simultaneously measured in a single shot The magnetic field's profile in the z direction, $B(z)$, was shown in Fig. 1(b). The field homogeneity was thus successfully determined for the first time in the EMFC experiment. Up to 500 T, the field homogeneity was estimated as good as the measurement error (~3 %) at z = ±1 mm, which has proven to be sufficiently good for the general solid-state physics measurements.

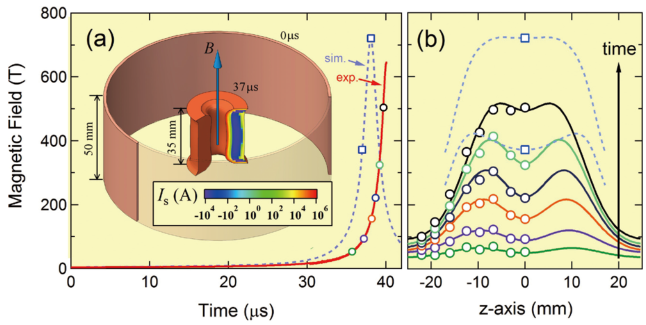

Fig. 1. (a) Magnetic field curves of the experiment (the solid curve, L_{lin} = 50 mm) and the simulation (the dashed curve, L_{lin} = 35 mm). The inset illustrates the liner's shape. For t = 0 μs, we show the liner used in the experiment (L_{lin} = 50 mm). For t = 37 μs, the simulated imploding liner in case of L_{lin} = 35 mm deforms into a barrel-like shape. The color map indicates the secondary current intensity, I_s, induced in the liner. (b) Spatial profiles of magnetic field intensity along the magnetic field axis at each time, which corresponds with the open symbols in (a). The solid-curves are the fitting of two Gaussian functions for the experimental data, and the dashed curves are the simulated spatial profiles in case of L_{lin} = 35 mm.

Two-hump structure of $B(z)$ in Fig. 1(b) is hardly explained by the mesh modeling of liner's dynamics developed by Miura and Nakao [4]. In Ref. 4, the liner's thickness was assumed to keep uniform along the z direction during the implosion. However, their model is far from accuracy in describing the real situation and is oversimplified. Therefore, we revised the simulation by independently calculating the dynamics of the liner mesh with its respective z coordinate, which allows us to obtain a nonuniform liner deformation.

The dashed curves in Figs. 1(a) and 1(b) are the simulation result in case of L_{lin} = 35 mm. The length of the primary coil (L_{pri}) is set to be 45 mm. The simulated liner's shape at 37 μs is illustrated in the inset of Fig. 1(a), and the color map indicates the secondary current intensity, I_s, induced in the liner. The barrel-like deformation of liner's inner wall shown in Fig. 1(a) induces the two hump structure of $B(z)$ in Fig. 1(b). Note that the liner's barrel-like deformation only takes place when $L_{lin} < L_{pri}$, whereas L_{lin} (50 mm) > L_{pri} (45 mm) at t = 0 μs in the real experiment. This fact implies a three-dimensional implosion process associated with a compression of the liner along the z-axis. The present work has pointed out that a three-dimensional analysis of an imploding liner is of particular importance for further record-breaking higher magnetic field in the EMFC, and for an increased controllability as well as a higher precision in the solid-state physics measurements.

References

[1] S. Takeyama and E. Kojima, J. Phys. D: Appl. Phys. **44**, 425003 (2011).
[2] D. Nakamura *et al.*, Rev. Sci. Instrum. **84**, 044702 (2013).
[3] D. Nakamura, H. Sawabe and S. Takeyama, Rev. Sci. Instrum. **85**, 036102 (2014).
[4] N. Miura and K. Nakao, Jpn. J. Appl. Phys. **29**, 1580 (1990).

Authors
D. Nakamura and S. Takeyama

Heat Pulse Measurements of Specific Heat in Pulsed Magnetic Fields

Kindo Group

Measurements of the specific heat (C_p) in magnetic fields have been widely used to investigate fundamental properties of a material. Although several attempts to provide specific heat data at high magnetic field have been made, experiments in pulsed magnets are subject to strong constrains that arise from the short timescale of the measurements. Therefore, calorimetric studies have all been limited to the magnetic field range accessible to continuous magnets (dc magnets), with very few exceptions of pulsed magnets having an unusually long (>250 ms) pulse field duration [1,2]. In this context, we have developed, for the first time, a calorimeter that can operate in short pulse duration of less than 50 ms [3].

We attempt to obtain a quick thermal response by reducing the physical size of the calorimeter. Our calorimeter consists of a $Au_{16}Ge_{84}$ thin-film thermometer, a $Ni_{50}Cr_{50}$ thin-film heater, 100 μm diameter Constantan relaxation wires, and a quartz thermal bath. The eliminations of a bulk thermometer and a bulk heater lead to a quick monitoring of the temperature and enable us to study thermodynamic properties, such as C_p and magnetocaloric effect (MCE), in

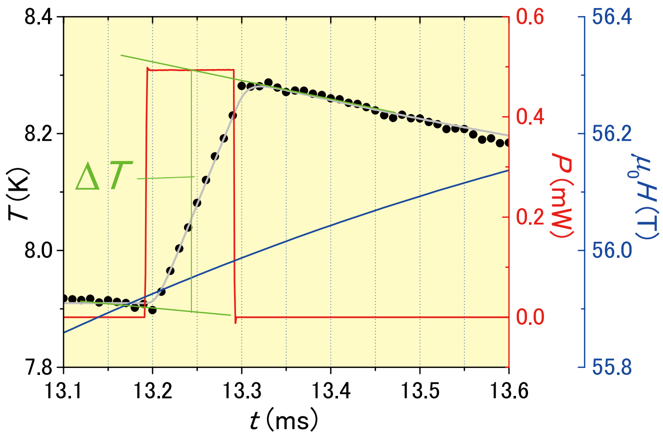

Fig. 1. Time dependence of the temperature (black dots), the power of the heat pulse (red), and the field profile (blue) during the 36 ms pulsed magnetic field. Gray curve represents a fit obtained with a simple heat equation.

the 36 ms pulsed magnet that is commonly used to reach fields above 50 T. As a test of our thin-film based calorimeter, we have measured the C_p of slab-shaped $Cu_3Mo_2O_9$ single crystalline samples (0.10 mg (sample 1) and 0.0285 mg (sample 2)) between 3 and 20 K in pulsed magnetic fields up to ~56 T.

Figure 1 shows the time dependence of sample temperature (black curve) during a specific heat measurement in the presence of 56 T pulsed magnetic fields. During the application of square heat pulse (red curve), the sample temperature linearly increased, and immediately after the heat pulse a clear step in temperature was observed. The short time scale of measurement (~0.5 ms) significantly reduces the uncertainty in magnetic field (blue curve); 0.2% of the applied field (56.0 ± 0.1 T) for observing a single temperature step. Since the step-like temperature change is the ideal situation for the heat pulse calorimetry, the change of the temperature (ΔT) can be estimated by the linear extrapolation (green lines in Fig. 1(a)), and the ΔQ is obtained by integrating the $P(t)$ curve. The molar specific heat was calculated by $C_p = \Delta Q \Delta T^{-1} m^{-1} M$, where m and M are the sample mass and the molar weight, respectively, and its temperature dependence was plotted in Fig. 2.

Figure 2 shows the $C_p(T)$ of sample 1 (black dots) and sample 2 (blue crosses) in various magnetic fields are shown together with PPMS data measured at 0, 7 and 13 T. $C_p(T)$

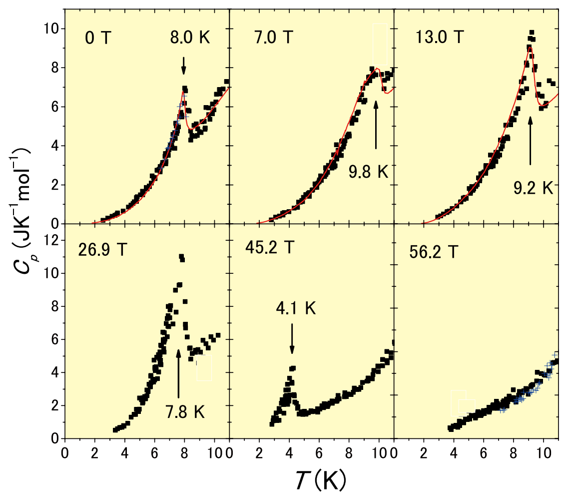

Fig. 2. A comparison of the specific heat data from the heat-pulse calorimeter (sample 1; black squares and sample 2; blue crosses) with those from the PPMS (red curves) near the phase transition in $Cu_3Mo_2O_9$. Arrows indicates the peak temperature in specific heat.

show λ-type pronounced peak and its peak temperature and the size of the anomaly varies as the applied magnetic field changes. Although the point-to-point scatter obtained from the present set-up is more than that of PPMS (red curve), the over-all temperature dependence of C_p, including the peak shape and its absolute value, agree well with the data measured in PPMS. We estimate that the absolute accuracy of the measurement is better than ±10% for temperature range from 3 to 20 K. The quantitative agreement between two sets of data shows that the experiment we are doing in pulsed field is the same as the experiments we have been doing in dc fields. The resultant $C_p(T)$ data can be analyzed in the conventional way to determine the entropy, specific heat exponent, and possibly the order of the phase transition.

We have developed an effective calorimeter for use in a pulsed magnetic field up to ~56 T and tested their performance with $Cu_3Mo_2O_9$ single crystalline samples. For $Cu_3Mo_2O_9$, this system exhibits an overall accuracy of better than ±10% for entire temperatures range of 3 to 20 K. This technique is now open to users of International Megagauss Science Laboratory.

References
[1] M. Jaime *et al.*, Nature **405**, 160 (2000).
[2] Y. Kohama, C. Marcenat, T. Klein, and M. Jaime, Rev. Sci. Instrum. **81**, 104902 (2010).
[3] Y. Kohama, Y. Hashimoto, S. Katsumoto, M. Tokunaga, and K. Kindo, Meas. Sci. Technol. **24**, 11505 (2013). (IOP select)

Authors
Y. Kohama, Y. Hashimoto, S. Katsumoto, M. Tokunaga, and K. Kindo

Electronic Phase Transitions of Graphite in the Quasi-Quantum Limit State

Tokunaga and Kindo Groups

The quantum limit state, where all carriers populate the lowest Landau level, exhibits various anomalous phenomena because of the strong correlation acting on the carriers confined by magnetic fields. This state can be realized only in extremely high magnetic fields, the order of 10^4 T, in ordinary metals.

Graphite is a semimetal having a small number of electrons and holes (~ 3 × 10^{18} cm^{-3} for each) and goes into the quasi-quantum limit state, where only the lowest electron-like (Landau index n = 0, spin ↑ and ↓) and hole-like (n = –1, ↑ and ↓) subbands are populated in magnetic fields above 7.4 T applied along the *c*-axis. With further increasing the field, emergence and collapse of a density wave state has been claimed through measurements of in-plane (ρ_{xx}) and out-of-plane (ρ_{zz}) resistivity [1]. In addition, recent magnetoresistance measurements up to 80 T suggested emergence and collapse of another density wave state at 53 T and 75 T, respectively [2]. The actual nesting vector in these density wave states and also the underlying structure of the subbands, however, remain unclear as yet because of the limited experimental technique available above 25 T.

We studied Hall resistivity (ρ_{xy}) and magnetization of graphite single crystals in pulsed high magnetic fields [3]. As the main feature of the results, the ρ_{xy} becomes almost zero as the field approaches 53 T, where ρ_{xx} and ρ_{zz} show anomalies as shown in Fig. 1. In the microscopic point of view, the Hall resistance is given by summation of the matrix elements of the current operator between the states having different Landau indices Δn = 1 and, hence, sensitive to the whole dispersion curves of the relevant subbands. The almost zero Hall resistance seems consistent with the existence of two populated subbands (n = 0↓ and n = –1↑) [1] rather than the less-symmetric three subband model (n = 0↑ , n = 0↓ and n = –1↑) [2]. Thereby, the quantum limit state likely emerges above 53 T. In this quantum limit state, density wave can be formed by the nesting between the Fermi points of the n = 0↓ and n = –1↑ subbands, which is equivalent to the BCS-like pairing state of excitons. Further studies are needed to clarify the nature of the additional phase transition at 75 T in this quantum limit state.

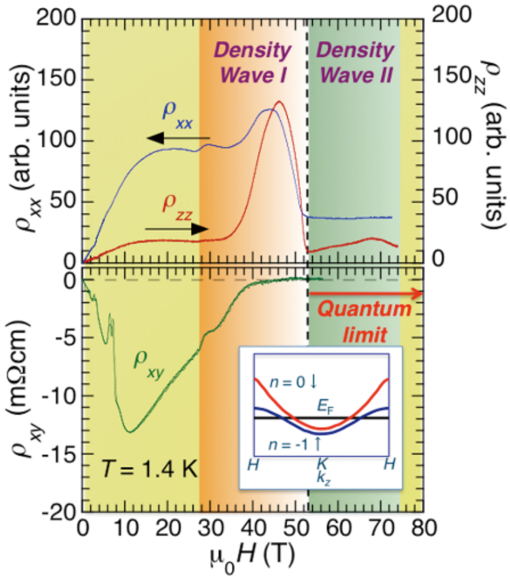

Fig. 1. (upper) In-plane (ρ_{xx}) and out-of-plane (ρ_{zz}) resistivity of graphite single crystals as a function of magnetic field applied along the c-axis at temperature of 1.4 K. (lower) Magnetic field dependence of in-plane Hall resistivity (ρ_{xy}) of graphite at 1.4 K. The colored areas represent different electronic phases suggested by transport measurements. The inset of the lower panel shows schematic illustration of the dispersion curves of the populated subbands above 53 T.

References
[1] H. Yaguchi and J. Singleton, J. Phys.: Condens. Matter **21**, 344207 (2009).
[2] B. Fauqué *et al.,* Phys. Rev. Lett. **110**, 266601 (2013).
[3] K. Akiba *et al.*, submitted to J. Phys. Soc. Jpn.

Authors
K. Akiba, A. Miyake, H. Yaguchi[a], A. Matsuo, K. Kindo, and M. Tokunaga
[a]Tokyo University of Science

---Laser and Synchrotron Research Center/ Synchrotron Radiation Laboratory-----------

Ultrafast Photo-Induced Transition of an Insulating VO_2 Thin Film into a Non-Rutile Metallic State

Shin Group

Vanadium dioxide (VO_2) is an exemplary strongly correlated material known for its dramatic insulator-to-metal transition around room temperature (Fig. 1(a)). The phase transition can also be triggered by external stimuli such as electric gating and light irradiation. VO_2 thus provides an interesting platform for novel functionalities. By using time-

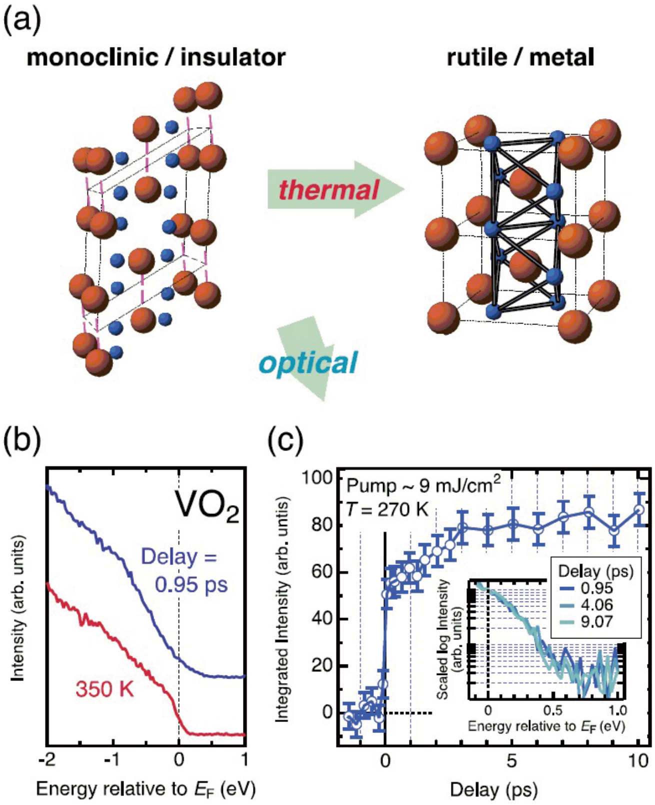

Fig. 1. Insulator-to-metal transition of VO_2. (a) Structural change from monoclinic insulating phase to rutile metal phase upon the thermal transition. (b) Time-resolve spectrum at delay = 0.95 ps (F ~ 9 mJ/cm^2, 270 K) compared with a static photoemission spectrum of a rutile metallic state recorded at 350 K. (c) Time evolution of spectral weight over [-0.2, 0.2 eV]. The inset shows the unoccupied side of the spectra for delay = 0.95, 4.05, 9.07 ps in the logarithmic scale.

resolved photoemission spectroscopy (TrPES) implemented by a high-harmonic generation method, we investigated the ultrafast photo-induced transition of VO_2, and provide insights into the non-equilibrium dynamics governed by strong correlations.

The valence-band spectrum of a VO_2 thin film was monitored in a pump-and-probe TrPES configuration. A metallic state emerged when the sample was impinged by a 170-fs pulse above a critical fluence F = 6 mJ/cm^2, which was directly evidenced by the ultrafast increase of the spectral weight at the Fermi level (E_F). The transition was accompanied by a spectral-weight transfer on a 1-eV scale characteristic of strong electron correlations. The photo-induced metallic state exhibited a unique spectrum that tails up to ~0.4 eV above E_F. This indicates that the emergent metallic state is different from the rutile state (Fig. 1(b)). After the impulsive impact, the spectral weight at E_F further increased until ~3 ps (Fig. 1(c), inset), indicating that the metallic state grew proliferatively. The ~0.4-eV tail also persisted for > 3 ps, the behavior of which cannot be explained by the photo-response of typical Mott insulators that relaxes within ~1 ps. These observations emphasize the importance of non-electronic degrees of freedom in the photo-induced dynamics of VO_2.

Reference

[1] R. Yoshida, T. Yamamoto, Y. Ishida, H. Nagao, T. Otsuka, K. Saeki, Y. Muraoka, R. Eguchi, K. Ishizaka, T. Kiss, S. Watanabe, T. Kanai, J. Itatani, and S. Shin, Phys. Rev. B **89**, 205114 (2014).

Authors

R. Yoshida, T. Yamamoto, Y. Ishida, H. Nagao[a], T. Otsuka[a], K. Saeki[a], Y. Muraoka[a], R. Eguchi[a], K. Ishizaka, T. Kiss, S. Watanabe, T. Kanai, J. Itatani, and S. Shin

[a]Okayama University

Development of the Polarization Control Segmented Cross Undulator at SPring-8 BL07LSU

I. Matsuda, Harada, and Shin Groups

Synchrotron-based soft X-ray spectroscopy has proven to be a powerful experimental technique for studying the atomic, molecular and electronic structures of materials. The energy range of soft X-rays covers the *K*-edge absorption of the most abundant elements on Earth (*e.g.* C, N, O, Si) and the *L*-edge absorption of the industrially important transition metals (Ti, V, Cr, Mn, Fe, Co, Ni, Cu and Zn). Soft X-ray spectroscopy has many unique characteristics, such as element specificity, chemical specificity and surface sensitivity. Furthermore, responses of a matter with different light polarization determine orbitals of the electronic states in solids, configurations of molecules on a surface, and spin/orbital magnetic moments of magnetic atoms. These properties make them versatile for application in a wide range of scientific fields including surface chemistry, environmental science and magnetism. Therefore, developments of polarization control soft X-ray sources have been one of the significant issues in condensed matter physics.

Recently, we have constructed a new soft X-ray beamline, BL07LSU, at SPring-8 to perform advanced soft X-ray spectroscopy for materials science. To realize the state-of-the-art performance, a novel segmented cross undulator (SCU) was developed and adopted as a soft X-ray light source. Figure 1 shows schematic drawing and photograph of the SCU. It consists of eight undulator segments and seven phase shifters (PS), and its total length is 27 m. Four segments generate horizontally linearly polarized radiation at the fundamental radiation (Figure-8 undulator), and the other four segments generate vertically linearly polarized radiation (Figure-∞ undulator). The horizontal and vertical undulator segments are placed alternately. Circular or tilted linearly polarized light can be obtained by superposing horizontally and vertically linearly polarized radiation, and the helicity of the circularly polarized radiation, for example, can be changed by the PSs. The PSs adjust the relative phase of the undulator radiation emitted from each segment by changing the path length of the electron orbit between segments with a local orbit bump. Linear polarization, P_L, and circular polarization, P_C, are evaluated by the rotating analyzer ellipsometry using the multilayer mirrors. The degrees of linear polarization (P_L) from four horizontal or four vertical segments are both 1.00. The degree of circular polarization (P_C) from four horizontal and four vertical

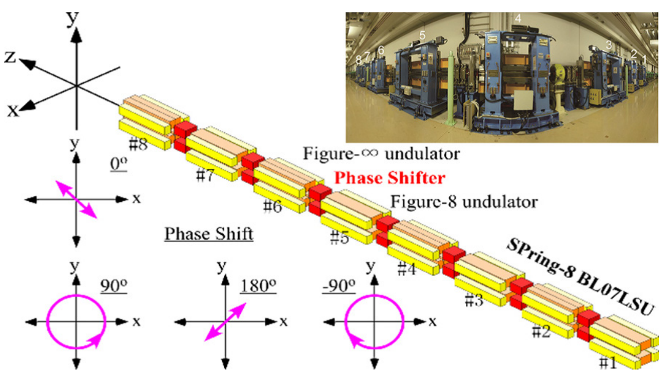

Fig. 1. Schematic and photograph of a novel segmented cross undulator at SPring-8 BL07LSU that generates polarization controlled soft X-ray.

segments are - 0.94 and 0.93 for left- and right-handed circularly polarized light, respectively.

The degree of polarization at SPring-8 BL07LSU is high enough to perform various soft X-ray spectroscopy using light polarization, such near-edge X-ray fine structure, X-ray magnetic circular dichroism, X-ray magneto-optical Kerr effect, and resonant soft X-ray diffraction. Moreover, the beamline optics and the experimental stations allow users to carry out the experiments also at small region (70 nm), with time resolutions (50 ps), and with high energy resolution (> 10,000).

Reference

[1] S. Yamamoto, Y. Senba, T. Tanaka, H. Ohashi, T. Hirono, H. Kimura, M. Fujisawa, J. Miyawaki, A. Harasawa, T. Seike, S. Takahashi, N. Nariyama, T. Matsushita, M. Takeuchi, T. Ohata, Y. Furukawa, K. Takeshita, S. Goto, Y. Harada, S. Shin, H. Kitamura, A. Kakizaki, M. Oshima, and I. Matsuda, Journal of Synchrotron Radiation **21**, 352 (2014).

Authors
I. Matsuda, S. Yamamoto, Y. Harada, and S. Shin

Discovery of a Giant Kerr Rotation in a Ferromagnetic Transition Metal by M-edge Resonant Magneto-Optic Kerr Effect

I. Matsuda and Shin Groups

Magneto-optical effects are one of the central topics in condensed matter physics. The effects have been used to study magnetism and spin transport in materials. Many experiments with the magneto-optical Kerr effect (MOKE) have been performed using linearly polarized laser light of a single wavelength typically in the visible region. Recently, there has been remarkable progress in new-generation light sources, such as the X-ray free-electron laser (FEL) and the high-harmonic generation (HHG) laser. These new monochromatic lasers have ultra-short pulse widths and tunable photon energies ranging from the extended violet to the X-ray region. Thus, MOKE measurements with photon energy tuned at the absorption edge (so-called resonant MOKE or RMOKE) are of considerable interest. Measurements with the new-generation light sources are expected to be element-specific and to trace spin dynamics in real time via time-resolved measurements.

In the present research, we have studied the Kerr rotation angle and ellipticity in the RMOKE at photon energies corresponding to the M-shell absorption edge of transition metal. We investigated the RMOKE in the well-known nickel film both theoretically and experimentally. The simulation was carried out with resonant scattering theory based on the Kramers-Heisenberg formula. The predicted Kerr rotation angle indicated a large MOKE (> 10°). Then, the large Kerr rotation angle was confirmed by rotating analyzer ellipsometry using vacuum ultraviolet (VUV) synchrotron radiation at KEK PF BL-18A. Figure 1 compares experimentally measured and calculated variations of θ_k with photon energy. The experiment reproduced large θ_k values (~10 degree) at the absorption edge: the overall features are in good agreement with the calculations, where the model parameter set has been independently determined with other core-level spectroscopies.

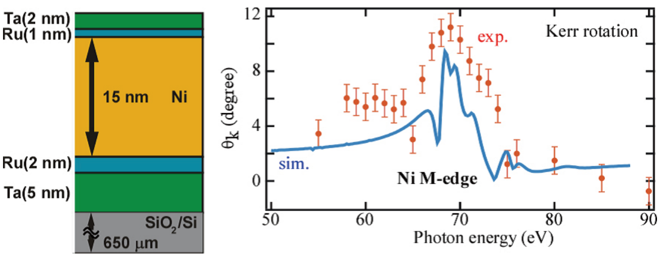

Fig. 1. Photon energy dependence of the Kerr rotation angle, θ_k, of the Ni film calculated with the resonant scattering theory (sim.) and measured experimentally with VUV synchrotron radiation (exp.). Measurement was performed at room temperature under a magnetic field of B = ± 0.47 T.

Since the RMOKE measurement is inherently element specific and is a photon-in and photon-out experiment, it is able to probe spin states of selected elements in complicated magnetic materials under external electromagnetic fields. Moreover, we observed a large Kerr rotation angle (> 10°) in the RMOKE, which is much larger than angles (<1°) typically found for the MOKE with visible light. Conventional MOKE measurement has always required lock-in amplifier techniques to obtain a high enough signal-to-noise ratio. However, the large Kerr rotation angle in the RMOKE we observed does not require such techniques. This advantage allows us to detect the magnetism or spin dynamics of a very small amount of the magnetic element in a material, such as a dilute magnetic semiconductor, or to measure very small structure, such as the magnetic nanostructure on a surface. This feature makes it possible to trace these ultrafast spin dynamics in terms of individual chemical species in *real time* when combined with FEL or HHG lasers.

Reference

[1] Sh. Yamamoto, M. Taguchi, M. Fujisawa, R. Hobara, S. Yamamoto, K. Yaji, T. Nakamura, K. Fujikawa, R. Yukawa, T. Togashi, M. Yabashi, M. Tsunoda, S. Shin, and I. Matsuda, Phys. Rev. B **89**, 064423 (2014).

Authors
I. Matsuda, Sh. Yamamoto, T. Nakamura[a], and S. Shin
[a]Japan Synchrotron Radiation Research Institute/SPring-8

Ultra-Broad Mode-Spacing Optical Frequency Comb

Kobayashi Group

A mode-locked oscillator produces bunch of regularly spaced longitudinal modes in an optical frequency region. It is called as an optical frequency comb. When the frequency comb was invented, it was regarded as a dream light source since one oscillator produces tens of thousands modes, corresponding to thousands of ultra-narrow linewidth cw lasers. Many people said that cw lasers were no longer necessary since making the mode-locked laser was easier than making very stable cw lasers. However, this story was not correct. One could not chose one comb tooth from neighboring modes because the mode spacing was too small to pick by using any dispersive optics. The mode-spacing is a repetition rate of the mode-locked (ML) oscillator, the high-repetition rate then makes broad mode spacing. The repetition rate of the ML laser is determined by the cavity length since only one pulse is propagating in a cavity. The smaller cavity then

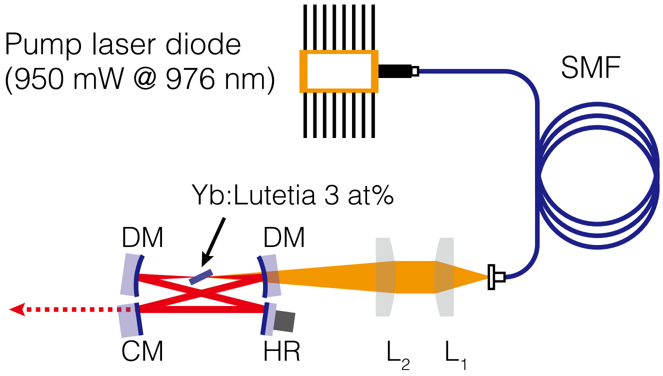

Fig. 1. Schematic of the experimental setup. DMs, dichroic mirrors; CM, chirp-compensation mirror; HR, high reflection mirror; L1 and L2, lenses.

produces the broader mode-spacing optical frequency comb. Another direction is to make higher resolution spectrometer or spectrograph to resolve each mode. The highest frequency resolution in a commercially available spectrometer is about 4 GHz in an optical frequency, then the higher repetition rate than 4 GHz is crucial to resolve comb teeth.

Here we report on our recent progress of high-repetition-rate ML oscillator [1]. We are concentrating on the laser-diode (LD) pumped Kerr-lens ML oscillator. There are some reasons to study this type of lasers. Typical high-repetition-rate comb is made by using Ti:sapphire laser pumped by a large green laser which is not easy to keep running for many days. However, many applications of the frequency comb require long-term operation. A single-mode-fiber (SMF) coupled LD can be kept running as long as we need without any degradation or miss alignment. The main drawback is its poor power. The highest power of the SMF coupled LD is limited below 1 W. Lower power pumping makes it difficult to realize high-repetition-rate ML oscillator. We invented new scheme of the ML oscillator with high finesse. This makes the intra-cavity power high enough to realize the Kerr-lens ML. By adopting Yb-doped ceramic as a gain medium, we have realized 6-GHz repetition rate oscillator with femto-second pulse duration.

Figure 1 shows the schematic of the small oscillator. ML oscillator consists of two concave mirrors and two plane mirrors. One of the plane mirror is specially coated

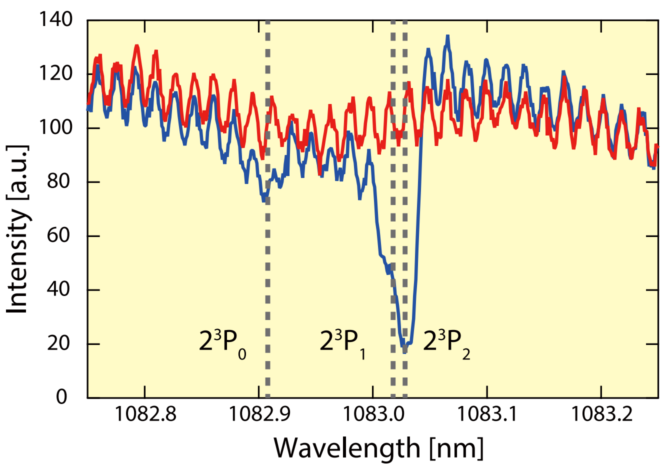

Fig. 2. Absorption spectroscopy of meta-stable He. Red curve shows the laser spectrum without He atoms. The modulation correspond comb structure. Blue curve was obtained with meta-stable He atoms. We can see clear two absorptions that correspond to the triplet S to triplet P transitions in a meta-stable state. 1S-2S transition is strictly prohibited so that the metastable life time is long enough to observe these transitions.

to compensate a chirp in the cavity. 1-mm-thick Yb:Lu_2O_3 ceramic was used for the laser gain. Obtained spectrum width was about 8 nm, and the measured pulse duration was 160 fs. By using commercially available optical spectrum analyzer, each comb mode was clearly resolved. This comb is applied for the precision spectroscopy of meta-stable He atoms, which has three absorption lines in the spectrum of this laser. Figure 2 shows the absorption spectroscopy of He obtained with 5.2-GHz repetition rate at this time. Three lines correspond 2^3S_1- 2^3P_0, 2^3S_1- 2^3P_1 and 2^3S_1- 2^3P_2 transitions. The energy spacing of 2^3P_0- 2^3P_1 is 30 GHz, and that of 2^3P_1- 2^3P_2 is 2 GHz, which is too small to resolve in this setup. The absolute frequency could be determined if the offset frequency is controlled, although it is not realized yet.

We have demonstrated the multi-GHz repetition-rate Kerr-lens ML oscillator with LD pumping for the first time to our best knowledge. It would open new applications with mode-resolved spectroscopy. The astronomical application is one of the promising candidate, in which this kind of laser could be used in order to find extra-solar planets.

Reference

[1] M. Endo, A. Ozawa, and Y. Kobayashi, Opt. Lett. **38**, 4502 (2013).

Authors

M. Endo and Y. Kobayashi

Generation of Attosecond Soft-X-Ray Bursts in the Water Window

Itatani Group

High harmonic generation using intense laser pulses is the most promising method to produce attosecond optical pulses. In the past decade, attosecond science has been extensively exploited using the advanced Ti:sapphire laser technology that can produce attosecond pulses in the extreme ultraviolet (EUV) below 200 eV in photon energies. Recent development of intense infrared sources that are based on optical parametric chirped-pulse amplification (OPCPA) has opened the opportunities to extend the spectral range of high harmonics from the EUV to the soft X ray region, but the lack of well-controlled reliable IR sources has been the problem to realize attosecond soft-X-ray spectroscopy.

In the present research [1], we have developed a novel IR light source that is based on OPCPA using BiB_3O_6 crystals pumped by Ti:sapphire lasers. This OPCPA system can amplify an octave-spanned bandwidth from 1100 to 2200 nm, which enables the phase-stable direct amplification of sub-two-cycle IR pulses. The light source produces 0.5-mJ,

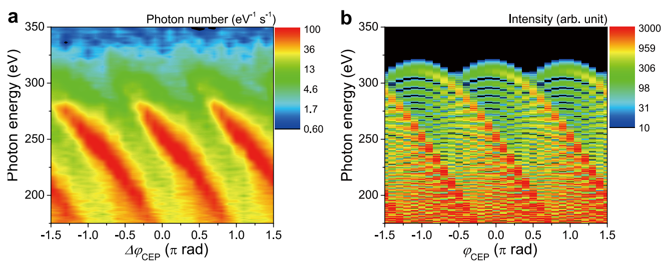

Fig. 1. (a) Experimentally obtained high harmonic spectra recorded at relative carrier-envelope phases in steps of 0.1π rad. (b) Simulated high harmonic spectra assuming 10-fs optical pulses at 1600 nm with an intensity of 4 × 10^{14} W/cm^2.

9-fs pulses with stable carrier-envelope phases (CEPs) at 1-kHz repetition rate. We have achieved excellent stabilities in the output energy and CEP, which are comparable to those of commercial Ti:sapphire lasers.

Figure 1(a) shows observed high harmonic spectra around the cutoff photon energy as a function of the CEP. The maximum photon energy reaches ~330 eV that is well beyond the carbon *K* edge at 284 eV. The shifting structures of the spectral peak is called the half-cycle cutoff, which is a clear signature of the generation of single isolated attosecond pulses. Figure 1(b) shows simulated results that are based on the strong-field approximation assuming the experimental parameters described in the caption of Fig. 1(a). The good agreement between the experimental and simulation results suggests the generation of isolated attosecond bursts in the water window. This result is an important milestone to extend the attosecond spectroscopy into the soft X ray region where element-specific ultrafast spectroscopy as well as novel attosecond techniques using high-energy electron wavepackets can be explored in the future.

Reference

[1] N. Ishii, K. Kaneshima, K. Kitano, T. Kanai, S. Watanabe, and J. Itatani, Nature Comm. **5**, 3331 (2014).

Authors

N. Ishii, K. Kaneshima, K. Kitano, T. Kanai, S. Watanabe[a], and J. Itatani
[a]Tokyo University of Science

Highlights of Joint Research

Supercomputer Center

The Supercomputer Center (SCC) is a part of the Materials Design and Characterization Laboratory (MDCL) of ISSP. Its mission is to serve the whole community of computational condensed-matter physics of Japan providing it with high performance computing environment. In particular, the SCC selectively promotes and supports large-scale computations. For this purpose, the SCC invites proposals for supercomputer-aided research projects and hosts the Steering Committee, as mentioned below, that evaluates the proposals.

The ISSP supercomputer system consists of three subsystems: System A, which is intended for a parallel computation with relatively smaller number of nodes connected tightly, and System B, which is intended for more nodes with relatively loose connections. In July, 2010, the SCC replaced the two supercomputer subsystems. The current system B is SGI Altix ICE 8400EX, which consists of 30 racks or 15360 cores whereas the system A is NEC SX-9, which consists of 4 nodes or 64 cpus. They have totally 200 TFlops. System C - FUJITSU PRIMEHPC FX10 was installed in April, 2013. It is highly compatible with K computer, the largest supercomputer in Japan. System C consists of 384 nodes, and each node has 1 SPARC64TM IXfx CPU (16 cores) and 32 GB of memory. The total system achieves 90.8 TFlops theoretical peak performance.

The hardware administration is not the only function of the SCC. The ISSP started hosting Computational Materials Science Initiative (CMSI), a new activity of promoting materials science study with next-generation parallel supercomputing. This activity is financially supported by the MEXT HPCI strategic program, and in CMSI, a number of major Japanese research institutes in various branches of materials science are involved. The SCC supports the activities of CMSI as its major mission.

All staff members of university faculties or public research institutes in Japan are invited to propose research projects (called User Program). The proposals are evaluated by the Steering Committee of SCC. Pre-reviewing is done by the Supercomputer Project Advisory Committee. In school year 2013 totally 245 projects were approved. The total points applied and approved are listed on Table. 1 below.

The research projects are roughly classified into the following three (the number of projects approved):

First-Principles Calculation of Materials Properties (107)
Strongly Correlated Quantum Systems (30)
Cooperative Phenomena in Complex, Macroscopic Systems (86)

All the three involve both methodology of computation and its applications. The results of the projects are reported in 'Activity Report 2013' of the SCC. Every year 3-4 projects are selected for "invited papers" and published at the beginning of the Activity Report. In the Activity Report 2013, the following three invited papers are included:

"One-hundred-million-atom electronic structure calculations on the K computer", Takeo HOSHI
"Strong correlation of electrons studied by computational approaches—Physics of superconductors and topological phases", Shiro SAKAI, Takahiro MISAWA, Youhei YAMAJI, Mayuru KURITA, and Masatoshi IMADA
"Coarse-Grained Simulation of Surfactant Membrane", Hayato SHIBA and Hiroshi NOGUCHI

Class	Max/Min Points	Application	Number of Projects	Total Points					
				Applied			Approved		
				System A	System B	System C	System A	System B	System C
A	100	any time	10	350	850	500	350	850	500
B	2k, 1k, 500	twice a year	56	40.7k	45.0k	6.6k	28.7k	29.8k	5.8k
C	20k, 10k, 2.5k	twice a year	130	793.5k	1043.0k	146.9k	486.5k	391.0k	98.6k
D	20k, 10k, 2.5k	any time	3	0	22.0k	0	0	19.0k	0
E	0, 30k, 2.5k	twice a year	24	-	653.0k	43.8k	-	283.5k	36.6k
S		twice a year	0	0	0	0	0	0	0
CMSI			22	-	-	-	-	-	92.5k
Total			245	834.6k	1,763.9k	197.8k	515.6k	724.2k	144.0k

Table 1. Research projects approved in 2013
The maximum points allotted to the project of each class are the sum of the points for the two systems; Computation for 1 CPU•hour corresponds to 0.32, 0.022, and 0.042 points for System-A, System-B, and System C, respectively.

Neutron Science Laboratory

The Neutron Science Laboratory (NSL) has been playing a central role in neutron scattering activities in Japan since 1961 by performing its own research programs as well as providing a strong General User Program for the university-owned various neutron scattering spectrometers installed at the JRR-3 (20MW) operated by Japan Atomic Energy Agency (JAEA) in Tokai (Fig. 1). In 2003, the Neutron Scattering Laboratory was reorganized as the Neutron Science Laboratory to further promote the neutron science with use of the instruments in JRR-3. Under the General User Program supported by NSL, 14 university-group-owned spectrometers in the JRR-3 reactor are available for a wide scope of researches on material science, and proposals close to 300 are submitted each year, and the number of visiting users under this program reaches over 6000 person-day/year. In 2009, NSL and Neutron Science Laboratory (KENS), High Energy Accelerator Research Organization (KEK) built a chopper spectrometer, High Resolution Chopper Spectrometer, HRC, at the beam line BL12 of MLF/J-PARC (Materials and Life Science Experimental Facility, J-PARC). HRC covers a wide energy and Q-range ($10\mu\text{eV} < \hbar\omega < 2\text{eV}$ and $0.02\text{Å}^{-1} < Q < 50\text{Å}^{-1}$), and therefore becomes complementary to the existing inelastic spectrometers at JRR-3. HRC started to accept general users through the J-PARC proposal system in FY2011.

Triple axis spectrometers, HRC, and a high resolution powder diffractometer are utilized for a conventional solid state physics and a variety of research fields on hard-condensed matter, while in the field of soft-condensed matter science, researches are mostly carried out by using the small angle neutron scattering (SANS-U) and/or neutron spin echo (iNSE) instruments. The upgraded time-of-flight (TOF) inelastic scattering spectrometer, AGNES, is also available through the ISSP-NSL user program.

On March 11, 2011, a great earthquake with Magnitude 9.0 hit North East Coast of Japan. Fortunately, JRR-3 was under regular inspection and no serious accidents or damages were reported. However, the lifeline of Tokai Village area was lost for more than two weeks, and it took more than two months before damage inspection of JRR-3 could be started. As of May of 2014, JRR-3 has not restarted yet. General User Programs of 2012 and 2013 were cancelled and that of 2014 has been suspended so far. In order to compensate the loss of the activity of NSL, a number of proposals accepted in 2011 - 2013 were transferred to overseas owing to kind offer from the major facilities, namely, ORNL, ILL, ANSTO, and HANARO.

Fig. 1. The reactor of JRR-3. The eight neutron scattering instruments are attached to the horizontal beam tubes in the reactor experimental hall. Two thermal and three cold guides are extracted from the reactor core towards the guide hall located to the left.

Fig. 2. The U.S.-Japan spectrometer, CTAX, installed at the cold guide-line CG4, High Flux Isotope Reactor (HFIR), in Oak Ridge National Laboratory. Members who contributed the relocation project of the U.S.-Japan spectrometer celebrate the completion of the project in October 2010.)

The NSL also operates the U.S.-Japan Cooperative Program on neutron scattering, providing further research opportunities to material scientists who utilize the neutron scattering technique for their research interests. In 2010, relocation of the U.S.-Japan triple-axis spectrometer, CTAX, was completed, and it is now open to users (Fig. 2).
http://neutrons.ornl.gov/instruments/HFIR/CG4C/

The activity report on Neutron Scattering Research in JFY2011 is given in NSL-ISSP Activity Report vol. 18 (2011), http://quasi.issp.u-tokyo.ac.jp/actrep/actrep-18-2011/index-pub_vol18.html.

International MegaGauss Science Laboratory

The objective of this laboratory (Fig. 1) is to study the physical properties of solid-state materials (such as semiconductors, magnetic materials, metals, insulators, superconducting materials) under ultra-high magnetic field conditions. Such a high magnetic field is also used for controlling the new material phase and functions. Our pulse magnets, at moment, can generate up to 87 Tesla (T) by non-destructive manner, and from 100 T up to 760 T (the world strongest as

Fig. 1. Building view of the International MegaGauss Science Laboratory (C-building) at ISSP.

Fig. 2. The building for the flywheel generator (left hand side) and a long pulse magnet station (right hand side). The flywheel giant DC generator is 350 ton in weight and 5 m high (bottom). The generator, capable of a 51 MW output power with the energy storage 210 MJ, is planned to energize the long pulse magnet generating 100 T without destruction.

an in-door record) by destructive methods. The laboratory is opened for scientists both from Japan and from overseas, especially from Asian countries, and many fruitful results are expected to come out not only from collaborative research but also from our in-house activities. One of our ultimate goals is to provide the scientific users as our joint research with magnets capable of a 100 T, milli-second long pulses in a non-destructive mode, and to offer versatile physical precision measurements. The available measuring techniques now involve magneto-optical measurements, cyclotron resonance, spin resonance, magnetization, and transport measurements. Recently, specific heat and calorimetric measurements are also possible to carry out with sufficiently high accuracy.

Our standard non-destructive-type pulse magnets are energized by single capacitor bank and can generate fields up to 75 T for ordinary use. Their simple sinusoidal waveforms are advantageous for precise and reliable measurements of various physical properties. Several on-demand magnets

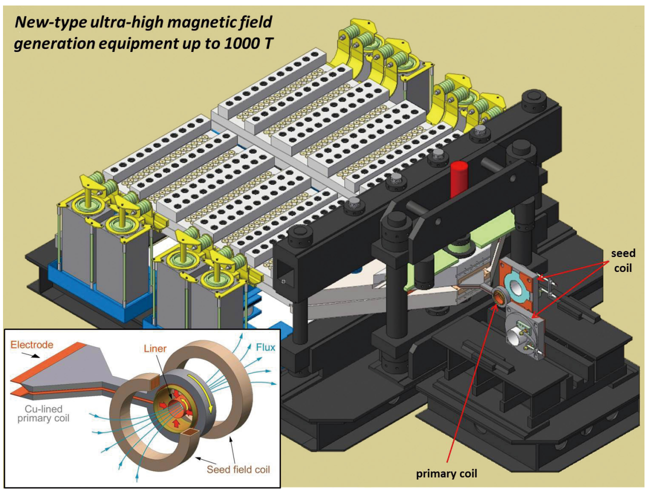

Fig. 3. (Build. C) The building for the electro-magnetic flux compression, generating over 700 T. 1000 T project started since 2010, and finally condenser banks of 9 MJ (5 MJ + 2 MJ +2 MJ) as a main system with the 2 MJ sub bank system for the seed field have been installed, and completed in the year of 2014.

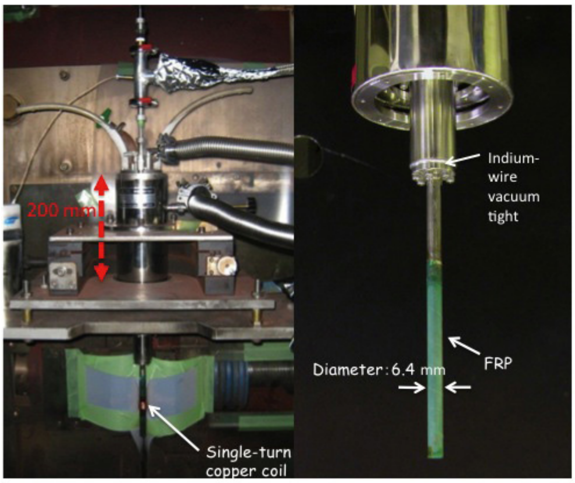

Fig. 4. Fig.4. A photo of the V-type single-turn coil equipped with 40 kV, (A:100+B:100=200 kJ) fast operating pulse power system. Measurements are carried out from room temperature down to 2 K by a specially designed cryostat.

having irregular shapes and sizes are developed for some particular experiments. We open six magnet cells for parallel experiments and accept more than 50 research projects per year in 2013.

A 210 MJ flywheel generator (Fig. 2), which is the world largest DC power supply (recorded in the Guinness Book of World Records) has been installed in the DC flywheel generator station at our laboratory, and used as an energy source of long pulse magnets. The magnet technologies are intensively devoted to the quasi-steady long pulse magnet (an order of 1-10 sec) energized by the giant DC power supply. The latest long-pulse magnet can generate fields up to 36 T with its pulse half-period of 1 sec.

Our interests cover the study on quantum phase transitions (QPTs) induced by high magnetic fields. Field-induced QPTs have been explored in various materials such as quantum spin systems, strongly correlated electron systems and other magnetic materials. Direct thermodynamic evidences of QPTs are obtained through magnetization and recently developed caloric measurements. For some QPTs, changes in symmetry at the transitions are sensitively resolved through measurements of electric polarization or optical imaging using a polarizing microscope. High resolution of electrical measurements realized the observation of quantum oscillations in high quality crystals through measurements of electrical resistivity, contactless impedance, and torque magnetometry.

Magnetic fields higher than 100 T can only be obtained with destructing a magnet coil, where ultra-high magnetic fields are obtained in a microsecond time scale. Our destructive techniques have undergone intensive developments. The project, financed by the ministry of education, culture, sports, science and technology, is now in progress, and goal is to generate 1000 T by the electromagnetic flux compression (EMFC) system (Fig. 3). The system which is unique to ISSP in the world scale is comprised of a power source of 5 MJ main condenser bank and 2 MJ condenser bank and has been accomplished its installation. Two magnet stations are constructed and both are energized from each power source. Both systems are fed with a 2 MJ condenser bank used for a seed-field coil, of which magnetic flux is to be compressed.

As an easy access to the megagauss science and technology, we have the single-turn coil (STC) system capable of generating the fields of up to 300 T by a fast-capacitor of 200 kJ. We have two STC systems, one is a horizontal type (H-type) and the other is a vertical type

	Alias	Type	B_{max}	Pulse width Bore	Power source	Applications	Others
Building C Room 101-113	Electro- Magnetic Flux Compression	destructive	730 T	μs 10 mm	5 MJ, 40kV	Magneto-Optical Magnetization	5 K – Room temperature
	Horizontal Single-Turn Coil	destructive	300 T 200 T	μs 5 mm 10 mm	0.2 MJ, 50 kV	Magneto-Optical measurements Magnetization	5 K – 400 K
	Vertical Single-Turn Coil	destructive	300 T 200 T	μs 5 mm 10 mm	0.2 MJ, 40 kV	Magneto-Optical Magnetization	2 K – Room temperature
Building C Room 114-120	Mid-Pulse Magnet	Non-destructive	60 T 70 T	40 ms 18 mm 40 ms 10 mm	0.9 MJ, 10 kV	Magneto-Optical measurements Magnetization Magneto-Transport Hall resistance Polarization Magneto-Striction Magneto-Imaging Torque Magneto- Calorimetry Heat Capacity	Independent Experiment in 5 site Lowest temperature 0.1 K
Building C Room 121	PPMS	Steady State	14 T			Resistance Heat Capacity	Down to 0.3 K
	MPMS	Steady State	7 T			Magnetization	
Building K	Short-Pulse magnet	Non-destructive	87 T (2-stage pulse) 85 T	5 ms 10 mm 5 ms 18 mm	0.5 MJ, 20 kV	Magnetization Magneto-Transport	2K – Room temperature
	Long-Pulse magnet	Non-destructive	36 T	1 s 30 mm	210 MJ, 2.7 kV	Resistance Magneto-Calorimetry	2K – Room temperature

Table 1. Available Pulse Magnets, Specifications

(V-type, Fig. 4). Various kinds of laser spectroscopy experiments such as the cyclotron resonance and the Faraday rotation using the H-type STC are available. On the other hand, for very low-temperature experiments, a combination of the V-type STC with a liquid helium bath cryostat is very useful and the magnetization measurements at temperature as low as 2 K can be performed up to 120 T with high precision.

Center of Computational Materials Science

K-computer at Kobe won the title of the world-fastest computer at TOP500 ranking announced at ISC11. Though it is in the 4th place in the list as of today, it is still providing the Japanese scientific community with an incomparable amount of computational resources. With the advancement of hardware and software technologies, large-scale numerical calculations have been making important contributions to materials science and will have even greater impact on the field in the near future. Center of Computational Materials Science (CCMS) is a specialized research center for promoting computer-aided materials science with massively parallel computers, such as K-computer. The center also functions as the headquarters of Computational Materials Science Initiative (CMSI), which is an inter-institutional organization for computational science of a broad range of disciplines, including molecular science, quantum chemistry, biological materials, and solid state physics. ISSP made contracts with 9 universities and 2 national institutes for supporting the activities of CMSI in which nearly 100 research groups are involved. The main purpose of CMSI is to establish a new community of computational science in which researches from different backgrounds work together on grand challenge problems, thereby developing computational infrastructures (new algorithms, coding styles, standard software packages, etc) and inspire young scientists.

CCMS has a branch office in the RIKEN AICS building on the Port Island Kobe, where K-computer is located, for supporting CMSI researchers getting together at the K-computer site to exchange idears of computational science, fine-tune various applications software, and develop better contact with staff members of RIKEN, the operating

Fig. 1. CMSI International Satellite Meeting 2013 in Kobe

Fig. 2. Workshop: Programming Techniques for K-Computer (Mishima)

institute of K-computer. Another mission of the Kobe branch of CCMS is exchanging ideas and techniques with researchers from other fields of computer science. (There are 5 major fields in the HPCI strategic program of MEXT, "biology", "materials and energy" (our field), "seismology, oceanography and meteorology", "industrial applications", and "high-energy physics and cosmology".)

The following is the selected list of meetings organized by CMSI and CCMS in SY2013:

- "CMSI Kobe Hands-On: xTAPP Tutorial" (Apr 23, Jul 30/2013, Kobe)
- "Workshop: Programming Techniques for K-Computer" (Jul 1-Jul 3/2013, Mishima)
- "Internaitional Workshop: EQPCM2013" (Jun 3-Jun 21/2013, Kashiwa)
- "CMSI Application Developments Seminar TOKKUN!" (Jun 5, Aug 5, Sep 3/2013, Kobe)
- "CMSI Kobe Hands-On: ALPS Tutorial" (Jul 10, Nov 6/2013, Kobe)
- "CMSI Kashiwa Hands-On: Machikaneyama2002 Tutorial" (Jul 26/2014, Kashiwa)
- "CMSI Division 1 Summer School" (Aug 12-Aug 16/2013, Zao)
- "CMSI Kobe Hands-On: Version Control System Tutorial" (Aug 22/2013, Kobe)
- "CMSI International Satellite Meeting 2013 in Kobe" (Oct 16-Oct 18 /2013, Kobe)
- "CMSI International Satellite Meeting 2013 in Nagoya" (Oct 17-Oct 19 /2013, Nagoya)
- "CMSI International Satellite Meeting 2013 in Tokyo" (Oct 18-Oct 19/2013, Hongo)
- "CMSI International Symposium 2013" (Oct 21-Oct 22/2013, Hongo)
- "CCMS Symposium" (Nov 19-Nov 20/2013, Kashiwa)
- "ISSP supercomputer - CMSI Joint Symposium" (Dec 10-Dec 13/2013, Kashiwa)
- "CMSI Kashiwa Hands-On: Version Control System Tutorial" (Jan 14/2014, Kashiwa)
- "Workshop: Programming Techniques for K-Computer" (Jan 28-Jan 30/2014, Atami)
- "CMSI Kashiwa Hands-On: xTAPP Tutorial" (Feb 26/2014, Kashiwa)
- "Joint Symposium of Elements Strategy Initiative, CMSI, SPring-8, J-PARC and KEK" (Feb 28-Mar 1/2014, Kashiwa)
- "CMSI Kobe Hands-On: Rokko Tutorial" (Mar 11/2014, Kobe)

Laser and Synchrotron Research Center (LASOR Center)

Laser and Synchrotron Research (LASOR) Center started from October, 2012. LASOR Center aims to promote material sciences using advanced photon technologies at ISSP by combining the "Synchrotron Radiation Laboratory" and "Advanced Spectroscopy Group". These two groups have long histories since 1980's and have kept strong leaderships in each photon science fields for a long time in the world. In the past several decades, the synchrotron-based and laser-based photon sciences have made remarkable progresses independently. However, recent progresses in both fields make it feasible to merge the synchrotron-based and laser based technologies to develop a new direction of photon and materials sciences. In the LASOR Center, extreme laser technologies such as ultrashort-pulse generation, ultraprecise control of optical pulses in the frequency domain, and high power laser sources for the generation of coherent VUV and SX light are intensively under development. The cutting edge soft X-ray beamline is also developed at the synchrotron facility SPring-8.

LASOR center aims three major spectroscopic methods [ultrafast, ultra-high resolution, and operand spectroscopy] by three groups [extreme laser science group, soft-X-ray spectroscopy and materials science group, and coherent photon science group], as illustrated in Fig.2. Under this framework, various advanced spectroscopy, such as ultra-high resolution photoemission, time-resolved, spin-resolved

Fig. 1. Open ceremony of LASOR center on October 2012.

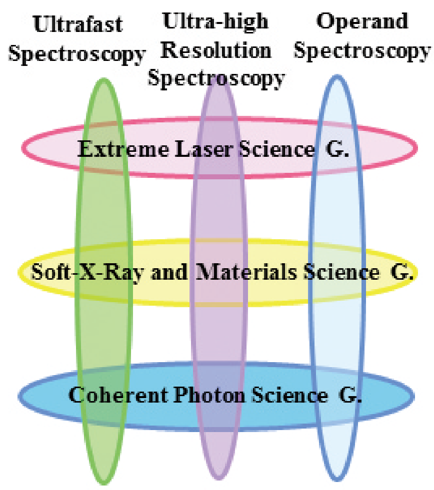

Fig. 2. Developments of advanced spectroscopy at LASOR center by three groups

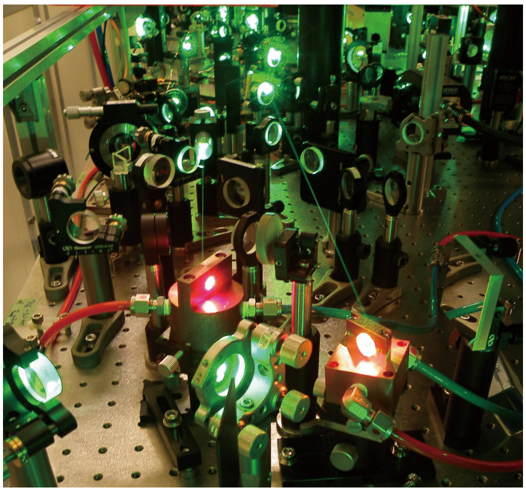

Fig. 3. Close look of a high-peak-power ultrashort-pulse laser

spectroscopy, diffraction, light scattering, imaging, microscopy and fluorescence spectroscopy are in progress by employing new coherent light sources based on laser and synchrotron technologies that cover a wide spectral range from X-ray to terahertz. In LASOR Center, a variety of materials sciences for semiconductors, strongly-correlated materials, molecular materials, surface and interfaces, and bio-materials are studied using advanced light sources and advanced spectroscopy. Another important aim of LASOR Center is the synergy of photon and materials sciences. Most of the research activities on the extreme laser development and their applications to material science are performed in the ISSP buildings D and E at Kashiwa Campus where large clean rooms and the vibration-isolated floor are installed. On the other hand, the experiments utilizing the advanced synchrotron source are performed at beamline BL07 in SPring-8 (Hyogo).

• Extreme Laser Science Group

The advancement of ultrashort-pulse laser technologies in the past decade has transformed the laser development at ISSP into three major directions, (i) towards ultrashort in the time domain, (ii) ultra high resolution in the spectral domain, and (iii) the extension of the spectral range, with extreme controllability of the laser sources. For ultrafast spectroscopy, we have developed carrier-envelope phase stable intense infrared light source that can produce sub-two cycle optical pulses for high harmonic and attosecond pulse generation. So far we observed coherent soft-X-ray radiation extending to a photon energy of ~330 eV. The simulation predicts the soft-X-ray field consists of single isolated attosecond pulses. For ultra-high resolution spectroscopy, fiber-laser-based light sources are intensively developed for producing EUV pulses for high resolution and time-resolved photoemission spectroscopy as well as extending the frequency comb to ultraviolet or infrared for various applications. The spectral range of intense optical pulses are being extended from visible to IR, MIR and THz ranges. Various types of high-repetition-rate ultrastable light sources are developed for laser-based ultrahigh resolution photoemission spectroscopy, high-average-power EUV generation in an enhancement cavity, and frequency comb spectroscopy for atomic physics, astronomical application, and frequency standards.

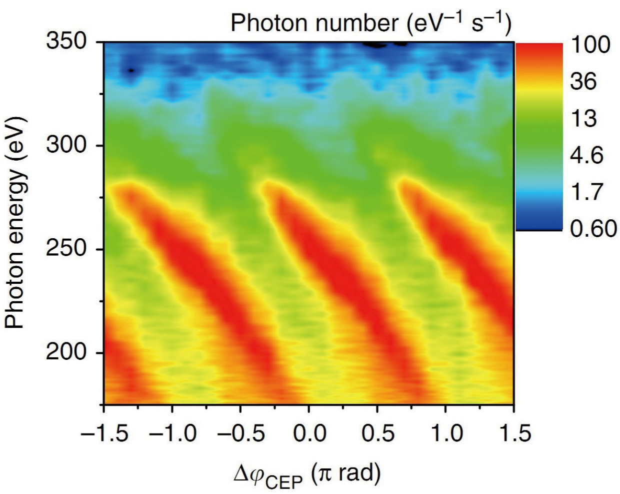

Fig. 4. Phase-dependence of high harmonic spectra in soft X rays.

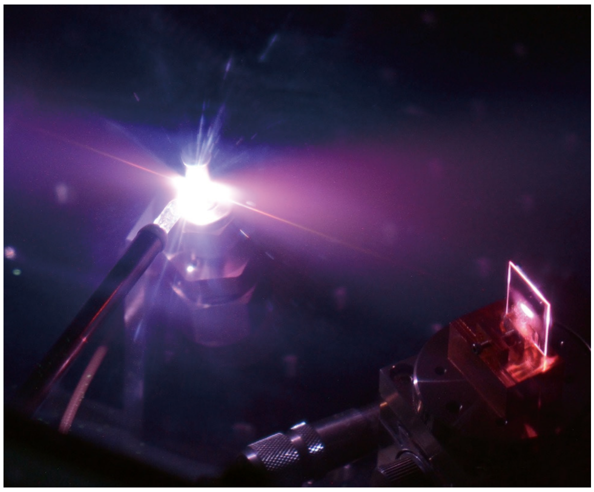

Fig. 5. 10-MHz high harmonic generation in an enhancement cavity.

• Soft-X-ray and Materials Science Group

Recently, VUV and SX lasers have been developed. They become very usuful for the materials science, if we develop the SX spectroscopy, such as the cutting-edge photoemission spectroscopy. Laser has a lot of fruitful properties. For examples, by using monochromatic light, ultra-high resolution angle-resolved photoemission spectroscopy (ARPES) is developed. The achieved resolution of 70-μeV is the highest resolution of the world. Fermiology of the materials science with μeV resolution is improved drastically by using the lasers. On the other hand, when we use pulsed laser light, the time resolved ARPES becomes possible. The time resolved photoemision in fs region is powerful to know the relaxation process of photo-induced phase transition. Furthermore, by using CW and circulary light in VUV region, the photoelec-

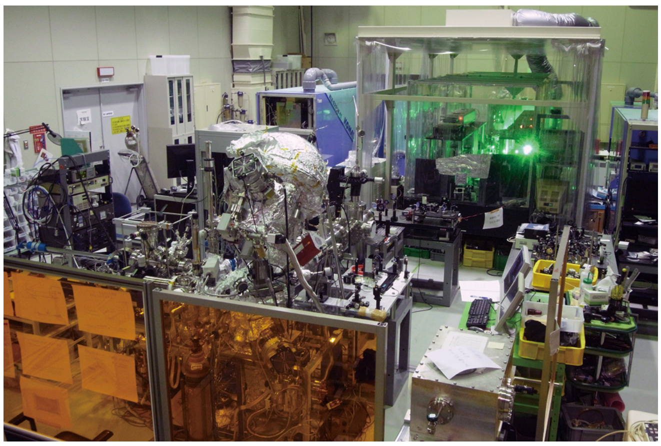

Fig. 6. Pump-probed photoemission system using 60-eV laser

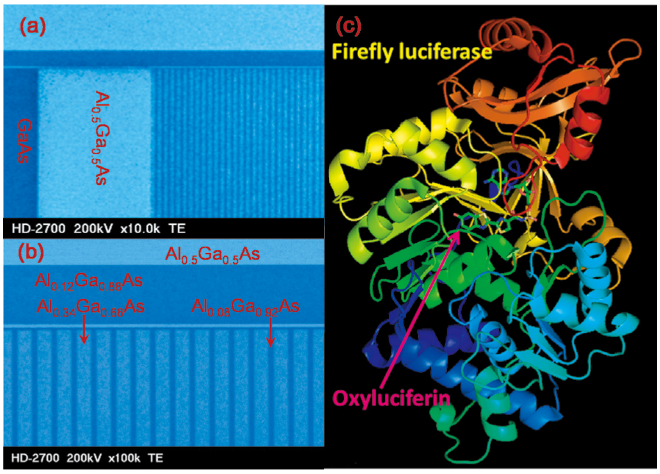

Fig. 7. Photonics devices under study: (left panel) semiconductor quantum wires and (right panel) firefly-bioluminescence system consisting of light emitter (oxyluciferin) and enzyme (luciferase)

tron microscopy(PEEM) is developed. The spatial resolution of nm region is very powerful for the nanomaterials.

• Coherent Photon Science Group

The coherent-photon science group has main interests in exploring a variety of coherent phenomena and non-equilibrium properties of excited states in condensed matters, in collaborations with research groups in charge of photoemission, operand-spectroscopy and extreme laser science. This group covers a wide range of materials, from semiconductors, ferromagnets, complexes and superconductors to biomaterials. Various ultrafast optics technologies such as femtosecond luminescence and pump-and-probe transmission/reflection spectroscopy are applied to studies on wavepacket dynamics, photo-induced phase transitions and carrier dynamics. Coherent control and observation of spin dynamics in magnetic materials and metamaterial structures by using high power terahertz radiation source is extensively studied. Advanced photonics devices are intensively studied, such as quantum nano-structure lasers with novel low-dimensional gain physics, low-power light-standard LEDs, very efficient multi-junction tandem solar cells for satellite use, and wonderful bio-/chemi-luminescent systems for wide bio-technology applications.

Synchrotron Radiation Laboratory

The Synchrotron Radiation Laboratory (SRL) was established in 1975 as a research division dedicated to solid state physics using synchrotron radiation (SR). In 1989, SRL started to hold the Tsukuba branch, in the Photon Factory (PF), High Energy Accelerator Research Organization (KEK). SRL maintains a Revolver undulator, two beamlines and three experimental stations; BL-18A for angle-resolved photoemission spectroscopy with SCIENTA electron analyzer, while undulator beamline BL-19A and BL-19B, for spin- and angle-resolved photoelectron spectroscopy (SARPES) and soft X-ray emission spectroscopy experiments, respectively. Recently, a high-yield spin detector, using very low energy electron diffraction, was developed at BL-19A. SAPRES measurements have now been performed with high-resolution and the experiments at the beamline have become important for exciting topics of surface/solid state physics such as topological insulators and ferromagnetic nanofilms.

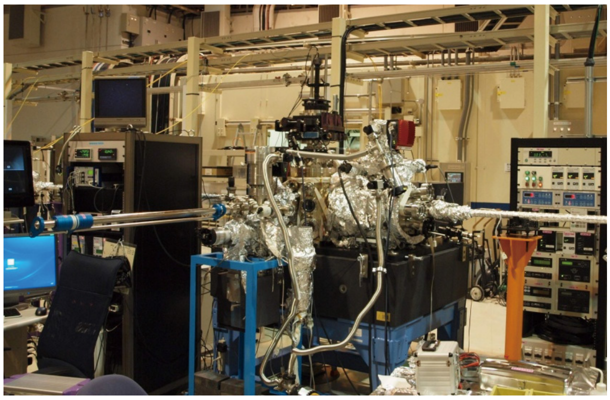

Fig. 1. 3D nano ESCA at SPring-8 BL07LSU

The SRL staffs have joined the Materials Research Division of the Synchrotron Radiation Research Organization (SRRO) of the University of Tokyo and they have played an essential role in constructing a new high brilliant soft X-ray beamline, BL07LSU, in SPring-8. The light source is the polarization-controlled 25-m long soft X-ray undulator. The monochromator is equipped with a varied-line-spacing plain grating, which covers the photon energy range from 250 eV to 2 keV. At the downstream of the beamline, four experimental stations have been developed for frontier spectroscopy researches: the three-dimensional (3D)

Fig. 2. XES station at SPring-8 BL07LSU

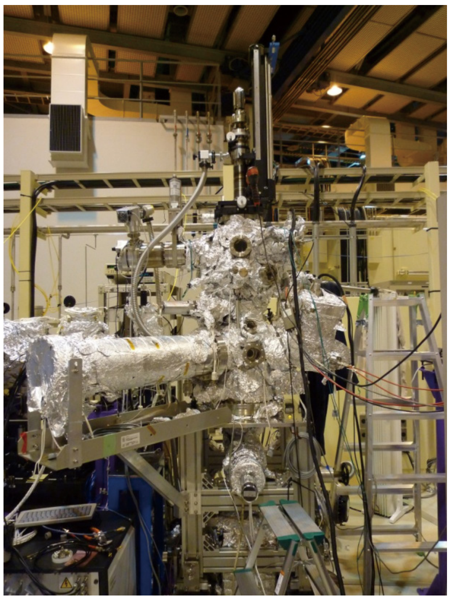

Fig. 3. TR-SX station at SPring-8 BL07LSU

nano-ESCA station, the soft X-ray emission spectroscopy (XES) station, the time-resolved soft X-ray spectroscopy (TR-SX) station, and the free-port station for any experimental apparatus. The beamline construction was completed in 2009 and SRL established the Harima branch laboratory in SPring-8. At SPring-8 BL07LSU, each end-station has achieved high performance: the 3D nano-ESCA reaches the spatial resolution of 70 nm, the XES station obtains spectra with energy resolving power E/ΔE larger than 5,000, and the TR-SX have established the laser-pump and SR-probe method with the time-resolution of 50 ps which corresponds to the SR pulse-width. The four end-stations have now been opened fully to outside users. In 2013, 153 researchers made their experiments during the SPring-8 operation time of 3400 hours.

Experimental Realization of a Quantum Breathing Pyrochlore Antiferromagnet

K. Kimura and S. Nakatsuji

Exploring novel and exotic phenomena associated with spin degrees of freedom has been central subject in condensed matter physics [1]. One of the most attractive systems in three dimension is a pyrochlore lattice magnet, which consists of corner-sharing regular tetrahedra of magnetic ions. The inherent geometrical frustration suppressing a conventional magnetic order often leads to a variety of unusual properties [1]. A key building unit of pyrochlore magnets is a single spin tetrahedron. Besides being a good starting point for considering the essence of physics of full pyrochlore lattice, it has been theoretically shown to possess interesting properties such as a doubly degenerate singlet state which can be labelled by scalar spin chirality [2]. To our knowledge, however, there has been no experimental realization of the S = 1/2 quantum spin tetrahedral system, partly because typical 3d transition metal ions with S = 1/2 (like Cu^{2+}) are difficult to keep the tetrahedral symmetry due to the inherent Jahn-Teller instability.

Here, we report the new Yb-based quantum spin system $Ba_3Yb_2Zn_5O_{11}$ [3]. Polycrystalline samples were synthesized by the standard solid state reaction method. The Rietveld refinement on powder X-ray diffraction pattern has revealed that this material crystallizes into the cubic structure with space group F-43m, and Yb^{3+} ions form a so-called breathing pyrochlore lattice [4] characterized by an alternating array of small and large Yb^{3+} regular tetrahedra (Fig. 1(a), inset). Analyses of the crystalline electric field (CEF) scheme of Yb^{3+} ions ($4f^{13}$) and magnetic susceptibility data down to 30 K show that the CEF ground state is approximated by a magnetic Kramers doublet with the isotropic effective g-factor g_{eff} = 2.66 for pseudospin-1/2. The very large gap (>500 K) to the excited states ensures that the low-temperature properties are described by pseudospin-1/2.

The temperature dependence of the magnetic susceptibility below 30 K is shown in Fig. 1(a). A broad maximum at around 4 K suggests a formation of a quantum spin singlet state due to antiferromagnetic interactions in a small Yb tetrahedron. This is supported by the magnetization curves at selected temperatures (Fig. 1(b)). Though linear above 4 K, the magnetization curves show a clear non-linear increase at B ~ 3 T below 4 K, a signature of the singlet-triplet crossover. These results are analyzed based on the pseudospin-1/2 single tetrahedron model with Heisenberg interactions J. The good agreement is obtained with J = -6.43 K and g_{eff} = 2.569, as indicated by the solid lines in Figs. 1(a) and 1(b), suggesting a formation of the doubly degenerate singlet state with chirality fluctuations predicted by the model [2]. Solid evidence for the double degeneracy is provided by magnetic specific heat C_M measured at ISSP (Fig. 2(a)). C_M down to 0.38 K exhibits a broad peak associated with the singlet formation without any signs of long-range order. Corresponding magnetic entropy S_M is shown in Fig. 2(b). The saturated value at 20 K is close to 75% of the value expected for a standard two level system Rln(2), and 25% of magnetic entropy remains below 0.38 K. This value is fully consistent with the doublet degeneracy of the singlet state expected from the single tetrahedral model. Moreover, as indicated by the red line of Figs. 2(a) and 2(b), C_M and S_M are well reproduced by the model.

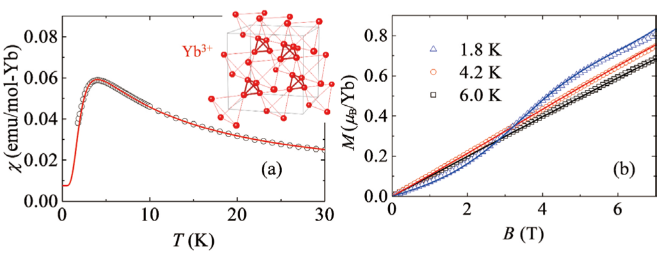

Fig. 1. (a) The temperature dependence of the magnetic susceptibility below 30 K. Inset: Breathing pyrochlore lattice formed by Yb ions. (b) The magnetization curves at selected temperatures. Solid lines in (a) and (b) represent calculated values based on the single tetrahedron model with Heisenberg J = -6.43 K and g_{eff} = 2.569.

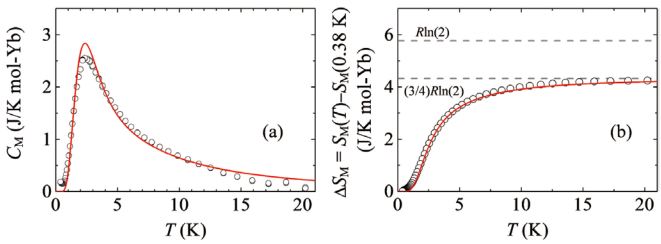

Fig. 2. The temperature dependence of (a) the magnetic specific heat C_M and (b) corresponding magnetic entropy S_M. Solid lines in (a) and (b) are fit to the single tetrahedron model. The dashed lines in (b) denote the entropy for a two level system Rln(2) and for a doubly degenerate singlet state (3/4)Rln(2).

All the data presented in this study therefore uncover the unique doubly degenerate singlet state with chirality fluctuations at T = 0.38 K. To the best of our knowledge, this is a new quantum state of matter which has never been established in existing materials. The mechanism for the lifting of the degeneracy is highly interesting and left for the future study.

References

[1] L. Balents, Nature **464**, 199 (2010).
[2] H. Tsunetsugu, J. Phys. Soc. Jpn. **70**, 640 (2001).
[3] K. Kimura, S. Nakatsuji, and T. Kimura, arXiv: 1404.6439
[4] Y. Okamoto, G. J. Nilsen, J. P. Attfield, and Z. Hiroi, Phys. Rev. Lett. **110**, 097203 (2013).

Authors
K. Kimura[a], S. Nakatsuji, and T. Kimura[a]
[a]Osaka University

Entanglement Spectra between Coupled Tomonaga-Luttinger Liquids

R. Lundgren, Y. Fuji, and S. Furukawa

Quantum entanglement has emerged as a new tool to characterize quantum phases. While the entanglement is nothing but "quantum correlation" that has been a central issue in condensed matter physics for a long time, new quantitative descriptions of the entanglement stimulated by quantum information theory have proved useful. The most frequently used quantity to describe the entanglement in quantum many-body problem is "entanglement entropy". However, there are other quantities which can be useful, and entanglement spectrum is one of them. Its relation to the spectrum of physical edge states is conjectured [1], and has been confirmed in several examples.

Here we report on a recent joint research [2] on entanglement spectra between two coupled Tomonaga-Luttinger

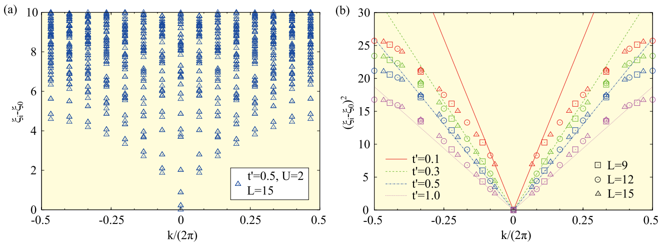

Fig. 1. The dispersion of entanglement spectra of a spin ladder model when a linear combination of two TL fields remains gapless while the other acquires a gap. The numerically obtained dispersion relation agrees well with the peculiar square-root dependence predicted by the theory.

liquids (TLLs). TLL is a ubiquitous effective field theory for quantum many-body problem in one dimension, and many physical systems such as quantum spin ladders and carbon nanotubes are described as coupled TLLs. There are variety of phases in coupled TLLs. In a class of gapless phases of coupled non-chiral TLLs, we find an entanglement spectrum with a dispersion relation proportional to the square root of the subsystem momentum. This result was derived using the field theory, and was then confirmed numerically for a spin ladder model. Such a dispersion is generally not expected for a spectrum of physical excitations, including those of edge states. We relate the unusual dispersion relation in the entanglement spectrum to a long-range interaction in the entanglement Hamiltonian. Our result sheds new light on the correspondence between the entanglement spectrum and the spectrum of the edge states.

This work was performed during a visit by R. Lundgren, a Ph. D. student at University of Texas, under the NSF East Asia and Pacific Summer Institutes for U.S. Graduate Students and the JSPS Summer Program, hosted by ISSP in cooperation with Department of Physics, the University of Tokyo.

References

[1] H. Li and F. D. M. Haldane, Phys. Rev. Lett. **101**, 010504 (2008).
[2] R. Lundgren, Y. Fuji, S. Furukawa, and M. Oshikawa, Phys. Rev. B **88**, 245137 (2013).

Authors

R. Lundgren[a], Y. Fuji, S. Furukawa[b], and M. Oshikawa
[a]University of Texas at Austin
[b]The University of Tokyo

Robust Protection from Backscattering in a Topological Insulator

Y. Ando, S. Shin and F. Komori

Surface of three-dimensional (3D) topological insulators (TIs) is a promising platform for novel device functions, whereon robust spin-polarized surface states occur due to topological feature of the bulk wave functions. High carrier mobility is expected on 3D TI surface because 180º backscattering is forbidden under the spin-helical texture of the topological surface states (TSSs). However, the prohibition range of backscattering has not been clarified yet. Here, we study how the elastic scattering is suppressed as functions of the scattering angle and electron energy in a single and unwarped upper Dirac cone of $Bi_{1.5}Sb_{0.5}Te_{1.7}Se_{1.3}$ [1]. The quaternary compound $Bi_{1.5}Sb_{0.5}Te_{1.7}Se_{1.3}$ is identified to a bulk-insulating TI, whose transport properties are dominated by the surface [2], and thus is suitable for investigating the TSS characteristics.

The elastic-scattering vector within the TSS on the cleaved surface was obtained from a quasiparticle interference (QPI) pattern, which is a Fourier-transformed constant-voltage *dI/dV* image measured using scanning tunneling microscopy at 5 K (Fig. 1). The observed elastic scattering amplitude within the TSS was critically suppressed beyond certain scattering-vector lengths, both in the $\bar{\Gamma}$-$\bar{M}$ and in $\bar{\Gamma}$-$\bar{K}$ directions. That is, there is a critical scattering-vector length,

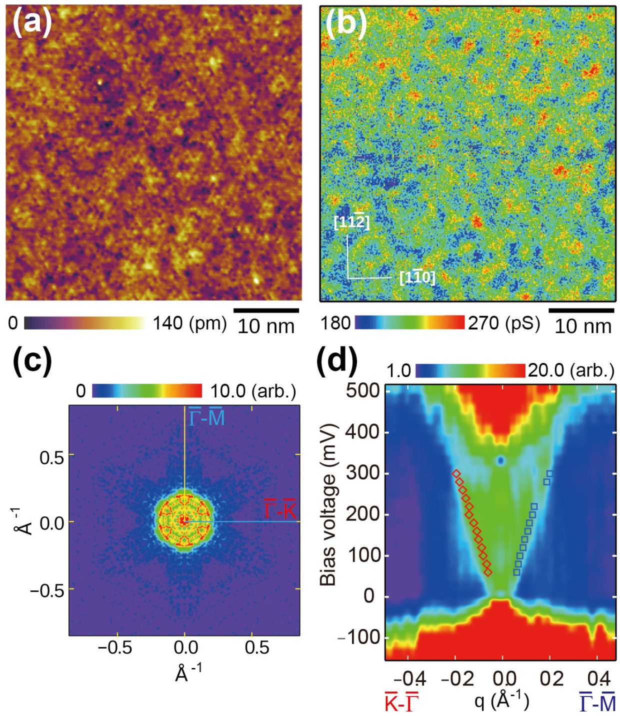

Fig. 1. (a) Topographic STM image of a cleaved surface of $Bi_{1.5}Sb_{0.5}Te_{1.7}Se_{1.3}$. (b) *dI/dV* image at the sample bias voltage V_b = 0.28 V. (c) Amplitude map of the elastic scatterings, or QPI map, derived by Fourier transformation (FT) of the *dI/dV* image shown in (b). (d) FT amplitude image in $\bar{\Gamma}$-$\bar{K}$ and in $\bar{\Gamma}$-$\bar{M}$ directions as functions of V_b. Critical scattering-vector lengths are plotted as red and blue symbols.

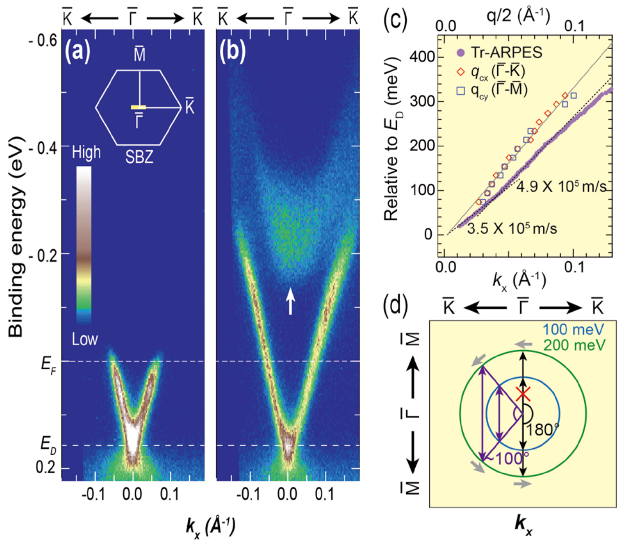

Fig. 2. (a,b) Intensity maps of ARPES before (a) and after (b) impinging a 170-fs pump laser pulse (1.5 eV). The dispersions above E_F are revealed by pumping the electrons into the unoccupied side. An arrow in (b) indicates the bottom of the bulk conduction band. (c) Comparison between critical scattering-vector lengths q_{cx} and q_{cy} (red and blue symbols) obtained from QPI images and the dispersion of the TSS (circles) from pump-probe ARPES. (d) Schematic of the elastic scattering within a nearly ideal Dirac TSS. Scattering angle larger than 100º is effectively prohibited.

qc, beyond which the scattering is effectively prohibited. The critical length increased with the increase of energy from the Dirac point as shown in Fig. 1(d). The band dispersions displayed in Fig. 2(a,b) were recorded by using angle-resolved photoemission spectroscopy (ARPES) implemented by a pump-and-probe method. Here, the dispersions above the Fermi level were revealed by pumping electrons into the unoccupied states (Fig. 2(b)). A nearly ideal Dirac-cone dispersion was observed within the bulk band gap. The locus of the Dirac point, bulk-conduction-band minimum, and the band velocity of the TSS were obtained. We find that the critical scattering vector length is 75 % shorter than the length of the 180^o backscattering vector (Fig. 2(c)). This indicates that the scattering in the TSS is effectively prohibited in a wide angular range of 100-180^o as schematically shown in Fig. 2(d). The robust protection from backscattering is good news for applications, but it poses a challenge to the theoretical understanding of the transport in the TSS.

References

[1] S. Kim, *et al.*, Phys. Rev. Lett. **112**, 136802 (2014).
[2] A. A. Taskin *et al.*, Phys. Rev. Lett. **109**, 066803 (2012).

Authors

S. Kim, S. Yoshizawa, Y Ishida, K. Eto[a], K. Segawa[a] Y. Ando[a], S. Shin, and F. Komori
[a]Osaka University

Microscopic Origin of π Electronic States in Silicene Revealed by Scanning Tunneling Microscopy

Y. Yamada-Takamura, T. Ozaki, and Y. Hasegawa

Silicene, a monolayer of silicon atoms forming a two-dimensional honeycomb lattice, has attracted significant attention in condensed matter physics because it has electronic states similar with its carbon counterpart, graphene and shares almost all the remarkable properties of graphene [1], such as massless Dirac fermion, pseudo spin, and the K/K' valleys. There are, however, some differences between the two ultimately thin materials; while graphene has a planar structure, silicene is buckled [1]; the atoms in the two sub-lattices have different heights, providing us a possibility of inducing a staggered potential by an application of an external electrical field [2]. Different from graphene, silicene exhibits significant spin-orbit coupling [3], making it bear topologically nontrivial electronic structure, which realizes the quantum spin Hall effect or two-dimensional topological insulator. The staggered potential can lift up degeneracy of the K and K' valleys, opening up a possibility of an effective spin polarized electron source [4].

Silicene has been formed so far on metal substrates, such as Ag [5-7] by depositing Si on the substrate. It can also be formed epitaxially on ZrB_2 thin film grown on Si(111) substrate [8]; by annealing silicon atoms segregate from the substrate to form the one-monolayer silicon thin film on the ZrB_2(0001). Because of the lattice matching between the 2×2 unit cell of ZrB_2(0001) and the $\sqrt{3}\times\sqrt{3}$ unit cell of silicene, the silicene on ZrB_2 exhibits a $\sqrt{3}\times\sqrt{3}$ reconstruction. Using a low-temperature scanning tunneling microscopy and spectroscopy (STM/STS), we investigated atomic and electronic structures of the silicon layer [9]. By comparing the experimental results with those of first-principles density functional theory calculations, we determined the atomic structure and discussed the electronic states and the bonding nature of each Si atoms within the unit cell.

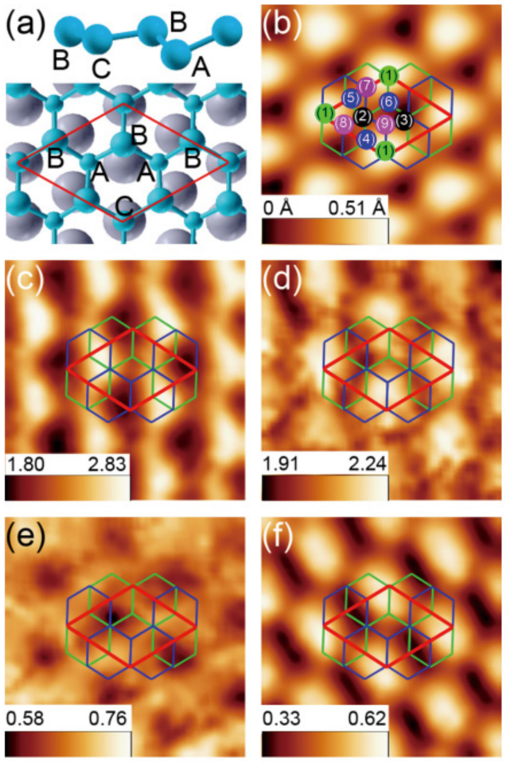

Fig. 1. (a) atomic structure of epitaxial silicene on ZrB_2(0001) derived from DFT calculations. Si atoms are colored in blue and Zr atoms are colored in grey. (b) STM image (2 nm × 2 nm) (c-f) tunneling conductance (*dI*/*dV*) images at the sample bias voltages of -0.47 V, -0.36 V, -0.12 V, and -0.02 V, respectively.

Figure 1 shows results taken by STM/STS. Figure 1(a) is an atomic structural model determined in the present study. Figure 1(b) is an STM image, and (c-f) are tunneling conductance (*dI*/*dV*) images taken at various bias voltages, that is, local density of states (LDOS) mappings at the corresponding energy level with respect to the Fermi energy.

The structural model (Fig. 1(a)) and the STM image (b) indicate that the protrusions observed in the STM image come from the atoms, marked C in the schematic, sitting on top of Zr atoms. Because of the local configuration, the buckling of the atom C is suppressed, making its orbitals hybridize in planar sp_2 manner. The tunneling spectra taken on the atoms indicate significant contribution of the p_z orbital to π/π^* valence/conduction bands, which was observed with angle-resolved photoemission (ARPES) [10]. The STS results also confirm the band gap due to the $\sqrt{3}\times\sqrt{3}$ buckled reconstruction observed by the ARPES study. On the other hand, atom A, which belongs to the same sub-lattice as atom C, exhibits buckling larger than the free-standing silicene, and possesses sp_3-like hybridized orbitals. The STM/STS results evidenced a clear correlation between hybridization of the orbitals of the Si atoms and the buckling.

References

[1] S. Cahangirov, M. Topsakal, E. Akturk, H. Sahin, and S. Ciraci, Phys. Rev. Lett. **102**, 236804 (2009).
[2] M. Ezawa, New J. Phys. **14**, 033003 (2012).
[3] C.-C. Liu, W. Feng, and Y. Yao, Phys. Rev. Lett. **107**, 076802 (2011).
[4] W.-F. Tsai, C.-Y. Huang, T.-R. Chang, H. Lin, H.-T. Jeng, and A. Bensil, Nat. Commun. **4**, 1500 (2013).
[5] P. Vogt, P. De Padova, C. Quaresima, J. Avila, E. Frantzeskakis, M. C. Asensio, A. Resta, B. Ealet, and G. Le Lay, Phys. Rev. Lett. **108**, 155501 (2012).
[6] L. Chen, C.-C. Liu, B. Feng, X. He, P. Cheng, Z. Ding, S. Meng, Y. Yao, and K. Wu, Phys. Rev. Lett. **109**, 056804 (2012).

[7] C.-L. Lin, R. Arafune, K. Kawahara, N. Tsukahara, E. Minamitani, Y. Kim, N. Takagi, and M. Kawai, Appl. Phys. Express **5**, 045802 (2012).
[8] A. Fleurence, R. Friedlein, T. Ozaki, H. Kawai, Y. Wang, and Y. Yamada-Takamura, Phys. Rev. Lett. **108**, 245501 (2012).
[9] A. Fleurence, Y. Yoshida, C.-C. Lee, T. Ozaki, Y. Yamada-Takamura, and Y. Hasegawa, Appl. Phys. Lett. **104**, 021605 (2014).
[10] R. Friedlein, A. Fleurence, J. T. Sadowski, and Y. Yamada-Takamura, Appl. Phys. Lett. **102**, 221603 (2013).

Authors
A. Fleurence[a], Y. Yoshida, C.-C. Lee[a], T. Ozaki[a], Y. Yamada-Takamura[a], and Y. Hasegawa
[a]Japan Advanced Institute of Science and Technology

Multiferroic Nanopillar Composites

Y. Matsumoto and M. Lippmaa

Composite materials can be used to elastically couple ferroelectrics and ferromagnets, producing a multiferroic material where the magnetization can be controlled by an electric field or the dielectric polarization by a magnetic field. In this work, a nanoscale pillar-and-matrix composite, consisting of a layered $Bi_5Ti_3FeO_{15}$ (BTFO) perovskite matrix and nanoscale pillars of a ferrimagnetic spinel $CoFe_2O_4$ (CFO), were used to study the effectiveness of nanoscale strain-mediated elastic coupling. The main advantage of this approach is that it may be possible to develop new types of multiferroics that can work close to room temperature and do not contain lead.

A three-dimensional model of the composite material is shown in Fig. 1(b), together with a surface electron microscope image in Fig. 1(a). The pillars form spontaneously during thin film growth due to immiscibility of the perovskite and spinel phases and extend throughout the thickness of the thin film, as shown in the cross-sectional transmission electron microscope image in Fig. 1c. Composition mapping shows nearly perfect segregation of Fe/Co and Bi/Ti in pillars with an average diameter of about 50 nm.

From the point of view of achieving elastic multiferroic coupling in a nanoscale composite, strain fields along the walls of the nanopillars are critically important. The behavior was analyzed by high-resolution electron microscopy, which showed that the nanostructure-matrix interface is heavily strained. The strain relaxes gradually in the BTFO matrix, as illustrated by the red radial arrows in Fig. 1(b). Ferroelectric switching in the BTFO matrix material was studied by piezoresponse force microscopy, showing that the polarization response depends on the volume fraction of nanopillars, reaching a maximum for a CFO volume of 35%. A bipolar poling pattern for this sample is shown in Fig. 2(b). Analysis showed the presence of both in-plane (*ab* plane) and out-of-plane (*c*-axis) polarization components, which is unusual for layered bismuth perovskite ferroelectrics where the polarization direction is in the *ab* plane. Thermodynamic Landau-Ginzburg-Devonshire (LGD) calculations showed that this is a direct result of the strain fields surrounding the nanopillars and may also be caused by the presence of shear domains at pillar boundaries that are not perfectly *c*-axis oriented. Magnetization analysis of the composites at 10 K showed that the saturation magnetization of CFO is not significantly affected by the 50 nm diameter of the nanopillars (Fig. 2a), reaching nearly the expected 4 μ_B/f.u. of bulk CFO.

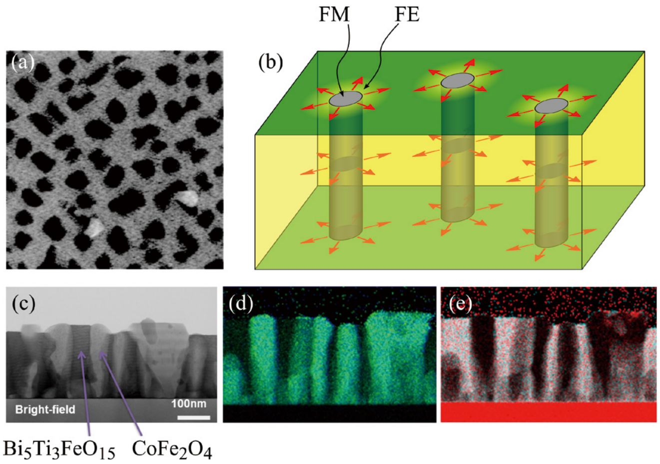

Fig. 1. (a) Scanning electron microscope image of the nanocomposite film surface and (b) a three-dimensional model of the composite material. The elastic strain field surrounding the nanopillars is marked with red arrows. (c) Cross-sectional electron microscope image and (d) Co/Fe and (e) Bi/Ti EDS mapping images.

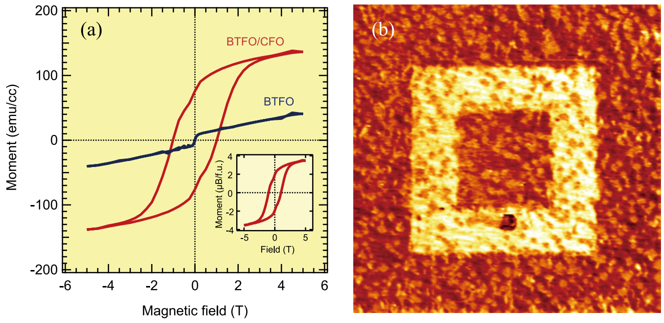

Fig. 2. (a) Magnetization comparison of a pure BTFO matrix and the BTFO/CFO nanocomposite film, showing the presence of ferromagnetism in the nanopillars. Inset shows the magnetization of a pure CFO sample. (b) A ferroelectrically poled pattern on the surface of a nanocomposite film, measured with a piezoresponse force microscope.

The work showed that systematic strain control is possible in spontaneously-formed nanopillar composites consisting of a spinel ferromagnet and a perovskite ferroelectric. The piezoresponse analysis showed that the three-dimensional nanoscale structuring and the associated strain fields are critical for obtaining suitable polarization behavior in the layered bismuth ferroelectrics. Work is now underway to determine the multiferroic response in such nanocomposite systems.

Reference

[1] A. Imai, X. Cheng, H. L. Xin, E. A. Eliseev, A. N. Morozovska, S. V. Kalinin, R. Takahashi, M. Lippmaa, Y. Matsumoto, and V. Nagarajan, ACS Nano **7**, 11079 (2013).

Authors
A. Imai[a,b], X. Cheng[b], H. L. Xin[c], E. A, Eliseev[d], A. N. Morozovska[d], S. V. Kalinin[e], R. Takahashi, M. Lippmaa, Y. Matsumoto[f], and V. Nagarajan[b]
[a]Tokyo Institute of Technology
[b]University of New South Wales
[c]Brookhaven National Laboratory
[d]National Academy of Sciences of Ukraine
[e]Oak Ridge National Laboratory
[f]Tohoku University

Development of High Pressure, High Field and Multi-Frequency ESR System Using Hybrid Type Pressure Cell

T. Sakurai, H. Ohta, and Y. Uwatoko

Pressure has been recognized as one of the most important parameters to explore novel phenomena around the quantum critical point for quantum spin systems. As the high field and multi-frequency ESR is a powerful means to study quantum spin systems from the microscopic point of view, it is very useful to introduce the parameter of pressure to the ESR measurement. We developed the high pressure, high field and multi-frequency ESR apparatus by combining the single-pass transmission type ESR apparatus using the pulsed high magnetic field up to 55 T and the unique piston cylinder pressure cell previously [1]. The most characteristic feature of this pressure cell is that all inner parts are made of zirconium oxide which has relatively good transmittance of electromagnetic wave. It enables us to observe ESR under pressure. However, the pressure range is limited below 1 GPa at most because the single layer cylinder is used and its inner and outer diameters are 3 and 8 mm, respectively. The limited sample space also affects the signal intensity. The signal to noise ratio is not enough to study spin states in detail. Moreover, several compounds have been suggested to have the critical pressures above 2 GPa recently [2]. Therefore, the new ESR apparatus which has higher pressure range and sensitivity is required. In this study, we have developed new ESR apparatus which uses the combination of the hybrid type pressure cell and the superconducting magnet to improve these two points [3].

Figure 1 shows the newly developed pressure cell for multi-frequency ESR measurement. The hybrid type cylinder which consists of inner NiCrAl cylinder and outer CuBe sleeve is used to achieve both larger sample space and higher pressure range above 2 GPa. The inner and outer diameters of the cylinder are 5 and 28 mm, respectively. The inner parts are all made of zirconium oxide. We confirmed that the pressure can be generated over 2.5 GPa at low temperature. However, they are sometimes cracked when the load is applied to generate the pressure over 2.5 GPa at low temperature. We have also developed new ESR apparatus using cryogen free superconducting magnet with wide bore. Gunn oscillator and backward wave oscillator which cover the frequency region from 50 to 400 GHz are used as the light source. The ESR signal is detected by an InSb detector and

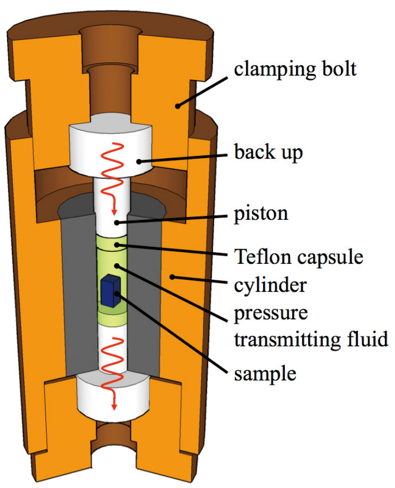

Fig. 1. Cut view of the hybrid type pressure cell for multi-frequency ESR measurement. Red lines show the electromagnetic wave.

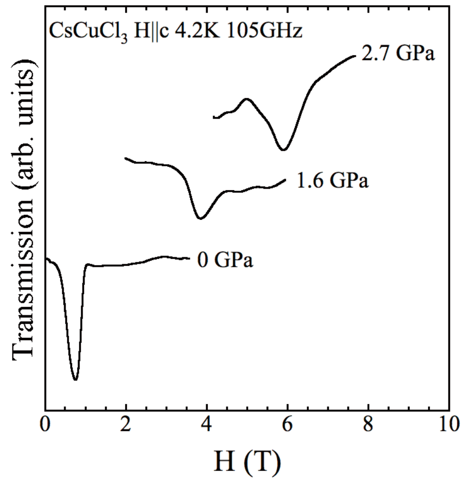

Fig. 2. Pressure dependence ESR spectra of $CsCuCl_3$ for H||c at 105 GHz.

the signal is amplified by the lock-in technique. The larger sample space and the use of the lock-in technique make the sensitivity higher than previous apparatus successfully. Figure 2 shows typical ESR spectra obtained by the developed high pressure ESR apparatus. $CsCuCl_3$ is a well known ABX_3 type antiferromagnet with T_N = 11 K. Figure 2 shows the antiferromagnetic resonance of this compound obtained at 4.2 K for H||c. It clearly shows that the resonance field shifts to the higher field side as the pressure is increased. This corresponds to the increase of the antiferromagnetic gap on applying the pressure [4]. The maximum pressure obtained in this measurement is 2.7 GPa as shown in Fig. 2. This result also shows that this high pressure ESR apparatus is promising tool to clarify the spin states of novel pressure induced phenomenon for quantum spin system.

References

[1] T. Sakurai *et al*., Rev. Sci. Instrum. **78**, 065107 (2007).
[2] T. Sakurai *et al*., J. Phys. Conf. Ser. **150**, 042171 (2009).
[3] K. Fujimoto *et al*., Appl. Magn. Reson. **44**, 893 (2013).
[4] T. Sakurai *et al*., J. Phys. Conf. Ser. **215**, 012184 (2010).

Author
T. Sakurai[a], S. Okubo[a], H. Ohta[a], K. Matsubayashi, and Y. Uwatoko
[a]Kobe University

One-Hundred-Million-Atom Electronic Structure Calculations on the K Computer

T. Hoshi

In the current (peta-scale) or next generation (exa-scale) computational physics, a crucial issue is ‘Application-Algorithm-Architecture co-design’ or inter-disciplinary collaborations among physics, applied mathematics and the high-performance computation field.

Here we report that one-hundred-million atom (100-nm-scale) electronic structure calculations were realized on the K computer [1,2]. The methodologies were based on the co-design. In particular, the novel iterative (Krylov-subspace) algorithms were constructed for the generalized shifted linear equations ($(zS-H)x=b$), instead of the conventional generalized eigen-value equation ($Hy=eSy$) (See [3,4] and reference therein). The methods give the real-space Green’s function, instead of eigen states. These solvers were implemented in our order-N calculation code ELSES (http://www.elses.jp/) with modeled (tight-binding) systems based on *ab* initio calculations. These solver algorithms are purely mathematical and applicable to large-matrix problems in many computational physics fields beyond electronic structure calculations.

In Fig. 1, the calculations show high parallel efficiency ('strong scaling') with up to the full core calculations of the K computer for one-hundred-million-atom (100-nm-scale) systems [1,2]. The calculated systems are amorphous-like conjugated polymer (aCP), poly-(9,9 dioctyl-fluorene) with N=102,238,848 atoms and sp^2-sp^3 nano-composite carbon solid (NCCS) with N=103,219,200 atoms. The high parallel efficiency stems not only from the fundamental mathematical theory but also from detailed techniques, such as programing techniques for saving memory and communication costs and a parallel file I/O [4].

An application study with NCCS is picked out [4]. The study is an early-stage one on the formation process of the nano-polycrystalline diamond (NPD), a novel ultra-hard material [5]. NPD is obtained by direct conversion sintering process from graphite under high pressure and high temperature and has characteristic 10-nm-scale lamellar-like structures. NPD is of industrial importance for its extreme hardness and strength and Sumitomo Electric Industries. Ltd. began commercial production from 2012. Our simulation is motivated by the investigation of possible precursor structures in the formation process of NPD and the structures should be nano-scale composites of sp^2 (graphite-like) and sp^3 (diamond-like) domains. Figure 2 shows the nano-domain analysis on the NCCS. The structure is a result of our simulation. The π-type crystalline orbital Hamiltonian population (πCOHP) analysis [4], an analysis method based on the Green's function, was used so as to distinguish the sp^2 and sp^3 domains. The analysis clarifies shapes of domains and structure of domain boundaries from huge electronic structure data and gives theoretical foundations of the composite.

General future aspects are (i) large-scale calculation methods for optical and transport properties and (ii) applications to various systems, such as organic materials.

The fundamental mathematical theory was constructed in the collaboration with applied mathematics researchers; T. Sogabe (Aichi Prefectural University) and S.-L. Zhang (Nagoya University) [3]. The code for massive parallelism was developed with the supercomputers, the systems B and C, at ISSP and the K computer was used in the research proposals of hp120170, hp120280 and hp130052.

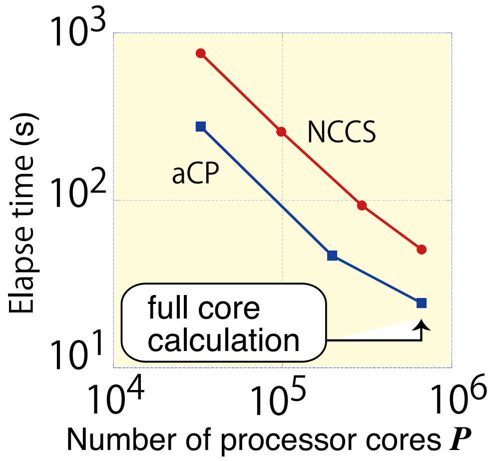

Fig. 1. Benchmark for the parallel efficiency ('strong scaling') on the K computer with one hundred million atoms. [1,2] The calculated systems are amorphous-like conjugated polymer (aCP), poly-(9,9 dioctyl-fluorene) and sp^2-sp^3 nano-composite carbon solid (NCCS).

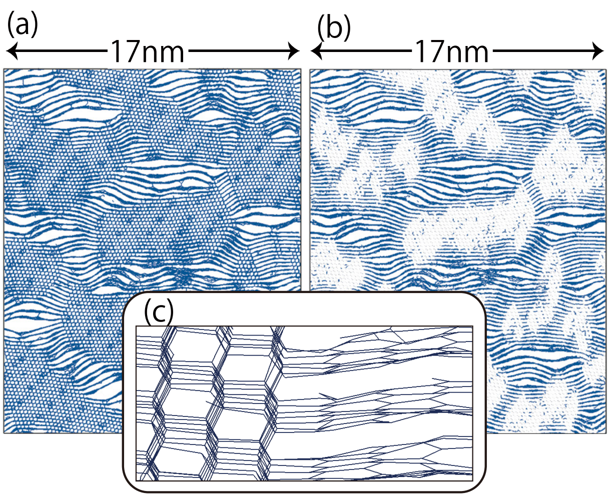

Fig. 2. Nano-domain analysis of NCCS visualized with the πCOHP [4]. The sp^2 (graphite-like) and sp^3 (diamond-like) domains are visualized in (a), while only the sp^2 domains are visualized in (b). A closeup of an sp^2- sp^3 domain boundary is shown in (c).

References

[1] T. Hoshi *et al.*, JPS Conf. Proc. **1**, 016004 (2014).
[2] T. Hoshi *et al.*, Proceedings of Science, in press (Preprint : http://arxiv.org/abs/1402.7285/)
[3] T. Hoshi *et al.*, J. Phys.: Condens. Matter **21**, 165502 (2012).
[4] T. Hoshi *et al.*, J. Phys. Soc. Jpn. **82**, 023710 (2013).
[5] T. Irifune *et al.*, Nature **421**, 599 (2003).

Author
T. Hoshi[a,b]
[a]Tottori University
[b]JST-CREST

Rolled Lamellar Structure of Surfactant Membranes Induced by Shear Flow

H. Shiba, H. Noguchi, and G. Gompper

Surfactant molecules in water self-assemble into various structures such as micelles and bilayer membranes, which display a rich variety of rheological properties. It is known that under shear flow, lamellar membranes can be oriented parallel or perpendicular to the shear-gradient direction. Surprisingly, under high shear flow, the membranes transform the planar lamellae to a closely-packed multi-lamellar vesicle structures, so-called the onion phase. The onion radius is reversible and can be described by a unique decreasing function of the shear rate. Although this onion phase was experimentally discovered 20 years ago,

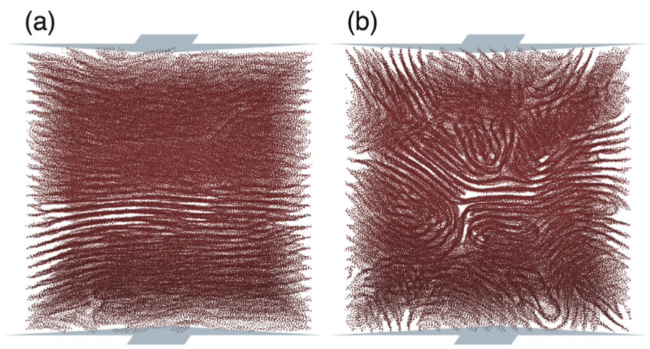

Fig. 1. Snapshot of surfactant membranes in simple shear flow. (a) A planar lamellae structure is formed at a low shear rate. (b) At a high shear rate, a rolled lamellar structure is formed perpendicularly to the flow direction. Top and bottom arrows represent the flow directions. The membranes are viewed from the flow direction.

the formation mechanism is not understood so far. Since the onion size is in a micro meter scale, it is far beyond applicable length scales for molecular simulations. Thus, we employed a highly coarse-grained membrane model, a meshless-membrane model, in which a membrane particle represents not a lipid molecule but a patch of the bilayer membrane. The particles self-assemble into membranes via multibody potential interactions.

At low shear rates, planar lamellae structures are formed at large membrane volume fractions (see Fig. 1a). At high shear rates, lamellar states exhibit undulation instability, leading to rolled or cylindrical membrane shapes oriented in the flow direction (see Fig. 1b). At even higher shear rate, the planar lamellae structures are formed again. The spatial symmetry and the structure factor of this rolled state agree with those of intermediate states during lamellar-to-onion transition measured by time-resolved small angle neutron and X-ray scattering experiments. A cylindrical or wavy lamellar structure was speculated to be this intermediate structure, but could not be distinguished from the scattering pattern alone. Our simulation results revealed that it is a rolled structure instead of regular cylindrical or wavy structures. The planar membranes become unstable in the flow gradient direction so that the membranes are rolled in perpendicular to the flow direction. We have not reproduced the onion structure itself. We will investigate the effects of defects and finite system size to pursue understanding of the onion phase.

Reference

[1] H. Shiba, H. Noguchi, and G. Gompper, J. Chem. Phys. **139**, 014702 (2013).

Authors
H. Shiba, H. Noguchi, and G. Gompper[a]
[a]Forschungszentrum Juelich

Neutron Scattering Study on Alternating Spin-3/2 Chain Compound $YCrGeO_5$

M. Hase, T. Masuda, and K. Kindo

Neutron scattering technique is known as a powerful tool to probe the spin correlation in magnetic materials. Among various types of neutron instruments the chopper spectrometer is designed particularly for collecting inelastic neutron scattering (INS) spectrum. Combination of position sensitive detectors and accumulative data-acquiring system leads to a state-of-art instrument for measuring the dynamical structure factor $S(\mathbf{q},\omega)$. Neutron Scattering Laboratory operates the High Resolution Chopper (HRC) spectrometer installed in J-PARC/MLF. The instrument covers the incident neutron energy range 10 meV ≤ E_i ≤ 500 meV and the scattering angle range 0.3° ≤ ψ ≤ 40°, which meets typical magnetic scattering in most of magnetic materials. In this highlight we introduce a recent study on an alternating spin-3/2 chain compound by using the HRC spectrometer.

The phase diagrams of the alternating spin chain systems for various magnitudes of spin were extensively studied theoretically [1-4]. The model Hamiltonian is $\mathcal{H} = J\Sigma_i(1-(-1)^i\delta)S_i \cdot S_{i+1}$. In case of spin-3/2 chain the spin alternation δ induces a spin gap at $0 < \delta < 0.42(2)$ and $0.42(2) < \delta \le 1$, and the ground state is non-magnetic singlet. Tomonaga-Luttinger liquid (TTL) state exists at $\delta = 0$ and 0.42(2). So far no experimental study has been reported because of absence of the model compound. Recently we found that $RCrGeO_5$ is a rare experimental realization of the spin-3/2 alternating spin chain. In this study we performed inelastic neutron scattering experiments on the polycrystalline sample of $YCrGeO_5$ to observe the magnetic excitation and to identify the spin Hamiltonian.

INS spectrums are shown in Figs. (a) and (b). The excitations are observed in the energy range of 8 meV ≤ $\hbar\omega$ ≤ 23 meV at 4.0 K and the intensity decreases with the increase of Q. The intensity is suppressed at higher temperature of 199 K. The results mean that the observed excitations are dominated by magnetic scattering. No excitation is observed at $\hbar\omega \le 8$ meV and this reveals the existence of the spin gap. The obtained powder INS spectrum was converted to the one-dimensional $S(q,\omega)$ [5] as shown in Fig. (c). The obtained profile was reproduced by empirical dispersion formula $\hbar\omega = \sqrt{A^2(\sin k)^2 + \Delta^2}$ with the parameters Δ = 10 meV and A = 20 meV. Figure (d) shows the dynamical structure factor calculated by DMRG with δ = 0.75 and Δ/J=1.1 and the calculation is consistent with the experiment. The measured magnitude of the spin gap is Δ = 10 meV

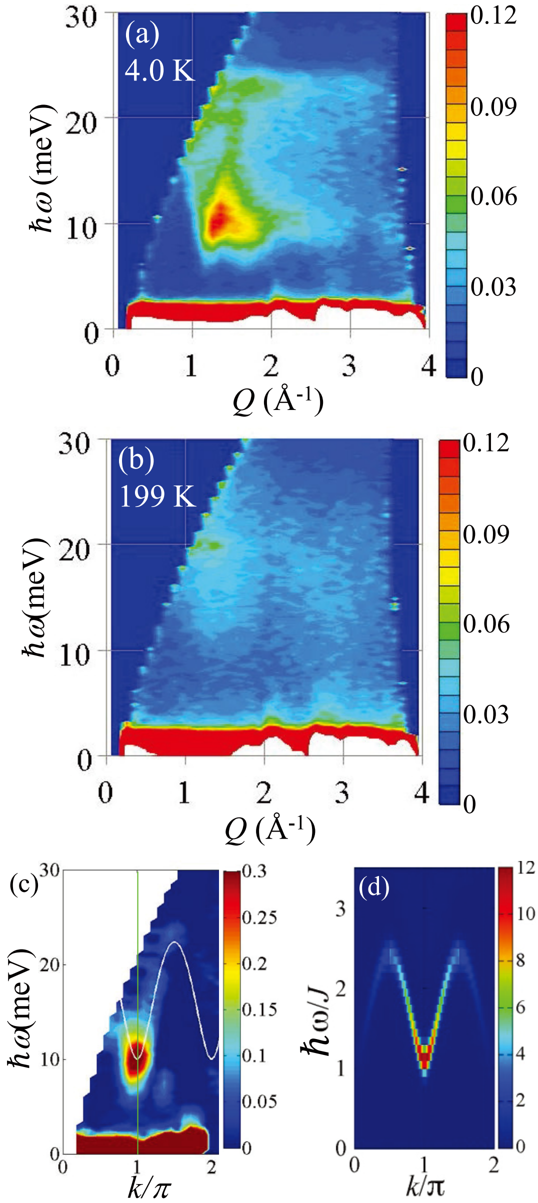

Fig. 1. (a) Inelastic neutron scattering (INS) spectrum of $YCrGeO_5$ at 4.0 K. (b) INS spectrum of $YCrGeO_5$ at 199 K. (c) INS spectrum converted to one-dimensional dynamical structure factor. (d) Calculated dynamical structure factor by DMRG method.

and this leads to J = 11meV. By using these parameters the magnetic susceptibility was quantitatively reproduced. Thus our study revealed that $YCrGeO_5$ is the first experimental realization of the spin-3/2 alternating spin chain.

As shown in Figs. (a) and (b) INS spectrum with high experimental resolution can be efficiently collected by using HRC spectrometer. Although the polycrystalline sample form, one-dimensional $S(q,\omega)$ can be obtained by the elaborated analysis. Combination of chopper spectrometer and polycrystalline sample will be a defacto standard in forthcoming era of neutron science.

References

[1] Y. Kato and A. Tanaka, J. Phys. Soc. Jpn. **63**, 1277 (1994).
[2] M. Kohno, M. Takahashi, and M. Hagiwara, Phys. Rev. B **57**, 1046 (1998).
[3] M. Yajima and M. Takahashi, J. Phys. Soc. Jpn. **65**, 39 (1996).
[4] S. Yamamoto, Phys. Rev. B **55**, 3603 (1997).
[5] K. Tomiyasu, M. Fujita, A. I. Kolesnikov, R. I. Bewley, M. J. Bull, and S. M. Bennington, Appl. Phys. Lett. **94**, 092502 (2009).

Authors

M. Hase[a], M. Soda, T. Masuda, D. Kawana, T.Yokoo[b], S. Itoh[b], A. Matsuo, K. Kindo, and M. Kohno[a]
[a]National Institute for Materials Science (NIMS)
[b]High Energy Accelerator Research Organization (KEK)

Detection of Berry's Phase in a Bulk Rashba Semiconductor

H. Murakawa, M. Tokunaga, and Y. Tokura

The geometrical information of the system parameter can be encoded in the wave function as a Berry's phase and governs the system properties. In quantum systems, Berry's phase can be a source for various emergent phenomena. Despite its ubiquity, there are few experimental observations of Berry's phase of bulk states. Here, we report detection of a nontrivial π Berry's phase in the bulk Rashba semiconductor BiTeI via analysis of the Shubnikov-de Haas (SdH) effect.

BiTeI has a polar crystal structure made up of stacked layers of bismuth (Bi), tellurium (Te) and iodine (I) atoms. Because of the absence of inversion symmetry and the strong polarity of the system, accompanied by the strong spin-orbit interaction of Bi, an extremely large Rashba spin splitting occurs in a bulk scale (Fig. 1A). As shown in Fig. 1B, two coaxial spin polarized Fermi surfaces verging

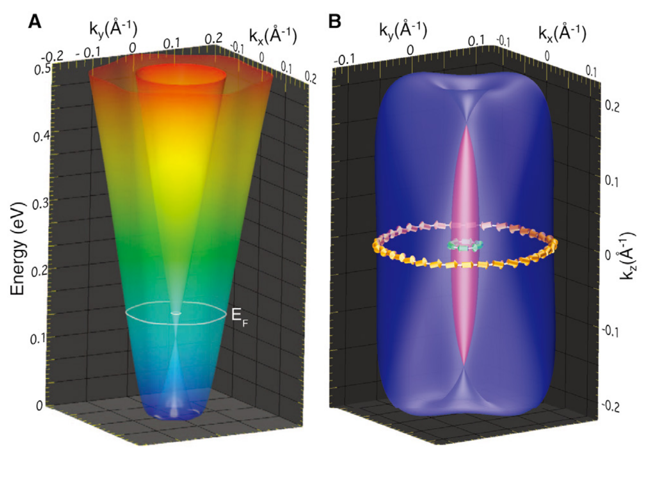

Fig. 1. (A) Energy band dispersion of the Rashba spin split band in BiTeI. (B) The inner and outer Fermi surfaces and helical spin textures (arrows) in BiTeI.

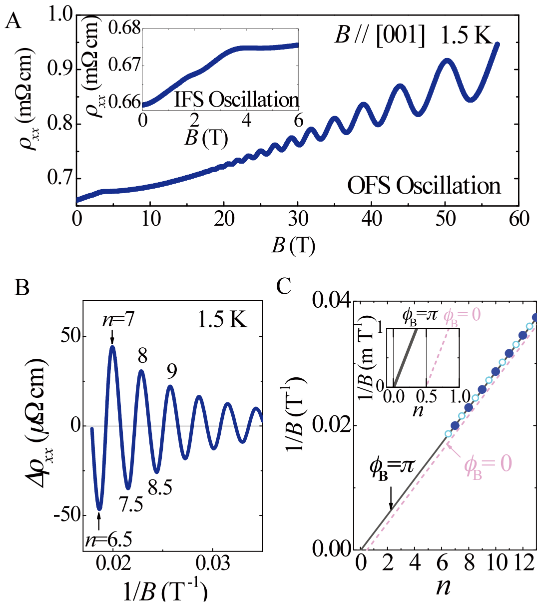

Fig. 2. (A) Magnetoresistivity of BiTeI sample. (B) The oscillatory component as a function of $1/B$. (C) Landau index plot of the outer Fermi. (inset) Magnified view around the intercept.

at Dirac point, namely, inner and outer Fermi surfaces (IFS and OFS, respectively) are formed. Theoretical prediction indicates that electrons on both FSs with the circular spin texture acquire π Berry's phase ($\phi_B = \pi$) and varies the system energy from the trivial case ($\phi_B = 0$). Under magnetic field, Landau levels in a Dirac system with $\phi_B = \pi$ locate at the middle of those in a system with $\phi_B = 0$. Thus, π Berry's phase can be detected as a π phase shift in quantum oscillation.

The extremely large Rashba spin splitting in BiTeI has great advantages on observing the Berry's phase. The large ratio of the extremal cross-sectional areas (A_N) of IFS and OFS enables the clear separation of the two sets of SdH oscillations. Moreover, the giant Rashba energy can dominate the Zeeman effect and preserve the circular spin texture even in a high magnetic field region. According to the Lifshitz-Onsager quantization rule, $A_N\hbar/eB = 2\pi(n + 1/2 - \phi_B/2\pi) = 2\pi(n + \gamma)$, Berry's phase is obtained as an intercept value γ in the linear relation between 1/B and Landau index number n. For precise evaluation, observation of the SdH oscillation down to lower Landau level is important. Therefore, high-magnetic field measurement with use of the non-destructive pulse magnet can be a powerful tool. Figure 2A shows the SdH oscillation from the OFS up to 56 T. We assign integer indices to the ρ_{xx} peak positions in $1/B$ and half integer indices to the ρ_{xx} valley positions (Fig. 2B). As shown in Fig. 2C, the interpolation line has almost zero intercept ($\gamma = 1/2 - \phi_B/2\pi = 0$), confirming the existence of π Berry's phase in the 3-dimensional Rashba semiconductor BiTeI.

Reference

[1] H. Murakawa, M. S. Bahramy, M. Tokunaga, Y. Kohama, C. Bell, Y. Kaneko, N. Nagaosa, H. Y. Hwang, and Y. Tokura, Science **342**, 1490 (2013).

Authors

H. Murakawa[a], M. S. Bahramy[b], M. Tokunaga, Y. Kohama, C. Bell[c], Y. Kaneko[a], N. Nagaosa[a,b], H.Y. Hwang[a,c], and Y. Tokura[a,b]
[a]Riken CEMS
[b]The University of Tokyo
[c]Stanford University

Discovery of Novel Phase of Solid Oxygen in Ultrahigh Magnetic Fields

T. C. Kobayashi and Y. H. Matsuda

Molecular oxygen has the spin S = 1 and the relation between the magnetic interaction and the crystal structure has been attracting attention of material scientists for a long time [1]. In the present work, we discovered a novel phase of solid oxygen as a result of the first-order structural phase transition by applying an extraordinarily strong magnetic field of up to 193 Tesla [2]. The change in the crystal symmetry due to the rearrangement of O_2 molecules is strongly suggested, which can make the new oxygen phase ferromagnetic. Since all known seven phases of solid oxygen have the antiferromagnetic nature, it is remarkable to obtain ferromagnetic oxygen.

The magnetization and magneto-transmission measurements have been performed in ultrahigh fields using a destructive manner, the single-turn coil technique. The magnetic field was applied in the α-phase of solid oxygen at low temperatures (T < 24 K). As shown in Fig. 1, we found that the magnetization rapidly increased at around 125 T. This is a clear evidence of the field-induced magnetic phase transition. Since the magnetization process has the large hysteresis, the transition is expected to be of first order. Figure 2 shows the time dependence of the magnetic field and two-dimensional magneto-transmission image. You can see that something drastic happens at very high magnetic fields. The field where this phenomenon is seen almost corresponds to the critical field of the magnetization jump shown in Fig. 1.

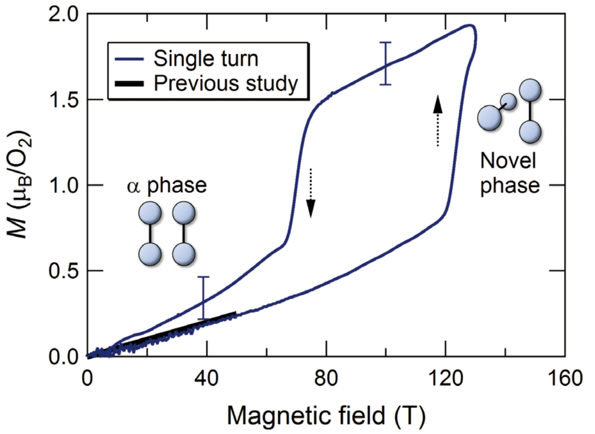

Fig. 1. The magnetization curve in α-oxygen at 9 K up to 129 T.

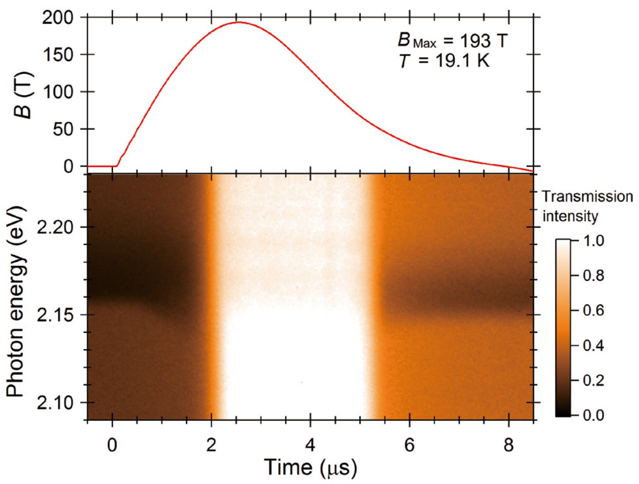

Fig. 2. (a) The waveform of the pulsed magnetic field. (b) The two-dimensional magneto-transmission image of α-oxygen.

The structural phase transition along with the magnetic transition explains the experimental findings; the significant increase of the light transmission is due to the reduction of the classical light scattering at the domain boundaries. In the strong magnetic field, the crystal structure becomes isotropic (cubic) from the anisotropic one (monoclinic). The origin of the phase transition is suggested to be the rearrangement of O_2 molecules, which is driven by the change in the exchange interaction depending on the spatial arrangement of the O_2 molecules.

The discovered novel phase is the eighth phase of solid oxygen, which has the different geometry of O_2 molecules from other seven phases. The state-of-the-art high magnetic field technique was essential in this discovery. Nowadays, in materials science, many treasures waiting for discovery are expected at the frontier of extreme high field.

References

[1] Y. A. Freiman, and H. J. Jodl, Phys. Rep. **401**, 1 (2004) and references therein.

[2] T. Nomura, Y. H. Matsuda, S. Takeyama, A. Matsuo, K. Kindo, J. L. Her, and T. C. Kobayashi, Phys. Rev. Lett., Editors' Suggestion, (2014) in press.

Authors

T. C. Kobayashi[a], T. Nomura, Y. H. Matsuda, S. Takeyama, A. Matsuo, K. Kindo, and J. L. Her[b]

[a]Okayama University

[b]Chang Gung University

Structure Determination of Silicene on Ag(111) by Low-Energy Electron Diffraction

K. Kawahara, T. Shirasawa, and N. Takagi

Silicene, a 2-dimensional honeycomb lattice of Si, attracts much attention since it is predicted to acquire exotic features such as massless Dirac fermions and high electron mobility [1]. As the spin orbit coupling of Si is 1000 times larger than that of C, silicene is one of the most interesting candidates for 2-dimensional topological insulator [2]. In addition, silicene should match with the current Si based technology. These characteristics make silicene promising in the next generation devices.

Several groups reported synthesis of silicene on Ag(111) [3-8]. Silicene forms 4×4 superstructure on the Ag(111) surface [4-8]. On a fundamental question '*Does 4×4 silicene have Dirac fermions?*', the arguments conflict among the research groups [4,7]. The electronic structure is connected with the atomic arrangement. Thus, by determining the atomic position, we can answer the above question. However, the geometric structure of 4x4 silicene has not been established. Several groups proposed the structural models of 4×4 silicene based on the result of scanning tunneling microscopy (STM) [4-8]. The reasonable model is a buckled structural model constructed by the STM and density functional theory (DFT) calculations [4-7]. In contrast, Feng *et al.* claimed that the corner-hole like features observed in the STM image are assigned to missing Si atoms and proposed a model in which hydrogen atoms terminate the dangling bonds of Si atoms [8]. The discrepancy arises from that the STM image is convolution of the geometric structure together with the electronic density of states. Hence we cannot determine the positions of the individual atoms in the 4x4 silicene only by

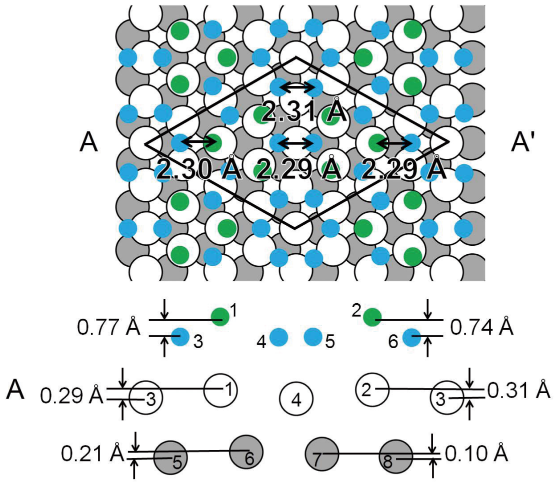

Fig. 1. The top and side views of the best-fit structure of 4×4 silicene. The side view is the cross section along the AA'. Green and blue balls represent Si atoms. The green Si atoms are moved up to the vacuum. White and Gray balls represent Ag atoms in the first and second layer, respectively.

STM measurements.

Electron diffraction is one of the most reliable and powerful techniques to determine the geometric structure. We have determined the geometric structure of 4×4 silicene by using low-energy electron diffraction [9]. We examined the regularly-buckled silicene, the buckled structure where six Si atoms are displaced and the structural model proposed by Feng *et al*. The optimized reliability factor (R-factor) of the buckled structure shown in Fig. 1 was 0.17. The optimized R factor of the model proposed by Feng *et al.* [8] was 0.48. The buckled structural model as Fig. 1 reproduced the experimental results very well. Figure 1 shows the top and cross sectional views of the best-fit structural model for 4×4 silicene. The green Si atoms are displaced perpendicularly to the surface and silicene forms into a buckled structure. The Si-Si bond lengths range from 2.29 to 2.31 Å, which are shorter than that for the bulk diamond structure. Substrate Ag atoms are displaced vertically at the interface. The R-factor is 0.52 for the model without the displacement of Ag, indicating that the displacement of Ag atoms is a key factor to determine the structure of 4×4 silicene. The displacement of Ag also reflects the strong interaction between silicene and Ag substrate, supporting the experimental results showing absence of the Dirac fermions [7]. In addition, the experimentally determined structure of 4×4 silicene matches quite well with that optimized by DFT calculations [4,5]. Thus, the geometric structure of 4×4 silicene on Ag(111) was completely clarified.

References

[1] S. Cahangirov *et al*., Phys. Rev. Lett. **102**, 236804 (2009).
[2] M. Ezawa, Phys. Rev. Lett. **109**, 055502 (2012).
[3] B. Lalmi *et al*.,Appl. Phys. Lett. **97**, 223109 (2010).
[4] P. Vogt *et al*.,Phys. Rev. Lett. **108**, 155501 (2012).
[5] C.-L. Lin *et al*., Appl. Phys. Express **5**, 045802 (2012).
[6] R. Arafune *et al*., Surf. Sci. **608**, 297 (2013).
[7] C.-L. Lin *et al*., Phys. Rev. Lett. **110**, 076801 (2013).
[8] B. Feng *et al*., Nano Lett.**12**, 3507 (2012).
[9] K. Kawahara *et al*., Surf. Sci. **623**, 25 (2014).

Authors

K. Kawahara[a], T. Shirasawa, R. Arafune[b], C.-L. Lin[a], T. Takahashi, M. Kawai[a], and N. Takagi[a]
[a]The University of Tokyo
[b]IMANA-NIMS

Observing Hot Carrier Distribution in an n-type Epitaxial Graphene on a SiC Substrate

H. Fukidome and I. Matsuda

A monolayer graphene is "supermaterial" that is the thinnest, lightest, and strongest material with ultrahigh electrical and thermal conductivity. Recently optical properties of the graphene have also attracted interests in the field of developing optoelectronic, plasmonic and nanophotonic devices. However, detailed mechanisms of the photo-induced phenomena of a graphene, such as the multiple carrier generation, have not been understood and, thus, the direct investigation of the non-equilibrium carrier dynamics has been strongly called for.

In the present research, we carried out femtoseconds(fs)-time- and angle-resolved photoemission experiment to observe the temporal variation of the Dirac electrons after the optical pumping in *real time*. The measurement was carried out using high-harmonic generation (HHG) laser system based on the Ti:Sappire laser (hν=1.57 eV). Photon energy of 28.26 eV for the HHG laser pulse is generated by irradiating the second harmonic laser pulses (hν =3.14 eV) at Ar gas and it is high enough to cover the electron momentum of the Dirac band at the K point in angle-resolved photoemission measurement. The time-resolved data were obtained using the pump (3.14 eV laser) and probe (HHG) method with a repetition rate of 1 kHz.

Figure 1(a) shows a series of angle-integrated spectra taken with a laser pumping power of 2.5 mW at various delay times. Dispersion of the Dirac bands, observed by angle-resolved photoemission at the K point, is shown in the inset. With laser pumping (t=0), the photoemission intensity of the upper Dirac band (UDB) decreases significantly while that of the lower Dirac band (LDB) remains constant. Around the energy corresponding to the Fermi energy, the spectral tail extends in energy. The slope of the spectral edge also becomes small. At each delay time, the

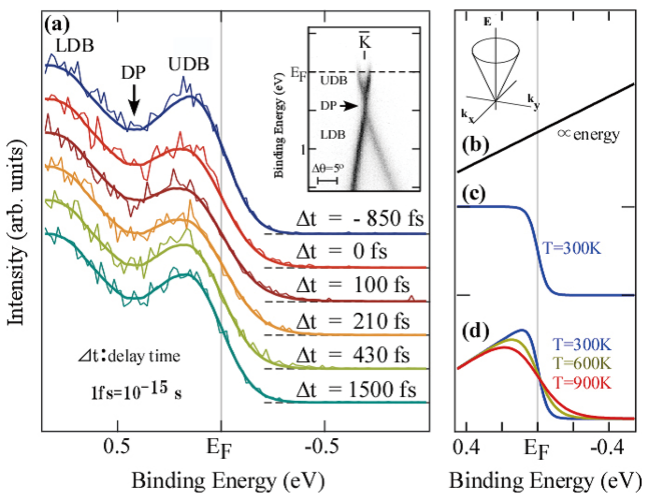

Fig. 1. (a) Comparison of the spectra at different delay times. The experimental spectra were taken at a photon energy of 28.26 eV at various delay times with pumping laser irradiation (hν=3.14 eV). The intensity variation for the UDB is clearly reproduced by the simulated result (d) while the intensity for the LDB is unchanged. The inset shows dispersion of the Dirac bands near the Fermi level (E_F). The upper Dirac band (UDB) and lower Dirac band (LDB) are labeled in the figure and the Dirac Point (DP) is indicated by an arrow. (b)–(d) Simulation of energy spectra for two cases of Dirac free electrons. The inset shows their two-dimensional band dispersion. (b) density of states, (c) Fermi–Dirac function, and (d) resulting spectra.

raw experimental data, drawn with thin colored lines, are curve-fitted with a function that is a product of density of states of graphene, Fig. 1 (b), and the Fermi-Dirac function, Fig. 1(c). In the spectral simulation of Fig. 1 (d), the Fermi edge shows a peak-like structure, and the peak top shifts toward higher binding energy at higher temperature. In Fig. 1(a), the fitting results are drawn through raw experimental data with bold colored lines. The temporal evolution in Fig. 1(a) is described by comparing it with the intensities simulated in Fig. 1(d) , and it reflects the time evolution of the electronic temperature, that is, the transient distribution of the hot carriers (electrons).

Reference

[1] T. Someya, H. Fukidome, Y. Ishida, R. Yoshida, T. Iimori, R. Yukawa, K. Akikubo, Sh. Yamamoto, S. Yamamoto, T. Yamamoto, T. Kanai, K. Funakubo, M. Suemitsu, J. Itatani, F. Komori, S. Shin, and I. Matsuda, Appl. Phys. Lett. **104**, 161103 (2014).

Authors

I. Matsuda, H. Fukidome[a], J. Itatani, S. Shin, and F. Komori
[a]Tohoku University

Electronic Structure of Carbon-Related Catalysts During Fuel Cell Operation by Soft X-Ray Emission Spectroscopy

H. Niwa, Y. Harada, and M. Oshima

Polymer electrolyte fuel cells (PEFCs) are expected to be promising power sources of high efficiency, low operating temperature, and low pollution for transportation and residential applications. Recently, carbon-based catalysts are getting considerable attention since adequately designed carbon-based catalysts show high ORR activities and are expected to be cathode catalysts alternative to conventional Pt-based catalysts [1,2]. The origin of their high ORR activities should be elucidated to further enhance the activities for commercialization. Previous electronic structure studies on carbon-based catalysts were mostly done at ex situ condition[3]. However, the results were not always conclusive because they did not observe the chemical state of each element under PEFC working condition. To further explore the ORR mechanism of carbon-based cathode catalysts,

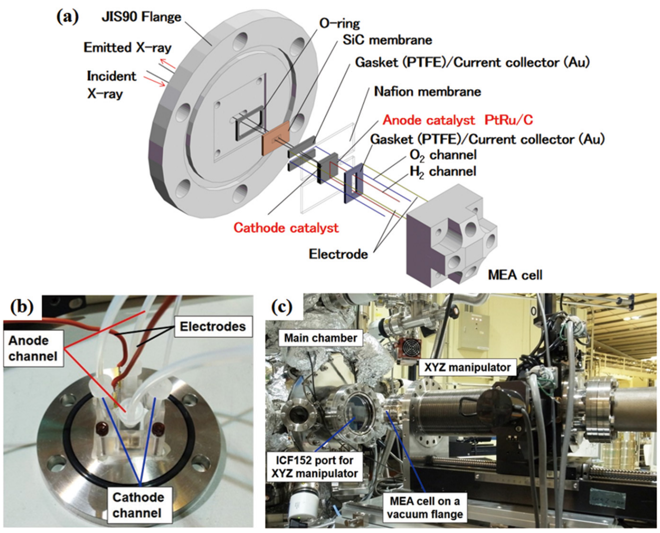

Fig. 1. (a) Schematic view of the MEA cell for operando SXE measurements. (b) Photograph of the MEA cell on a vacuum flange. (c) Photograph of a XYZ manipulator and a main chamber.

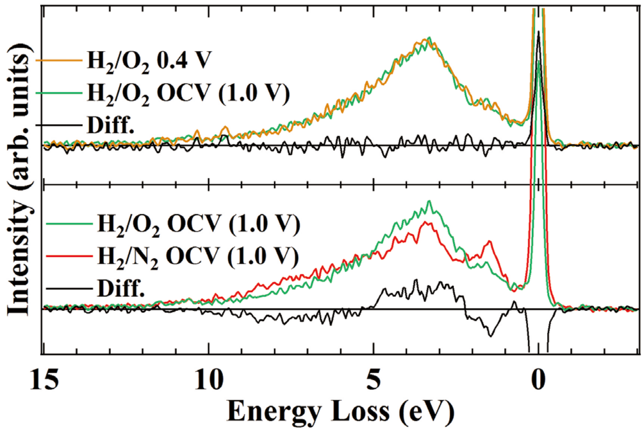

Fig. 2. Smoothed Fe 2*p* SXE spectra compared with the open circuit voltage (lower panel) and the same gas condition (upper panel). Black solid lines are difference spectra.

operando observation of the electronic structure is strongly required.

Here we report a novel electrochemical cell system developed for operando soft X-ray emission spectroscopy of cathode catalysts for polymer electrolyte fuel cells at BL07LSU of SPring-8[4]. Incorporating a membrane electrode assembly on a vacuum compatible flange (Fig. 1), the system enables direct observation of element-specific electronic structure that changes with gaseous and potential conditions for electrochemical reaction. We have successfully observed the electronic structure of iron in the iron phthalocyanine-based cathode catalyst under various working conditions by the operando soft X-ray emission spectroscopy. At open circuit voltage it is found that an oxidized iron site exists even after reductive high temperature pyrolysis and is active for oxygen adsorption (Fig. 2), which is not expected from ex situ results for powder samples where metallic iron site inactive for ORR dominates.

References

[1] W. Y. Wong, W. R.W. Daud, A. B. Mohamad, A. A. H. Kadhum, E. H. Majlan, and K. S. Loh, Diam. Relat. Mater. **22**, 12 (2012).
[2] F. Jaouen, E. Proietti, M. Lefèvre, R. Chenitz, J.-P. Dodelet, G. Wu, H. T. Chung, C. M. Johnston, and P. Zelenay, Ene. Environ. Sci. **4**, 114 (2011).
[3] U. I. Kramm, I. Abs-Wurmbach, I. Herrmann-Geppert, J. Radnik, S. Fiechter, and P. Bogdanoff, J. Electrochem. Soc. **158**, B69 (2011).
[4] H. Niwa, H. Kiuchi , J. Miyawaki, Y. Harada, M. Oshima, Y. Nabae, and T. Aoki, Electrochem. Commun. **35**, 57 (2013).

Authors

H. Niwa, H. Kiuchi[a], J. Miyawaki, Y. Harada, M. Oshima[a], Y. Nabae[b], and T. Aoki[c]
[a]The University of Tokyo
[b]Tokyo Institute of Technology
[c]Toshiba Fuel Cell Power Systems Corporation

Clarification of Mechanism of Ferromagnetism in Ferromagnetic Semiconductor

M. Kobayashi, A. Tanaka, and Y. Harada

A ferromagnetic semiconductor (FMS), in which a host semiconductor is doped with a low concentration of magnetic ions, has attracted much attention in spintronics, which exploits the properties of magnets for electronics

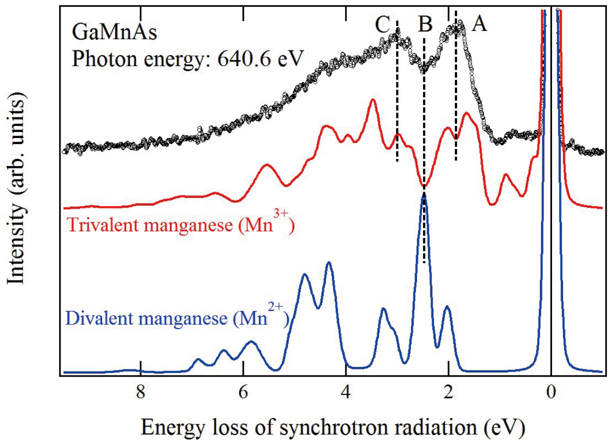

Fig. 1. Soft X-ray emission spectrum of GaMnAs and simulation results. The simulation result for Mn^{3+} (red) is in good agreement with the experimental spectrum (black).

indispensable in industry. These semiconductors have both electrical properties of a semiconductor and magnetic properties of a doped magnetic element. $Ga_{1-x}Mn_xAs$ (GaMnAs) is a typical ferromagnetic semiconductor obtained by doping a small amount of manganese (Mn) into gallium arsenide (GaAs). Its practical application as a spintronics material is being examined because it exhibits ferromagnetism at a relatively high temperature. However, the mechanism of ferromagnetism in GaMnAs has not been conclusively determined, and various physical models have been proposed.

In this study, to address the electronic structure of the doped Mn ions, we report the results of Mn L_3 x-ray absorption spectroscopy (XAS) and resonant inelastic x-ray scattering (RIXS) measurements of $Ga_{1-x}Mn_xAs$ (x = 0.04) at SPring-8 BL23SU and BL07LSU [1], respectively. RIXS is a powerful tool to investigate electronic excitations in element- and symmetry-specific ways including *d-d* and charge-transfer (CT) excitations for open shell 3*d* orbitals [2], and magnetic excitations for spin or charge-ordered systems [3]. These excitations are sensitive to electron correlation, crystalline symmetry, and the strength of hybridization with the ligand band. The RIXS spectra obtained for $Ga_{1-x}Mn_xAs$ are compared with configuration-interaction (CI) cluster-model calculations [4], and the electronic structure parameters are estimated.

The obtained XAS spectrum was compared with the CI cluster model calculations. Both the calculated spectra for the Mn^{2+} and Mn^{3+} states well reproduce the experimental XAS spectrum and we cannot determine the effective charge on the Mn site. On the other hand, the RIXS spectra provide definitive information: the RIXS spectra in Fig. 1 show a broad profile even at energy resolutions high enough to distinguish individual *d-d* excitation peaks of MnO. An analysis by the CI calculations indicates that the Mn ground

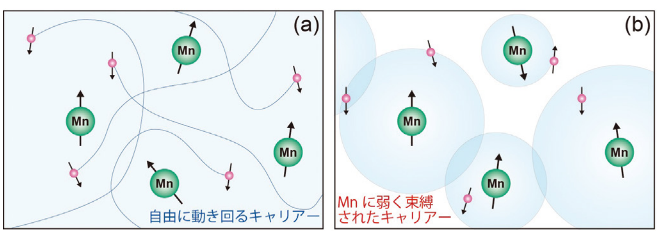

Fig. 2. Models for mechanism of ferromagnetism in $Ga_{1-x}Mn_xAs$: (a) Zener's *p-d* exchange model and (b) magnetic polaron model. The direction of the arrows in the upper figure indicates the direction of magnets.

states mainly consist of the Mn^{3+} electronic configuration composed of the charge-transferred states ($d^5\underline{L}$ and $d^6\underline{L}^2$), in which the ligand hole is weakly bound to the Mn $3d^5$ state (which can be explained by the magnetic polaron model: Fig. 2(b)), rather than the pure Mn^{2+} state (which can be explained by the Zener's *p-d* exchange model: Fig. 2(a)). In order to reproduce the experimental broadening of the Mn *d-d* excitation, not only the (Gaussian) broadening by the energy resolution but also the 0.5 eV Lorentzian broadening is required. The additional Lorentzian broadening in the RIXS spectra can be attributed to the lifetime broadening in the final state of the RIXS process where fast decay of the *d-d* excitations to an electron-hole pair in the host valence and conduction bands occurs because of the hybridization between the Mn 3*d* orbital and the ligand band.

References

[1] G. Ghiringhelli, M. Matsubara, C. Dallera, F. Fracassi, A. Tagliaferri, N. B. Brookes, A. Kotani, and L. Braicovich, Phys. Rev. B **73**, 035111 (2006).

[2] M. L. Tacon, G. Ghiringhelli, J. Chaloupka, M. M. Sala, V. Hinkov, M. W. Haverkort, M. Minola, M. Bakr, K. J. Zhou, S. Blanco-Canosa, C. Monney, Y. T. Song, G. L. Sun, C. T. Lin, G. M. D. Luca, M. Salluzzo, G. Khaliullin, T. Schmitt, L. Braicovich, and B. Keimer, Nat. Phys. **7**, 725 (2011).

[3] A. Tanaka and T. Jo, J. Phys. Soc. Jpn. **63**, 2788 (1994).

Authors

M. Kobayashi[a], H. Niwa[a], Y. Takeda[b], A. Fujimori[a], Y. Senba[c], H. Ohashi[c], A. Tanaka[d], S. Ohya[a], P. N. Hai[a], M. Tanaka[a], Y. Harada, and M. Oshima[a]

[a]The University of Tokyo
[b]Japan Atomic Energy Agency
[c]Japan Synchrotron Radiation Research Institute (JASRI)
[d]Hiroshima University

Selective Probing of the OH or OD Stretch Vibrations in Liquid Water Using Resonant Inelastic Soft X-ray Scattering

Y. Harada, T. Tokushima, and S. Shin

The unique property of water, such as high boiling and melting point compared to molecules like non-metal hydride, or less density in solid form than in liquid form, are

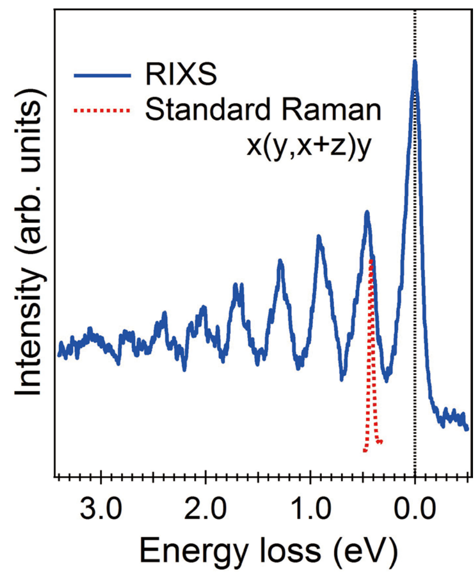

Fig. 1. The water vibronic structure observed in the RIXS spectrum. Dotted red curve is a standard Raman spectrum of liquid water in the same experimental configuration x(y, x+z)y [2] as the O 1*s* RIXS.

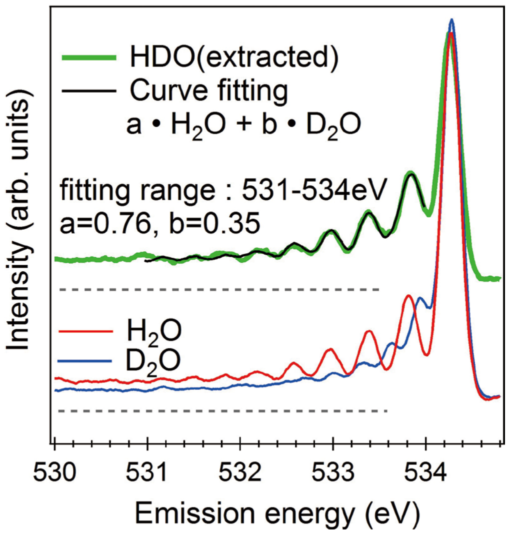

Fig. 2. Isotope effect on the multiple vibrational excitations of water. For each spectrum the background level is indicated by a dashed line. The extracted HDO spectrum is fitted with a linear combination of the H_2O and D_2O spectra in the range from 531–534 eV.

explained by an attractive force between water molecules, called 'hydrogen bond'. There are many proposed local structural models that describe the water network. Among them, a continuum model, where hydrogen bonds in water are distorted, broken and reformed continuously, but water itself is composed of a single component, or a mixture (micro-heterogeneity) model, where the network is considered as a mixture of various hydrogen bond configurations, are well known. However, the model that describes better the hydrogen bond property of liquid water, is still under debate.

In this work, we have succeeded in revealing validity of the mixture (micro-heterogeneity) model by selective observation of hydrogen-bond-broken water molecules and in detecting with high sensitivity the difference in the degree of hydrogen bond strength between light (normal) water and heavy water (in which both hydrogen atoms have been replaced with deuterium) using soft X-ray resonant inelastic scattering at BL07LSU and BL17SU of SPring-8[1]. High-resolution O 1s resonant inelastic X-ray scattering spectra of liquid H_2O/D_2O/HDO, obtained by excitation near the pre-edge resonance (Fig. 1) show, in the elastic line region, well-separated multiple vibrational structures corresponding to the internal OH stretch vibration in the ground state of water. The energy of the first-order vibrational excitation is strongly blue-shifted with respect to the main band in the Infrared/Raman spectra of water [2], indicating that water molecules with a highly weakened or broken donating hydrogen bond are correlated with the pre-edge structure in the X-ray absorption spectrum. As shown in Fig. 2, the vibrational profile of pre-edge excited HDO water is well fitted with 50±20% greater OH-stretch contribution compared to OD, which strongly supports a preference for OH being the weakened or broken H-bond in agreement with the well-known picture that D_2O makes stronger H-bonds than H_2O [3,4]. Accompanying path-integral molecular dynamics simulations show that this is particularly the case for strongly asymmetrically H-bonded molecules, i.e. those that are selected by pre-edge excitation. These results are expected to lead to the clarification of the role of water in various chemical and catalytic reactions as well as water in biological organisms where hydrogen bond plays an important role.

References

[1] Y. Harada, T. Tokushima, Y. Horikawa, O. Takahashi, H. Niwa, M. Kobayashi, M. Oshima, Y. Senba, H. Ohashi, K. T. Wikfeldt, A. Nilsson, L. G. M. Pettersson, S. Shin, Phys. Rev. Lett. **111**, 193001 (2013).
[2] G. E. Walrafen, M. S. Hokmabadi, and W.-H. Yang, J. Chem. Phys. **85**, 6964 (1986).
[3] J.D. Smith, C. D. Cappa, K. R. Wilson, R. C. Cohen, P. L. Geissler, R. J. Saykally, Proc. National Acad. Sci. (USA) **102**, 14171 (2005).
[4] Y. Nagata, R.E. Pool, E.H.G. Backus, M. Bonn, Phys. Rev. Lett. **109**, 226101 (2012).

Authors

Y. Harada, T. Tokushima[a], Y. Horikawa, O. Takahashi[b], H. Niwa[c], M. Kobayashi[c], M. Oshima[c], Y. Senba[d], H. Ohashi[d], K. T. Wikfeldt[e,f], A. Nilsson[g,h], L. G. M. Pettersson[h], and S. Shin
[a]RIKEN/SPring-8
[b]Hiroshima University
[c]The University of Tokyo
[d]JASRI/SPring-8
[e]University of Iceland
[f]NORDITA, AlbaNova University Center
[g]SLAC National Accelerator Laboratory
[h]AlbaNova University Center, Stockholm University

Emergent Quantum Phases in Condensed Matter – from topological to first-principles approaches (EQPCM2013)

June 3-21, 2013

H. Aoki, R. Arita, S. Fujimoto, M. Imada, S. Onoda, Y. Tada ,Y. Takada, and M. Oshikawa

In condensed matter theory, a variety of collective phenomena emerging in real materials are often explained or predicted first in terms of effective models, and then the description is made more precise with first-principles calculations based on the *ab initio* Hamiltonian. These two approaches require different backgrounds and are in many instances pursued separately. However, given the rapid progress in the both approaches and a rich variety of novel quantum phenomena found in recent years, bridging between the two is important more than ever. This Workshop/Symposium was organized in order to facilitate such an exchange with interactions among active theorists with diverse backgrounds.

During the Symposium period (June 12-14, 2013), results from the frontline of research, including experimental works, were reported in 33 talks and 47 poster presentations. The “hot” topics at the Symposium included Skyrmions in magnetic materials, transport in topological insulators, electron correlations in topological insulators, quantum spin ice, quantum spin liquids, and quantum entanglements in topological phases. The cumulative total attendance of the three-day symposium reached 351, indicating the success in attracting people from different fields.

The rest of the program was designated as the Workshop period. Typically, each day of the Workshop started with a 90-minute pedagogical lecture in the morning, followed by two 30-minute talks in the afternoon mostly by junior scientists. This format was conceived in order to stimulate exchanges among scientists with different backgrounds, and to encourage junior scientists. In fact, the ample free time between and after the talks was filled with lively informal discussions. During the Workshop period, there were 14 pedagogical lectures and 20 30-minute talks. The pedagogical lectures reviewed fundamentals of current topics and covered both effective-model based and first-principles approaches. They were particularly useful for the participants to become acquainted with unfamiliar concepts and methods. The 30-minute talks by junior scientists were of surprisingly high quality, demonstrating the high standards of young generation in the emerging fields.

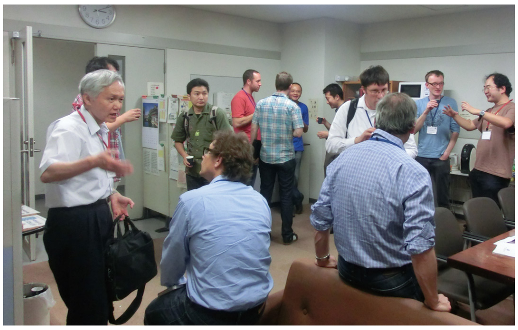

This Workshop/Symposium was sponsored by ISSP, as well as Computational Materials Science Initiative of Japan, Elements Strategy Initiative Center for Magnetic Materials, Grant-in-Aid for Scientific Research on Innovative Areas “Topological Quantum Phenomena in Condensed Matter with Broken Symmetries”, and Institute for Complex Adaptive Matter (ICAM-I2CAM, NSF Grant DMR-0844115).

The program and other details of the Workshop/Symposium can be found at the web page http://www.issp.u-tokyo.ac.jp/public/EQPCM/

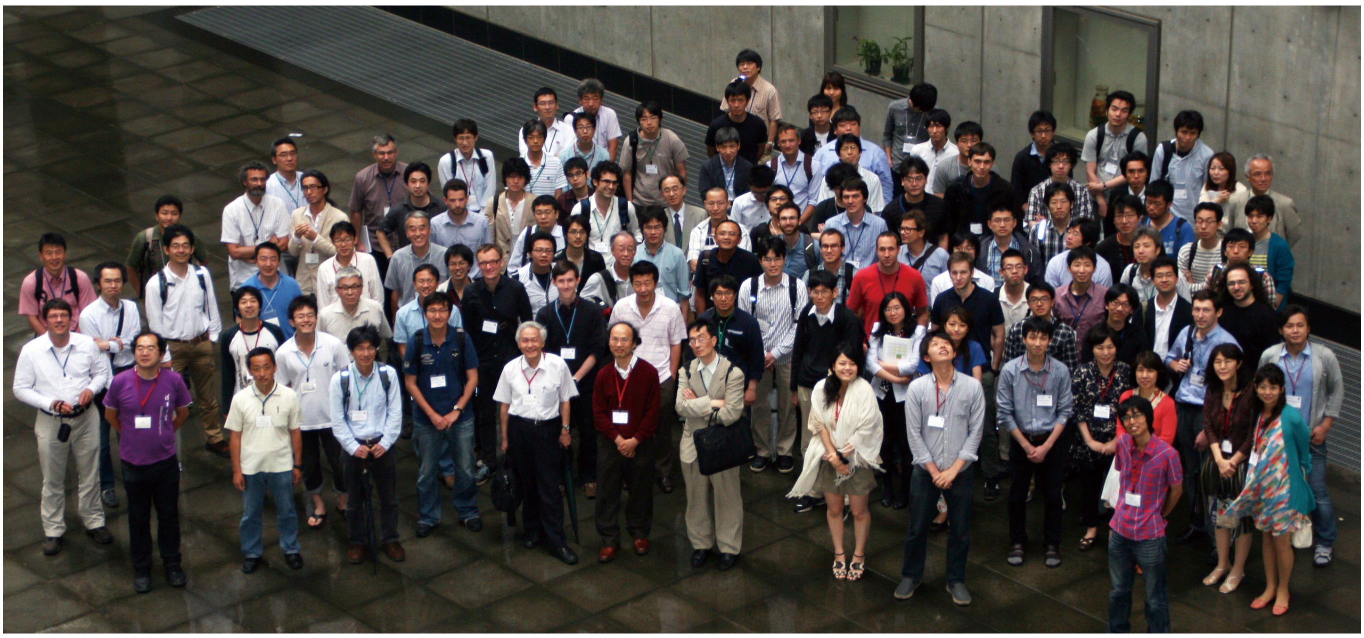

The 2nd DYCE-Asia and ISSP-international Workshop on Life Science and Photonics

December 17-18, 2013
H. Akiyama and H. Yokoyama

As the first ISSP international workshop on life science, the 2nd DYCE-ASIA workshop on “Life Science and Photonics” was held at Media Hall, Kashiwa Library, in Kashiwa Campus of The University of Tokyo. It was planned as an interdisciplinary scientist meeting of life scientists, physicists, and semiconductor photonics engineers. In this workshop, interesting recent topics including (1) bio-imaging for science and medical applications, (2) spectroscopy of bio-related materials, and (3) bioluminescence science and applications, were presented. About 60 people attended the workshop, including invited 15 speakers mainly from Asia-Pacific economies. Each speaker gave plain introduction to non-specialist audiences.

Life science and photonics are both very rapidly growing fields in this century, and we need to enhance mutual understanding and interactions among scientists in these fields. Moreover, these fields should lead near-future economy growth. Indeed, industrial developments related to photonics science are recently very active particularly in Asia-Pacific economies/countries. Therefore, this workshop was organized as the 2nd DYCE-ASIA workshop: DYCE (Optical science of dynamically-correlated electrons in semiconductors) was the title of a joint-research program from November 2008 to March 2013, supported via KAKENHI, or Grants-in-Aid for Scientific Research on Innovative Areas, by MEXT, Japan. The DYCE-ASIA workshop was started in order to extend the domestic DYCE research in Japan to Asian and international economies/countries.

The 2nd DYCE-ASIA workshop was officially supported by and organized as a project of Asia-Pacific Economic Cooperation (APEC), because the above-mentioned aims of the DYCE-ASIA workshop exactly match the goals of Policy Partnership on Science, Technology and Innovation (PPSTI) in APEC. This workshop was financially supported by KAKENHI grant (No. 20104001) and ISSP.

We got many thankful comments from foreign attendants as shown below.

— Thank you for the excellent work organizing the II DYCE and hosting at Todai. The workshop was very well organized and interesting. As for me, I had the opportunity to present my work and see and discuss the work of other researchers interested in solving the mechanism of bioluminescence colors. I also had the opportunity to see other interesting works about bio-photonics, of special interest were the technologies dealing with fluorescence imaging and microscopy, and to interact with researchers from other areas. Finally, I wish to thank the opportunity to see state of the art laser technologies in your labs. I hope in the near future to host a workshop or advanced school of bioluminescence in Brazil.

— Thank you so much indeed for the invitation. I enjoyed taking part in the Workshop. I love Japan very much and I am very happy every time visiting your so nice and beautiful country. As for the Workshop, I believe that the in general its quality was good. It was helpful in many senses (for me, at least). The program was interesting, the quality of presentations was fine, the number of participants was about right. The minor problem for me was the accommodation. The air conditioner (the heater) in my room was awful. Very noisy and without auto temperature control. I hope that the University will replace air conditioners for modern ones in the near future. Anyway, I enjoyed very my visiting you and hope to see you soon.

— The workshop was extremely well organized. All the invited speakers are very knowledgeable and they are in the top of their scientific fields. I tremendously learnt a lot from these 2 days workshop. Very focused topics! The poster session has also brought a different flavor to the workshop as we had more time to scientifically discuss with each individual. My overall impression is very positive about the work and I would love to participate in the next DYCE if possible. Please keep up the good work.

— Many thanks for your organizing such a wonderful event. I have been back to Taipei on last Thursday. Please kindly consider the development of 1300 nm femtosecond laser light, which would be very useful for clinical imaging.

— Thanks for your nice organization and warm hospitality during the 2nd DYCE-Asia. The topic of "Life Science and Photons" is very interesting and reflects the hot application trend of laser technologies. Although the conference is of a small

scale, it attracts the most important researchers in this field and in the world. Such a conference is definitely important to Asia researchers. I enjoyed it very much. I think such a topic-limited conference is very good and should be continued in the future.

— I'd like to thank you again for your kind arrangement of the 2nd DYCE workshop and the lab tour, and the nice dinner for six of us together. As a beginner, I learned a lot from our speakers about life science /firefly and the status of 1300nm microscopy. I discussed with several DYCE members and possibly some further collaboration work in the near future. I think (at least for Taiwanese participants): we can cover the air fees to Japan to reduce the financial loading of the DYCE program. The guest house at U. Tokyo is very nice and convenient. Thank you for everything.

— I would like to thank you for the kind invitation and the warm welcome in the University of Tokyo. It was great meeting you and the other colleagues that work on bioluminescence. I would like to reiterate that I am very interested in starting collaboration with your group. I will re-read your latest excellent publications and I will come up with some proposals on how we can complement our expertise.

— Overall, the symposium is of very high quality and efficient. A collection of frontier technologies, results, and ideas is presented in the symposium. The results on bioluminescence are particularly interesting. It reflects the outreaching effort of the excellent team. The team and related scholars have achieved tremendously in various photonics technologies, especially on novel light sources. As shown in the abstract book, the topics are well selected. The participating scholars also did a great job in presenting their work. The meeting venue is located in the library and next to on-campus cafeteria. The arrangement is very practical and efficient. The lab tour is rather impressive. It takes resources, intelligent and dedicated scholars, creativity and relentless efforts to build up such a world class laboratory, as shown in the tour. It shows Japan can definitely lead the world in realizing frontier ideas with cutting edge technologies. Last, but not the least, the interaction among the participants is most warming and rekindling. Behind the excellent works, there are so many details that are often left out from the official presentation. The coffee breaks and the get-together lunches and dinners nicely fill the gap on behind the scene stories and allow the building of friendship. In the next workshop, participation of more graduate students is highly encouraged. The logistics is also excellently done, simple and effective.

ISSP Workshops

Future Research of Material Science Using Vacuum-Ultraviolet and Soft X-ray Synchrotron Light

May 28-29, 2013
J. Fujimori, T. Kinoshita, K. Amamiya, T. Okuda, S. Shin, J. Yoshinobu, and F. Komori

Vacuum-ultraviolet and soft X-ray beamlines have been updated in the synchrotron light facilities in Japan including SPring-8 and Photon Factory. In the end stations of these beamlines, advanced techniques for the studies of new materials are now available by the improvement of polarization control and expansion of wavelength range with high energy resolution, and so on. Using these, we can expect more precise and quantitative measurements for studying new properties of the materials. However, the synchrotron radiation facilities have lacked enough opportunities to share information on their individual development plan. This is not ideal for the present trend in the research of solid state physics that a target material is intensively investigated by several complimentary methods for the thorough understanding of its properties and functionalities through cooperative research. In this workshop, there were reports on the current status and future plan of each synchrotron radiation facility in Japan and on the recent results at the advanced beamlines including some of the oversea facilities as well as on the plan of Tohoku medium-size synchrotron radiation facility. Based on these reports, we discussed the future research using vacuum-ultraviolet and soft X-ray synchrotron light. The workshop provided an important opportunity for the community of this research area that the beamline scientists from all the facilities and active users in Japan intensively discussed the future of their research field together.

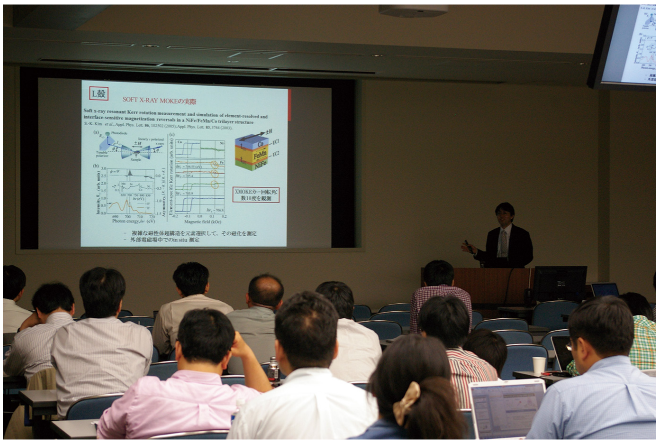

Energent Quantum Phases in Condensed Matter (EQPCM2013)

June 12-14, 2013
Y. Takada and M. Oshikawa

This ISSP workshop was held as the symposium part of the international workshop of the same title. See the section of “International Conferences and Workshops”.

Polar Oxides for Energy Conversion

June 26, 2013
M. Lippmaa, Y. Matsumoto, and I. Takeuchi

The focus of this workshop was on new oxide materials related to energy conversion applications. In particular, new types of polar oxides may offer a way to design internal electric field gradients in oxide heterostructures for achieving efficient photocarrier separation. In addition to basic solar cell geometries, the desire is to use functional oxides that fulfill two roles simultaneously, harvesting solar light by photocarrier generation and catalytically enhancing photoelectrochemical reactions on the surface. The presentations covered a broad range of related topics: catalytic materials, synthesis techniques, surface analysis, crystal design, phase transition mechanisms, and microstructural analysis. About 40 people attended the workshop, most of whom are young researchers. The event was thus a good venue for in-depth discussions on new materials and new ideas on oxide materials design. Two longer invited talks gave the attendees a chance to think about more general materials lifecycle issues and to see a practical example how new materials, in this case thermoelastic alloys, transition from pure basic science research to an actual application.

Extreme High Magnetic Field Science: Towards Fusion of Field, Materials and Probe

October 30-November 1, 2013
K. Kindo, H. Ota, T. Sasaki, T. Shimizu, S. Takeyama, M. Tokunaga, H. Nojiri, M. Hagiwara, Y. Hosokoshi, Y. H. Matsuda, M. Yoshizawa, and S. Mitsudo

Recently, large high-magnetic field laboratories have been built in many countries all over the world. Progress in the last decade on both generation- and measurement-techniques makes it possible to carry out various experiments under high magnetic fields. New development of materials science has started, as well, such as a fusion of high field with other fields (*e.g.* synchrotron radiation light source or laser). A fusion of high magnetic field, new materials and probe is required to develop an advanced research on materials science for the next decade. High Magnetic Field Co-laboratory Project also contributes to the progress of high field science. The project was planned to connect Japanese large high field laboratories strongly and has been realized partially. An exchange of researcher has been promoted in accordance with the project. This workshop was held to discuss the issues noted below.

1) Search for a new research subject for the next decade and training of young researchers
2) Development of research subject fused with other fields
3) Complete realization of High Magnetic Field Co-laboratory Project

The three issues were discussed not only by the high field laboratories but also by the users community. It was very significant for the high field community that all researchers concerned with high field gathered together to discuss the above issues and exchange recent information.

Materials and Physical Sciences Related to Energy and Environment

November 11-13, 2013

H. Mori, K. Kanoda, T. Sasaki, J. Takeya, F. Komori, M. Shibayama, J. Yoshinobu, O. Yamamuro, H. Akiyama, O. Sugino, Y. Harada, and M. Lippmaa

After the 2011 Tohoku earthquake, the scientific studies towards energy conversion and green environment have been extensively carried out. This workshop has focused on fundamental researches of novel materials and physical sciences related to energy and environment.

The energy conversion system and recent novel materials have hierarchical structures. For example, solar cell is a complex system, composed of synthetic molecules, charge transfer pairs, p-n interface, semiconducting layers, and buttery device. As attractive soft material, ionic liquid is also a hierarchical system with nano-meso-micro correlation lengths. The scientific keywords of these systems are "multi-energy scale", "dynamic structure", and "excited state". Therefore, it is important to perform researches integratedly.

In this workshop, the active 39 researchers have afforded 30-min. keynotes and 20-min. oral presentations in the sessions of "solar cell･artificial photosynthesis", "photo-catalyst", "battery", "surface science", "molecular materials･organic electronics", "bio-materials", and "hydrogen-based-materials". The 24 graduate students and young researchers have presented their researches in the poster session. Totally, 198 participants for 3 days participated in the workshop with hot discussions. It is meaningful that prominent researchers in a wide range of scientific fields presented their cutting-edge research results and exchange their information.

Condensed Matter Physics under Pulsed Ultrahigh Pressures and Magnetic Fields

November 25-26, 2013

K. G. Nakamura, T. Suemoto, N. Sarukura, S. Koshihara, H. Noziri, and M. Yoshimura

Ultrahigh pressures (>1TPa) and magnetic fields (>1kT) are recently realized by using a high-power laser, and electronic and structure dynamics in condensed matter can be studied under these extreme conditions. In this symposium, we discussed generation techniques of such extreme fields, current research activities, and future topics. The symposium consisted of sessions on (1) physics under strong magnetic fields, (2) physics under ultrahigh pressures, and (3) ultrafast measurements, with seventeen presentations. On the topics (1) there were presentations of a recent generation technique of the kT magnetic field using high-power laser plasma and measurements with synchrotron radiation, laser, and neutron diffraction under pulsed magnetic fields. On the topics (2), the generation of laser-induced ultrahigh pressures over TPa, which cannot be accessed by static compression, and combination research works with X rays from XFEL (X-ray Free Electron Laser) were presented. In addition, studies on planetary science using shock-induced high pressures were also presented. On the topics (3), single-shot measurement techniques are presented to study ultrafast phenomena using laser combined with pulsed electrons and X rays. Throughout the symposium, we discussed the problems of pulsed high pressure and magnetic fields and potential for studying unique properties of materials under non-equilibrium conditions.

Local Symmetry Breaking and Quantum Properties in Strongly Correlated Electron Systems

November 27-29, 2013
T. Arima, H. Harima, S. Nakatsuji, and Z. Hiroi

Symmetry is one of the most important concepts to determine the physical properties of solid states. For example, many interesting phenomena such as unconventional superconductivity, multiferroicity, and spin Hall effect are relevant to the breaking of the global space-inversion symmetry and resultant antisymmetric spin-orbit interaction. The antisymmetric spin-orbit interaction can be activated at non-centrosymmetric atomic sites even in materials with global space inversion symmetry. At such non-centrosymmetric sites, an odd-parity ligand field also allows the emergence of odd-parity multipoles like magnetic quadrupole and electric octupole moments, which may open the door to new paradigms in material science.

This workshop was organized to shed light on the possible exotic properties induced by the breaking of local inversion symmetry coupled with the electron correlation and spin-orbit coupling. During the workshop, off-diagonal responses, quantum transport, and exotic superconductivity were intensively discussed in terms of multipoles. In particular, many itinerant systems hosting the degree-of-freedom of various multipole moments were intensively discussed. The number of participants reached 87, consisting of researchers in the fields of 4f-electron systems (rare-earth compounds), 5f systems (uranium compounds), and d-electron systems (transition-metal compounds). The discussions across the various communities in solid state science made the workshop very successful.

Joint Research Meeting of ISSP Supercomputer Joint Use and CMSI Annual Activity Report 2013

December 10-13, 2013
H. Akai, N. Kawashima, O. Sugino, S. Todo, H. Noguchi, T. Oguchi, A. Oshiyama, T. Kawakatsu, S. Tsuneyuki, N. Hatano, S. Kasamatsu, H. Watanabe, Y. Noguchi, H. Shiba, and S. Morita

Every year, we hold a workshop for the joint research of the ISSP supercomputers. This year, the meeting was co-organized with The Computational Materials Science Initiative (CMSI), of which ISSP is the headquarters. During the four days of the meeting, we had 58 oral presentations, and 49 poster presentations. 192 scientists participated. The subjects of the presentations ranged from the most fundamental low-temperature behaviors of quantum matters to semi-conductor device, and new energy resources. We invited five distinguished speakers: K. Nakajima (U. Tokyo), Z. Hiroi (ISSP), K. Hukushima (U. Tokyo), M. Kato (Tokyo Inst. Tech.) and Y. Oyanagi (Kobe Univ.). We had active discussions for oral and poster presentations. The results of questionnaire on ISSP supercomputer were also presented and supercomputer architectures suitable to computational material science were discussed. The following three people are presented awards.

Young Researcher Encouragement Award: Kazuya Ishimura (Institute for Molecular Science).

Visual Award: Takuma Yagasaki (Okayama University).

Poster Award: Hiroshi Watanabe (Institute for Solid State Physics).

Joint Researches in Foreign Neutron Facilities

January 29-30, 2014

T. Masuda, M. Shibayama, H. Yoshizawa, and O. Yamamuro

Since the Great East Japan Earthquake on 11th March in 2011, Japan Research Reactor (JRR3) has suspended its operation and the Neutron Scattering Laboratory (NSL) has had difficulty in the domestic joint research using neutron spectrometers installed in JRR3. Now the NSL provides the neutron users the travel budgets for the neutron experiments at foreign facilities and supports the joint researches. In this workshop the users presented and discussed the researches performed at the foreign facilities. The field covers wide range including magnetism, strongly correlated electrons, glass, and soft matter. As for magnetism, the topics on geometrically frustrated systems were focused; the complex magnetic structure in chiral magnet, novel magnetic phase in quantum spin ice, the interplay between magnetic structure and electric polarization in multiferroics, etc. As for strongly correlated electrons system, studies on magnetic excitations and structures in various types of superconductors including high-T_c Cu oxides, Fe pnictides, and heavy-fermion materials were presented. It should be noted that the development and application of high pressure cell were implemented even in the restricted machine time at foreign facilities. Structural and dynamical analyses on new materials in the field of soft matter and quasi-elastic scatterings on cluster structure and ion liquid in the field of glass were reported. With 25 talks and 17 posters, the discussions at the workshop were hot and fruitful, indicating the scientists in the field of neutron scattering are actively doing their research and even enjoying this hard situation.

Present Activity and Future Prospect of BL07LSU in SPring-8

February 19, 2014

S. Shin, F. Komori, I. Matsuda, and Y. Harada

Five years has passed since the University of Tokyo started constructing an undulator beamline BL07LSU in SPring-8, and it is the middle of the project period using exclusively the beamline for joint studies. Polarization-controlled high-brilliance light is now available in the beamline, and used for advanced spectroscopy at the end-stations for material science. The number of publications from the beamline users has increased recently, and attracted much attention over the world. As a result, the overseas researchers continuously apply their joint studies there, and more than 30 % of the beam time for the joint studies is used with the foreign collaborators at present. In this workshop, the present status of the undulator light and the recent results at the end-stations were reported, and the advancement of the beamline in the next five years was discussed. In particular, future use of the polarization switching was proposed in relation to the development of the variable-polarization undulator. For the next two years, three long-term projects have been accepted at the three stationary end-stations for time-resolved spectroscopy, three-dimensional nano ESCA and soft X-ray emission spectroscopy. Each research plan with common keywords of operando and polarization control was introduced and discussed. New research plans using the free port were presented as well.

Subjects of Joint Research

平成 25 年度　共同利用課題一覧（前期）　Joint Research List (2013 First Term)

嘱託研究員（Commission Researcher）

No.	課題名	氏名	所属		Title	Name	Organization
1	幾何学的フラストレートした化合物の極低温磁化測定	柄木　良友	琉球大学	教育学部	Ultra low temperature measurements for geometrically frustrated materials	Yoshitomo Karaki	University of the Ryukyus
2	^{3}He-^{4}He 希釈冷凍機を用いた走査トンネル顕微鏡の改良と極低温スピン偏極 STM の開発	河江　達也	九州大学	大学院工学研究院	Development of very low-temperature spin-polarized STM with a ^{3}He-^{4}He dilution refrigerator	Tatsuya Kawae	Kyushu University
3	二次元超伝導の渦糸および近接効果に関する理論研究	林　伸彦	大阪府立大学	ナノ科学・材料研究センター	Theoretical study on vortices in two-dimensional superconductors	Nobuhiko Hayashi	Osaka Prefecture University
4	AgPdCu 合金圧力セルを用いた磁場中比熱測定	河江　達也	九州大学	大学院工学研究院	Development of pressure cell for specific heat measurements under magnetic field	Tatsuya Kawae	Kyushu University
5	有機伝導体の圧力効果	村田　惠三	大阪市立大学	大学院理学研究科	Effect of pressure on the organic conductor	Keizo Murata	Osaka City University
6	多重極限関連装置の調整	高橋　博樹	日本大学	文理学部	Adjustment of cubic anvil apparatus	Hiroki Takahashi	Nihon University
7	Ce 化合物の単結晶試料評価とその圧力効果	藤原　哲也	山口大学	大学院理工学研究科	Effect of pressure on the Ce compounds	Tetsuya Fujiwara	Yamaguchi University
8	磁性体の圧力効果	巨海　玄道	久留米工業大学		Effect of pressure on the magnetic materials	Gendo Oomi	Kurume Institute of Technology
9	圧力下 NMR 測定法に関する開発	藤原　直樹	京都大学	大学院人間・環境学研究科	Development of NMR measurement method under high pressure	Naoki Fujiwara	Kyoto University
10	低温用マルチアンビル装置の開発	辺土　正人	琉球大学	理学部	Development of multi-anvil apparatus for low temperature	Masato Hedo	University of the Ryukyus
11	中性子回析に用いる圧力装置の開発	片野　進	埼玉大学	大学院理工学研究科	Developments of high pressure cell for neutron diffraction	Susumu Katano	Saitama University
12	擬一次元有機物質の圧力下物性研究	糸井　充穂	日本大学	医学部	Study on pressure induced superconductivity of quasi organic conductor	Miho Itoi	Nihon University

No.	課題名	氏名	所属		Title	Name	Organization
13	高圧下の比熱測定装置の開発	梅原　出	横浜国立大学	工学部	Development of apparatus for specific heat measurements under high pressure	Izuru Umehara	Yokohama National University
14	磁化測定装置の開発	名嘉　節	物質・材料研究機構		Development of the magnetometer	Takashi Naka	National Institute for Materials Science
15	3d 遷移金属化合物の圧力下における磁気特性	鹿又　武	東北学院大学	工学総合研究所	Investigation of magnetic properties for 3d transition intermetallic compounds under pressure	Takeshi Kanomata	Tohoku Gakuin University
16	重い電子系物質における圧力下電気抵抗測定	礒田　誠	香川大学	教育学部	Effect of pressure on the electrical resistivity of heavy fermi on compounds	Makoto Isoda	Kagawa University
17	小型集束型小角散乱装置の高性能化及びそれによる応用研究	古坂　道弘	北海道大学	大学院工学研究院	Development of a compact focusing small-angle neutron scattering instrument and application research using the instrument	Michihiro Furusaka	Hokkaido University
18	中性子極小角散乱実験装置のアップグレード	金子　純一	北海道大学	大学院工学研究院	Upgrade of ULS system	Junichi Kaneko	Hokkaido University
19	中性子散乱装置の共同利用・開発による強相関電子系物質の構造物性の研究	岩佐　和晃	東北大学	大学院理学研究科	Structural studies of strongly correlated electron systems by neutron scattering method and instrumental development	Kazuaki Iwasa	Tohoku University
20	中性子モノクロメータの改良と中性子４軸回折計 FONDER の制御プログラムの改良	木村　宏之	東北大学	多元物質科学研究所	Improvement of neutron monochromator and control program for four circle neutron diffractometer FONDER	Hiroyuki Kimura	Tohoku University
21	中性子散乱装置のアップグレードと共同利用研究の推進	藤田　全基	東北大学	金属材料研究所	Upgrading of the neutron scattering device and promotion of the research and public use	Masaki Fujita	Tohoku University
22	中性子散乱装置のアップグレード後の研究計画の実施と共同利用の推進	大山　研司	東北大学	金属材料研究所	Propelling the inter university research cooperation	Kenji Ohoyama	Tohoku University
23	中性子散乱装置のアップグレード後の研究計画の実施と共同利用の推進	平賀　晴弘	高エネルギー加速器研究機構	物質構造科学研究所	Implementation of the research plan under the cooperation-use program after upgrading neutron scattering instruments	Haruhiro Hiraka	KEK
24	中性子散乱装置のアップグレード後の研究計画の実施と共同利用の推進	田畑　吉計	京都大学	大学院工学研究科	Progress of the joint research by using the neutron scattering instruments	Yoshikazu Tabata	Kyoto University
25	中性子散乱装置のアップグレード後の研究計画の実施と共同利用の推進	松村　武	広島大学	大学院先端物質科学研究科	Promotion of joint research after the upgrade of neutron scattering instruments	Takeshi Matsumura	Hiroshima University
26	J-PARC/MLF と JRR-3 共存時代に向けた３軸型中性子散乱装置の高度化	松浦　直人	総合科学研究機構		Upgrade of 3-axis neutron spectrometer for the oncoming coexistence of J-PARC/MLF and JRR-3	Masato Matsuura	CROSS
27	中性子分光器を用いた強相関電子系物質の微視的研究	桑原　慶太郎	茨城大学	大学院理工学研究科	Neutron scattering study of strongly correlated electron systems by using neutron spectrometers	Keitaro Kuwahara	Ibaraki University
28	高度化した３軸分光器を用いた共同利用の推進と物質科学研究の実施	横山　淳	茨城大学	理学部	Executing user program and study of material science with the advanced triple-axis spectrometers	Makoto Yokoyama	Ibaraki University
29	冷中性子スピン干渉計の応用と MINE ビームラインの整備	田崎　誠司	京都大学	大学院工学研究科	Development of cold neutron spin interferometry and improvements of MINE beam line	Seiji Tasaki	Kyoto University

No.	課題名	氏名	所属		Title	Name	Organization
30	膜貫通ペプチドのフリップフロップ誘起能の評価	中野　実	富山大学	大学院医学薬学研究部	Induction of phospholipid flip-flop by transmembrane peptides	Minoru Nakano	University of Toyama
31	C1-3 ULS 極小角散乱装置 IRT	杉山　正明	京都大学	原子炉実験所	Development of micro-focusing small-angle neutron scattering spectrometer	Masaaki Sugiyama	Kyoto University
32	集光テスト用小型 SANS の開発及び冷中性子反射率計・干渉計のアップグレード	日野　正裕	京都大学	原子炉実験所	Improvement of MIEZE spectrometer and cold neutron reflectometer and interferometer	Masahiro Hino	Kyoto University
33	集光テスト用小型 SANS の開発及び冷中性子反射率計・干渉計のアップグレード	北口　雅暁	名古屋大学	素粒子宇宙起源研究機構	Development of compact SANS and improvement of cold neutron reflectometer and interferometer	Masaaki Kitaguchi	Nagoya University
34	中性子散乱用高圧セルの開発および高圧下における中性子散乱実験	藤原　哲也	山口大学	大学院理工学研究科	Neutron scattering experiments under high pressure and development of high pressure cell for neutron scattering	Tetsuya Fujiwara	Yamaguchi University
35	流動場でのソフトマターの構造変化に関する研究	高橋　良彰	九州大学	先導物質化学研究所	Studies on structural change of soft matter under flow field	Yoshiaki Takahashi	Kyushu University
36	三軸分光器を用いた極端条件下における物質科学研究の実施	阿曽　尚文	琉球大学	理学部	Material science studies under extreme conditions by using triple-axis spectrometers	Naofumi Aso	University of the Ryukyus
37	非イオン界面活性剤水溶液ゲル構造に対する高分子添加効果	川端　庸平	首都大学東京	大学院理工学研究科	Effect of polymer addition to gel structures in a nonionic surfactant solution	Youhei Kawabata	Tokyo Metropolitan University
38	中性子散乱研究計画の実施と共同利用の推進	伊藤　晋一	高エネルギー加速器研究機構		Propelling the inter university research cooperation	Shinichi Itoh	KEK
39	冷中性子干渉イメージング装置開発研究	大竹　淑恵	理化学研究所	光量子工学研究領域	Research and development of interferometric imaging instruments for cold neutron	Yoshie Otake	RIKEN
40	高度化した三軸分光器を用いた共同利用の推進とスピンダイナミクスの研究	佐藤　卓	東北大学	多元物質科学研究所	Promoting user program and investigating spin dynamics using advanced triple-axis spectrometers	Taku Sato	Tohoku University
41	高度化した三軸分光器を用いた強相関電子系物質の研究	南部　雄亮	東北大学	多元物質科学研究所	Study of strongly correlated electron systems using advanced triple-axis spectrometers	Yusuke Nambu	Tohoku University
42	高温超伝導体の高分解能光電子分光	藤森　淳	東京大学	大学院理学系研究科	Ultra-high resolution photoemission spectroscopy on high Tc superconductor	Atsushi Fujimori	The University of Tokyo
43	60-eV レーザーを用いた時間分解光電子分光の開発	石坂　香子	東京大学	大学院工学系研究科	The development of time-resolved photoemission using 60eV laser	Kyoko Ishizaka	The University of Tokyo
44	鉄系超伝導体のレーザー光電子分光	下志万　貴博	東京大学	大学院工学系研究科	Laser-ARPES on Fe superconductor	Takahiro Shimojima	The University of Tokyo
45	Bi 系超伝導体の角度分解光電子分光	竹内　恒博	名古屋大学	エコトピア科学研究所	Angle-resolved photoemission study on high T_c cuprate	Tsunehiro Takeuchi	Nagoya University
46	高分解能光電子分光による強相関物質の研究	横谷　尚睦	岡山大学	大学院自然科学研究科	Ultra-high resolution study on strongly correlated materials	Takayoshi Yokoya	Okayama University

No.	課題名	氏名	所属		Title	Name	Organization
47	酸化バナジウムの高分解能光電子分光	江口　律子	岡山大学	大学院自然科学研究科	Photoemission study on vanadium oxides	Ritsuko Eguchi	Okayama University
48	有機化合物の光電子分光	金井　要	東京理科大学	理工学部	Photoemission study on organic compounds	Kaname Kanai	Tokyo University of Science
49	重い電子系ウラン化合物の高分解能光電子分光	藤森　伸一	日本原子力研究開発機構	量子ビーム応用研究部門	Ultra high resolution photoemission study on heavy fermion uranium compounds	Shinichi Fujimori	Japan Atomic Energy Agency
50	レーザー PEEM による磁性体の研究	小野　寛太	高エネルギー加速器研究機構	物質構造科学研究所	Study on magnetism by laser PEEM	Kanta Ono	KEK
51	レーザー光電子分光による酸化物薄膜の研究	津田　俊輔	物質・材料研究機構		Laser-Photoemission Study on Oxide Films	Shunsuke Tsuda	National Institute for Materials Science
52	4f 電子系物質の高分解能光電子分光	松波　雅治	自然科学研究機構	分子科学研究所	Photoemission study on 4f materials	Masaharu Matsunami	National Institutes of Natural Sciences
53	超高空間分解能光電子顕微鏡による磁区構造観察	中川　剛志	九州大学	大学院総合理工学研究院	Observation of magnetic domain structures by ultra-high resolution photoemission electron microscopy	Takeshi Nakagawa	Kyushu University
54	Mn 化合物の時間分解光電子分光	大川　万里生	東京理科大学	理学部	Time resolved photoemission on Mn compounds	Mario Okawa	Tokyo University of Science
55	時間分解光電子分光による重い電子系の研究	関山　明	大阪大学	大学院基礎工学研究科	Study on heavy fermion materials by time-resolved photoemission	Akira Sekiyama	Osaka University
56	高分解能光電子分光による酸化バナジウムの研究	藤原　秀紀	大阪大学	大学院基礎工学研究科	Study on vanadium oxides by high resolution photoemission	Hidenori Fujiwara	Osaka University
57	角度分解光電子分光法による遷移金属酸化物の表面 / 界面電子状態の研究	吉松　公平	東京大学	大学院理学系研究科	Angle-resolved photoemission study of the interfacial states of transition-metal oxides	Kohei Yoshimatsu	The University of Tokyo
58	高輝度放射光軟 X 線を用いた時間分解光電子分光による表面ダイナミクス研究	近藤　寛	慶應義塾大学	理工学部	Study of surface dynamics by time-resolved photoemission spectroscopy with high-brilliant soft x-ray synchrotron radiation	Hiroshi Kondoh	Keio University
59	軟 X 線アンジュレータビームラインの分光光学系の開発研究	雨宮　健太	高エネルギー加速器研究機構	物質構造科学研究所	Research and development of soft X-ray undulator beamline	Kenta Amemiya	KEK
60	高輝度光源計画における直入射ビームラインおよびその利用計画の検討	伊藤　健二	高エネルギー加速器研究機構	物質構造科学研究所	Design and case study for the high-resolution atoms- and molecules-spectroscopy beamline at the Super SOR facility	Kenji Ito	KEK
61	光電子スピン検出器の開発・研究	奥田　太一	広島大学	放射光科学研究センター	Research and development of a new photoelectron spin detector	Taichi Okuda	Hiroshima University
62	光電子顕微鏡による磁性ナノ構造物質の磁化過程	木下　豊彦	高輝度光科学研究センター		Magnetization in process of magnetic nano structure by PEEM	Toyohiko Kinoshita	Japan Synchrotron Radiation Institute
63	高輝度極紫外ビームラインの設計・評価	小野　寛太	高エネルギー加速器研究機構	物質構造科学研究所	Design and characterization of brilliance VUV beamline	Kanta Ono	KEK

No.	課題名	氏名	所属		Title	Name	Organization
64	高輝度極紫外ビームラインの設計・評価	木村　真一	自然科学研究機構	分子科学研究所	Design and characterization of brilliance VUV beamline	Shinichi Kimura	National Institutes of Natural Sciences
65	高輝度光源ビームラインにおける分光光学系の設計・開発	後藤　俊治	高輝度光科学研究センター		Design of the new undulator beamline at SPring-8	Shunji Goto	Japan Synchrotron Radiation Institute
66	〃	大橋　治彦	高輝度光科学研究センター		〃	Haruhiko Ohashi	Japan Synchrotron Radiation Institute
67	高輝度軟 X 線を利用した強相関物質の電子状態研究	組頭　広志	高エネルギー加速器研究機構	物質構造科学研究所	Study of electronic states in strongly correlated materials with high brilliant soft-X ray.	Hiroshi Kumigashira	KEK
68	時間分解光電子分光法による光触媒材料のキャリアダイナミクス研究	小澤　健一	東京工業大学	大学院理工学研究科	Study of carrier dynamics in photocatalysis materials by time-resolved photoemission spectroscopy	Kenichi Ozawa	Tokyo Institute of Technology
69	軟 X 線時間分解分光実験による磁性研究	木村　昭夫	広島大学	大学院理学研究科	Study of magnetic properties by time-resolved soft X-ray spectroscopy	Akio Kimura	Hiroshima University
70	高輝度軟 X 線を利用する光電子顕微鏡装置の設計・開発	坂本　一之	千葉大学	大学院融合科学研究科	Research and designing of a PEEM spectrometer for high brilliance soft X ray	Kazuyuki Sakamoto	Chiba University
71	二次元表示型スピン分解光電子エネルギー分析器の開発	大門　寛	奈良先端科学技術大学院大学	物質創成科学研究科	Development of 2D display type spin resolved photoelectron energy analyzer	Hiroshi Daimon	Nara Institute of Science and Technology
72	偏光制御軟 X 線アンジュレータの研究開発	北村　英男	理化学研究所		Research and development of polarization-controlled soft X-ray undulator	Hideo Kitamura	RIKEN
73	Si（111）表面相転移におけるキャリアダイナミクスの研究	虻川　匡司	東北大学	多元物質科学研究所	Study of carrier dynamics during Si(111) surface transition	Tadashi Abukawa	Tohoku University
74	軟 X 線吸収／発光分光法によるリチウムイオン電池電極材料の電子物性研究	細野　英司	産業技術総合研究所	エネルギー技術研究部門	Study on the electronic property of electrode materials for Li-ion batteries by soft X-ray absorption/emission spectroscopy	Eiji Hosono	National Institute of Advanced Industrial Science and Technology
75	超高分解能軟 X 線発光分光による水素吸蔵合金中の水素の波動関数の局在性に関する研究	関場　大一郎	筑波大学	数理物質系	Study on the localization of wave functions of hydrogen atom in hydrogen storage alloys using ultrahigh resolution soft X-ray emission spectroscopy	Daiichiro Sekiba	University of Tsukuba
76	価数異常を伴う量子臨界現象	三宅　和正	豊田理化学研究所		Quantum criticality associated with valence instability	Kazumasa Miyake	Toyota Physical and Chemical Research Institute
77	有機薄膜の物性測定	田島　裕之	兵庫県立大学	大学院物質理学研究科	Characterization of organic thin films	Hiroyuki Tajima	University of Hyogo
78	光電子分光、共鳴軟 X 線回折	和達　大樹	東京大学	大学院工学系研究科	Spades photoemission spectroscopy・resonant soft x-ray scattering	Hiroki Wadati	The University of Tokyo
79	幾何学的フラストレーション系における量子物性の研究	木村　健太	大阪大学	大学院基礎工学研究科	Quantum state of matter in geometrically-frustrated systems	Kenta Kimura	Osaka University

一般研究員（General Researcher）

No.	課題名	氏名	所属		Title	Name	Organization
1	スピン液体 $Tb_2Ti_2O_7$ の比熱測定	高津　浩	首都大学東京	大学院理工学研究科	Specific heat measurements on a spin liquid candidate $Tb_2Ti_2O_7$	Hiroshi Takatsu	Tokyo Metropolitan University
2	〃	谷口　智洋	首都大学東京	大学院理工学研究科	〃	Tomohiro Taniguchi	Tokyo Metropolitan University
3	強相関伝導系のパルス磁場中の超音波測定	吉澤　正人	岩手大学	大学院工学研究科	Ultrasonic measurements of strongly correlated systems in pulsed magnetic field	Masahito Yoshizawa	Iwate University
4	〃	竹澤　遼	岩手大学	大学院工学研究科	〃	Haruka Takezawa	Iwate University
5	強相関電子系化合物の秩序相に対する結晶対称性および軌道縮退の効果	横山　淳	茨城大学	理学部	Effects of crystal symmetry and orbital degeneracy in ordered states of strongly correlated electron systems	Makoto Yokoyama	Ibaraki University
6	〃	石川　沙羅	茨城大学	大学院理工学研究科	〃	Sara Ishikawa	Ibaraki University
7	固体ヘリウム４の非古典的回転慣性の遮断効果	青木　悠樹	東京工業大学	大学院総合理工学研究科	Blocking effect of nonclassical rotational momentum inertia for Solid Helium 4	Yuki Aoki	Tokyo Institute of Technology
8	〃	岩佐　泉	神奈川大学	理学部	〃	Izumi Iwasa	Kanagawa University
9	〃	三浦　尊	東京工業大学	大学院理工学研究科	〃	Takeru Miura	Tokyo Institute of Technology
10	新しいスピンフィルターを用いた超流動ヘリウム３スピン流制御の研究	山口　明	兵庫県立大学	大学院物質理学研究科	New spin filter for spin current control in superfluid helium-3	Akira Yamaguchi	University of Hyogo
11	〃	鎌田　尚史	兵庫県立大学	大学院物質理学研究科	〃	Naofumi Kamada	University of Hyogo
12	新奇な強磁性転移をもつパイロクロア化合物 $Yb_2Ti_2O_7$ の磁気相図	安井　幸夫	明治大学	理工学部	Magnetic phase diagram of pyrochlore compound $Yb_2Ti_2O_7$ with anomalous ferromagnetic transition	Yukio Yasui	Meiji University
13	超流動ヘリウム３-A 相の半整数量子渦の研究	石川　修六	大阪市立大学	大学院理学研究科	Study of half quantized vortex in superfluid ^{3}He-A phase	Osamu Ishikawa	Osaka City University
14	〃	國松　貴之	大阪市立大学	大学院理学研究科	〃	Takayuki Kunimatsu	Osaka City University
15	有機ラジカルを用いた新規磁性体の低温磁気測定	山口　博則	大阪府立大学	大学院理学系研究科	Low temperature magnetic properties of new organic radical compounds	Hironori Yamaguchi	Osaka Prefecture University
16	〃	岩瀬　賢治	大阪府立大学	大学院理学系研究科	〃	Kenji Iwase	Osaka Prefecture University

No.	課題名	氏名	所属		Title	Name	Organization
17	有機ラジカルを用いた新規磁性体の低温磁気測定	奥　雄太	大阪府立大学	大学院理学系研究科	Low temperature magnetic properties of new organic radical compounds	Yuta Oku	Osaka Prefecture University
18	スピンクロスオーバー伝導体に対する圧力効果	高橋　一志	神戸大学	大学院理学研究科	Pressure effect on spin crossover conductors	Kazuyuki Takahashi	Kobe University
19	〃	川向　希昂	神戸大学	大学院理学研究科	〃	Kiko Kawamukai	Kobe University
20	フラーライド単結晶の伝導性と磁性	森山　広思	東邦大学	理学部	Magnetic and transport properties of fullereide single crystals	Hiroshi Moriyama	Toho University
21	〃	山本　翔平	東邦大学	大学院理学研究科	〃	Shohei Yamamoto	Toho University
22	高温高圧下おいて水素分子が石英の結晶構造に与える影響	篠崎　彩子	東京大学	大学院理学系研究科	Effect of hydrogen molecules to crystal structure of quartz under high pressure	Ayako Shinozaki	The University of Tokyo
23	充填スクッテルダイト構造を有する新熱電変換材料の開発	関根　ちひろ	室蘭工業大学	大学院工学研究科	Development of new thermoelectric materials with filled-skutterudite structure	Chihiro Sekine	Muroran Institute of Technology
24	〃	川合　拓馬	室蘭工業大学	大学院工学研究科	〃	Takuma Kawaai	Muroran Institute of Technology
25	超硬質窒化炭素の高温高圧合成	寒川　匡哉	岡山理科大学	理学部	Synthesis of superhard carbon nitride at high temperature and high pressure	Masaya Sougawa	Okayama University of Science
26	超高圧プレスを用いた新規プロトニクス酸化物のソフト化学的合成法の検討	山口　周	東京大学	大学院工学研究科	Oxide-protonics materials synthesis by combined use of soft chemical method and high pressure	Shu Yamaguchi	The University of Tokyo
27	〃	三好　正悟	東京大学	大学院工学研究科	〃	Shogo Miyoshi	The University of Tokyo
28	〃	田中　和彦	東京大学	大学院工学研究科	〃	Kazuhiko Tanaka	The University of Tokyo
29	〃	ドロクサリブ　ロラス　ティンブル	東京大学	大学院工学研究科	〃	Doloksaribu Rolas Timbul	The University of Tokyo
30	〃	飯田　勇気	東京大学	大学院工学研究科	〃	Yuki Iida	The University of Tokyo
31	溶融亜鉛メッキ合金相の応力誘起変態	山口　周	東京大学	大学院工学研究科	Stress-induced phase transformation of Fe-Zn alloy formed in hot-dip process	Shu Yamaguchi	The University of Tokyo
32	〃	三好　正悟	東京大学	大学院工学研究科	〃	Shogo Miyoshi	The University of Tokyo
33	〃	田中　和彦	東京大学	大学院工学研究科	〃	Kazuhiko Tanaka	The University of Tokyo

No.	課題名	氏名	所属		Title	Name	Organization
34	溶融亜鉛メッキ合金相の応力誘起変態	上田　涼平	東京大学	大学院工学研究科	Stress-induced phase transformation of Fe-Zn alloy formed in hot-dip process	Ryohei Ueda	The University of Tokyo
35	スピンクロスオーバー伝導体の電流電圧特性の光応答	高橋　一志	神戸大学	大学院理学研究科	Photo response of I-V characteristics of spin crossover conductors	Kazuyuki Takahashi	Kobe University
36	〃	袋井　克平	神戸大学	大学院理学研究科	〃	Kappei Fukuroi	Kobe University
37	分子性導電体の磁気・光物性研究	松田　真生	熊本大学	大学院自然科学研究科	Studies on magnetic and optical properties of molecular conductors	Masaki Matsuda	Kumamoto University
38	〃	浜田　佑美	熊本大学	大学院自然科学研究科	〃	Yumi Hamada	Kumamoto University
39	有機伝導体の低温物性測定	鳥塚　潔	法政大学	理工学部	Measurements of low temperature properties of organic thin films (2)	Kiyoshi Torizuka	Hosei University
40	1/5 欠損正方格子ハバードモデルの磁気相図	山下　靖文	日本大学	工学部	Magnetic phase diagram of the 1/5-depleted square-lattice Hubbard model	Yasufumi Yamashita	Nihon University
41	B サイト秩序型ペロブスカイト酸化物のエピタキシャル薄膜におけるマルチフェロイック特性	大久保　勇男	物質・材料研究機構	国際ナノアーキテクトニクス研究拠点	Multiferroicity in epitaxial films of B-site ordered perovskite oxides	Isao Ohkubo	National Institute for Materials Science
42	太陽電池応用を目指したシリコン材料プロセスの研究	伊高　健治	弘前大学	北日本新エネルギー研究所	Research of the process of silicon products for solar cell application	Kenji Itaka	Hirosaki University
43	カーボンナノマテリアル表面からの２次電子放出機構の研究	田中　慎一郎	大阪大学	産業科学研究所	Mechanism of the secondary-electron emission from the surface of carbon nanomaterials	Shin-ichiro Tanaka	Osaka University
44	機械的応力のシリコン表面化学への影響に関する研究	成島　哲也	自然科学研究機構	分子科学研究所	Effect on silicon surface chemistry under external mechanical stress	Tetsuya Narushima	National Institutes of Natural Sciences
45	表面プラズモンを支持する金属単結晶面の作成と解析 (3)	渡辺　量朗	東京理科大学	大学院総合化学研究科	Fabrication and analysis of single crystal metal surfaces supporting surface plasmons (3)	Kazuo Watanabe	Tokyo University of Science
46	〃	長井　健太	東京理科大学	大学院総合化学研究科	〃	Kenta Nagai	Tokyo University of Science
47	量子ホール効果測定のための高移動度半導体試料作成	福田　昭	兵庫医科大学	教養部門	Development of the high mobility semiconductor sample for the measurements in the quantum Hall regime	Akira Fukuda	Hyogo College of Medicine
48	〃	寺澤　大樹	兵庫医科大学	教養部門	〃	Daiju Terasawa	Hyogo College of Medicine
49	SiC 表面上のエピタキシャルシリコン酸化物超薄膜のバンドギャップ接続に関する研究	鈴木　孝将	福岡大学	工学部	Study on band-gap profiles of epitaxial ultra-thin films on SiC surfaces	Takayuki Suzuki	Fukuoka University
50	〃	栃原　浩	福岡大学	工学部	〃	Hiroshi Tochihara	Fukuoka University

No.	課題名	氏名	所属		Title	Name	Organization
51	金属／半導体表面上ナノ構造の形成とその非線形発光の時間分解測定	河村　紀一	日本放送協会放送技術研究所	表示・機能素子研究部	Time resolved spectroscopy of harmonics from nano-structures on metal/semiconductor surfaces	Norikazu Kawamura	NHK Science & Technical Research Laboratories
52	(Ho,Y)Rh_2Si_2 単結晶の磁気転移	繁岡　透	山口大学	大学院理工学研究科	Magnetic transitions of (Ho,Y)Rh_2Si_2 single crystal	Toru Shigeoka	Yamaguchi University
53	〃	藤原 哲也	山口大学	大学院理工学研究科	〃	Tetsuya Fujiwara	Yamaguchi University
54	〃	森田　哲広	山口大学	大学院理工学研究科	〃	Tetsuhiro Morita	Yamaguchi University
55	$EuCo_2P_2$ の高圧力下磁化測定	藤原　哲也	山口大学	大学院理工学研究科	Magnetization measurements of $EuCo_2P_2$ under high pressures	Tetsuya Fujiwara	Yamaguchi University
56	〃	中田　琢也	山口大学	大学院理工学研究科	〃	Takuya Nakada	Yamaguchi University
57	Fe_3Mo_3N の高圧下電気抵抗率測定	和氣　剛	京都大学	大学院工学研究科	Resistivity measurement of Fe_3Mo_3N under high pressure	Takeshi Waki	Kyoto University
58	〃	安藤　拓矢	京都大学	大学院工学研究科	〃	Takuya Ando	Kyoto University
59	$LaFe_2P_2$ の輸送特性の圧力効果	藤原 哲也	山口大学	大学院理工学研究科	Pressure effect on the electrical transport properties of $LaFe_2P_2$	Tetsuya Fujiwara	Yamaguchi University
60	Mn_2Sb 系メタ磁性体の高圧下における磁気状態	小山　佳一	鹿児島大学	大学院理工学研究科	Magnetic state of Mn_2Sb metamagnets under high pressure	Keiichi Koyama	Kagoshima University
61	〃	松本　佳大	鹿児島大学	大学院理工学研究科	〃	Yoshihiro Matsumoto	Kagoshima University
62	Ni-Mn-Ga 系強磁性形状記憶合金の磁化の圧力依存性	安達　義也	山形大学	大学院理工学研究科	Pressure dependence of magnetization for the ferromagnetic shape-memory alloys of Ni-Mn-Ga system	Yoshiya Adachi	Yamagata University
63	〃	池田　大地	山形大学	大学院理工学研究科	〃	Daichi Ikeda	Yamagata University
64	R-TM-Ge 系新物質の基本物性評価	北川　健太郎	高知大学	教育研究部	Investigation for basic properties in a new R-TM-Ge system	Kentaro Kitagawa	Kochi University
65	TmB_4 の磁気準周期秩序相における圧力効果	伊賀　文俊	茨城大学	理学部	Pressure effect on the magnetic quasi-period ordered phase in TmB_4	Fumitoshi Iga	Ibaraki University
66	〃	道村　真司	埼玉大学	研究機構	〃	Shinji Michimura	Saitama University
67	セリウム系磁性超伝導体における微小磁気モーメントの圧力下磁化測定 III	阿曽　尚文	琉球大学	理学部	Magnetization studies under pressure in Ce-based magnetic superconductors with small magnetic moments II	Naofumi Aso	University of the Ryukyus

No.	課題名	氏名	所属		Title	Name	Organization
68	圧力下磁場中点接合分光実験の試み	本山　岳	島根大学	大学院総合理工学研究科	Development of a new method of point-contact-spectroscopy under pressure	Gaku Motoyama	Shimane University
69	〃	太刀掛　勇哉	兵庫県立大学	大学院物質理学研究科	〃	Yuya Tachikake	University of Hyogo
70	価数揺動系 SmS ならびに Yb 系準結晶における高圧下物性研究	出口　和彦	名古屋大学	大学院理学研究科	High-pressure study on mixed-valence SmS and Yb-quasicrystal	Kazuhiko Deguchi	Nagoya University
71	〃	井村　敬一郎	名古屋大学	大学院理学研究科	〃	Keiichiro Imura	Nagoya University
72	〃	松川　周矢	名古屋大学	大学院理学研究科	〃	Shuya Matsukawa	Nagoya University
73	希土類化合物の純良単結晶育成と圧力下低温物性	中野　智仁	新潟大学	大学院自然科学研究科	Single-crystal growth of the rare-earth compound and its low-temperature properties under pressure	Tomohito Nakano	Niigata University
74	〃	大屋　七海	新潟大学	大学院自然科学研究科	〃	Nami Ohya	Niigata University
75	希土類強磁性体 RAl_2 の異方的磁気体積効果	大橋　政司	金沢大学	理工研究域	Anisotropic magnetovolume effect of rare earth ferromagnet RAl_2	Masashi Ohashi	Kanazawa University
76	幾何学的フラストレート系の圧力効果の研究	武田　直也	新潟大学	工学部	Pressure effect of geometric frustration system	Naoya Takeda	Niigata University
77	〃	青山　悠司	新潟大学	大学院自然科学研究科	〃	Yuji Aoyama	Niigata University
78	強相関型セリウム化合物および合金の量子相転移と磁性	村山　茂幸	室蘭工業大学	大学院工学研究科	Quantum phase transition and magnetism in the strongly correlated Ce compounds and alloys	Shigeyuki Murayama	Muroran Institute of Technology
79	〃	雨海　有佑	室蘭工業大学	大学院工学研究科	〃	Yusuke Amakai	Muroran Institute of Technology
80	〃	水野　博貴	室蘭工業大学	大学院工学研究科	〃	Hiroki Mizuno	Muroran Institute of Technology
81	三角格子磁性体 $NaM(Acac)_3$benzen (M=Ni,Mn,Fe) の低温磁性	栁木　良友	琉球大学	教育学部	Low temperature magnetism of triangular lattice antiferromagnet $NaM(Acac)_3$benzene (M=Ni,Mn,Fe)	Yoshitomo Karaki	University of the Ryukyus
82	磁化測定用対向アンビル型高圧力発生装置の開発 (2)	藤原 哲也	山口大学	大学院理工学研究科	Development of opposed-anvil type high pressure apparatus for magnetization measurement II	Tetsuya Fujiwara	Yamaguchi University
83	重い電子系物質における ^{3}He 温度領域での磁化測定	河江　達也	九州大学	大学院工学研究院	Magnetization measurements in ^{3}He temperature region for heavy fermion systems	Tatsuya Kawae	Kyushu University
84	〃	佐藤　由昌	九州大学	大学院工学府	〃	Yoshiaki Sato	Kyushu University

No.	課題名	氏名	所属		Title	Name	Organization
85	重い電子系物質における ^{3}He 温度領域での磁化測定	古谷　圭一	九州大学	大学院工学府	Magnetization measurements in ^{3}He temperature region for heavy fermion systems	Keiichi Furuya	Kyushu University
86	多形化合物 $DyIr_2Si_2$ の磁気特性	繁岡　透	山口大学	大学院理工学研究科	Magnetic property of polymorphic compound $DyIr_2Si_2$	Toru Shigeoka	Yamaguchi University
87	〃	藤原 哲也	山口大学	大学院理工学研究科	〃	Tetsuya Fujiwara	Yamaguchi University
88	〃	蔵田 裕也	山口大学	大学院理工学研究科	〃	Yuya Kurata	Yamaguchi University
89	低次元有機伝導体の温度圧力相図の構築	村田　惠三	大阪市立大学	大学院理学研究科	Temperature-pressure phase diagram of low dimensional organic conductors	Keizo Murata	Osaka City University
90	〃	福本　雄平	大阪市立大学	大学院理学研究科	〃	Yuhei Fukumoto	Osaka City University
91	導電性ラングミュア・ブロジェット膜の高圧下の電気的性質に関する研究	三浦　康弘	桐蔭横浜大学	大学院工学研究科	Studies on electrical properties of conductive Langmuir-Blodgett films under high pressure	Yasuhiro Miura	Toin University of Yokohama
92	新規遷移金属炭化物の高圧合成	丹羽　健	名古屋大学	大学院工学研究科	High pressure synthesis of new transition metal carbides	Ken Niwa	Nagoya University
93	〃	岩崎　純也	名古屋大学	大学院工学研究科	〃	Junya Iwasaki	Nagoya University
94	新規遷移金属窒化物の超高圧合成	長谷川　正	名古屋大学	大学院工学研究科	High pressure synthesis of novel transition metal nitrides	Masashi Hasegawa	Nagoya University
95	〃	鈴木　健太郎	名古屋大学	大学院工学研究科	〃	Kentaro Suzuki	Nagoya University
96	SU(N) スピンをもつ２次元一般化 Heisenberg 模型の有限温度転移	鈴木　隆史	兵庫県立大学	大学院工学研究科	Finite temperature phase transition in 2d SU(N)-spin Heisenberg models	Takafumi Suzuki	University of Hyogo
97	テンソルネットワーク変分法の開発	原田　健自	京都大学	大学院情報学研究科	Development of tensor network variational methods	Kenji Harada	Kyoto University
98	三角スピンチューブのスピンダイナミクス	真中　浩貴	鹿児島大学	大学院理工学研究科	Spin dynamics of triangular spin tubes	Hirotaka Manaka	Kagoshima University
99	中性子散乱研究用大型単結晶試料の結晶性評価	阿曽　尚文	琉球大学	理学部	Crystal quality evaluation of large single crystals for neutron scattering	Naofumi Aso	University of the Ryukyus
100	$DyPd_2Ge_2$ 単結晶の逐次磁気転移	繁岡　透	山口大学	大学院理工学研究科	Successive magnetic transitions of $DyPd_2Ge_2$ single crystal	Toru Shigeoka	Yamaguchi University
101	〃	藤原 哲也	山口大学	大学院理工学研究科	〃	Tetsuya Fujiwara	Yamaguchi University

No.	課題名	氏名	所属		Title	Name	Organization
102	$DyPd_2Ge_2$ 単結晶の逐次磁気転移	田端　克好	山口大学	大学院理工学研究科	Successive magnetic transitions of $DyPd_2Ge_2$ single crystal	Katsuyoshi Tabata	Yamaguchi University
103	パイロクロア磁性体 $Tb_{2+x}Ti_{2-x}O_{7-y}$ の比熱研究	高津　浩	首都大学東京	大学院理工学研究科	Specific heat studies of a pyrochlore-lattice magnet $Tb_{2+x}Ti_{2-x}O_{7-y}$	Hiroshi Takatsu	Tokyo Metropolitan University
104	〃	清原　達也	首都大学東京	大学院理工学研究科	〃	Tatsuya Kiyohara	Tokyo Metropolitan University
105	新規三元化合物 $CeZn_2Ge_2$ の輸送特性	藤原　哲也	山口大学	大学院理工学研究科	Electrical transport properties of new ternary compound $CeZn_2Ge_2$	Tetsuya Fujiwara	Yamaguchi University
106	〃	中田　琢也	山口大学	大学院理工学研究科	〃	Takuya Nakada	Yamaguchi University
107	鉄系超伝導体 $FeTe_{1-x}S_x$ のアニール効果	山崎　照夫	東京理科大学	理工学部	Effect of annealing in the Fe-based superconductor $FeTe_{1-x}S_x$	Teruo Yamazaki	Tokyo University of Science
108	$(Ho,Gd)Rh_2Si_2$ 単結晶の高磁場磁化	繁岡　透	山口大学	大学院理工学研究科	High field magnetization of $(Ho,Gd)Rh_2Si_2$ single crystal	Toru Shigeoka	Yamaguchi University
109	〃	森田　哲広	山口大学	大学院理工学研究科	〃	Tetsuhiro Morita	Yamaguchi University
110	$(Ho,Y)Rh_2Si_2$ 単結晶の高磁場磁化	繁岡　透	山口大学	大学院理工学研究科	High field magnetization of $(Ho,Y)Rh_2Si_2$ single crystal	Toru Shigeoka	Yamaguchi University
111	〃	藤井　洋	山口大学	大学院理工学研究科	〃	Yoh Fujii	Yamaguchi University
112	Co を含む遍歴電子メタ磁性体の強磁場測定	道岡　千城	京都大学	大学院理学研究科	High field magnetization of the itinerant metamagnet with cobalt ions	Chishiro Michioka	Kyoto University
113	〃	今井　正樹	京都大学	大学院理学研究科	〃	Masaki Imai	Kyoto University
114	〃	原口　祐哉	京都大学	大学院理学研究科	〃	Yuya Haraguchi	Kyoto University
115	$LaCoO_3$ 系の強磁場誘起スピン転移の研究	佐藤　桂輔	茨城工業高等専門学校	自然科学	Field induced spin-state transition in $LaCoO_3$	Keisuke Sato	Ibaraki National College of Technology
116	スピン・電荷・軌道の自由度をもつ新規フラストレート物質の磁性	植田　浩明	京都大学	大学院理学研究科	Magnetism of novel frustrated materials with spin, charge, orbital degrees of freedom	Hiroaki Ueda	Kyoto University
117	〃	小林　慎太郎	京都大学	大学院理学研究科	〃	Shintaro Kobayashi	Kyoto University
118	〃	田口　篤史	京都大学	大学院理学研究科	〃	Atsushi Taguchi	Kyoto University

No.	課題名	氏名	所属		Title	Name	Organization
119	ナローギャップ半導体 $Fe_{1-x}Co_xSb_2$ の強磁場誘起強磁性の探索	田畑　吉計	京都大学	大学院工学研究科	Search for a high-field induced ferromagnetic state in the narrow-gap semiconductor $Fe_{1-x}Co_xSb_2$	Yoshikazu Tabata	Kyoto University
120	パルス磁場下比熱測定法による物性研究	稲垣　祐次	九州大学	大学院工学研究院	High field study by specific heat measurements under pulsed magnetic field	Yuji Inagaki	Kyushu University
121	ホイスラー化合物 $Ru_{2-x}Fe_xCrSi$ の強磁場磁化	廣井　政彦	鹿児島大学	大学院理工学研究科	Magnetizaiton of Heusler compounds $Ru_{2-x}Fe_xCrSi$ in high magnetic field	Masahiko Hiroi	Kagoshima University
122	〃	西井上　創羅	鹿児島大学	大学院理工学研究科	〃	Soura Nishiinoue	Kagoshima University
123	モリブデン酸銅におけるマルチクロミズム現象の観測	浅野　貴行	九州大学	大学院理学研究院	Observation of multi-chromic phenomena in the $CuMoO_4$	Takayuki Asano	Kyushu University
124	〃	福井　博章	九州大学	大学院理学府	〃	Hiroaki Fukui	Kyushu University
125	希土類金属間化合物の強磁場物性研究	海老原　孝雄	静岡大学	理学部	Physical phenomena at high magnetic fields in rear earth intermetallic compounds	Takao Ebihara	Shizuoka University
126	〃	土屋　政人	静岡大学	大学院理学研究科	〃	Masato Tsuchiya	Shizuoka University
127	近藤半導体 (Yb, R)B_{12} (R=Zr, Sc) の 80T 級磁場下での強磁場物性	伊賀　文俊	茨城大学	理学部	High field physical property of Kondo insulator (Yb, R)B_{12} (R=Zr, Sc) up to 80T class by using the pulse magnet	Fumitoshi Iga	Ibaraki University
128	〃	石井　克弥	茨城大学	大学院理工学研究科	〃	Katsuya Ishii	Ibaraki University
129	金属ナノクラスターネットワークの磁気抵抗測定	稲田　貢	関西大学	システム理工学部	Electronic transport properties of metal cluster networks under high-magnetic field	Mitsuru Inada	Kansai University
130	〃	小川　智矢	関西大学	大学院理工学研究科	〃	Tomoya Ogawa	Kansai University
131	高ドープ高温超伝導体のパルス強磁場下輸送現象	渡辺　孝夫	弘前大学	大学院理工学研究科	Transport phenomena in strongly-doped high-T_c superconductors under pulsed high magnetic fields	Takao Watanabe	Hirosaki University
132	〃	掛谷　一弘	京都大学	大学院工学研究科	〃	Itsuhiro Kakeya	Kyoto University
133	〃	臼井　友洋	弘前大学	大学院理工学研究科	〃	Tomohiro Usui	Hirosaki University
134	高圧合成希土類 12 ホウ化物の磁化特性	伊賀　文俊	茨城大学	理学部	Magnetic property of rare earth dodecaborides produced by high pressure synthesis	Fumitoshi Iga	Ibaraki University
135	四元系 η- カーバイド型化合物の強磁場磁化測定	和氣　剛	京都大学	大学院工学研究科	High field magnetization measurement of quartery η-carbide-type compounds	Takeshi Waki	Kyoto University

No.	課題名	氏名	所属		Title	Name	Organization
136	四元系 η - カーバイド型化合物の強磁場磁化測定	安藤　拓矢	京都大学	大学院工学研究科	High field magnetization measurement of quartary η-carbide-type compounds	Takuya Ando	Kyoto University
137	水熱合成法による新規 V 系酸化物の比熱測定	原　茂生	中央大学	理工学部	Heat capacity measurement of novel vanadium based oxide	Shigeo Hara	Chuo University
138	低次元有機磁性体の強磁場磁化測定	細越　裕子	大阪府立大学	大学院理学系研究科	High-field magnetization measurements of organic low-dimensional magnets	Yuko Hosokoshi	Osaka Prefecture University
139	〃	天谷　直樹	大阪府立大学	大学院理学系研究科	〃	Naoki Amaya	Osaka Prefecture University
140	〃	菊地　健太郎	大阪府立大学	大学院理学系研究科	〃	Kentaro Kikuchi	Osaka Prefecture University
141	鉄系ホイスラー化合物 $Fe_2Mn_{1-x}V_xSi$ の高磁場磁化測定	伊藤　昌和	鹿児島大学	大学院理工学研究科	High field magnetization of Heusler compound $Fe_2Mn_{1-x}V_xSi$	Masakazu Ito	Kagoshima University
142	複合極限装置のためのワイドボアパルスマグネットの開発	萩原　政幸	大阪大学	極限量子科学研究センター	Development of a wide-bore pulse magnet for experimental apparatus used under multiple extreme conditions	Masayuki Hagiwara	Osaka University
143	〃	谷口　一也	大阪大学	極限量子科学研究センター	〃	Kazuya Taniguchi	Osaka University
144	近藤半導体 $(Yb,R)B_{12}$ のワンターンコイル 120T パルス磁場下での強磁場磁化過程	伊賀　文俊	茨城大学	理学部	High field magnetization of Kondo insulator $(Yb,R)B_{12}$ by using one-turn coil in a 120T pulse magnet	Fumitoshi Iga	Ibaraki University
145	〃	林　健人	茨城大学	大学院理工学研究科	〃	Kento Hayashi	Ibaraki University
146	パイロクロア型イリジウム酸化物の強磁場下の物性研究	松平　和之	九州工業大学	大学院工学研究院	Transport and magnetic properties of pyrochlore iridates under high field magnetic field	Kazuyuki Matsuhira	Kyushu Institute of Technology
147	〃	後藤　岳	九州工業大学	大学院工学府	〃	Gaku Goto	Kyushu Institute of Technology
148	幾何学的フラストレーションを有する磁性体の強磁場下での振舞い	香取　浩子	東京農工大学	大学院工学研究院	Properties of geometrically frustrated magnets in high magnetic fields	Hiroko Katori	Tokyo University of Agriculture and Technology
149	〃	安藤　悠一	東京農工大学	大学院工学府	〃	Yuichi Ando	Tokyo University of Agriculture and Technology
150	超強磁場を利用した NiMn 基および CoCr 基合金の低温異常現象の観察および起源解明	伊東　航	仙台高等専門学校		Observation and clarification of the origin of anomalous behaviors at low temperature under strong magnetic field in NiMn based and CoCr based alloys	Wataru Ito	Sendai National College of Technology
151	〃	キョ　キョウ	東北大学	大学院工学研究科	〃	Xiao XU	Tohoku University
152	二次元遍歴電子磁性体の強磁場下での磁化過程	太田　寛人	東京農工大学	大学院工学研究院	Magnetic behavior of 2-dimensional itinerant electronic magnets under high magnetic field	Hiroto Ohta	Tokyo University of Agriculture and Technology

No.	課題名	氏名	所属		Title	Name	Organization
153	二次元遍歴電子磁性体の強磁場下での磁化過程	野口　大介	東京農工大学	大学院工学府	Magnetic behavior of 2-dimensional itinerant electronic magnets under high magnetic field	Daisuke Noguchi	Tokyo University of Agriculture and Technology
154	非破壊パルス強磁場を用いたグラファイトの磁場誘起密度波多重相の研究	矢口　宏	東京理科大学	理工学部	Study of the magnetic-field induced multiple density-wave state in graphite using non-destructive pulsed magnetic fields	Hiroshi Yaguchi	Tokyo University of Sceince
155	$Ca_{2-x}Sr_xRuO_4$ における不純物効果のレーザー光電子分光による研究	溝川　貴司	東京大学	大学院新領域創成科学研究科	Laser photoemission study of impurity effect in $Ca_{2-x}Sr_xRuO_4$	Takashi Mizokawa	The University of Tokyo
156	二次元 Dirac 電子系における多体効果のナノスケール制御	吹留　博一	東北大学	電気通信研究所	Nanoscale control of many-body effects in 2D Dirac electron systems	Hirokazu Fukidome	Tohoku University
157	MBE 法による窒化物半導体ナノ超格子の高分解能 X 線回折測定	小柴　俊	香川大学	工学部	High resolution XRD studies of nitride semiconductor nano meter superlattices by modulated beam epitaxy	Shyun Koshiba	Kagawa University
158	〃	中井　裕子	香川大学	大学院工学研究科	〃	Yuko Nakai	Kagawa University
159	窒素デルタドーピング構造半導体中の等電子トラップの光学特性評価	矢口　裕之	埼玉大学	大学院理工学研究科	Optical characterization of individual isoelectronic traps in nitrogen delta-doped semiconductors	Hiroyuki Yaguchi	Saitama University
160	〃	高宮　健吾	埼玉大学	大学院理工学研究科	〃	Kengo Takamiya	Saitama University
161	〃	山崎 泰由	埼玉大学	大学院理工学研究科	〃	Yasuyuki Yamazaki	Saitama University
162	窒素ラジカル変調制御法を用いた RF-MBE による GaNAs/GaAs 多重量子井戸構造を含んだ p-i-n 接合の特性評価	小柴　俊	香川大学	工学部	Electrical Properties of GaNAs/GaAs MQWs p-i-n junctions grown by RF-MBE using modulated nitrogen radical beam source	Shyun Koshiba	Kagawa University
163	〃	太田　奈津美	香川大学	大学院工学研究科	〃	Natsumi Ohta	Kagawa University
164	テラヘルツ分光装置を用いた酸化物磁性材料の研究	大越　慎一	東京大学	大学院理学系研究科	Study of magnetic oxide using terahertz spectroscopy	Shin-ichi Ohkoshi	The University of Tokyo
165	〃	生井　飛鳥	東京大学	大学院理学系研究科	〃	Asuka Namai	The University of Tokyo
166	〃	吉清　まりえ	東京大学	大学院理学系研究科	〃	Marie Yoshikiyo	The University of Tokyo
167	マルチフェロイック物質 $YBaCuFeO_5$ の単結晶評価	安井　幸夫	明治大学	理工学部	Characterization of single crystals of multiferroic system $YBaCuFeO_5$	Yukio Yasui	Meiji University
168	Bi ナノワイヤーにおける量子振動実験	長谷川　靖洋	埼玉大学	工学部	Experiment of quantum oscillation by Bi nanowire	Yasuhiro Hasegawa	Saitama University
169	半導体基板上に成長したグラフェンナノリボンおよびシリセンの電子物性	中辻　寛	東京工業大学	大学院総合理工学研究科	Electronic structure of graphene and silicene grown on semiconductor substrates	Kan Nakatsuji	Tokyo Institute of Technology

No.	課題名	氏名	所属		Title	Name	Organization
170	銀超薄膜上のシリセンの構造解析	平原　徹	東京大学	大学院理学系研究科	Structure analysis of silicene formed on ultrathin Ag films	Toru Hirahara	The University of Tokyo
171	強磁場による準結晶の量子臨界現象の研究	出口　和彦	名古屋大学	大学院理学研究科	High magnetic field experiments of quantum critical quasicrystal	Kazuhiko Deguchi	Nagoya University
172	〃	松川　周矢	名古屋大学	大学院理学研究科	〃	Shuya Matsukawa	Nagoya University
173	$BiCo_{1-x}(Fe,Ni)_xO_3$ のパルス強磁場中スピン状態転移	岡　研吾	東京工業大学	応用セラミックス研究所	Field induced spin-state transition in $BiCo_{1-x}(Fe,Ni)_xO_3$	Kengo Oka	Tokyo Institute of Technology
174	極低温超高分解能レーザー光電子分光装置による超伝導ギャップ測定	岡崎　浩三	東京大学	大学院理学系研究科	Superconducting-gap measurements by low-temperature high-resolution laser photoemission spectroscopy	Kozo Okazaki	The University of Tokyo
175	〃	堀尾　眞史	東京大学	大学院理学系研究科	〃	Masafumi Horio	The University of Tokyo
176	鉄水素化物の高圧合成と地球のコアに溶け込む水素量の推定	飯塚　理子	愛媛大学	地球深部ダイナミクス研究センター	Synthesis of iron hydride at high pressure and study for hydrogen melting in core of the Earth	Riko Iizuka	Ehime University
177	非磁性基底二重項を持つ $PrIr_2Zn_{20}$ の磁場中比熱測定	鬼丸　孝博	広島大学	大学院先端物質科学研究科	Specific heat measurements in magnetic field on $PrIr_2Zn_{20}$ with the nonmagnetic doublet ground state	Takahiro Onimaru	Hiroshima University
178	〃	松本　圭介	広島大学	大学院先端物質科学研究科	〃	Keisuke Matsumoto	Hiroshima University
179	〃	島田　祐樹	広島大学	大学院先端物質科学研究科	〃	Yuki Shimada	Hiroshima University
180	Mg_2Si 単結晶および焼結体のホール測定	平山　尚美	東京理科大学	基礎工学部	Hall measurement of single-crystalline and sintered polycrystalline Magnesium Silicide (Mg_2Si)	Naomi Hirayama	Tokyo University of Sceince
181	カルコパイライト $CuFeS_2$ の低温磁性相の探索	小林　夏野	青山学院大学	理工学部	Investigation of magnetic property in chalcopyrite $CuFeS_2$	Kaya Kobayashi	Aoyama Gakuin University
182	価数揺動物質の高圧力中輸送特性の研究	仲間　隆男	琉球大学	理学部	Transport properties of valence fluctuating compounds under pressure	Takao Nakama	University of the Ryukyus
183	〃	仲村　愛	琉球大学	大学院理工学研究科	〃	Ai Nakamura	University of the Ryukyus
184	〃	平仲　裕一	琉球大学	大学院理工学研究科	〃	Yuichi Hiranaka	University of the Ryukyus
185	希土類金属間化合物の高圧下における磁性と輸送特性	仲間　隆男	琉球大学	理学部	Magnetism and transport properties of rare-earth intermetallic compounds under high pressure	Takao Nakama	University of the Ryukyus
186	〃	照屋　淳志	琉球大学	大学院理工学研究科	〃	Atsushi Teruya	University of the Ryukyus

No.	課題名	氏名	所属		Title	Name	Organization
187	希土類金属間化合物の高圧下における磁性と輸送特性	上門　太郎	琉球大学	大学院理工学研究科	Magnetism and transport properties of rare-earth intermetallic compounds under high pressure	Taro Uejyo	University of the Ryukyus
188	$EuCd_{11}$ の高圧下における電子状態の研究	本多　史憲	東北大学	金属材料研究所	Electronic state in $EuCd_{11}$ under high pressure	Fuminori Honda	Tohoku University
189	角度分解光電子分光による鉄系超伝導体における擬ギャップの研究	園部　竜也	東京大学	大学院工学系研究科	APRES Study on Pseudogap in Iron-Pnictides	Tatsuya Sonobe	The University of Tokyo
190	極性層状ビスマス化合物におけるバルクとサブ表面のスピン分裂バンド構造	坂野　昌人	東京大学	大学院工学系研究科	Spin-splitting in bulk and near surface of layered polar Bi-based semiconductors	Masato Sakano	The University of Tokyo
191	空間反転対称性の破れた超伝導体の結晶性評価	古川　はづき	お茶の水女子大学	大学院人間文化創成科学研究科	Evaluation of single crystal quality of non-centrosymmetric superconductors	Hazuki Furukawa	Ochanomizu University
192	〃	石井　梨恵子	お茶の水女子大学	大学院人間文化創成科学研究科	〃	Rieko Ishii	Ochanomizu University
193	〃	呉　麻美子	お茶の水女子大学	大学院人間文化創成科学研究科	〃	Mamiko Kure	Ochanomizu University
194	空間反転対称性の破れた超伝導体のヘリカル磁束格子の観測	古川　はづき	お茶の水女子大学	大学院人間文化創成科学研究科	Helical vortex phase on non-centrosymmetric superconductors	Hazuki Furukawa	Ochanomizu University
195	〃	石井　梨恵子	お茶の水女子大学	大学院人間文化創成科学研究科	〃	Rieko Ishii	Ochanomizu University
196	〃	呉　麻美子	お茶の水女子大学	大学院人間文化創成科学研究科	〃	Mamiko Kure	Ochanomizu University
197	Sr_2RuO_4 の異常金属状態の研究	古川　はづき	お茶の水女子大学	大学院人間文化創成科学研究科	Anomalous vortex state of Sr_2RuO_4	Hazuki Furukawa	Ochanomizu University
198	〃	納谷　麻衣子	お茶の水女子大学	大学院人間文化創成科学研究科	〃	Maiko Naya	Ochanomizu University
199	$ErNi_2B_2C$ とその関連物質における自発的磁束格子の観測	古川　はづき	お茶の水女子大学	大学院人間文化創成科学研究科	Spontaneous vortex lattice in $ErNi_2B_2C$ and its related compounds	Hazuki Furukawa	Ochanomizu University
200	〃	石井　梨恵子	お茶の水女子大学	大学院人間文化創成科学研究科	〃	Rieko Ishii	Ochanomizu University
201	新しいボロン・クラスター系物質の開発と陽電子ビーム法による分析	金沢　育三	東京学芸大学	自然科学系	Making of new boron-cluster materials and analysis by slow-positron beam	Ikuzo Kanazawa	Tokyo Gakugei University
202	〃	今井　恵利華	東京学芸大学	大学院教育学研究科	〃	Erika Imai	Tokyo Gakugei University
203	低次元頂点及び辺共有した四面体のフラストレーション効果と磁化過程	浅野　貴行	九州大学	大学院理学研究院	Frustration effect and magnetization process of low-dimensional corner-edge-sharing tetrahedron compounds	Takayuki Asano	Kyushu University

No.	課題名	氏名	所属		Title	Name	Organization
204	低次元頂点及び辺共有した四面体のフラストレーション効果と磁化過程	川見　洋一郎	九州大学	大学院理学府	Frustration effect and magnetization process of low-dimensional corner- edge-sharing tetrahedron compounds	Yoichiro Kawami	Kyushu University
205	熱耐久性を有する高性能塗布型有機トランジスタ材料の開発	岡本　敏宏	東京大学	大学院新領域創成科学研究科	Development of solution-processable high performance organic semiconductos with thermal durability	Toshihiro Okamoto	The University of Tokyo
206	〃	三津井　親彦	東京大学	大学院新領域創成科学研究科	〃	Chikahiko Mitsui	The University of Tokyo
207	〃	山岸　正和	東京大学	大学院新領域創成科学研究科	〃	Masakazu Yamagishi	The University of Tokyo
208	〃	中村　健一	愛媛大学	工学部	〃	Ken-ichi Nakamura	Ehime University
209	〃	吉本　和美	東京大学	大学院新領域創成科学研究科	〃	Kazumi Yoshimoto	The University of Tokyo
210	$La_{1-x}Ca_xMnO_{3+\delta}$ の反強磁性と熱電特性に関する研究	中津川　博	横浜国立大学	大学院工学研究院	Antiferromagnetism and thermoelectric properties in $La_{1-x}Ca_xMnO_{3+\delta}$	Hiroshi Nakatsugawa	Yokohama National University
211	新規梯子格子磁性体 3-Br-4-F-V の NMR 測定	山口　博則	大阪府立大学	大学院理学系研究科	NMR study of new spin-ladder material 3-Br-4-F-V	Hironori Yamaguchi	Osaka Prefecture University
212	〃	宮外　浩嗣	大阪府立大学	大学院理学系研究科	〃	Hirotsugu Miyagai	Osaka Prefecture University
213	theta-BEDT-TTF 塩の電荷秩序と電荷グラス形成に関する研究	宮川　和也	東京大学	大学院工学系研究科	Studies of formation of charge ordered state and charge glass state in theta-(BEDT-TTF) system	Kazuya Miyagawa	The University of Tokyo
214	〃	佐藤　拓朗	東京大学	大学院工学系研究科	〃	Takuro Sato	The University of Tokyo
215	$LaFe_2P_2$ の輸送特性の圧力効果	中田　琢也	山口大学	大学院理工学研究科	Pressure effect on the electrical transport properties of $LaFe_2P_2$	Takuya Nakada	Yamaguchi University
216	磁化測定用対向アンビル型高圧力発生装置の開発 (2)	中田　琢也	山口大学	大学院理工学研究科	Development of opposed-anvil type high pressure apparatus for magnetization measurement II	Takuya Nakada	Yamaguchi University
217	超流動ヘリウム 3 -A 相の半整数量子渦の研究	木村　豊	大阪市立大学	大学院理学研究科	Study of half quantized vortex in superfluid ^{3}He-A phase	Yutaka Kimura	Osaka City University

物質合成・評価設備 P クラス（Materials Synthesis and Characterization P Class Researcher）

No.	課題名	氏名	所属		Title	Name	Organization
1	時間分解分光法を用いた超臨界流体中パルスレーザープラズマによるダイヤモンドイド合成における反応メカニズムの探索	シュタウス スヴェン	東京大学	大学院新領域創成科学研究科	Investigation of the reaction mechanisms of diamondoid synthesis by pulsed laser plasmas generated in supercritical fluids by time-resolved spectroscopy	Sven Stauss	The University of Tokyo

No.	課題名	氏名	所属		Title	Name	Organization
2	時間分解分光法を用いた超臨界流体中パルスレーザープラズマによるダイヤモンドイド合成における反応メカニズムの探索	姫野　翔平	東京大学	大学院新領域創成科学研究科	Investigation of the reaction mechanisms of diamondoid synthesis by pulsed laser plasmas generated in supercritical fluids by time-resolved spectroscopy	Shohei Himeno	The University of Tokyo
3	パイロクロア型希土類酸化物の単結晶育成と磁気フラストレーションの研究	松平　和之	九州工業大学	大学院工学研究院	Single crystal growth and study of frustrated magnetism in pyrochlore rare-earth oxides	Kazuyuki Matsuhira	Kyushu Institute of Technology

物質合成・評価設備 G クラス（Materials Synthesis and Characterization G Class Researcher）

No.	課題名	氏名	所属		Title	Name	Organization
1	超臨界水を用いた有機・無機複合廃棄物からのマテリアルリサイクル	大友　順一郎	東京大学	大学院新領域創成科学研究科	Material recycling from organic-inorganic composite waste using supercritical water	Junichiro Otomo	The University of Tokyo
2	〃	松本　祐太	東京大学	大学院新領域創成科学研究科	〃	Yuta Matsumoto	The University of Tokyo
3	ペロブスカイト型酸素キャリアを用いたケミカルルーピングシステムの開発	大友　順一郎	東京大学	大学院新領域創成科学研究科	The study on perovskite based oxygen carrier materials for CLC/CLR applications	Junichiro Otomo	The University of Tokyo
4	〃	オーチェン ジェームス オーチェン	東京大学	大学院新領域創成科学研究科	〃	Ochieng James OCHIENG	The University of Tokyo
5	ケミカルループ法の還元過程における酸化物イオン伝導体の担体効果	大友　順一郎	東京大学	大学院新領域創成科学研究科	Influence of the oxide ion conductor on the reduction process of a chemical-looping method	Junichiro Otomo	The University of Tokyo
6	〃	菊池　典晃	東京大学	大学院新領域創成科学研究科	〃	Noriaki Kikuchi	The University of Tokyo
7	プロトン伝導性固体電解質を用いた有機ハイドライド脱水素・水素化の電極反応特性	大友　順一郎	東京大学	大学院新領域創成科学研究科	Electrochemical redox of organic chemical hydrides with proton conducting solid electrolyte	Junichiro Otomo	The University of Tokyo
8	〃	野田　直人	東京大学	大学院新領域創成科学研究科	〃	Naoto Noda	The University of Tokyo
9	金属酸化物の酸化還元を利用した蓄電システムの開発	大友　順一郎	東京大学	大学院新領域創成科学研究科	Development of energy storage system using redox of metal oxide	Junichiro Otomo	The University of Tokyo
10	〃	高坂　文彦	東京大学	大学院新領域創成科学研究科	〃	Fumihiko Kosaka	The University of Tokyo
11	酸化セリウムナノマテリアルのキャラクタリゼーション	佐々木　岳彦	東京大学	大学院新領域創成科学研究科	Characterization for ceria-based nanomaterials	Takehiko Sasaki	The University of Tokyo
12	〃	梶　智大	東京大学	大学院新領域創成科学研究科	〃	Tomohiro Kaji	The University of Tokyo
13	酸化物イオン伝導体とプロトン伝導体を用いた新規二次電池の開発	大友　順一郎	東京大学	大学院新領域創成科学研究科	Development of novel rechargeable battery utilizing oxide ion conductor and proton conductor	Junichiro Otomo	The University of Tokyo

No.	課題名	氏名	所属		Title	Name	Organization
14	酸化物イオン伝導体とプロトン伝導体を用いた新規二次電池の開発	櫻井　健一朗	東京大学	大学院新領域創成科学研究科	Development of novel rechargeable battery utilizing oxide ion conductor and proton conductor	Kenichiro Sakurai	The University of Tokyo
15	中温作動型燃料電池におけるプロトン伝導型固体電解質の開発	大友　順一郎	東京大学	大学院新領域創成科学研究科	Development of proton conducting electrolyte for inter mediate fuel cells	Junichiro Otomo	The University of Tokyo
16	〃	庄野　洋平	東京大学	大学院新領域創成科学研究科	〃	Yohei Shono	The University of Tokyo
17	高プロトン伝導性リン酸ガラス - セラミックスの合成およびイオン伝導特性の解明	大友　順一郎	東京大学	大学院新領域創成科学研究科	Synthesis of proton conducting phosphate glass-ceramics and elucidation of property of ion conduction	Junichiro Otomo	The University of Tokyo
18	〃	門田　稔	東京大学	大学院新領域創成科学研究科	〃	Minoru Kadota	The University of Tokyo
19	フラストレート磁性とスピン軌道相互作用の協調・競合効果	有馬　孝尚	東京大学	大学院新領域創成科学研究科	Interplay between frustrated magnetism and spin-orbit interaction	Taka-hisa Arima	The University of Tokyo
20	〃	阿部　伸行	東京大学	大学院新領域創成科学研究科	〃	Nobuyuki Abe	The University of Tokyo
21	〃	豊田　新悟	東京大学	大学院新領域創成科学研究科	〃	Shingo Toyoda	The University of Tokyo
22	SOFC 空気極における製造プロセス由来微量成分の電極性能に対する影響評価	大友　順一郎	東京大学	大学院新領域創成科学研究科	Evaluation of correlation between SOFC cathode performance and trace element behavior in a SOFC production process	Junichiro Otomo	The University of Tokyo
23	〃	大石　淳矢	東京大学	大学院新領域創成科学研究科	〃	Junya Oishi	The University of Tokyo
24	ケミカルループ法におけるカルシウムフェライト系材料の酸化還元反応特性	大友　順一郎	東京大学	大学院新領域創成科学研究科	Redox kinetics of calcium ferrite materials in chemical looping combustion	Junichiro Otomo	The University of Tokyo
25	〃	磯貝　俊介	東京大学	大学院新領域創成科学研究科	〃	Shunsuke Isogai	The University of Tokyo
26	固体酸化物形燃料電池の劣化挙動におけるインピーダンススペクトルと電極構造の解析	大友　順一郎	東京大学	大学院新領域創成科学研究科	Analysis of electrochemical impedance spectra and electrode structure for the identification of degradation mechanisms in solid oxide fuel cells	Junichiro Otomo	The University of Tokyo
27	〃	伊原　冬樹	東京大学	大学院新領域創成科学研究科	〃	Fuyuki Ihara	The University of Tokyo
28	高温高圧水を利用した有機修飾微粒子の連続式合成技術の開発	大友　順一郎	東京大学	大学院新領域創成科学研究科	The development of continuous synthesis of organic-modified particles in high temperature and pressure water	Junichiro Otomo	The University of Tokyo
29	〃	生駒　健太郎	東京大学	大学院新領域創成科学研究科	〃	Kentaro Ikoma	The University of Tokyo
30	超臨界水を反応場とした複合酸化物ナノ粒子の合成	大友　順一郎	東京大学	大学院新領域創成科学研究科	Synthesis of nano-sized oxide particles using supercritical water as a reaction medium	Junichiro Otomo	The University of Tokyo

No.	課題名	氏名	所属		Title	Name	Organization
31	超臨界水を反応場とした複合酸化物ナノ粒子の合成	横　哲	東京大学	大学院新領域創成科学研究科	Synthesis of nano-sized oxide particles using supercritical water as a reaction medium	Akira Yoko	The University of Tokyo
32	多重安定性を示す光誘起分子磁性体のサイズ効果の研究	糸井　充穂	日本大学	医学部	Size effect on photo-switchable molecular magnet $K_{0.3}Co[Fe(CN)_6]_{0.77}\cdot 3.4H_2O$	Miho Itoi	Nihon University
33	新規な相転移を示すフラストレート磁性体の物性評価	植田　浩明	京都大学	大学院理学研究科	Characterization of frustrated magnets with novel phase transitions	Hiroaki Ueda	Kyoto University
34	〃	小林　慎太郎	京都大学	大学院理学研究科	〃	Shintaro Kobayashi	Kyoto University
35	〃	後藤　真人	京都大学	大学院理学研究科	〃	Masato Goto	Kyoto University
36	超臨界二酸化炭素中パルスレーザーアブレーションのプラズマ分光診断	占部　継一郎	東京大学	大学院新領域創成科学研究科	Spectroscopic plasma diagnostics of pulsed laser ablation generated in supercritical carbon dioxide	Keiichiro Urabe	The University of Tokyo
37	超臨界二酸化炭素中パルスレーザープラズマによるダイヤモンドイドの合成	シュタウス スヴェン	東京大学	大学院新領域創成科学研究科	Synthesis of diamondoids by pulsed-laser plasmas in supercritical CO_2	Sven Stauss	The University of Tokyo
38	〃	加藤　智嗣	東京大学	大学院新領域創成科学研究科	〃	Satoshi Kato	The University of Tokyo
39	ナノ構造制御に基づく環境、エネルギー材料の開発	細野　英司	産業技術総合研究所	エネルギー技術研究部門	Development of the environmental and energy materials by the nanostructure control	Eiji Hosono	National Institute of Advanced Industrial Science and Technology
40	新規磁石材料の微細構造解析	齋藤　哲治	千葉工業大学	工学部	Microstructural studies of newly developed permanent magnet materials	Tetsuji Saito	Chiba Institute of Technology
41	酸化物薄膜 / ナノ構造体の配向成長法の確立と物理特性制御	中島　智彦	産業技術総合研究所	先進製造プロセス研究部門	Orientation growth and physical property of oxide thin films and nanostructured materials	Tomohiko Nakajima	National Institute of Advanced Industrial Science and Technology
42	金属炭化物微粒子の超伝導磁気特性	吉田　喜孝	いわき明星大学	科学技術学部	Magnetic property in superconducting fine particles of metal carbides	Yoshitaka Yoshida	Iwaki-Meisei University
43	ハーフメタル型ホイスラー合金の磁性と輸送特性に関する研究	重田　出	鹿児島大学	大学院理工学研究科	Study on the magnetic and transport properties of half-metallic Heusler alloys	Iduru Shigeta	Kagoshima University
44	〃	春森　浩平	鹿児島大学	大学院理工学研究科	〃	Kouhei Harumori	Kagoshima University
45	ホイスラー型化合物の磁性と伝導の研究	廣井　政彦	鹿児島大学	大学院理工学研究科	Study on the magnetic and electrical properties of Heusler compounds	Masahiko Hiroi	Kagoshima University
46	新規ペロヴスカイト系関連酸化物の磁気物性	長谷川　正	名古屋大学	大学院工学研究科	Magnetism of novel perovskite related oxides	Masashi Hasegawa	Nagoya University
47	〃	志村　元	名古屋大学	大学院工学研究科	〃	Gen Shimura	Nagoya University

No.	課題名	氏名	所属		Title	Name	Organization
48	正 20 面体希土類クラスターを特徴とする金属合金の構造、電子物性と磁性	廣戸　孝信	東京理科大学	大学院基礎工学研究科	Crystal structures, electric and magnetic properties of alloys composed of icosahedral rare-earth cluster	Takanobu Hiroto	Tokyo University of Sceince
49	13 族クラスター固体の電子物性に関する研究	木村　薫	東京大学	大学院新領域創成科学研究科	Electronic properties of group 13 elements-based cluster solids	Kaoru Kimura	The University of Tokyo
50	〃	高際　良樹	東京大学	大学院新領域創成科学研究科	〃	Yoshiki Takagiwa	The University of Tokyo
51	〃	北原　功一	東京大学	大学院新領域創成科学研究科	〃	Kouichi Kitahara	The University of Tokyo
52	〃	柳原　大輔	東京大学	大学院新領域創成科学研究科	〃	Yanagihara Daisuke	The University of Tokyo
53	Cu-X（X=Co, Fe, Ni）系合金中の磁性微粒子析出過程と磁気特性の関係	竹田　真帆人	横浜国立大学	大学院工学研究院	Precipitation behavior and magnetic properties of fine magnetic particles in Cu-X base alloys	Mahoto Takeda	Yokohama National University
54	〃	李　東海	横浜国立大学	大学院工学府	〃	Lee donghae	Yokohama National University
55	〃	金　俊燮	横浜国立大学	大学院工学府	〃	KIM JUNSEOP	Yokohama National Univirsity

物質合成・評価設備 U クラス（Materials Synthesis and Characterization U Class Researcher）

No.	課題名	氏名	所属		Title	Name	Organization
1	Mn および Cr を含む $(Fe,Mg)_2SiO_4$ 単結晶の合成	杉浦　直治	東京大学	大学院理学系研究科	Synthesis of $(Fe,Mg)_2SiO_4$ single crystals doped with Mn and Cr	Naoji Sugiura	The University of Tokyo

長期留学研究員（Long Term Young Researcher）

No.	課題名	氏名	所属		Title	Name	Organization
1	銅酸化物高温超伝導体 Bi2212 の極紫外レーザー時間分解 ARPES	山本　貴士	東京理科大学	大学院理学研究科	EUV-laser time and angle resolved photoemission of high temperature cuprate Bi2212	Takashi Yamamoto	Tokyo University of Sceince
2	カテコール縮環型 TTF 誘導体を用いた新規誘起伝導体の合成と構造、性質	伊藤　悠太	東邦大学	大学院理学研究科	Synthesis, structures, and properties of novel organic conductors based on catechol-fused TTF derivatives	Yuta Ito	Toho University
3	プロトン - 電子相関系分子性導体の重水素効果	山田　翔太	東邦大学	大学院理学研究科	Deutelation effect of proton-electron correlated molecular conductor	Shota Yamada	Toho University
4	低次元電子系の高周波伝導率の測定	設楽　航	東京理科大学	大学院基礎工学研究科	Measurement of the high-frequency conductivities of the low-dimensional electron systems	Wataru Shitara	Tokyo University of Sceince

中性子（Neutron Scattering Researcher）

No.	課題名	氏名	所属		Title	Name	Organization
・申請装置 4G: GPTAS							
1	GPTAS（汎用 3 軸中性子分光器）IRT 課題	佐藤　卓	東北大学	多元物質科学研究所	IRT: GPTAS (Triple Axis Spectrometer)	Taku J Sato	Tohoku University
2	重い電子系 URu_2Si_2 の磁気励起	網塚　浩	北海道大学	大学院理学研究院 物理学部門	Magnetic excitation of heavy-electron system URu_2Si_2	Hirsohi Amitsuka	Hokkaido University
3	$La_{1-x}U_xRu_2Si_2$ (x > 0.9) における磁気秩序構造と磁気励起	網塚　浩	北海道大学	大学院理学研究院 物理学部門	Magnetic ordering structure and excitation in $La_{1-x}U_xRu_2Si_2$ (x > 0.9)	Hirsohi Amitsuka	Hokkaido University
4	空間反転対称性を持たない超伝導体 $CeIrSi_3$ の非整合磁気構造	阿曽　尚文	琉球大学	理学部物質地球科学科	Incommensurate magnetic structure in a non-centrosymmetric superconductor $CeIrSi_3$	Naofumi Aso	University of the Ryukyus
5	新しい重い電子系超伝導体 $CePt_2In_7$ の磁気反射の探索	阿曽　尚文	琉球大学	理学部物質地球科学科	Search for magnetic reflections in a new heavy fermion superconductor $CePt_2In_7$	Naofumi Aso	University of the Ryukyus
6	$EuCo_2P_2$ の磁気構造解析	藤原　哲也	山口大学	理工学研究科	Magnetic structure analysis of $EuCo_2P_2$	Tetsuya Fujiwara	Yamaguchi University
7	重い電子系新物質 $Ce_2Pt_3Ge_5$ の磁気構造解析	藤原　哲也	山口大学	理工学研究科	Magnetic structure analysis of new heavy fermion material $Ce_2Pt_3Ge_5$	Tetsuya Fujiwara	Yamaguchi University
8	スピンアイスにおけるトポロジカル相転移	門脇　広明	首都大学東京	理工学研究科	Topological phase transitions in spin ice	Hiroaki Kadowaki	Tokyo Metropolitan University
9	時間分割中性子散乱測定による磁気構造変化過程の実時間追跡	元屋　清一郎	東京理科大学	理工学部	Real-time observation of magnetic structural change by means of time-resolved neutron scattering experiments	Kiyoichiro Motoya	Tokyo University of Science
10	磁気構造の長時間変化と磁性原子希釈効果	元屋　清一郎	東京理科大学	理工学部	Dilution effect of magnetic atoms on the long-time variation of magnetic structure	Kiyoichiro Motoya	Tokyo University of Science
11	AFeAs (A = Li, Na) の超伝導対称性	南部　雄亮	東北大学	多元物質科学研究所	Superconducting pairing symmetry in AFeAs (A = Li, Na)	Yusuke Nambu	Tohoku University
12	強磁性超伝導体 UCoGe におけるスピン揺らぎの研究	佐藤　憲昭	名古屋大学	大学院理学研究科	Study on spin fluctuations of the superconducting ferromagnet UCoGe	Noriaki Sato	Nagoya University
13	$CeTe_3$ および $TbTe_3$ における量子臨界現象および磁性と超伝導の相関の研究	佐藤　憲昭	名古屋大学	大学院理学研究科	Study on the quantum criticality and correlation of magnetism and superconductivity in $CeTe_3$ and $TbTe_3$	Noriaki Sato	Nagoya University
14	重い電子系超伝導体 $CeRh_xIr_{1-x}In_5$ における磁性と超伝導の相関の研究	佐藤　憲昭	名古屋大学	大学院理学研究科	Study on the correlation of magnetism and superconductivity in $CeRh_xIr_{1-x}In_5$	Noriaki Sato	Nagoya University
15	$Dy_3Al_5O_{12}$ ガーネットにおけるクーロン相の探索	佐藤　卓	東北大学	多元物質科学研究所	Search for Coulomb phase in the $Dy_3Al_5O_{12}$ garnet	Taku J Sato	Tohoku University

No.	課題名	氏名	所属		Title	Name	Organization
16	強誘電体の相転移機構（変位型及び秩序 無秩序型）に関する統一的理解の確立	重松　宏武	山口大学	教育学部	Establishment of the unified explanation about the phase transition mechanism (displacive and order-disorder types) in ferroelectrics	Hirotake Shigematsu	Yamaguchi University
17	$HoRh_2Si_2$ の成分分離逐次磁気転移	繁岡　透	山口大学	理工学研究科	Successive components-separated magnetic transitions in $HoRh_2Si_2$	Toru Shigeoka	Yamaguchi University
18	強磁性量子臨界点近傍の遍歴電子フラストレート磁性体 Fe_3Mo_3N およびその Co 置換系の動的スピン相関	田畑　吉計	京都大学	大学院工学研究科材料工学専攻	Dynamic spin correlations of itinerant-electron frustrated magnets in the vicinity of a FM-QCP Fe_3Mo_3N and its co-substituted systems	Yoshikazu Tabata	Kyoto University
19	中性子回折による六方晶フェライト $(Ba_{1-x}Sr_x)_2Zn_2Fe_{12}O_{22}$ および $Ba(Fe_{1-x}Sc_x)_{12}O_{19}$ の超交換相互作用研究	内海　重宜	諏訪東京理科大学	システム工学部	Superexchange interaction of hexagonal ferrites $(Ba_{1-x}Sr_x)_2Zn_2Fe_{12}O_{22}$ and $Ba(Fe_{1-x}Sc_x)_{12}O_{19}$ studied by neutron diffraction	Shigenori Utsumi	Tokyo University of Science, Suwa
20	重い電子系ウラン化合物の秩序状態に対する一軸応力効果	横山　淳	茨城大学	理学部	Effect of uniaxial stress on ordered state in U-based heavy-fermion compound	Makoto Yokoyama	Ibaraki University
21	鉄系超伝導体のスピン揺動	李　哲虎	産業技術総合研究所	エネルギー技術研究部門	Spin fluctuations of iron-based superconductors	Chul-Ho Lee	National Institute of Advanced Industrial Science and Technology
22	$EuRu_2P_2$ の磁気構造解析	藤原　哲也	山口大学	理工学研究科	Magnetic structure analysis of $EuRu_2P_2$	Tetsuya Fujiwara	Yamaguchi University
23	パイロクア磁性体における格子―軌道―スピン観測とスピン流、異常ホール効果への影響	古川　はづき	お茶の水女子大学	大学院人間文化創成科学研究科	Neutron study on pyrochlore oxide materials	Hazuki Furukawa	Ochanomizu University
24	電子誘電性を示す分子性有機導体 θ -$(BEDT\text{-}TTF)_2CsZn(SCN)_4$ における格子ダイナミクスの研究	松浦　直人	東北大学	金属材料研究所	Investigation of lattice dynamics reflecting electronic ferroelectricity in a charge-transfer complex θ -$(BEDT\text{-}TTF)_2CsZn(SCN)_4$	Masato Matsuura	Tohoku University
・申請装置 5G: PONTA							
25	PONTA（高性能偏極中性子散乱装置）IRT 課題	益田　隆嗣	東京大学	物性研究所	IRT: PONTA (Polarized Neutron Triple Axis Spectrometer)	Takatsugu Masuda	The University of Tokyo
26	PONTA（高性能偏極中性子散乱装置）IRT 課題 偏極中性子線を用いた磁気散乱中性子線ホログラフィー	林　好一	東北大学	金属材料研究所	IRT: PONTA (Polarized Neutron Triple Axis Spectrometer)	Koichi Hayashi	Tohoku University
27	高エネルギー磁気励起測定による Bi2201 の磁気励起分散の研究	榎木　勝徳	九州工業大学	大学院工学研究院物質工学研究系	Study of magnetic excitation dispassion in Bi2201 by measurement of high-energy excitation	Masanori Enoki	Kyushu Institute of Technology
28	一次元フラストレート鎖量子磁性体 $CaCuVO_4$ (OD) の磁気励起	萩原　雅人	東京大学	物性研究所	Magnetic excitation of one dimensional quantum frustrated chain $CaCuVO_4$(OD)	Masato Hagihala	The University of Tokyo
29	一次元鎖量子磁性体 $LiCuVO_4$ の SDW_2 相での弾性散乱測定	萩原　雅人	東京大学	物性研究所	Neutron diffraction at SDW_2 phase on one dimensional quantum magnetic $LiCuVO_4$	Masato Hagihala	The University of Tokyo
30	スピンギャップ系物質 $Pb_2V_3O_9$ の磁気構造と磁気励起	益田　隆嗣	東京大学	物性研究所	Magnetic structure and magnetic excitation in the spin gap material $Pb_2V_3O_9$	Takatsugu Masuda	The University of Tokyo
31	電子誘電性を示す分子性有機導体 β'-$(BEDT\text{-}TTF)_2ICl_2$ における格子ダイナミクスの研究	松浦　直人	東北大学	金属材料研究所	Investigation of lattice dynamics reflecting electronic ferroelectricity in a charge-transfer complex β'-$(BEDT\text{-}TTF)_2ICl_2$	Masato Matsuura	Tohoku University

No.	課題名	氏名	所属		Title	Name	Organization
32	時間分割中性子散乱測定による磁気構造変化過程の実時間追跡	元屋　清一郎	東京理科大学	理工学部　物理学科	Real-time observation of magnetic structural change by means of time-resolved neutron scattering experiments	Kiyoichiro Motoya	Tokyo University of Science
33	磁気構造の長時間変化と磁性原子希釈効果	元屋　清一郎	東京理科大学	理工学部　物理学科	Dilution effect of magnetic atoms on the long-time variation of magnetic structure	Kiyoichiro Motoya	Tokyo University of Science
34	多段メタ磁性体 $Ca_3Co_2O_6$ における磁気構造の長時間変化への disorder の効果	茂吉　武人	東京理科大学	理工学部	Disorder effects on the long-time variation of magnetic structure in a multistep metamagnet $Ca_3Co_2O_6$	Taketo Moyoshi	Tokyo University of Science
35	三角格子系 Na_xNiO_2 の磁気構造	茂吉　武人	東京理科大学	理工学部	Magnetic structure of a triangular system Na_xNiO_2	Taketo Moyoshi	Tokyo University of Science
36	マルチフェロイック $CuFeO_2$ における 2 軸圧力による磁気・強誘電ドメイン配向制御	中島　多朗	東京理科大学	理学部物理学教室	Biaxial-pressure control of multiferroic domain structure in spin-driven ME multiferroic $CuFeO_2$	Taro Nakajima	Tokyo University of Science
37	偏極中性子回折によるアルカリ金属ナノクラスター強磁性体の研究	中野　岳仁	大阪大学	理学研究科物理学専攻	Neutron diffraction study on ferromagnetism of alkali-metal nanocluster array by spin-polarized beam	Takehito Nakano	Osaka University
38	$NiGa_2S_4$ におけるスピンネマティック相関の検出	南部　雄亮	東北大学	多元物質科学研究所	Detection of spin nematic correlation in the 2D magnet $NiGa_2S_4$	Yusuke Nambu	Tohoku University
39	カゴメ格子・三角格子積層系 $YBaCo_4O_7$ の磁気励起	左右田　稔	東京大学	物性研究所	Magnetic excitation of $YBaCo_4O_7$ with kagome and triangular lattices	Minoru Soda	The University of Tokyo
40	$A_2CoSi_2O_7$(A=Ca and Ba) におけるエレクトロマグノン	左右田　稔	東京大学	物性研究所	Electromagnon in $A_2CoSi_2O_7$ (A=Ca and Ba)	Minoru Soda	The University of Tokyo
41	希釈イジング反強磁性体 $Ho_xY_{1-x}Ru_2Si_2$ の磁気秩序相における異常スピンダイナミクス	田畑　吉計	京都大学	大学院工学研究科材料工学専攻	Anomalous spin dynamics in the magnetic ordered state of the diluted Ising antiferromagnet $Ho_xY_{1-x}Ru_2Si_2$	Yoshikazu Tabata	Kyoto University
42	導電性三角格子磁性体 $PdCrO_2$ の反強磁性秩序と異常伝導	高津　浩	首都大学東京	理工学研究科物理学専攻	Antiferromagnetism and its relation to the anomalous conductivity in the metallic triangular-lattice magnet $PdCrO_2$	Hiroshi Takatsu	Tokyo Metropolitan University
43	秩序型ペロブスカイト $CaCu_3Ti_4O_{12}$ のフォノン	留野　泉	秋田大学	教育文化学部	Phonons in ordered perovskite $CaCu_3Ti_4O_{12}$	Izumi Tomeno	Akita University
44	立方晶 $BaTiO_3$ のフォノンの温度依存性	留野　泉	秋田大学	教育文化学部	Temperature dependence of phonons in cubic $BaTiO_3$	Izumi Tomeno	Akita University
45	$Pr_{0.5}Sr_{0.5}MnO_3$ の高温フォノン	留野　泉	秋田大学	教育文化学部	Phonon in $Pr_{0.5}Mn_{0.5}MnO_3$ at high temperature	Izumi Tomeno	Akita University
46	$PbCuSO_4(OH)_2$ の磁場によって誘起される新奇量子相	安井　幸夫	明治大学	理工学部	Magnetic-field-induced anomalous quantum phase of $PbCuSO_4(OH)_2$)	Yukio Yasui	Meiji University
47	偏極中性子を用いた $Cu_3Mo_2O_9$ 単結晶の磁気構造の決定	長谷　正司	物質・材料研究機構	量子ビームユニット中性子散乱グループ	Determination of the magnetic structure of a $Cu_3Mo_2O_9$ single crystal using polarized neutrons	Masashi Hase	National Institute for Materials Science
48	$(CuZn)_3Mo_2O_9$ 単結晶の磁気反射の測定	長谷　正司	物質・材料研究機構	量子ビームユニット中性子散乱グループ	Investigation of magnetic reflections in a $(CuZn)_3Mo_2O_9$ single crystal	Masashi Hase	National Institute for Materials Science

No.	課題名	氏名	所属		Title	Name	Organization
49	混晶系 $Ba_{1-x}Ca_xTiO_3$ のフォノン	留野　泉	秋田大学	教育文化学部	Phonons in $Ba_{1-x}Ca_xTiO_3$	Izumi Tomeno	Akita University
・申請装置 6G: TOPAN							
50	TOPAN（東北大理：３軸型偏極中性子分光器）IRT 課題	岩佐　和晃	東北大学	大学院理学研究科	IRT: TOPAN (Tohoku-University Polarization Analysis Neutron Spectrometer)	Kazuaki Iwasa	Tohoku University
51	新規 T' 構造ホールドープ銅酸化物 $Pr_{2-x}Ca_xCuO_4$ における磁気相関の研究	藤田　全基	東北大学	金属材料研究所	Study of spin correlations in novel T'-structured cuprate oxide $Pr_{2-x}Ca_xCuO_4$	Masaki Fujita	Tohoku University
52	高精度測定による Fe-LSCO の異方的磁気秩序ピークの起源の研究	藤田　全基	東北大学	金属材料研究所	Origin of anisotropic magnetic peak in Fe-LSCO studied with high resolution measurement	Masaki Fujita	Tohoku University
53	新規フラストレーションスピン梯子系 $BiCu_2PO_6$ における磁気相関の温度発展	藤田　全基	東北大学	金属材料研究所	Thermal evolution of magnetic correlations in novel frustrated spin-ladder system $BiCu_2PO_6$	Masaki Fujita	Tohoku University
54	遍歴電子反強磁性体 Mn_3Si における動的スピン階層構造の研究	平賀　晴弘	東北大学	金属材料研究所	Study on dynamical spin hierarchical structure in itinerant-electron antiferromagnet Mn_3Si	Haruhiro Hiraka	Tohoku University
55	$PrIr_2Zn_{20}$ における非 Kramers 二重項による四極子秩序の検証	岩佐　和晃	東北大学大学院	理学研究科	Search for a quadrupole ordering due to a non-Kramers doublet in $PrIr_2Zn_{20}$	Kazuaki Iwasa	Tohoku University
56	近藤半導体 $CeOs_4Sb_{12}$ における磁場によってエンハンスされる秩序変数	岩佐　和晃	東北大学大学院	理学研究科	An order parameter enhanced by magnetic field in the Kondo semiconductor $CeOs_4Sb_{12}$	Kazuaki Iwasa	Tohoku University
57	$Ce_{0.7}La_{0.3}B_6$ の一軸圧下中性子回折	桑原　慶太郎	茨城大学大学院	理工学研究科応用粒子線科学専攻	Neutron diffraction study of $Ce_{0.7}La_{0.3}B_6$ under uniaxial pressure	Keitaro Kuwahara	Ibaraki University
58	CeTe における圧力誘起反強四極子秩序	松村　武	広島大学	大学院先端物質科学研究科	Pressure induced antiferroquadrupole order in CeTe	Takeshi Matsumura	Hiroshima University
59	$Ce_{0.5}La_{0.5}B_6$ における磁気八極子秩序の検証	松村　武	広島大学	大学院先端物質科学研究科	Magnetic octupole order in $Ce_{0.5}La_{0.5}B_6$	Takeshi Matsumura	Hiroshima University
60	水素貯蔵材料アルミニウム錯体水素化物における水素放出過程の回折と非弾性散乱による研究	富安　啓輔	東北大学	高等教育開発推進センター	Diffraction and inelastic scattering studies of decomposition process in hydrogen storage material, hydride with aluminum complex	Keisuke Tomiyasu	Tohoku University
・申請装置 C1-1: HER							
61	HER (高エネルギー分解能３軸型中性子分光器) IRT 課題	横山　淳	茨城大学	理学部理学科	IRT: HER (High Energy Resolution Triple-Axis Spectrometer)	Makoto Yokoyama	Ibaraki University
62	$La_{1-x}U_xRu_2Si_2$ $(x > 0.9)$ における磁気秩序構造と磁気励起	網塚　浩	北海道大学	大学院理学研究院 物理学部門	Magnetic ordering structure and excitation in $La_{1-x}U_xRu_2Si_2$ $(x > 0.9)$	Hirsohi Amitsuka	Hokkaido University
63	空間反転対称性をもたない超伝導体 $CeRhSi_3$ の磁気励起	阿曽　尚文	琉球大学	理学部物質地球科学科	Magnetic fluctuations in a non-centrosymmetric superconductor $CeRhSi_3$	Naofumi Aso	University of the Ryukyus

No.	課題名	氏名	所属		Title	Name	Organization
64	量子臨界点近傍にある $YbCo_2Zn_{20}$ の磁気励起	阿曽　尚文	琉球大学	理学部物質地球科学科	Magnetic excitations in $YbCo_2Zn_{20}$ in vicinity of a quantum critical point	Naofumi Aso	University of the Ryukyus
65	高エネルギー磁気励起測定による Bi2201 の磁気励起分散の研究	榎木　勝徳	九州工業大学	大学院工学研究院物質工学研究系	Study of magnetic excitation dispassion in Bi2201 by measurement of high-energy excitation	Masanori Enoki	Kyushu Institute of Technology
66	新規 T' 構造ホールドープ銅酸化物 $Pr_{2-x}Ca_xCuO_4$ における磁気相関の研究	藤田　全基	東北大学	金属材料研究所	Study of spin correlations in novel T'-structured cuprate oxide $Pr_{2-x}Ca_xCuO_4$	Masaki Fujita	Tohoku University
67	高精度測定による Fe-LSCO の異方的磁気秩序ピークの起源の研究	藤田　全基	東北大学	金属材料研究所	Origin of anisotropic magnetic peak in Fe-LSCO studied with high resolution measurement	Masaki Fujita	Tohoku University
68	新規フラストレーションスピン梯子系 $BiCu_2PO_6$ における磁気相関の温度発展	藤田　全基	東北大学	金属材料研究所	Thermal evolution of magnetic correlations in novel frustrated spin-ladder system $BiCu_2PO_6$	Masaki Fujita	Tohoku University
69	一次元フラストレート鎖量子磁性体 $CaCuVO_4$ (OD) の磁気励起	萩原　雅人	東京大学	物性研究所	Magnetic excitation of one dimensional quantum frustrated chain $CaCuVO_4$(OD)	Masato Hagihala	The University of Tokyo
70	$DyFe_2Zn_{20}$ における異方性変化を伴う逐次磁気相転移	岩佐　和晃	東北大学大学院	理学研究科	Successive magnetic phase transition accompanying drastic variation in magnetic anisotropy of $DyFe_2Zn_{20}$	Kazuaki Iwasa	Tohoku University
71	量子スピンアイスの研究	門脇　広明	首都大学東京	理工学研究科	Quantum spin ice	Hiroaki Kadowaki	Tokyo Metropolitan University
72	スピン・ネマティック相関の検出	益田　隆嗣	東京大学	物性研究所	Detection of spin nematic correlation	Takatsugu Masuda	The University of Tokyo
73	スピンギャップ系物質 $Pb_2V_3O_9$ の磁気構造と磁気励起	益田　隆嗣	東京大学	物性研究所	Magnetic structure and magnetic excitation in the spin gap material $Pb_2V_3O_9$	Takatsugu Masuda	The University of Tokyo
74	スピン格子結合系 $CuFeO_2$ のスピン波分散関係の一軸応力変化	満田　節生	東京理科大学	理学部物理学教室	Spin wave dispersion relation in a spin-lattice coupled system $CuFeO_2$ under uniaxial stress	Setsuo Mitsuda	Tokyo University of Science
75	鉄系スピンラダー $BaFe_2Se_3$ の磁気揺動	南部　雄亮	東北大学	多元物質科学研究所	Spin dynamics of the iron-based spin ladder compound $BaFe_2Se_3$	Yusuke Nambu	Tohoku University
76	AFeAs (A = Li, Na) の超伝導対称性	南部　雄亮	東北大学	多元物質科学研究所	Superconducting pairing symmetry in AFeAs (A = Li, Na)	Yusuke Nambu	Tohoku University
77	強磁性超伝導体 UCoGe におけるスピン揺らぎの研究	佐藤　憲昭	名古屋大学	大学院理学研究科	Study on spin fluctuations of the superconducting ferromagnet UCoGe	Noriaki Sato	Nagoya University
78	$CeTe_3$ および $TbTe_3$ における量子臨界現象および磁性と超伝導の相関の研究	佐藤　憲昭	名古屋大学	大学院理学研究科	Study on the quantum criticality and correlation of magnetism and superconductivity in $CeTe_3$ and $TbTe_3$	Noriaki Sato	Nagoya University
79	重い電子系超伝導体 $CeRh_xIr_{1-x}In_5$ における磁性と超伝導の相関の研究	佐藤　憲昭	名古屋大学	大学院理学研究科	Study on the correlation of magnetism and superconductivity in $CeRh_xIr_{1-x}In_5$	Noriaki Sato	Nagoya University
80	量子スピン反強磁性三量体系 2b $3CuCl_2$ $2H_2O$ の磁気励起	佐藤　卓	東北大学	多元物質科学研究所	Magnetic excitations in quantum spin antiferromagnetic trimer system 2b $3CuCl_2$ $2H_2O$	Taku J Sato	Tohoku University

No.	課題名	氏名	所属		Title	Name	Organization
81	$Dy_3Al_5O_{12}$ ガーネットにおけるクーロン相の探索	佐藤　卓	東北大学	多元物質科学研究所	Search for Coulomb phase in the $Dy_3Al_5O_{12}$ garnet	Taku J Sato	Tohoku University
82	カゴメ格子・三角格子積層系 $YBaCo_4O_7$ の磁気励起	左右田　稔	東京大学	物性研究所	Magnetic excitation of $YBaCo_4O_7$ with kagome and triangular lattices	Minoru Soda	The University of Tokyo
83	$A_2CoSi_2O_7$(A=Ca and Ba) におけるエレクトロマグノン	左右田　稔	東京大学	物性研究所	Electromagnon in $A_2CoSi_2O_7$ (A=Ca and Ba)	Minoru Soda	The University of Tokyo
84	強磁性量子臨界点近傍の遍歴電子フラストレート磁性体 Fe_3Mo_3N およびその Co 置換系の動的スピン相関	田畑　吉計	京都大学	大学院工学研究科材料工学専攻	Dynamic spin correlations of itinerant-electron frustrated magnets in the vicinity of a FM-QCP Fe_3Mo_3N and its co-substituted systems	Yoshikazu Tabata	Kyoto University
85	S=1/2 三角格子ハイゼンベルク反強磁性体 $Ba_3CoSb_2O_9$ の磁気励起と量子再規格化	田中　秀数	東京工業大学	大学院理工学研究科物性物理学専攻	Quantum renormalization of magnetic excitations in S=1/2 triangular lattice Heisenberg antiferromagnet $Ba_3CoSb_2O_9$	Hidekazu Tanaka	Tokyo Institute of Technology
86	水素貯蔵材料アルミニウム錯体水素化物における水素放出過程の回折と非弾性散乱による研究	富安　啓輔	東北大学	高等教育開発推進センター	Diffraction and inelastic scattering studies of decomposition process in hydrogen storage material, hydride with aluminum complex	Keisuke Tomiyasu	Tohoku University
87	電荷スピン両フラストレート系 1147 フェライトの中性子散乱による電気磁気効果探査	蒲沢　和也	総合科学研究機構	東海事業センター	Neutron scattering study for both charge and spin frustrated system of the 4th pyrochlore lattice of cubic 1147 ferrite $HoBaFe_4O_7$	Kazuya Kamazawa	CROSS-Tokai
88	鉄系超伝導体のスピン揺動	李　哲虎	産業技術総合研究所	エネルギー技術研究部門	Spin fluctuations of iron-based superconductors	Chul-Ho Lee	National Institute of Advanced Industrial Science and Technology
89	$PrRh_2Ge_2$ の逐次磁気転移	繁岡　透	山口大学	理工学研究科	Successive magnetic transitions in $PrRh_2Ge_2$	Toru Shigeoka	Yamaguchi University
90	逐次相転移を示した三角格子物質 $Co_2(OD)_3Br$ のフラストレーション磁性とスピン揺らぎ	鄭　旭光	佐賀大学	大学院工学系研究科		Xu-Guang Zheng	Saga University
91	atacamite 型四面体構造 $Mn_2(OD)_3Cl$, $Mn_2(OD)_3Br$ のスピン揺らぎ	鄭　旭光	佐賀大学	大学院工学系研究科	Investigation of spin fluctuations in atacamite-type pyrochlore compounds $Mn_2(OD)_3Cl$ and $Mn_2(OD)_3Br$	Xu-Guang Zheng	Saga University
・申請装置 C1-2: SANS-U							
92	SANS-U（二次元位置測定小角散乱装置）IRT 課題	柴山　充弘	東京大学	物性研究所	IRT: SANS-U (Small Angle Neutron Scattering Instrument)	Mitsuhiro Shibayama	The University of Tokyo
93	時分割 SANS 測定によるイオン液体中で特有なゲル化反応速度論の構造化学的研究	藤井　健太	東京大学	物性研究所	Gelation process of tetra-PEG ion gel studied by time-resolved small angle neutron scattering	Kenta Fujii	The University of Tokyo
94	phosphonate 型イオン液体を溶解剤とするセルロースの溶存構造	藤井　健太	東京大学	物性研究所	Solution structure of phosphonate-based ionic liquid containing cellulose	Kenta Fujii	The University of Tokyo
95	空間反転対称性の破れた超伝導体のヘリカル磁束格子の観測	古川　はづき	お茶の水女子大学	大学院人間文化創成科学研究科	Helical vortex phase on non-centrosymmetric superconductors	Hazuki Furukawa	Ochanomizu University
96	新規 Fe 系超伝導体の磁束格子実験	古川　はづき	お茶の水女子大学	大学院人間文化創成科学研究科	SANS experiment on flux line lattice on new Fe pnictide superconductors	Hazuki Furukawa	Ochanomizu University

No.	課題名	氏名	所属		Title	Name	Organization
97	希釈冷凍機温度領域における $CeMIn_5$(M=Co, Ir) の磁束の磁気形状因子の異常	古川　はづき	お茶の水女子大学	大学院人間文化創成科学研究科	Anomalous magnetic form factor in the vortex state on $CeMIn_5$ (M=Co, Ir)	Hazuki Furukawa	Ochanomizu University
98	中性子小角散乱実験による Sr_2RuO_4 の異常金属状態の研究	古川　はづき	お茶の水女子大学	大学院人間文化創成科学研究科	Anomalous vortex state in Sr_2RuO_4 studied by SANS experiments	Hazuki Furukawa	Ochanomizu University
99	Rheo-SANS を用いたずり応力場におけるグリース増ちょう剤の構造解析	平山　朋子	同志社大学	理工学部	Structural analysis of thickener in grease under shear stress by means of Rheo-SANS	Tomoko Hirayama	Doshisha University
100	エポキシ樹脂の重合誘起相分離と架橋構造	金谷　利治	京都大学	化学研究所	Polymerization induced phase separation of epoxy resin and network structure	Toshiji Kanaya	Kyoto University
101	非イオン界面活性剤水溶液で形成されるベシクルの臨界ベシクル濃度近傍での構造とダイナミクス	川端　庸平	首都大学東京	理工学研究科	Static and dynamic structures of vesicles near the critical vesicle concentration in a nonionic surfactant aqueous solution	Youhei Kawabata	Tokyo Metropolitan University
102	架橋点が疎水性相互作用からなる非晶性高分子ゲルの広い空間スケールでの構造	松葉　豪	山形大学	大学院理工学研究科	Wide spatial scale structure of hydrophobic crosslinked gels in amorphous polymers	Go Matsuba	Yamagata University
103	温度および塩濃度応答性界面不活性／界面活性転移高分子のミセル形成とナノ構造転移	松岡　秀樹	京都大学	工学研究科	Micelle formation and nanostructure transition of temperature and salt concentration responsive non-surface active/surface active transition polymers	Hideki Matsuoka	Kyoto University
104	超巨大磁気抵抗を示すペロブスカイト型マンガン酸化物における自己相似プロファイルの研究	松浦　直人	東北大学	金属材料研究所	Investigation of power law profile of the ferromagnetic cluster in perovskite manganite	Masato Matsuura	Tohoku University
105	POPC ナノディスクの構造とダイナミクス	中野　実	富山大学大学院	医学薬学研究部（薬学）	Structure and dynamics of POPC nanodiscs	Minoru Nakano	University of Toyama
106	膜貫通ペプチドのフリップフロップ誘起能の評価	中野　実	富山大学大学院	医学薬学研究部（薬学）	Induction of flip-flop by transmembrane peptides	Minoru Nakano	University of Toyama
107	膜脂質のダイナミクスに及ぼす膜の曲率の評価	中野　実	富山大学大学院	医学薬学研究部（薬学）	Effects of curvature on dynamics of membrane lipids	Minoru Nakano	University of Toyama
108	界面不活性の働きをする界面活性剤	貞包　浩一朗	高エネルギー加速器研究機構	物質構造科学研究所中性子研究系	Amphiphilic molecules acting as a surface inactive substance	Koichiro Sadakane	KEK
109	高圧条件下における２成分混合溶液の新奇な臨界挙動	貞包　浩一朗	高エネルギー加速器研究機構	物質構造科学研究所中性子研究系	Novel critical behavior in a mixture of water/organic solvent under high-pressure condition	Koichiro Sadakane	KEK
110	水／有機溶媒／塩混合溶液系の秩序構造に対する圧力の効果	貞包　浩一朗	高エネルギー加速器研究機構	物質構造科学研究所中性子研究系	Pressure-induced phase transition in a mixture of water/organic solvent/salt	Koichiro Sadakane	KEK
111	PEG/PDMS 相互連結相構造を有する高分子ゲルの構造解析	酒井　崇匡	東京大学	工学系研究科	Structural study on end-linked PEG/PDMS hydrogels	Takamasa Sakai	The University of Tokyo
112	毛髪の内部構造解析	柴山　充弘	東京大学	物性研究所	Structural analysis of hair	Mitsuhiro Shibayama	The University of Tokyo
113	温度応答性部位を有する Tetra ゲルの構造解析	柴山　充弘	東京大学	物性研究所	Structural analysis of thermo-responsive Tetra-gel	Mitsuhiro Shibayama	The University of Tokyo

No.	課題名	氏名	所属		Title	Name	Organization
114	Rheo-FocusingSANS を用いたずり粘稠効果に伴う紐状ミセル伸長機構の解明	柴山　充弘	東京大学	物性研究所	Rheo-Focusing SANS study on shear induced transition of wormlike micelle	Mitsuhiro Shibayama	The University of Tokyo
115	燃料電池電極用触媒インクの構造解析	柴山　充弘	東京大学	物性研究所	Structural studies on catalyst for fuel cell electrodes	Mitsuhiro Shibayama	The University of Tokyo
116	水性アクリル樹脂分散体における粒子構造解析	柴山　充弘	東京大学	物性研究所	Particle structure for aqueous acrylic polymer dispersion	Mitsuhiro Shibayama	The University of Tokyo
117	フェノール樹脂ゲル化過程の不均一性解析	柴山　充弘	東京大学	物性研究所	Inhomogeneity of phenolic resins during gelation process	Mitsuhiro Shibayama	The University of Tokyo
118	α - シヌクレインにおける初期会合過程のその場観測	杉山　正明	京都大学	原子炉実験所	In situ SANS observation of the early stage on aggregation process of α-synuclein	Masaaki Sugiyama	Kyoto University
119	糖鎖クラスターを修飾した巨大錯体分子の構造解析	杉山　正明	京都大学	原子炉実験所	Structural analysis of huge complexes decorated with sugar cluster surfaces	Masaaki Sugiyama	Kyoto University
120	含水飽和圧縮モンモリロナイトの原子炉型中性子小角散乱によるキャラクタリゼーション	高橋　宏明	東北大学	工学研究科	Characterization of water-saturated compacted montmorillonites by reactor type small-angle neutron scattering	Hiroaki Takahashi	Tohoku University
121	イミダゾリウム系イオン液体とベンゼン誘導体との混合状態	高椋　利幸	佐賀大学	大学院工学系研究科	Mixing state of imidazolium-based ionic liquids and benzene derivatives	Toshiyuki Takamuku	Saga University
122	イオン液体によるタンパク質３次構造の安定化	高椋　利幸	佐賀大学	大学院工学系研究科	Stabilization of tertiary structure of proteins by ionic liquids	Toshiyuki Takamuku	Saga University
123	結び目を有する環状高分子の溶液中のコンフォメーション	高野　敦志	名古屋大学	大学院工学研究科化学・生物工学専攻	Conformation of knotted ring polymers in solutions	Atsushi Takano	Nagoya University
124	(環状高分子＋線状高分子）ブレンド試料中の環状高分子の回転半径に及ぼす線状高分子の添加効果	高野　敦志	名古屋大学	大学院工学研究科化学・生物工学専攻	Addition effect of linear polymer in ring/linear polymer blend on radius of gyration of ring polymer	Atsushi Takano	Nagoya University
125	イオン液体と界面活性剤の混合物の相分離現象	吉田　亨次	福岡大学	理学部	Phase separation of ionic liquids and surfactant mixtures	Koji Yoshida	Fukuoka University
126	中性子スピンエコー法を基軸とした Staphylococcal nuclease の水溶液中でのメゾスコピックダイナミクス研究	遠藤　仁	日本原子力研究開発機構	量子ビーム応用研究部門	Mesoscopic dynamics of staphylococcal nuclease in aqueous solution investigated by neutron spin echo technique	Hitoshi Endo	Japan Atomic Energy Agency
127	生理活性を持つリン脂質二重膜のメゾスコピック物性研究	遠藤　仁	日本原子力研究開発機構	量子ビーム応用研究部門	Mesoscopic properties of bioactive lipid bilayer	Hitoshi Endo	Japan Atomic Energy Agency
128	DNA 界面密生相の構造物性解析	藤田　雅弘	理化学研究所	前田バイオ工学研究室	Structural and physical properties of DNA brush layer	Masahiro Fujita	RIKEN
129	多分岐ポリエチレンオキサイドを用いたイオンゲルの網目構造とその溶媒効果	藤井　健太	東京大学	物性研究所中性子科学研究施設	Solvent effect on the network structure of Tetra-PEG ion gel	Kenta Fujii	The University of Tokyo
130	Fe 系超伝導体の磁束研究	古川　はづき	お茶の水女子大学	大学院人間文化創成科学研究科	Vortex study on Fe-based superconductors	Hazuki Furukawa	Ochanomizu University

No.	課題名	氏名	所属		Title	Name	Organization
131	中性子小角散乱法による多孔性放射線合成ゲルのナノ構造解析	佐藤　信浩	京都大学	原子炉実験所	SANS analysis on the nano structure of radiation-synthesized porous polymer gels	Nobuhiro Sato	Kyoto University
・申請装置 C1-3: ULS							
132	ULS（極小角散乱装置）IRT 課題	大竹　淑恵	理化学研究所	仁科加速器センター	IRT: ULS (Ultra Small Angle Scattering Instrument)	Yoshie Otake	RIKEN
・申請装置 C1-3: mf-SANS							
133	C1-3 小型集束型小角散乱装置 IRT 課題	古坂　道弘	北海道大学	大学院工学研究科	IRT: mf-SANS (mini-focusing Small Angle Neutron Scattering Instrument)	Michihiro Furusaka	Hokkaido University
・申請装置 C2-3-1: iNSE							
134	iNSE（中性子スピンエコー分光器）IRT 課題	柴山　充弘	東京大学	物性研究所	IRT: iNSE (New issp Neutron Spin Echo Spectrometer)	Mitsuhiro Shibayama	The University of Tokyo
135	界面活性剤ゲルの膜面内ダイナミクス	川端　庸平	首都大学東京	理工学研究科	Dynamics in gel-like surfactant membrane	Youhei Kawabata	Tokyo Metropolitan University
136	非イオン界面活性剤水溶液で形成されるベシクルの臨界ベシクル濃度近傍での構造とダイナミクス	川端　庸平	首都大学東京	理工学研究科	Static and dynamic structures of vesicles near the critical vesicle concentration in a nonionic surfactant aqueous solution	Youhei Kawabata	Tokyo Metropolitan University
137	リラクサー PMN-xPT におけるフラクタル揺らぎの研究	松浦　直人	東北大学	金属材料研究所	Study of fractal dynamics in relaxor ferroelectric PMN-30%PT	Masato Matsuura	Tohoku University
138	POPC ナノディスクの構造とダイナミクス	中野　実	富山大学大学院	医学薬学研究部	Structure and dynamics of POPC nanodiscs	Minoru Nakano	University of Toyama
139	水／有機溶媒／塩混合溶液系の秩序構造に対する圧力の効果	貞包　浩一朗	高エネルギー加速器研究機構	物質構造科学研究所中性子研究系	Pressure-induced phase transition in a mixture of water/organic solvent/salt	Koichiro Sadakane	KEK
140	Tetra-PEG イオンゲル・ハイドロゲルの動的挙動の解析	柴山　充弘	東京大学	物性研究所	Segment dynamics analysis of Tetra-PEG ionic liquid gels and hydrogels	Mitsuhiro Shibayama	The University of Tokyo
141	イオン液体によるタンパク質３次構造の安定化	高椋　利幸	佐賀大学	大学院工学系研究科	Stabilization of tertiary structure of proteins by ionic liquids	Toshiyuki Takamuku	Saga University
142	イオン液体と界面活性剤の混合物の相分離現象	吉田　亨次	福岡大学	理学部	Phase separation of ionic liquids and surfactant mixtures	Koji Yoshida	Fukuoka University
143	中性子スピンエコー法を基軸とした Staphylococcal nuclease の水溶液中でのメゾスコピックダイナミクス研究	遠藤　仁	日本原子力研究開発機構	量子ビーム応用研究部門	Mesoscopic dynamics of staphylococcal nuclease in aqueous solution investigated by neutron spin echo technique	Hitoshi Endo	Japan Atomic Energy Agency
144	生理活性を持つリン脂質二重膜のメゾスコピック物性研究	遠藤　仁	日本原子力研究開発機構	量子ビーム応用研究部門	Mesoscopic properties of bioactive lipid bilayer	Hitoshi Endo	Japan Atomic Energy Agency

No.	課題名	氏名	所属		Title	Name	Organization
・申請装置 C3-1-1: AGNES							
145	AGNES（高分解能パルス冷中性子分光器）IRT 課題	山室　修	東京大学	物性研究所	IRT: AGNES (Angle Focusing Cold Neutron Spectrometer)	Osamu Yamamuro	The University of Tokyo
146	GeTe 系の液液転移と個別原子拡散	千葉　文野	慶應義塾大学	理工学部物理学科	Liquid-liquid transition and individual atomic diffusion in GeTe system	Ayano Chiba	Keio University
147	ポリ 4- メチルペンテン -1 のガス透過と局所ダイナミクスの相関	井上　倫太郎	京都大学	化学研究所	Correlation between local dynamics and gas permeability of poly(4-methyl-1-pentene)	Rintaro Inoue	Kyoto University
148	非晶性高分子の分子運動への超臨界二酸化炭素の影響	金子　文俊	大阪大学	大学院理学研究科高分子科学専攻	Influence of supercritical carbon dioxide on dynamical properties of amorphous polymers	Fumitoshi Kaneko	Osaka University
149	ペロブスカイト型酸水素化物におけるヒドリドダイナミクス	小林　洋治	京都大学	工学研究科	Mobile hydride in perovskite oxyhydrides	Yoji Kobayashi	Faculty of Engineering, Kyoto University
150	中性子準弾性散乱によるアルキルイミダゾリウム系イオン液体におけるアルキル鎖運動の系統的研究	古府　麻衣子	東京大学	物性研究所	Systematic QENS study on dynamics of alkyl-chain in alkylimidazolium ionic liquids	Maiko Kofu	The University of Tokyo
151	H_2-SF_6 ハイドレート中の水素の拡散ダイナミクス	古府　麻衣子	東京大学	物性研究所	Diffusion of hydrogen molecules in H_2-SF_6 hydrate	Maiko Kofu	The University of Tokyo
152	メタノール水溶液における疎水性水和による水分子の拡散遅延効果	丸山　健二	新潟大学	理学部化学科	The retardation effect of hydrophobic hydration on diffusion dynamics of water molecules in methanol aqueous solution	Kenji Maruyama	Niigata University
153	水酸化テトラアルキルアンモニウムを包接した配位高分子中での水酸化物イオンの運動	貞清　正彰	九州大学	カーボンニュートラル・エネルギー国際研究所	Motion of hydroxide ions inside a metal-organic framework including alkyl ammonium hydroxides	Masaaki Sadakiyo	Kyushu Univeristy
154	ナノ細孔中に封じ込められたシクロヘキサンの新奇な相転移に伴うダイナミクスの変化の解明	辰巳　創一	東京工業大学	理工学研究科化学専攻	Elucidation of the dynamical change involved in newly discovered phase transition of nano-confined cyclohexane	Soichi Tatsumi	Tokyo Institute of Technology
155	メソポーラス有機シリカ中に閉じ込めた水とメタノールのダイナミクス	山口　敏男	福岡大学	理学部	Dynamics of water and methanol molecules confined in mesoporous organic silica	Toshio Yamaguchi	Fukuoka University
156	両性イオン - グリシンの水溶液のダイナミクスと水和構造	山室　憲子	東京電機大学	理工学部	Dynamics and hydration structures of aqueous solutions of zwitterionic glycine	Noriko Yamamuro	Tokyo Denki University
157	逆浸透膜表面での水のダイナミクス	山室　修	東京大学	物性研究所	Dynamics of water on surface of reverse osmosis membranes	Osamu Yamamuro	The University of Tokyo
158	多孔性配位高分子 MIL-53 におけるプロトン伝導ダイナミクス	山室　修	東京大学	物性研究所	Proton conducting dynamics in porous coordination polymer MIL-53	Osamu Yamamuro	The University of Tokyo
159	マルチフェロイック物質 $CuFe_{1-x}MxO_2$ (M=Al,Mn) の中性子準弾性散乱	林　慶	東北大学	大学院工学研究科応用物理学専攻	Quasielastic neutron scattering of multiferroic $CuFe_{1-x}MxO_2$ (M=Al,Mn)	Kei Hayashi	Tohoku University
・申請装置 C3-1-2: MINE1							

No.	課題名	氏名	所属		Title	Name	Organization
160	MINE1（京大炉：多層膜中性子干渉計・反射率計）IRT 課題	日野　正裕	京都大学	原子炉実験所	IRT: MINE (Multilayer Interferometer and Refrectmeter for Neutron) 1	Masahiro Hino	Kyoto University
161	MIEZE 分光法を用いた量子井戸滞在時間の実時間測定	日野　正裕	京都大学	原子炉実験所	Direct measurement of dwell time in quasi-bound state by mean of MIEZE spectroscopy	Masahiro Hino	Kyoto University
162	2 次元中性子集光デバイスの開発	日野　正裕	京都大学	原子炉実験所	Development of 2D focusing supermirror device	Masahiro Hino	Kyoto University
163	中性子スピン位相イメージングを用いた電流分布の可視化 III	田崎　誠司	京都大学	工学研究科原子核工学専攻	Visualization of electric current distribution using neutron spin phase imaging III	Seiji Tasaki	Kyoto University
164	冷中性子による全断面積測定	田崎　誠司	京都大学	工学研究科原子核工学専攻	Measurement of total cross section for cold neutron	Seiji Tasaki	Kyoto University
・申請装置 C3-1-2: MINE2							
165	MINE2（京大炉：多層膜中性子干渉計・反射率計）IRT 課題	日野　正裕	京都大学	原子炉実験所	IRT: MINE (Multilayer Interferometer and Refrectmeter for Neutron) 2	Masahiro Hino	Kyoto University
166	経路を完全分離する Jamin 型冷中性子干渉計の開発と応用	舟橋　春彦	京都大学	高等教育研究開発推進機構	Jamin-type cold-neutron interferometer with completely separated two paths	Haruhiko Funahashi	Kyoto University
167	MIEZE 分光法を用いた量子井戸滞在時間の実時間測定	日野　正裕	京都大学	原子炉実験所	Direct measurement of dwell time in quasi-bound state by mean of MIEZE spectroscopy	Masahiro Hino	Kyoto University
168	2 次元中性子集光デバイスの開発	日野　正裕	京都大学	原子炉実験所	Development of 2D focusing supermirror device	Masahiro Hino	Kyoto University
169	中性子反射率法による各種 DLC 被膜／潤滑油界面の構造解析	平山　朋子	同志社大学	理工学部	Structural analysis of interface of DLC/lubricant by means of neutron reflectometry	Tomoko Hirayama	Doshisha University
170	中性子反射率法による潤滑下摩擦低減のための金属基板上ポリマーブラシ層の膜厚・密度測定	平山　朋子	同志社大学	理工学部	Thickness and density of polymer brush layer on metal surface under lubrication measured by neutron reflectometry	Tomoko Hirayama	Doshisha University
171	中性子反射率法による疎水性表面上におけるアルカン分子の密度測定	平山　朋子	同志社大学	理工学部	Density of alkane molecules on hydrophobic surface measured by neutron reflectometry	Tomoko Hirayama	Doshisha University
172	中性子反射率によるポリメチルメタクリレート薄膜におけるガラス転移温度の分布	井上　倫太郎	京都大学	化学研究所	Distribution of glass transition temperature in poly(methyl methacrylate) thin film studied by neutron reflectivity	Rintaro Inoue	Kyoto University
173	ディップコート薄膜の熱的物性挙動	井上　倫太郎	京都大学	化学研究所	Thermal properties of dip-coated polymer thin film	Rintaro Inoue	Kyoto University
174	超冷中性子光学系のためのデバイス開発	北口　雅暁	京都大学	原子炉実験所	Development of optical devices for ultra cold neutrons	Masaaki Kitaguchi	Kyoto University
175	高分子 / 水界面領域におけるタンパク質吸着状態に関する研究	松野　寿生	九州大学	大学院工学研究院　応用化学部門 (機能)	Study of adsorbed proteins at the polymer/water interfaces	Hisao Matsuno	Kyushu University

No.	課題名	氏名	所属		Title	Name	Organization
176	混合液体と接触した高分子界面の凝集状態	田中　敬二	九州大学	大学院工学研究院応用化学部門	Aggregation State of Interface between Polymers and Mixed Non-solvents	Keiji Tanaka	Kyushu University
177	中性子スピン位相イメージングを用いた電流分布の可視化 III	田崎　誠司	京都大学	工学研究科原子核工学専攻	Visualization of electric current distribution using neutron spin phase imaging III	Seiji Tasaki	Kyoto University
178	波動関数の振幅を制御した多層膜中性子反射鏡の開発	田崎　誠司	京都大学	工学研究科原子核工学専攻	Improvement of multilayer neutron mirrors by controlling amplitude of the internal wavefunction	Seiji Tasaki	Kyoto University
179	多層膜スピンスプリッターによる高空間分解能磁気イメージング法の開発	林田　洋寿	日本原子力研究開発機構	J-PARC センター	Development of new magnetic imaging technique with high spatial resolution using multilayer spin splitter	Hirotoshi Hayashida	Japan Atomic Energy Agency
180	多層膜冷中性子干渉計による重力起因位相の精密測定（II）	関　義親	理化学研究所	仁科加速器研究センター	Precision measurement of gravitationally induced phase with multilayer cold neutron interferometer II	Yoshichika Seki	RIKEN
・申請装置 T1-1: HQR							
181	HQR（高分解能中性子散乱装置）IRT 課題	吉沢　英樹	東京大学	物性研究所	IRT: HQR (High Q Resolution Triple Axis Spectrometer)	Hideki Yoshizawa	The University of Tokyo
182	$EuCo_2P_2$ の磁気構造解析	藤原　哲也	山口大学	理工学研究科	Magnetic structure analysis of $EuCo_2P_2$	Tetsuya Fujiwara	Yamaguchi University
183	$EuRu_2P_2$ の磁気構造解析	藤原　哲也	山口大学	理工学研究科	Magnetic structure analysis of $EuRu_2P_2$	Tetsuya Fujiwara	Yamaguchi University
184	重い電子系新物質 $Ce_2Pt_3Ge_5$ の磁気構造解析	藤原　哲也	山口大学	理工学研究科	Magnetic structure analysis of new heavy fermion material $Ce_2Pt_3Ge_5$	Tetsuya Fujiwara	Yamaguchi University
185	空間反転対称性を欠く二次元的系 $CeNiC_2$ の磁気構造	片野　進	埼玉大学	理工学研究科	Magnetic structures of the non-centrosymmetrical 2D system $CeNiC_2$	Susumu Katano	Saitama University
186	スピン・ネマティック相関の検出	益田　隆嗣	東京大学	物性研究所	Detection of spin nematic correlation	Takatsugu Masuda	The University of Tokyo
187	磁性イオン置換によりフラストレーションを制御したスピン誘導型強 誘電体 $CuFeO_2$ の交差相関物性	満田　節生	東京理科大学	理学部物理学教室	Cross-correlation in spin-driven ME multiferroic $CuFeO_2$ with Mn-magnetic doping	Setsuo Mitsuda	Tokyo University of Science
188	スピン格子結合系 $CuFeO_2$ のスピン波分散関係の一軸応力変化	満田　節生	東京理科大学	理学部物理学教室	Spin wave dispersion relation in a spin-lattice coupled system $CuFeO_2$ under uniaxial stress	Setsuo Mitsuda	Tokyo University of Science
189	時間分割中性子散乱測定による磁気構造変化過程の実時間追跡	元屋　清一郎	東京理科大学	理工学部	Real-time observation of magnetic structural change by means of time-resolved neutron scattering experiments	Kiyoichiro Motoya	Tokyo University of Science
190	磁気構造の長時間変化と磁性原子希釈効果	元屋　清一郎	東京理科大学	理工学部	Dilution effect of magnetic atoms on the long-time variation of magnetic structure	Kiyoichiro Motoya	Tokyo University of Science
191	多段メタ磁性体 $Ca_3Co_2O_6$ における磁気構造の長時間変化への disorder の効果	茂吉　武人	東京理科大学	理工学部	Disorder effects on the long-time variation of magnetic structure in a multistep metamagnet $Ca_3Co_2O_6$	Taketo Moyoshi	Tokyo University of Science

No.	課題名	氏名	所属		Title	Name	Organization
192	三角格子系 Na_xNiO_2 の磁気構造	茂吉　武人	東京理科大学	理工学部　物理学科	Magnetic structure of a triangular system Na_xNiO_2	Taketo Moyoshi	Tokyo University of Science
193	マルチフェロイック $CuFeO_2$ における２軸圧力による磁気・強誘電ドメイン配向制御	中島　多朗	東京理科大学	理学部物理学教室	Biaxial-pressure control of multiferroic domain structure in spin-driven ME multiferroic $CuFeO_2$	Taro Nakajima	Tokyo University of Science
194	鉄系超伝導体母物質 FeTe のスピン・格子結合に対する一軸圧力効果	中島　多朗	東京理科大学	理学部物理学教室	Uniaxial pressure effect on a parent compound of Fe-based superconductor FeTe	Taro Nakajima	Tokyo University of Science
195	二次元三角格子反強磁性体の圧力効果	南部　雄亮	東北大学	多元物質科学研究所	Pressure effects on the 2D triangular antiferromagnet	Yusuke Nambu	Tohoku University
196	$CeTe_3$ および $TbTe_3$ における量子臨界現象および磁性と超伝導の相関の研究	佐藤　憲昭	名古屋大学	大学院理学研究科	Study on the quantum criticality and correlation of magnetism and superconductivity in $CeTe_3$ and $TbTe_3$	Noriaki Sato	Nagoya University
197	$MnSb_2O_6$ の磁場中磁気構造	佐藤　卓	東北大学	多元物質科学研究所	Magnetic structure of $MnSb_2O_6$ under external field	Taku J Sato	Tohoku University
198	強誘電体の相転移機構（変位型及び秩序 無秩序型）に関する統一的理解の確立	重松　宏武	山口大学	教育学部	Establishment of the unified explanation about the phase transition mechanism (displacive and order-disorder type) in ferroelectrics	Hirotake Shigematsu	Yamaguchi University
199	Rb_2MoO_4 における多形転移とソフトフォノン	重松　宏武	山口大学	教育学部	Polymorph transition and soft phonon in Rb_2MoO_4	Hirotake Shigematsu	Yamaguchi University
200	$PrRh_2Ge_2$ の逐次磁気転移	繁岡　透	山口大学	理工学研究科	Successive magnetic transitions in $PrRh_2Ge_2$	Toru Shigeoka	Yamaguchi University
201	$HoRh_2Si_2$ の成分分離逐次磁気転移	繁岡　透	山口大学	理工学研究科	Successive components-separated magnetic transitions in $HoRh_2Si_2$	Toru Shigeoka	Yamaguchi University
202	秩序型ペロブスカイト $CaCu_3Ti_4O_{12}$ のフォノン	留野　泉	秋田大学	教育文化学部	Phonons in ordered perovskite $CaCu_3Ti_4O_{12}$	Izumi Tomeno	Akita University
203	逐次相転移を示した三角格子物質 $Co_2(OD)_3Br$ のフラストレーション磁性とスピン揺らぎ	鄭　旭光	佐賀大学	大学院工学系研究科		Xu-Guang Zheng	Saga University
204	電荷スピン両フラストレート系 1147 フェライトの中性子散乱による電気磁気効果探査	蒲沢　和也	総合科学研究機構	東海事業センター	Neutron scattering study for both charge and spin frustrated system of the 4th pyrochlore lattice of cubic 1147 ferrite $HoBaFe_4O_7$	Kazuya Kamazawa	CROSS-Tokai
205	立方晶 $BaTiO_3$ のフォノンの温度依存性	留野　泉	秋田大学	教育文化学部	Temperature dependence of phonons in cubic $BaTiO_3$	Izumi Tomeno	Akita University
206	混晶系 $Ba_{1-x}Ca_xTiO_3$ のフォノン	留野　泉	秋田大学	教育文化学部	Phonons in $Ba_{1-x}Ca_xTiO_3$	Izumi Tomeno	Akita University
207	$Pr_{0.5}Sr_{0.5}MnO_3$ の高温フォノン	留野　泉	秋田大学	教育文化学部	Phonon in $Pr_{0.5}Mn_{0.5}MnO_3$ at high temperature	Izumi Tomeno	Akita University
208	atacamite 型四面体構造 $Mn_2(OD)_3Cl$, $Mn_2(OD)_3Br$ のスピン揺らぎ	鄭　旭光	佐賀大学	大学院工学系研究科	Investigation of spin fluctuations in atacamite-type pyrochlore compounds $Mn_2(OD)_3Cl$ and $Mn_2(OD)_3Br$	Xu-Guang Zheng	Saga University

No.	課題名	氏名	所属		Title	Name	Organization
・申請装置 T1-2: AKANE							
209	AKANE（東北大金研：三軸型中性子分光器 ）IRT 課題	平賀　晴弘	東北大学	金属材料研究所	IRT: AKANE (Advanced Kinken Neutron Spectrometer)	Haruhiro Hiraka	Tohoku University
210	高エネルギー磁気励起測定による Bi2201 の磁気励起分散の研究	榎木　勝徳	九州工業大学	大学院工学研究院物質工学研究系	Study of magnetic excitation dispassion in Bi2201 by measurement of high-energy excitation	Masanori Enoki	Kyushu Institute of Technology
211	新規 T' 構造ホールドープ銅酸化物 $Pr_{2-x}Ca_xCuO_4$ における磁気相関の研究	藤田　全基	東北大学	金属材料研究所	Study of spin correlations in novel T'-structured cuprate oxide $Pr_{2-x}Ca_xCuO_4$	Masaki Fujita	Tohoku University
212	高精度測定による Fe-LSCO の異方的磁気秩序ピークの起源の研究	藤田　全基	東北大学	金属材料研究所	Origin of anisotropic magnetic peak in Fe-LSCO studied with high resolution measurement	Masaki Fujita	Tohoku University
213	新規フラストレーションスピン梯子系 $BiCu_2PO_6$ における磁気相関の温度発展	藤田　全基	東北大学	金属材料研究所	Thermal evolution of magnetic correlations in novel frustrated spin-ladder system $BiCu_2PO_6$	Masaki Fujita	Tohoku University
214	遍歴電子反強磁性体 Mn_3Si における動的スピン階層構造の研究	平賀　晴弘	東北大学	金属材料研究所	Study on dynamical spin hierarchical structure in itinerant-electron antiferromagnet Mn_3Si	Haruhiro Hiraka	Tohoku University
215	マルチフェロイック物質 $SmMn_2O_5$ の磁気秩序と強誘電性	木村　宏之	東北大学	多元物質科学研究所	Antiferromagnetism and ferroelectricity in multiferroic compounds of $SmMn_2O_5$	Hiroyuki Kimura	Tohoku University
216	MPO_4 (M: 遷移金属) のカイラル磁気構造の検証	高阪　勇輔	青山学院大学	理工学部物理数理学科	Chiral magnetism in MPO_4 (M: transition metal)	Yusuke Kousaka	Aoyama-Gakuin University
217	CrX (Cr=Si, Ge) のカイラル磁気構造の検証	高阪　勇輔	青山学院大学	理工学部物理数理学科	Chiral magnetic structure in CrX (X=Si, Ge)	Yusuke Kousaka	Aoyama-Gakuin University
218	幾何学的フラストレート系 $(Mn,Mg)Cr_2O_4$ におけるらせん磁気構造のクロスオーバー	高阪　勇輔	青山学院大学	理工学部物理数理学科	Crossover between conical and screw magnetic phase in $(Mn,Mg)Cr_2O_4$	Yusuke Kousaka	Aoyama-Gakuin University
219	Mn_2Sb のスピン揺らぎの研究	小山　佳一	鹿児島大学	大学院理工学研究科	Experimental study of spin fluctuation on Mn_2Sb	Keiichi Koyama	Kagoshima University
220	磁場中中性子回折による YbPd の金属的電荷秩序構造の研究	光田　暁弘	九州大学	理学研究院	Study on metallic charge order in YbPd by neutron diffraction in a magnetic field	Akihiro Mitsuda	Kyushu Univerisity
221	鉄系超伝導体のスピン揺動	李　哲虎	産業技術総合研究所	エネルギー技術研究部門	Spin fluctuations of iron-based superconductors	Chul-Ho Lee	National Institute of Advanced Industrial Science and Technology
・申請装置 T1-3: HERMES							
222	HERMES（東北大金研：中性子粉末回折装置）IRT 課題	大山　研司	東北大学	金属材料研究所	IRT: HERMES (Kinken Powder Diffractometer for High Efficiency and High Resolution MeasurementS)	Kenji Ohoyama	Tohoku University
223	希土類 遷移金属複合酸化物の磁気構造	土井　貴弘	北海道大学	大学院理学研究院化学部門	Magnetic structure of lanthanide transition metal oxides	Yoshihiro Doi	Hokkaido University

No.	課題名	氏名	所属		Title	Name	Organization
224	新規 $AA'BO_4$ 型構造をもつ混合イオン伝導体の結晶構造とイオン伝導経路の解明	藤井　孝太郎	東京工業大学	大学院理工学研究科	Structural investigation of the novel $AA'BO_4$-type materials mixed oxide-ionic and electronic conducting materials	Kotaro Fujii	Tokyo Institute of Technology
225	異常高原子価鉄を持つ $(Ba,Sr)FeO_3$ の磁気構造と相境界の解明	陰山　洋	京都大学工学研究科	物質エネルギー化学専攻	Investigation for magnetic structure and phase boundary of $(Ba,Sr)FeO_3$ with an unusually high valence strate of iron	Hiroshi Kageyama	Kyoto University
226	正方格子 d1 超伝導体 $BaTi_2Sb_2O$ の低温構造	陰山　洋	京都大学工学研究科	物質エネルギー化学専攻	Low temperature structural analysis in $BaTi_2Sb_2O$ with a d1 square lattice	Hiroshi Kageyama	Kyoto University
227	ペロブスカイト型酸窒化物に対する水素化物イオン挿入	陰山　洋	京都大学工学研究科	物質エネルギー化学専攻	Hydride-incorporation into perovskite-type oxynitride	Hiroshi Kageyama	Kyoto University
228	ニオブドープ・ペロブスカイトコバルト酸化物の構造の解明	陰山　洋	京都大学工学研究科	物質エネルギー化学専攻	Structural investigation of neodymium-doped cobaltate perovskites	Hiroshi Kageyama	Kyoto University
229	$(CuCl)LaNb_2O_{7-x}F_x$ の構造決定	小林　洋治	京都大学	工学研究科	Structural determination of $(CuCl)LaNb_2O_{7-x}F_x$	Yoji Kobayashi	Faculty of Engineering, Kyoto University
230	新規カイラル磁性体 MPO_4 (M: 遷移金属) の磁気構造解析	高阪　勇輔	青山学院大学	理工学部物理数理学科	Magnetic structure analysis in new chiral magnetic compounds MPO_4 (M: transition metal)	Yusuke Kousaka	Aoyama-Gakuin University
231	新規カイラル磁性体 CrX (X=Si, Ge) の磁気構造解析	高阪　勇輔	青山学院大学	理工学部物理数理学科	Magnetic structure analysis in new chiral magnetic compounds CrX (X=Si, Ge)	Yusuke Kousaka	Aoyama-Gakuin University
232	電子ドープ型マンガン酸化物の磁化の反転と磁気構造	松川　倫明	岩手大学	工学部	Magnetization reversal and magnetic structure in electron doped manganites	Michiaki Matsukawa	Iwate University
233	二層三角格子反強磁性体 $Fe_2Ga_2S_5$ の結晶構造と磁気構造	南部　雄亮	東北大学	多元物質科学研究所	Crystal and magnetic structures of the bilayer triangular antiferromagnet $Fe_2Ga_2S_5$	Yusuke Nambu	Tohoku University
234	新しい S=3/2 三角格子反強磁性体の結晶構造と磁気構造	南部　雄亮	東北大学	多元物質科学研究所	Crystal and magnetic structures of a new S=3/2 triangular antiferromagnet	Yusuke Nambu	Tohoku University
235	リチウムイオンを含む新規複合酸化物の結晶構造解析	単　躍進	宇都宮大学	工学研究科	Crystal structure analysis of a novel multiple oxide with lithium and tellurium	Yue Jin Shan	Utsunomiya University
236	新しいタイプの遍歴電子フラストレート磁性体 Fe_6W_6C, Co_6W_6C における磁気相関	田畑　吉計	京都大学	大学院工学研究科材料工学専攻	Spin correlatons in novel itinerant-electron frustrated magnets Fe_6W_6C and Co_6W_6C	Yoshikazu Tabata	Kyoto University
237	機械的特性に優れた新規磁性化合物 M_2AX の磁気構造解析	田畑　吉計	京都大学	大学院工学研究科材料工学専攻	Magnetic structure of novel magnetic compounds with outstanding mechanical properties M_2AX	Yoshikazu Tabata	Kyoto University
238	スピン２の籠目格子反強磁性体 $Cs_2Mn_3LiF_{12}$ の基底状態	田中　秀数	東京工業大学	大学院理工学研究科物性物理学専攻	Ground state of spin-2 kagome lattice antiferromagnet Cs_2MnLiF_{12}	Hidekazu Tanaka	Tokyo Institute of Technology
239	ナノ細孔中に封じ込められたシクロヘキサンの新奇な相転移に伴う構造変化の解明	辰巳　創一	東京工業大学	理工学研究科化学専攻	Elucidation of the structural change involved in newly discovered phase transition of nano-confined cyclohexane	Soichi Tatsumi	Tokyo Institute of Technology
240	クロム複硫化物の結晶構造と磁気転移	手塚　慶太郎	宇都宮大学	工学研究科物質環境化学専攻	Crystal structures and magnetic transitions of chromium complex Sulfides	Keitaro Tezuka	Utsunomiya University

No.	課題名	氏名	所属		Title	Name	Organization
241	水素貯蔵材料アルミニウム錯体水素化物における水素放出過程の回折と非弾性散乱による研究	富安　啓輔	東北大学	高等教育開発推進センター	Diffraction and inelastic scattering studies of decomposition process in hydrogen storage material, hydride with aluminum complex	Keisuke Tomiyasu	Tohoku University
242	イミダゾリウム系イオン液体の短・中距離構造	山室　修	東京大学	物性研究所	Short- and intermediate-range structures of imidazolium-based ionic liquids	Osamu Yamamuro	The University of Tokyo
243	層状ペロブスカイト型酸化物の結晶構造とイオン拡散経路	八島　正知	東京工業大学	大学院理工学研究科	Crystal structure and ion conduction pathway of layered perovskite-type oxides	Masatomo Yashima	Tokyo Institute of Technology
244	格子間酸素を利用したイオン伝導性セラミックスの結晶構造とイオン拡散経路	八島　正知	東京工業大学	大学院理工学研究科	Crystal structure and diffusion pathway of oxide ions in ionic conducting ceramics via interstitial oxide ions	Masatomo Yashima	Tokyo Institute of Technology
245	新しい三角格子系物質 MODX [M:Cu,Ni,Co etc; X:Cl,Br,I] の幾何学的フラストレーション磁性と磁気構造の解明	鄭　旭光	佐賀大学	大学院工学系研究科	Study of geometric frustration in a new triangular lattice series compounds MODX	Xu-Guang Zheng	Saga University
246	三角格子系水酸塩化物 $M_2(OD)_3X$[M:Cu,Ni,Cu etc; X:Cl,Br,I] の幾何学的フラストレーション磁性と磁気構造の解明 II	鄭　旭光	佐賀大学	大学院工学系研究科	Study of geometric frustration in triangular-lattice $M_2(OD)_3X$[M:Cu,Ni,Cu etc; X:Cl,Br,I]	Xu-Guang Zheng	Saga University
247	鉄系超伝導体の結晶構造と超伝導の相関	李　哲虎	産業技術総合研究所	エネルギー技術研究部門	Relationship between crystal structure and superconductivity in Fe-based superconductors	Chul-Ho Lee	National Institute of Advanced Industrial Science and Technology
248	白金含有ペロブスカイト型酸化物の中性子回折測定	野村　勝裕	産業技術総合研究所	ユビキタスエネルギー研究部門	Neutron diffraction study of platinum containing perovskite oxides	Katsuhiro Nomura	National Institute of Advanced Industrial Science and Technology
249	高い保磁力を有する FeCo ナノ粒子の結晶構造	飯久保　智	九州工業大学	大学院生命体工学研究科	Crystal structure of a FeCo nano-particle with high coercive force	Satoshi Iikubo	Kyushu Institute of Technology
250	可視光応答型酸窒化物光触媒の構造物性	八島　正知	東京工業大学	大学院理工学研究科	Structure-property correlation of visible-light responsive metal-oxynitride photocatalysis	Masatomo Yashima	Tokyo Institute of Technology
・申請装置 C2-2: FONDER							
251	FONDER（中性子 4 軸回折装置）IRT 課題	野田　幸男	東北大学	多元物質科学研究所	IRT: FONDER (Four-circle-Off-center-type Neutron Diffractometer)	Yukio Noda	Tohoku University
252	$DyFe_2Zn_{20}$ における異方性変化を伴う逐次磁気相転移	岩佐　和晃	東北大学大学院	理学研究科	Successive magnetic phase transition accompanying drastic variation in magnetic anisotropy of $DyFe_2Zn_{20}$	Kazuaki Iwasa	Tohoku University
253	マルチフェロイック物質 $SmMn_2O_5$ の磁気秩序と強誘電性	木村　宏之	東北大学	多元物質科学研究所	Antiferromagnetism and ferroelectricity in multiferroic compounds of $SmMn_2O_5$	Hiroyuki Kimura	Tohoku University
254	塑性歪みを加えた Pt_3Fe 反強磁性体における強磁性の発現機構	小林　悟	岩手大学	工学部マテリアル工学科	Mechanism of ferromagnetism in plastically deformed Pt_3Fe antiferromagnet	Satoru Kobayashi	Iwate University
255	金属的電荷秩序を示す YbPd の低温構造の解明	光田　暁弘	九州大学	理学研究院	Study on low-temperature structure of YbPd performing metallic charge order	Akihiro Mitsuda	Kyushu Univerisity
256	磁性イオン置換したスピンフラストレーション系物質 $CuFeO_2$ の磁気構造	満田　節生	東京理科大学	理学部物理学教室	Magnetic structures in spin frustration system $CuFeO_2$ with magnetic doping	Setsuo Mitsuda	Tokyo University of Science

No.	課題名	氏名	所属		Title	Name	Organization
257	ビスマス系強誘電体単結晶における巨大圧電性の起源解明	野口　祐二	東京大学	先端科学技術研究センター	Mechanism of a giant piezoelectric response for Bi-based ferroelectric single crystals	Yuji Noguchi	The University of Tokyo
258	KH_2AsO_4 の低温構造と相転移	重松　宏武	山口大学	教育学部	Low temperature structure and the phase transition of KH_2AsO_4	Hirotake Shigematsu	Yamaguchi University
259	スピン三重項超伝導体 Sr_2RuO_4 の一軸圧力下中性子散乱実験	山崎　照夫	東京理科大学	理工学部物理学科	Neutron scattering of the triplet superconductor Sr_2RuO_4 under uniaxial pressures	Teruo Yamazaki	Tokyo University of Science
260	I 型クラスレートにおける非調和振動	金子　耕士	日本原子力研究開発機構	量子ビーム応用研究部門	Anharmonicity in type-I clathrates	Koji Kaneko	Japan Atomic Energy Agency
261	β - パイロクロア化合物における精密構造解析	金子　耕士	日本原子力研究開発機構	量子ビーム応用研究部門	Detailed structural analysis on beta-pyrochlore compounds	Koji Kaneko	Japan Atomic Energy Agency
・申請装置 Accessory							
262	アクセサリー IRT 課題	上床　美也	東京大学	物性研究所	IRT: Accessory	Yoshiya Uwatoko	The University of Tokyo

平成 25 年度　共同利用課題一覧（後期）　Joint Research List (2013 Latter Term)

嘱託研究員（Comission Researcher）

No.	課題名	氏名	所属		Title	Name	Organization
1	AgPdCu 合金圧力セルを用いた磁場中比熱測定	河江　達也	九州大学	大学院工学研究院	Development of pressure cell for specific heat measurements under magnetic field	Tatsuya Kawae	Kyushu University
2	有機伝導体の圧力効果	村田　惠三	大阪市立大学	大学院理学研究科	Effect of pressure on the organic conductor	Keizo Murata	Osaka City University
3	多重極限関連装置の調整	高橋　博樹	日本大学	文理学部	Adjustment of cubic anvil apparatus	Hiroki Takahashi	Nihon University
4	希土類化合物の単結晶試料評価とその圧力効果	藤原　哲也	山口大学	大学院理工学研究科	Effect of pressure on the Ce compounds	Tetsuya Fujiwara	Yamaguchi University
5	磁性体の圧力効果	巨海　玄道	久留米工業大学		Effect of pressure on the magnetic materials	Gendo Oomi	Kurume Institute of Technology
6	圧力下 NMR 測定法に関する開発	藤原　直樹	京都大学	大学院人間・環境学研究科	Development of NMR measurement method under high pressure	Naoki Fujiwara	Kyoto University
7	低温用マルチアンビル装置の開発	辺土　正人	琉球大学	理学部	Development of multi-anvil apparatus for low temperature	Masato Hedo	University of the Ryukyus
8	中性子回析に用いる圧力装置の開発	片野　進	埼玉大学	大学院理工学研究科	Developments of high pressure cell for neutron diffraction	Susumu Katano	Saitama University
9	擬一次元有機物質の圧力下物性研究	糸井　充穂	日本大学	医学部	Study on pressure induced superconductivity of quasi organic conductor	Miho Itoi	Nihon University
10	高圧下の比熱測定装置の開発	梅原　出	横浜国立大学	工学部	Development of apparatus for specific heat measurements under high pressure	Izuru Umehara	Yokohama National University
11	磁化測定装置の開発	名嘉　節	物質・材料研究機構		Development of the magnetometer	Takashi Naka	National Institute for Materials Science
12	3d 遷移金属化合物の圧力下における磁気特性	鹿又　武	東北学院大学	工学総合研究所	Investigation of magnetic properties for 3d transition intermetallic compounds under pressure	Takeshi Kanomata	Tohoku Gakuin University
13	重い電子系物質における圧力下電気抵抗測定	礒田　誠	香川大学	教育学部	Effect of pressure on the electrical resistivity of heavy fermi on compounds	Makoto Isoda	Kagawa University
14	小型集束型小角散乱装置の高性能化及びそれによる応用研究	古坂　道弘	北海道大学	大学院工学研究院	Development of a compact focusing small-angle neutron scattering instrument and application research using the instrument	Michihiro Furusaka	Hokkaido University
15	中性子極小角散乱実験装置のアップグレード	金子　純一	北海道大学	大学院工学研究院	Upgrade of ULS system	Junichi Kaneko	Hokkaido University

No.	課題名	氏名	所属		Title	Name	Organization
16	中性子散乱装置の共同利用・開発による強相関電子系物質の構造物性の研究	岩佐　和晃	東北大学	大学院理学研究科	Structural studies of strongly correlated electron systems by neutron scattering method and instrumental development	Kazuaki Iwasa	Tohoku University
17	中性子モノクロメータの改良と中性子４軸回折計 FONDER の制御プログラムの改良	木村　宏之	東北大学	多元物質科学研究所	Improvement of neutron monochrometor and control program for four circle neutron diffractometer FONDER	Hiroyuki Kimura	Tohoku University
18	中性子散乱装置のアップグレードと共同利用研究の推進	藤田　全基	東北大学	金属材料研究所	Upgrading of the neutron scattering device and promotion of the research and public use	Masaki Fujita	Tohoku University
19	中性子散乱装置のアップグレード後の研究計画の実施と共同利用の推進	大山　研司	東北大学	金属材料研究所	P ropelling the inter university research cooperation	Keji Ohoyama	Tohoku University
20	中性子散乱装置のアップグレード後の研究計画の実施と共同利用の推進	平賀　晴弘	高エネルギー加速器研究機構	物質構造科学研究所	Implementation of the research plan under the cooperation-use program after upgrading neutron scattering instruments	Haruhiro Hiraka	KEK
21	中性子散乱装置のアップグレード後の研究計画の実施と共同利用の推進	田畑　吉計	京都大学	大学院工学研究科	Progress of the joint research by using the neutron scattering instruments	Yoshikazu Tanabe	Kyoto University
22	中性子散乱装置のアップグレード後の研究計画の実施と共同利用の推進	松村　武	広島大学	大学院先端物質科学研究科	Promotion of joint research after the upgrade of neutron scattering instruments	Takeshi Matsumura	Hiroshima University
23	J-PARC/MLF と JRR-3 共存時代に向けた３軸型中性子散乱装置の高度化	松浦　直人	総合科学研究機構		Upgrade of 3-axis neutron spectrometer for the oncoming coexistence of J-PARC/MLF and JRR-3	Masato Matsuura	CROSS
24	中性子分光器を用いた強相関電子系物質の微視的研究	桑原　慶太郎	茨城大学	大学院理工学研究科	Neutron scattering study of strongly correlated electron systems by using neutron spectrometers	Keitaro Kuwahara	Ibaraki University
25	高度化した３軸分光器を用いた共同利用の推進と物質科学研究の実施	横山　淳	茨城大学	理学部	Executing user program and study of material science with the advanced triple-axis spectrometers	Makoto Yokoyama	Ibaraki University
26	冷中性子スピン干渉計の応用と MINE ビームラインの整備	田崎　誠司	京都大学	大学院工学研究科	Development of cold neutron spin interferometry and improvements of MINE beam line	Seiji Tasaki	Kyoto University
27	膜貫通ペプチドのフリップフロップ誘起能の評価	中野　実	富山大学	大学院医学薬学研究部	Induction of phospholipid flip-flop by transmembrane peptides	Minoru Nakano	University of Toyama
28	C1-3　ULS 極小角散乱装置 IRT	杉山　正明	京都大学	原子炉実験所	Development of micro-focusing small-angle neutron scattering spectrometer	Masaaki Sugiyama	Kyoto University
29	集光テスト用小型 SANS の開発及び冷中性子反射率計・干渉計のアップグレード	日野　正裕	京都大学	原子炉実験所	Improvement of MIEZE spectrometer and cold neutron reflectometer and interferometer	Masahiro Hino	Kyoto University
30	集光テスト用小型 SANS の開発及び冷中性子反射率計・干渉計のアップグレード	北口　雅暁	名古屋大学	現象解析研究センター	Development of compact SANS and improvement of cold neutron reflectometer and interferometer	Masaaki Kitaguchi	Nagoya University
31	中性子散乱用高圧セルの開発および高圧下における中性子散乱実験	藤原　哲也	山口大学	大学院理工学研究科	Neutron scattering experiments under high pressure and development of high pressure cell for neutron scattering	Tetsuya Fujiwara	Yamaguchi University
32	流動場でのソフトマターの構造変化に関する研究	高橋　良彰	九州大学	先導物質化学研究所	Studies on structural change of soft matter under flow field	Yoshiaki Takahashi	Kyushu University

No.	課題名	氏名	所属		Title	Name	Organization
33	三軸分光器を用いた極端条件下における物質科学研究の実施	阿曽　尚文	琉球大学	理学部	Material science studies under extreme conditions by using triple-axis spectrometers	Naofumi Aso	University of the Ryukyus
34	非イオン界面活性剤水溶液における臨界ベシクル濃度近傍での２分子膜の熱揺らぎ	川端　庸平	首都大学東京	大学院理工学研究科	Thermal fluctuation of bilayers near the critical vesicle concentration in a nonionic surfactant aqueous solution	Youhei Kawabata	Tokyo Metropolitan University
35	中性子散乱研究計画の実施と共同利用の推進	伊藤　晋一	高エネルギー加速器研究機構		Propelling the inter university research cooperation	Shinichi Itoh	High Energy Accelerator Research Institute
36	冷中性子干渉イメージング装置開発研究	大竹　淑恵	理化学研究所	光量子工学研究領域	Research and development of interferometric imaging instruments for cold neutron	Yoshie Otake	RIKEN
37	高度化した三軸分光器を用いた共同利用の推進とスピンダイナミクスの研究	佐藤　卓	東北大学	多元物質科学研究所	Promoting user program and investigating spin dynamics using advanced triple-axis spectrometers	Taku Sato	Tohoku University
38	高度化した三軸分光器を用いた強相関電子系物質の研究	南部　雄亮	東北大学	多元物質科学研究所	Study of strongly correlated electron systems using advanced triple-axis spectrometers	Yusuke Nambu	Tohoku University
39	強磁場量子ビーム科学のためのパルスマグネットの開発	鳴海　康雄	東北大学	金属材料研究所	Developments of pulse magnets for synchrotron and neutron experiments in pulsed high magnetic fields	Yasuo Narumi	Tohoku University
40	高温超伝導体の高分解能光電子分光	藤森　淳	東京大学	大学院理学系研究科	Ultra-high resolution photoemission spectroscopy on high T_c superconductor	Atsushi Fujimori	The University of Tokyo
41	60-eV レーザーを用いた時間分解光電子分光の開発	石坂　香子	東京大学	大学院工学系研究科	The development of time-resolved photoemission using 60 eV laser	Kyoko Ishizaka	The University of Tokyo
42	鉄系超伝導体のレーザー光電子分光	下志万　貴博	東京大学	大学院工学系研究科	Laser-ARPES on Fe superconductor	Takahiro Shimojima	The University of Tokyo
43	Bi 系超伝導体の角度分解光電子分光	竹内　恒博	名古屋大学	エコトピア科学研究所	Angle-resolved photoemission study on high T_c cuprate	Tsunehiro Takeuchi	Nagoya University
44	高分解能光電子分光による強相関物質の研究	横谷　尚睦	岡山大学	大学院自然科学研究科	Ultra-high resolution study on strongly correlated materials	Takayoshi Yokoya	Okayama University
45	酸化バナジウムの高分解能光電子分光	江口　律子	岡山大学	大学院自然科学研究科	Photoemission study on vanadium oxides	Ritsuko Eguchi	Okayama University
46	有機化合物の光電子分光	金井　要	東京理科大学	理工学部	Photoemission study on organic compounds	Kaname Kanai	Tokyo University of Science
47	重い電子系ウラン化合物の高分解能光電子分光	藤森　伸一	日本原子力研究開発機構	量子ビーム応用研究部門	Ultra high resolution photoemission study on heavy fermion uranium compounds	Shinichi Fujimori	Japan Atomic Energy Agency
48	レーザー光電子分光による酸化物薄膜の研究	津田　俊輔	物質・材料研究機構		Laser-photoemission study on oxide films	Shunsuke Tsuda	National Institute for Materials Science
49	4f 電子系物質の高分解能光電子分光	松波　雅治	自然科学研究機構	分子科学研究所	Photoemission study on 4f materials	Masaharu Matsunami	National Institutes of Natural Sciences

No.	課題名	氏名	所属		Title	Name	Organization
50	超高空間分解能光電子顕微鏡による磁区構造観察	中川　剛志	九州大学	大学院総合理工学府	Observation of magnetic domain structures by ultra-high resolution photoemission electron microscopy	Takeshi Nakagawa	Kyushu University
51	Mn 化合物の時間分解光電子分光	大川　万里生	東京理科大学	理学部	Time resolved photoemission on Mn compounds	Mario Okawa	Tokyo University of Science
52	光電子分光、共鳴軟 X 線回析	和達　大樹	東京大学	大学院工学系研究科	Spades photoemission spectroscopy-resonant soft x-ray scattering	Hiroki Wadati	The University of Tokyo
53	極低温・超高分解能光電子分光を用いた超伝導機構の研究	岡崎　浩三	東京大学	大学院理学系研究科	Study of the mechanism of superconductivity by low temperature and high resolution photoemission spectroscopy	Kozo Okazaki	The University of Tokyo
54	収差補正型光電子顕微鏡の建設と利用研究	小嗣　真人	高輝度光科学研究センター		Construction and utilization research of aberration correction photoelectron emission microscopy	Masato Kotsugi	Japan Synchrotron Radiation Institute
55	時間分解・マイクロビームラインの開発と研究	室　隆桂之	高輝度光科学研究センター		Development of micr- and time-resolved beamline	Takayuki Muro	Japan Synchrotron Radiation Institute
56	ナノクラスター物質の発光測定	田島　裕之	兵庫県立大学	大学院物質理学研究科	Luminescence studies on nanoclusters	Hiroyuki Tajima	The Univerisity of Hyogo
57	高輝度放射光軟 X 線を用いた時間分解光電子分光による表面ダイナミクス研究	近藤　寛	慶應義塾大学	理工学部	Study of surface dynamics by time-resolved photoemission spectroscopy with high-brilliant soft X-ray synchrotron radiation	Hiroshi Kondoh	Keio University
58	軟 X 線アンジュレータビームラインの分光光学系の開発研究	雨宮　健太	高エネルギー加速器研究機構	物質構造科学研究所	Research and development of soft X-ray undulator beamline	Kenta Amemiya	High Energy Accelerator Research Institute
59	光電子スピン検出器の開発・研究	奥田　太一	広島大学	放射光科学研究センター	Research and development of a new photoelectron spin detector	Taichi Okuda	Hiroshima University
60	光電子顕微鏡による磁性ナノ構造物質の磁化過程	木下　豊彦	高輝度光科学研究センター		Magnetization in process of magnetic nano structure by PEEM	Toyohiko Kinoshita	Japan Synchrotron Radiation Institute
61	高輝度極紫外ビームラインの設計・評価	小野　寛太	高エネルギー加速器研究機構	物質構造科学研究所	Design and characterization of brilliance VUV beamline.	Kanta Ono	High Energy Accelerator Research Institute
62	高輝度光源ビームラインにおける分光光学系の設計・開発	後藤　俊治	高輝度光科学研究センター	放射光研究所	Design of the new undulator beamline at SPring-8	Shunji Goto	Japan Synchrotron Radiation Institute
63	〃	大橋　治彦	高輝度光科学研究センター	放射光研究所	〃	Haruhiko Ohashi	Japan Synchrotron Radiation Institute
64	高輝度軟 X 線を利用した強相関物質の電子状態研究	組頭　広志	高エネルギー加速器研究機構	物質構造科学研究所	Study of electronic states in strongly correlated materials with high brilliant soft-Xray	Hiroshi Kumigashira	High Energy Accelerator Research Institute
65	時間分解光電子分光法による光触媒材料のキャリアダイナミクス研究	小澤　健一	東京工業大学	大学院理工学研究科	Study of carrier dynamics in photocatalysis materials by time-resolved photoemission spectroscopy	Kenichi Ozawa	Tokyo Institute of Technology
66	軟 X 線時間分解分光実験による磁性研究	木村　昭夫	広島大学	大学院理学研究科	Study of magnetic properties by time-resolved soft X-ray spectroscopy	Akio Kimura	Hiroshima University

No.	課題名	氏名	所属		Title	Name	Organization
67	高輝度軟 X 線を利用する光電子顕微鏡装置の設計・開発	坂本　一之	千葉大学	大学院融合科学研究科	Research and designing of a PEEM spectrometer for high brilliance soft X ray	Kazuyuki Sakamoto	Chiba University
68	二次元表示型スピン分解光電子エネルギー分析器の開発	大門　寛	奈良先端科学技術大学院大学	物質創成科学研究科	Development of 2D-display-type spin-resolved photoelectron energy analyzer	Hiroshi Daimon	Nara Institute of Science and Technology
69	時間分解光電子回折実験の要素技術開発	林　好一	東北大学	金属材料研究所	Technical development of time-resolved photoelectron diffraction experiment	Koichi Hayashi	Tohoku University
70	軟 X 線吸収／発光分光法によるリチウムイオン電池電極材料の電子物性研究	細野　英司	産業技術総合研究所	エネルギー技術研究部門	Study on the electronic property of electrode materials for Li-ion batteries by soft X-ray absorption/emission spectroscopy	Eiji Hosono	National Institute of Advanced Industrial Science and Technology
71	超高分解能軟 X 線発光分光による水素吸蔵合金中の水素の波動関数の局在性に関する研究	関場　大一郎	筑波大学	数理物質系	Study on the localization of wave functions of hydrogen atom in hydrogen storage alloys using ultrahigh resolution soft X-ray emission spectroscopy	Daiichiro Sekiba	University of Tsukuba
72	時間分解光電子分光による重い電子系の研究	関山　明	大阪大学	大学院基礎工学研究科	Study on heavy Fermion materials by time-resolved photoemission	Akira Sekiyama	Osaka University
73	高分解能光電子分光による酸化バナジウムの研究	藤原　秀紀	大阪大学	大学院基礎工学研究科	Study on vanadium oxides by high resolution photoemission	Hidenori Fujiwara	Osaka University
74	軟 X 線発光・共鳴非弾性散乱分光の磁気円・線二色性測定システムの構築	菅　滋正	大阪大学	産業科学研究所	Construction of a noble system for circular and linear dichroism in soft X-ray emission and RIXS spectroscopy	Shigemasa Suga	Osaka University

一般研究員（General Researcher）

No.	課題名	氏名	所属		Title	Name	Organization
1	S=2 一次元ハイゼンベルグ反強磁性体の極低温磁化測定	萩原　政幸	大阪大学	極限量子科学研究センター	Magnetization measurements on an S=2 one-dimensional Heisenberg antiferromagnet at ultra-low temperatures	Masayuki Hagiwara	Osaka University
2	5f 及び 3d 電子系強磁性超伝導体の研究	出口　和彦	名古屋大学	大学院理学研究科	Study of 5f and 3d ferromagnetic superconductors	Kazuhiko Deguchi	Nagoya University
3	〃	國方　翔太	名古屋大学	大学院理学研究科	〃	Shouta Kunikata	Nagoya University
4	カゴ状構造を有する異方的超伝導体 $Y_5Ir_6Sn_{18}$ の超伝導ギャップ構造の決定	加瀬　直樹	新潟大学	大学院自然科学研究科	Superconducting gap structures of $Y_5Ir_6Sn_{18}$ determined by angle-resolved specific heat measurements	Naoki Kase	Niigata University
5	〃	増村　昌三	新潟大学	大学院自然科学研究科	〃	Shozo Masumura	Niigata University
6	トポロジカル物質のパルス磁場中の超音波測定	吉澤　正人	岩手大学	大学院工学研究科	Ultrasonic measurements of topological materials in pulsed magnetic field	Masahito Yoshizawa	Iwate University
7	〃	藤井　千旭	岩手大学	大学院工学研究科	〃	Chiaki Fujii	Iwate University

No.	課題名	氏名	所属		Title	Name	Organization
8	パイロクロア磁性体 $Tb_{2-x}Ti_{2+x}O_7$ の比熱測定	高津　浩	首都大学東京	大学院理工学研究科	Specific heat measurements of the pyrochlore magnet $Tb_{2-x}Ti_{2+x}O_7$	Hiroshi Takatsu	Tokyo Metropolitan University
9	〃	清原　達也	首都大学東京	大学院理工学研究科	〃	Tatsuya Kiyohara	Tokyo Metropolitan University
10	非磁性基底二重項を持つ $PrIr_2Zn_{20}$ における La 希釈効果	鬼丸　孝博	広島大学	大学院先端物質科学研究科	La substitution effect on the magnetic properties of $PrIr_2Zn_{20}$ with the nonmagnetic doublet ground state	Takahiro Onimaru	Hiroshima University
11	〃	松本　圭介	広島大学	大学院先端物質科学研究科	〃	Keisuke Matsumoto	Hiroshima University
12	〃	島田　祐樹	広島大学	大学院先端物質科学研究科	〃	Yuki Shimada	Hiroshima University
13	有機ラジカルを用いた新規磁性体の低温磁気測定	山口　博則	大阪府立大学	大学院理学系研究科	Low temperature magnetic properties of new organic radical compounds	Hironori Yamaguchi	Osaka Prefecture University
14	〃	岩瀬　賢治	大阪府立大学	大学院理学系研究科	〃	Kenji Iwase	Osaka Prefecture University
15	〃	奥　雄太	大阪府立大学	大学院理学系研究科	〃	Yuta Oku	Osaka Prefecture University
16	量子スピンアイス系 $Yb_2Ti_2O_7$ の特異な磁気相転移	安井　幸夫	明治大学	理工学部	Anomalous magnetic transition of quantum spin ice system $Yb_2Ti_2O_7$	Yukio Yasui	Meiji University
17	六方晶 ordered perovskite 三角格子反強磁性体 $Ba_3MTa_2O_9$ (M=Co, Ni) の低温磁性	小野　俊雄	大阪府立大学	大学院理学系研究科	Low temperature magnetic properties of hexagonal ordered perovskite triangular antiferromagnetic system $Ba_3MTa_2O_9$ (M=Co, Ni)	Toshio Ono	Osaka Prefecture University
18	磁性体の中性子散乱による研究	桑原　慶太郎	茨城大学	大学院理工学研究科	Neutron scattering study of magnetic materials	Keitaro Kuwahara	Ibaraki University
19	コバルト錯体からなる分子性導電体の磁気・光物性研究	松田　真生	熊本大学	大学院自然科学研究科	Studies on magnetic and optical properties of molecular conductors composed of a Co complex	Masaki Matsuda	Kumamoto University
20	〃	小崎　祐太郎	熊本大学	大学院自然科学研究科	〃	Yutaro Kozaki	Kumamoto University
21	鉄錯体からなる分子性導電体の磁気・光物性研究	松田　真生	熊本大学	大学院自然科学研究科	Studies on magnetic and optical properties of molecular conductors composed of a Fe complex	Masaki Matsuda	Kumamoto University
22	〃	西　美樹	熊本大学	大学院自然科学研究科	〃	Miki Nishi	Kumamoto University
23	熱耐久性を有する高性能塗布型有機トランジスタ材料の開発	岡本　敏宏	東京大学	大学院新領域創成科学研究科	Development of solution-processable high performance organic semiconductors with thermal durability	Toshihiro Okamoto	The University of Tokyo
24	〃	三津井　親彦	東京大学	大学院新領域創成科学研究科	〃	Chikahiko Mitsui	The University of Tokyo

No.	課題名	氏名	所属		Title	Name	Organization
25	熱耐久性を有する高性能塗布型有機トランジスタ材料の開発	山岸　正和	東京大学	大学院新領域創成科学研究科	Development of solution-processable high performance organic semiconductors with thermal durability	Masakazu Yamagishi	The University of Tokyo
26	〃	吉本　和美	東京大学	大学院新領域創成科学研究科	〃	Kazumi Yoshimoto	The University of Tokyo
27	〃	中村　健一	愛媛大学	工学部	〃	Ken-ichi Nakamura	Ehime University
28	新規梯子格子磁性体 3-Br-4-F-V の NMR 測定	山口　博則	大阪府立大学	大学院理学系研究科	NMR study of new spin-ladder material 3-Br-4-F-V	Hironori Yamaguchi	Osaka Prefecture University
29	〃	宮外　浩嗣	大阪府立大学	大学院理学系研究科	〃	Hirotsugu Miyagai	Osaka Prefecture University
30	1/5 欠損正方格子ハバードモデルにおけるエッジ状態とベリー位相	山下　靖文	日本大学	工学部	Edge state and Berry phase of the 1/5-depleted square-lattice Hubbard model at 1/4-filling	Yasufumi Yamashita	Nihon University
31	1/5 欠損正方格子上のハバード模型におけるチャーン数の計算	丸山　勲	福岡工業大学	情報工学部	Calculation of the Chern Number in the 1/5-depleted square-lattice Hubbard model.	Isao Maruyama	Fukuoka Institute of Technology
32	特異な分散を示す強相関電子系における量子相転移	宮原　慎	福岡大学	理学部	Quantum phase transition in strongly correlated electron systems with anomalous dispersion relations	Shin Miyahara	Fukuoka University
33	ダブルペロブスカイト酸化物薄膜における秩序構造制御とその輸送・誘電特性評価	北村　未歩	東京大学	大学院工学系研究科	Control of orderd-structure and evaluations of transport and dielectric properties in double perovskite oxide films	Miho Kitamura	The University of Tokyo
34	パルスレーザー堆積法による多成分系ナノ相分離酸化物薄膜の構造と物性	松本　祐司	東北大学	大学院工学研究科	Structural and material-property characterization of multi component oxide films with nano-scale phase separation	Yuji Matsumoto	Tohoku University
35	太陽電池用シリコンプロセスにおける副生成物の分析	伊高　健治	弘前大学	北日本新エネルギー研究所	Analysis of the by-product under the direct silica reduction process for solar cells	Kenji Itaka	Hirosaki University
36	機能性酸化物薄膜の作製と評価	坪内　賢太	東京大学	大学院新領域創成科学研究科	Fablication and characterization of functional oxide thin film	Kenta Tsubouchi	The University of Tokyo
37	Bi ナノワイヤーにおける量子振動実験	長谷川　靖洋	埼玉大学	工学部	Experiment of quantum oscillation by Bi nanowire	Yasuhiro Hasegawa	Saitama University
38	Mg_2Si 単結晶および焼結体のホール測定	平山　尚美	東京理科大学	基礎工学部	Hall measurement of single-crystalline and sintered polycrystalline magnesium silicide Mg_2Si	Naomi Hirayama	Tokyo University of Science
39	Pb 置換 BI 系超伝導体のホール係数測定	神戸　士郎	山形大学	大学院理工学研究科	Hall coefficient measurement of Pb-substituted Bi-based superconductors	Shiro Kambe	Yamagata University
40	〃	菅野　駿	山形大学	大学院理工学研究科	〃	Shun Kanno	Yamagata University
41	〃	呉　勇傑	山形大学	大学院理工学研究科	〃	Yongjie Wu	Yamagata University

No.	課題名	氏名	所属		Title	Name	Organization
42	Pb 置換 BI 系超伝導体のホール係数測定	羅　添文	山形大学	大学院理工学研究	Hall coefficient measurement of Pb-substituted Bi-based superconductors	Luo Tianwen	Yamagata University
43	機械的応力のシリコン表面化学への影響に関する研究	成島　哲也	自然科学研究機構	分子科学研究所	Effect on silicon surface chemistry under external mechanical stress	Tetsuya Narushima	National Institutes of Natural Sciences
44	金属／半導体表面上ナノ構造の形成とその非線形発光の時間分解測定	河村　紀一	日本放送協会	放送技術研究所	Time resolved spectroscopy of harmonics from nano-structures on metal/semiconductor surfaces	Norikazu Kawamura	NHK Science & Technical Research Laboratories
45	新しい金属ドープ・ボロン・クラスター系物質と陽電子ビーム法による分析	金沢　育三	東京学芸大学	自然科学系	Making of new metal-doped boron-cluster materials and analysis by slow-positron beam	Ikuzo Kanazawa	Tokyo Gakugei University
46	〃	今井　恵利華	東京学芸大学	大学院教育学研究科	〃	Erika Imai	Tokyo Gakugei University
47	半導体基板上に成長したグラフェンナノリボンおよびシリセンの電子物性	中辻　寛	東京工業大学	大学院総合理工学研究科	Electronic structure of graphene and silicene grown on semiconductor substrates	Kan Nakatsuji	Tokyo Institute of Technology
48	重い電子系超伝導の実空間観察のための超低温・強磁場の小型 STM の開発	河江　達也	九州大学	大学院工学研究院	Development of a miniature STM for low-temperature and high-field measurements of heavy fermion superconductors	Tatsuya Kawae	Kyushu University
49	〃	高田　弘樹	九州大学	大学院工学府	〃	Hiroki Takata	Kyushu University
50	二ホウ化物薄膜上のエピタキシャルシリセン及びゲルマニウム層の低温走査トンネル顕微鏡観察	高村　由起子	北陸先端科学技術大学院大学	マテリアルサイエンス研究科	Low temperature scanning tunneling microscopy investigations of epitaxial silicene and germanium layer on diboride thin films	Yukiko Takamura	Japan Advanced Institute of Science and Technology
51	〃	ライナー　フリードライン	北陸先端科学技術大学院大学	マテリアルサイエンス研究科	〃	Rainer FRIEDLEIN	Japan Advanced Institute of Science and Technology
52	〃	アントワーヌ　フロランス	北陸先端科学技術大学院大学	マテリアルサイエンス研究科	〃	Antoine FLEURENCE	Japan Advanced Institute of Science and Technology
53	〃	青柳　航平	北陸先端科学技術大学院大学	マテリアルサイエンス研究科	〃	Kohei Aoyagi	Japan Advanced Institute of Science and Technology
54	(Ho,Y)Rh_2Si_2 単結晶の磁気転移 2	繁岡　透	山口大学	大学院理工学研究科	Magnetic transitions of (Ho,Y)Rh_2Si_2 single crystal (2)	Toru Shigeoka	Yamaguchi University
55	〃	藤井　洋	山口大学	大学院理工学研究科	〃	Yoh Fujii	Yamaguchi University
56	$EuFe_2P_2$ の高圧力下磁化測定	藤原　哲也	山口大学	大学院理工学研究科	Magnetization measurements under high pressures in $EuFe_2P_2$	Tetsuya Fujiwara	Yamaguchi University
57	〃	田端　克好	山口大学	大学院理工学研究科	〃	Katsuyoshi Tabata	Yamaguchi University
58	$EuRu_2P_2$ の高圧力下磁化測定 (2)	藤原　哲也	山口大学	大学院理工学研究科	Magnetization measurements under high pressures in $EuRu_2P_2$ (II)	Tetsuya Fujiwara	Yamaguchi University

No.	課題名	氏名	所属		Title	Name	Organization
59	$EuRu_2P_2$ の高圧力下磁化測定 (2)	中田　琢也	山口大学	大学院理工学研究科	Magnetization measurements under high pressures in $EuRu_2P_2$ (II)	Takuya Nakada	Yamaguchi University
60	$Mn_{2-x}Cu_xSb$ 磁性体の高圧下における磁気状態	小山　佳一	鹿児島大学	大学院理工学研究科	Magnetic state of $Mn_{2-x}Cu_xSb$ magnet under high pressure	Keiichi Koyama	Kagoshima University
61	〃	松本　佳大	鹿児島大学	大学院理工学研究科	〃	Yoshihiro Matsumoto	Kagoshima University
62	Ni-Mn-Ga 系強磁性形状記憶合金の磁化の圧力依存性	安達　義也	山形大学	大学院理工学研究科	Pressure dependence of magnetization for the ferromagnetic shape-memory alloys of Ni-Mn-Ga system	Yoshiya Adachi	Yamagata University
63	〃	池田　大地	山形大学	大学院理工学研究科	〃	Daichi Ikeda	Yamagata University
64	$PrBa_2Cu_4O_8$ と $PrBa_2Cu_3O_{7-\delta}$ の混合セラミックスの高圧下電気抵抗率測定	久田　旭彦	徳島大学	大学院ソシオ・アーツ・アンド・サイエンス研究部	Electrical resistivity of mixtures of $PrBa_2Cu_4O_8$ and $PrBa_2Cu_3O_{7-\delta}$ ceramics under high pressure	Akihiko Hisada	The University of Tokushima
65	TmB_4 の磁気準周期秩序相における圧力効果	伊賀　文俊	茨城大学	理学部	Pressure effect on the magnetic quasi-period ordered phase in TmB_4	Fumitoshi Iga	Ibaraki University
66	セリウム系化合物における微小磁気モーメントの圧力下磁化測定	阿曽　尚文	琉球大学	理学部	Magnetization studies under pressure in Ce-based compounds with small magnetic moments	Naofumi Aso	University of the Ryukyus
67	ホイスラー化合物 $Fe_{2-x}Co_xMnSi$ の圧力下電気抵抗率	伊藤　昌和	鹿児島大学	大学院理工学研究科	Electrical transport properties of Heusler compound $Fe_{2-x}Co_xMnSi$	Masakazu Ito	Kagoshima University
68	〃	山下　敏広	鹿児島大学	大学院理工学研究科	〃	Toshihiro Yamashita	Kagoshima University
69	圧力下での磁気および価数ゆらぎが生み出す Eu 化合物の新しい電子状態の探索	本多　史憲	東北大学	金属材料研究所	Investigation of exotic electronic properties of Eu compounds driven by magnetic and valence fluctuation under high pressure	Fuminori Honda	Tohoku University
70	〃	大貫　惇睦	琉球大学	理学部	〃	Yoshichika Onuki	University of the Ryukyus
71	価数揺動物質の高圧力中輸送特性の研究	仲間　隆男	琉球大学	理学部	Transport properties of valence fluctuating compounds under pressure	Takao Nakama	University of the Ryukyus
72	〃	仲村　愛	琉球大学	大学院理工学研究科	〃	Ai Nakamura	University of the Ryukyus
73	〃	平仲　裕一	琉球大学	大学院理工学研究科	〃	Yuichi Hiranaka	University of the Ryukyus
74	回転希釈冷凍機を用いた量子固体・量子液体研究	白濱　圭也	慶應義塾大学	理工学部	Studies of quantum fluids and solids using rotating dilution refrigerators	Keiya Shirahama	Keio University
75	〃	高橋　大輔	足利工業大学	共通課程	〃	Daisuke Takahashi	Ashikaga Institute of Technology

No.	課題名	氏名	所属		Title	Name	Organization
76	回転希釈冷凍機を用いた量子固体・量子液体研究	村川　智	慶應義塾大学	理工学部	Studies of quantum fluids and solids using rotating dilution refrigerators	Satoshi Murakawa	Keio University
77	〃	立木　智也	慶應義塾大学	大学院理工学研究科	〃	Tsuiki Tomoya	Keio University
78	回転超流動ヘリウム３のテクスチャーダイナミクスの研究	佐々木　豊	京都大学	低温物質科学研究センター	Texture dynamics of rotating superfluid ^{3}He	Yutaka Sasaki	Kyoto University
79	希土類化合物の純良単結晶育成と圧力下電気抵抗測定	中野　智仁	新潟大学	大学院自然科学研究科	Single-crystal growth of the rare-earth compound and low-temperature resistivity under high pressure	Tomohito Nakano	Niigata University
80	〃	安達　季並	新潟大学	大学院自然科学研究科	〃	Kinami Adachi	Niigata University
81	固体ヘリウムの超流動に見られる様な「新規超流動現象の基礎研究」	井上　和朗	芝浦工業大学	工学部	Fundamental study of new types of superfluidity as seen in solid ^{4}He	Kazuo Inoue	Shibaura Institute of Technology
82	〃	久保田　実	芝浦工業大学	総合研究所	〃	Minoru Kubota	Shibaura Institute of Technology
83	〃	荒木　秀明	長岡工業高等専門学校	物質工学科	〃	Hideaki Araki	Nagaoka National College of Technology
84	磁化測定用対向アンビル型高圧力発生装置の開発 (3)	藤原　哲也	山口大学	大学院理工学研究科	Development of opposed-anvil type high pressure apparatus for magnetization measurement (III)	Tetsuya Fujiwara	Yamaguchi University
85	〃	森田　哲広	山口大学	大学院理工学研究科	〃	Tetsuhiro Morita	Yamaguchi University
86	重い電子系反強磁性体 $CeNiIn_4$ の圧力誘起量子臨界現象の研究	大原　繁男	名古屋工業大学	大学院工学研究科	Study of pressure induced quantum critical phenomena for heavy fermion antiferromagnet $CeNiIn_4$	Shigeo Ohara	Nagoya Institute of Technology
87	〃	松本　裕司	名古屋工業大学	大学院工学研究科	〃	Yuji Matsumoto	Nagoya Institute of Technology
88	〃	小林　拓也	名古屋工業大学	大学院工学研究科	〃	Takuya Kobayashi	Nagoya Institute of Technology
89	重い電子系物質における ^{3}He 温度領域での磁化測定	河江　達也	九州大学	大学院工学研究科	Magnetization measurements in ^{3}He temperature region for heavy fermion systems	Tatsuya Kawae	Kyushu University
90	〃	佐藤　由昌	九州大学	大学院工学府	〃	Yoshiaki Sato	Kyushu University
91	〃	古谷　圭一	九州大学	大学院工学府	〃	Keiichi Furuya	Kyushu University
92	遷移金属間化合物の高圧下における磁性と輸送特性	仲間　隆男	琉球大学	理学部	Magnetism and transport properties of intermetallic compounds under high pressure	Takao Nakama	University of the Ryukyus

No.	課題名	氏名	所属		Title	Name	Organization
93	遷移金属間化合物の高圧下における磁性と輸送特性	照屋　淳志	琉球大学	大学院理工学研究科	Magnetism and transport properties of intermetallic compounds under high pressure	Atsushi Teruya	University of the Ryukyus
94	〃	上門　太郎	琉球大学	大学院理工学研究科	〃	Taro Uejyo	University of the Ryukyus
95	多形化合物 RIr_2Si_2(R= 希土類）の磁気転移	繁岡　透	山口大学	大学院理工学研究科	Magnetic transition of polymorphic compound RIr_2Si_2 (R=rare earth)	Toru Shigeoka	Yamaguchi University
96	〃	蔵田　裕也	山口大学	大学院理工学研究科	〃	Yuya Kurata	Yamaguchi University
97	中間価数状態を示す SmS ならびに Yb 系準結晶・近似結晶における高圧下物性研究	出口　和彦	名古屋大学	大学院理学研究科	High-pressure study on mixed-valence SmS, Yb-quasi and -approximant crystals	Kazuhiko Deguchi	Nagoya University
98	〃	井村　敬一郎	名古屋大学	大学院理学研究科	〃	Keiichiro Imura	Nagoya University
99	〃	松川　周矢	名古屋大学	大学院理学研究科	〃	Shuya Matsukawa	Nagoya University
100	超流動ヘリウム 3-A 相の半整数量子渦の研究	石川　修六	大阪市立大学	大学院理学研究科	Study of the half quantized vortex in superfluid ^{3}He-A phase	Osamu Ishikawa	Osaka City University
101	〃	國松　貴之	大阪市立大学	大学院理学研究科	〃	Takayuki Kunimatsu	Osaka City University
102	超流動ヘリウム 3-A_1 相におけるスピン流に伴う電場効果の検出	山口　明	兵庫県立大学	大学院物質理学研究科	Detection of an electrical field induced by spin current in superfluid ^{3}He-A_1 phase	Akira Yamaguchi	The Univerisity of Hyogo
103	〃	鎌田　尚史	兵庫県立大学	大学院物質理学研究科	〃	Naofumi Kamada	The Univerisity of Hyogo
104	有機分子性導体の高圧物性の研究	鳥塚　潔	法政大学	理工学部	Studies on high pressure properties of organic molecular conductors	Kiyoshi Torizuka	Hosei University
105	捩り振り子測定による固体ヘリウム４のずれ弾性測定	青木　悠樹	東京工業大学	大学院総合理工学研究科	Shear modulus measurement of solid helium-4 by torsional oscillator	Yuki Aoki	Tokyo Institute of Technology
106	〃	岩佐　泉	神奈川大学	理学部	〃	Izumi Iwasa	Kanagawa University
107	〃	三浦　尊	東京工業大学	大学院総合理工学研究科	〃	Takeru Miura	Tokyo Institute of Technology
108	強磁性元素を含む非磁性半導体のフェルミ面計測	小林　夏野	青山学院大学	理工学部	Measuring Fermi surfaces of paramagnetic semiconductors containing ferromagnetic elements	Kaya Kobayashi	Aoyama Gakuin University
109	新奇な量子相転移現象の数値的研究	原田　健自	京都大学	大学院情報学研究科	Numerical study of unconventional quantum phase transitions	Kenji Harada	Kyoto University

No.	課題名	氏名	所属		Title	Name	Organization
110	Fe_6W_6C の異常な熱膨張	和氣　剛	京都大学	大学院工学研究科	Anomalous thermal expansion in Fe_6W_6C	Takeshi Waki	Kyoto University
111	Fe-$MgSiO_3$-H_2 系の高温高圧下におけるふるまいの解明	八木　健彦	愛媛大学	地球深部ダイナミクス研究センター	Behavior of Fe-$MgSiO_3$-H_2 system under high pressure and temperature condition	Takehiko Yagi	Ehime University
112	高圧その場ラマン散乱測定による後期遷移金属多窒化物の窒素状態の評価	丹羽　健	名古屋大学	大学院工学研究科	Evaluation for bonding character of dinitrogen in transition metal pernitrides inferred from high-pressure in-situ Raman scattering measurements	Ken Niwa	Nagoya University
113	〃	鈴木　健太郎	名古屋大学	大学院工学研究科	〃	Kentaro Suzuki	Nagoya University
114	高圧下におけるベンゼンの重合反応	篠崎　彩子	東京大学	大学院理学系研究科	Polymerization of benzene under high pressure condition.	Ayako Shinozaki	The University of Tokyo
115	高圧下におけるペロブスカイト Eu(Ti,Zr)O_3 の構造変化	陰山　洋	京都大学	大学院工学研究科	Structural change in Eu(Ti,Zr)O_3 under high pressure	Hiroshi Kageyama	Kyoto University
116	〃	山本　隆文	京都大学	大学院工学研究科	〃	Takafumi Yamamoto	Kyoto University
117	〃	吉井　龍太	京都大学	大学院工学研究科	〃	Ryuta Yoshii	Kyoto University
118	〃	中野　晃佑	京都大学	大学院工学研究科	〃	Kousuke Nakano	Kyoto University
119	高温高圧下おいて水素分子がコーサイトの結晶構造に与える影響	篠崎　彩子	東京大学	大学院理学系研究科	Effect of hydrogen molecules to crystal structure of coesite under high pressure	Ayako Shinozaki	The University of Tokyo
120	充填スクッテルダイト構造を有する新超伝導体の物質探索	関根　ちひろ	室蘭工業大学	大学院工学研究科	Search for new superconductors with filled-skutterudite structure	Chihiro Sekine	Muroran Institute of Technology
121	〃	崔　云	室蘭工業大学	大学院工学研究科	〃	Un Sai	Muroran Institute of Technology
122	新規 B_1 型酸化物固溶体の超高圧合成	長谷川　正	名古屋大学	大学院工学研究科	High pressure syntheses of novel B_1-type oxide solid solutions	Masashi Hasegawa	Nagoya University
123	〃	嶋田　大輝	名古屋大学	大学院工学研究科	〃	Hiroki Shimada	Nagoya University
124	新規 C-N 系化合物の超高圧合成	長谷川　正	名古屋大学	大学院工学研究科	High pressure syntheses of novel C-N compounds	Masashi Hasegawa	Nagoya University
125	〃	小田　喬史	名古屋大学	大学院工学研究科	〃	Takashi Oda	Nagoya University
126	造礁性サンゴ骨格の微細組織観察	甕　聡子	北海道大学	大学院理学院	Observation on crystallographic texture of reef-building coral skeleton	Satoko Motai	Hokkaido University

No.	課題名	氏名	所属		Title	Name	Organization
127	大型プレスを用いた IV 族遷移金属炭化物の高圧合成	丹羽　健	名古屋大学	大学院工学研究科	High pressure synthesis of IV group transition metal carbides using large volume high pressure apparatus	Ken Niwa	Nagoya University
128	〃	志村　元	名古屋大学	大学院工学研究科	〃	Gen Shimura	Nagoya University
129	超硬質窒化炭素の高温高圧合成 (2)	寒川　匡哉	岡山理科大学	大学院理学研究科	Synthesis of superhard carbon nitride at high temperature (II)	Masaya Sougawa	Okayama University of Science
130	〃	田中　大	岡山理科大学	大学院理学研究科	〃	Dai Tanaka	Okayama University of Science
131	超高圧プレスを用いた新規プロトニクス酸化物のソフト化学的合成法の検討	山口　周	東京大学	大学院工学系研究科	Oxide-protonics materials synthesis by combined use of soft chemical method and high pressure	Shu Yamaguchi	The University of Tokyo
132	〃	三好　正悟	東京大学	大学院工学系研究科	〃	Shogo Miyoshi	The University of Tokyo
133	〃	田中　和彦	東京大学	大学院工学系研究科	〃	Kazuhiko Tanaka	The University of Tokyo
134	〃	ドロクサリブ ロラス ティンブル	東京大学	大学院工学系研究科	〃	Doloksaribu Rolas Timbul	The University of Tokyo
135	〃	飯田　勇気	東京大学	大学院工学系研究科	〃	Yuki Iida	The University of Tokyo
136	溶融亜鉛メッキ合金相の応力誘起変態	山口　周	東京大学	大学院工学系研究科	Stress-induced phase transformation of Fe-Zn alloy formed in hot-dip process	Shu Yamaguchi	The University of Tokyo
137	〃	三好　正悟	東京大学	大学院工学系研究科	〃	Shogo Miyoshi	The University of Tokyo
138	〃	田中　和彦	東京大学	大学院工学系研究科	〃	Kazuhiko Tanaka	The University of Tokyo
139	〃	上田　涼平	東京大学	大学院工学系研究科	〃	Ryohei Ueda	The University of Tokyo
140	空間反転対称性の破れた超伝導体の結晶性評価	古川　はづき	お茶の水女子大学	大学院人間文化創成科学研究科	Evaluation of single crystal quality of non-centrosymmetric superconductors	Hazuki Furukawa	Ochanomizu University
141	〃	石井　梨恵子	お茶の水女子大学	大学院人間文化創成科学研究科	〃	Rieko Ishii	Ochanomizu University
142	〃	呉　麻美子	お茶の水女子大学	大学院人間文化創成科学研究科	〃	Mamiko Kure	Ochanomizu University
143	三角スピンチューブのスピンダイナミクス	真中　浩貴	鹿児島大学	大学院理工学研究科	Spin dynamics of triangular spin tubes	Hirotaka Manaka	Kagoshima University

No.	課題名	氏名	所属		Title	Name	Organization
144	三元合金 $CuFePt_6$ 単結晶の評価	高橋　美和子	筑波大学	数理物質系	Characterization for a single crystal of ternary alloy $CuFePt_6$	Miwako Takahashi	University of Tsukuba
145	中性子散乱研究用大型単結晶試料の結晶性評価	阿曽　尚文	琉球大学	理学部	Crystal quality evaluation of large single crystals for neutron scattering	Naofumi Aso	University of the Ryukyus
146	鉄系超伝導体関連物質の高エネルギー X 線回折による単結晶試料確認	佐藤　卓	東北大学	多元物質科学研究所	Quality check of Fe-based superconductor related materials using high energy X-ray diffraction	Taku Sato	Tohoku University
147	$CeCoIn_5$ の磁束の磁気形状因子の異常	古川　はづき	お茶の水女子大学	大学院人間文化創成科学研究科	Anomalous magnetic form factor in the vortex state on $CeCoIn_5$	Hazuki Furukawa	Ochanomizu University
148	$ErNi_2B_2C$ とその関連物質における自発的磁束格子の観測	古川　はづき	お茶の水女子大学	大学院人間文化創成科学研究科	Spontaneous vortex lattice in $ErNi_2B_2C$ and its related compounds	Hazuki Furukawa	Ochanomizu University
149	〃	石井　梨恵子	お茶の水女子大学	大学院人間文化創成科学研究科	〃	Rieko Ishii	Ochanomizu University
150	Sr_2RuO_4 の異常金属状態の研究	古川　はづき	お茶の水女子大学	大学院人間文化創成科学研究科	Anomalous vortex state of Sr_2RuO_4	Hazuki Furukawa	Ochanomizu University
151	〃	納谷　麻衣子	お茶の水女子大学	大学院人間文化創成科学研究科	〃	Maiko Naya	Ochanomizu University
152	$Tb_2Ti_2O_7$ における量子スピン液体状態の研究	門脇　広明	首都大学東京	大学院理工学研究科	Quantum spin liquid in $Tb_2Ti_2O_7$	Hiroaki Kadowaki	Tokyo Metropolitan University
153	〃	谷口　智洋	首都大学東京	大学院理工学研究科	〃	Tomohiro Taniguchi	Tokyo Metropolitan University
154	スピン液体 $Tb_2Ti_2O_7$ の比熱測定	高津　浩	首都大学東京	大学院理工学研究科	Specific heat measurements on a spin liquid candidate $Tb_2Ti_2O_7$	Hiroshi Takatsu	Tokyo Metropolitan University
155	〃	清原　達也	首都大学東京	大学院理工学研究科	〃	Tatsuya Kiyohara	Tokyo Metropolitan University
156	空間反転対称性の破れた超伝導体のヘリカル磁束格子の観測	古川　はづき	お茶の水女子大学	大学院人間文化創成科学研究科	Helical vortex phase on non-centrosymmetric superconductors	Hazuki Furukawa	Ochanomizu University
157	〃	石井　梨恵子	お茶の水女子大学	大学院人間文化創成科学研究科	〃	Rieko Ishii	Ochanomizu University
158	〃	呉　麻美子	お茶の水女子大学	大学院人間文化創成科学研究科	〃	Mamiko Kure	Ochanomizu University
159	重い電子系新物質 $Ce_2Pt_3Ge_5$ の比熱測定 (2)	藤原　哲也	山口大学	大学院理工学研究科	Specific heat measurement in new heavy fermion system $Ce_2Pt_3Ge_5$ (II)	Tetsuya Fujiwara	Yamaguchi University
160	〃	中田　琢也	山口大学	大学院理工学研究科	〃	Takuya Nakada	Yamaguchi University

No.	課題名	氏名	所属		Title	Name	Organization
161	多形化合物 RIr_2Si_2（R= 希土類）の磁気特性	繁岡　透	山口大学	大学院理工学研究科	Magnetic property of polymorphic compound RIr_2Si_2 (R=rare earth)	Toru Shigeoka	Yamaguchi University
162	〃	蔵田　裕也	山口大学	大学院理工学研究科	〃	Yuya Kurata	Yamaguchi University
163	鉄系超伝導体関連物質の輸送特性	佐藤　卓	東北大学	多元物質科学研究所	Transport properties of Fe-based superconductor related materials	Taku Sato	Tohoku University
164	複合スピン系の比熱測定	佐藤　卓	東北大学	多元物質科学研究所	Heat capacity of complex spin system	Taku Sato	Tohoku University
165	$(Ho,Gd)Rh_2Si_2$ 単結晶の高磁場磁化 2	繁岡　透	山口大学	大学院理工学研究科	High field magnetization of $(Ho,Gd)Rh_2Si_2$ single crystal (2)	Toru Shigeoka	Yamaguchi University
166	〃	森田　哲広	山口大学	大学院理工学研究科	〃	Tetsuhiro Morita	Yamaguchi University
167	スピネル $FeCr_2S_4$ の高磁場物性	伊藤　昌和	鹿児島大学	大学院理工学研究科	Magnetic properties of spinel $FeCr_2S_4$ in high magnetic field	Masakazu Ito	Kagoshima University
168	〃	山下　敏広	鹿児島大学	大学院理工学研究科	〃	Toshihiro Yamashita	Kagoshima University
169	パルス磁場下比熱測定法による物性研究	稲垣　祐次	九州大学	大学院工学研究院	High field study by specific heat measurements under pulsed magnetic field	Yuji Inagaki	Kyushu University
170	モリブデン酸銅の強磁場磁化過程とサイズ効果	浅野　貴行	九州大学	大学院理学研究院	High-field magnetization process and size effect in copper molybdate	Takayuki Asano	Kyushu University
171	〃	福井　博章	九州大学	大学院理学府	〃	Hiroaki Fukui	Kyushu University
172	価数揺動状態にある Yb 化合物 $YbInCu_4$ の Yb-In 固溶系における強磁場磁化過程	道岡　千城	京都大学	大学院理学研究科	High field magnetization of a valence fluctuated Yb compound $YbInCu_4$ and its family compounds	Chishiro Michioka	Kyoto University
173	〃	今井　正樹	京都大学	大学院理学研究科	〃	Masaki Imai	Kyoto University
174	〃	中東　太一	京都大学	大学院理学研究科	〃	Taichi Nakahigashi	Kyoto University
175	希土類金属間化合物の強磁場物性研究	海老原　孝雄	静岡大学	大学院理学研究科	Physical phenomena at high magnetic fields in rear earth intermetallic compounds	Takao Ebihara	Shizuoka University
176	〃	土屋　政人	静岡大学	大学院理学研究科	〃	Masato Tsuchiya	Shizuoka University
177	幾何学的フラストレート磁性体の強磁場磁化測定	菊池　彦光	福井大学	大学院工学研究科	Magnetization studies of the frustrated magnets	Hikomitsu Kikuchi	University of Fukui

No.	課題名	氏名	所属		Title	Name	Organization
178	幾何学的フラストレート磁性体の強磁場磁化測定	浅野　泰典	福井大学	大学院工学研究科	Magnetization studies of the frustrated magnets	Yasunori Asano	University of Fukui
179	強相関ナローギャップ半導体 $Fe_{1-x}Mn_xSb_2$ の強磁場物性	田畑　吉計	京都大学	大学院工学研究科	High field magnetic properties of the strongly correlated narrow-gap semiconductor $Fe_{1-x}Mn_xSb_2$	Yoshikazu Tabata	Kyoto University
180	近藤半導体 (Yb, R)B_{12} (R=Zr, Sc, Y) の 80T 級磁場下での強磁場物性	伊賀　文俊	茨城大学	理学部	High field physical property of Kondo insulator (Yb, R)B_{12} (R=Zr, Sc, Y) up to 80T class by using the pulse magnet	Fumitoshi Iga	Ibaraki University
181	〃	林　健人	茨城大学	大学院理工学研究科	〃	Kento Hayashi	Ibaraki University
182	高圧合成希土類 12 ホウ化物の磁化特性	伊賀　文俊	茨城大学	理学部	Magnetic property of rare earth dodecaborides produced by high pressure synthesis	Fumitoshi Iga	Ibaraki University
183	三角格子反強磁性体混晶系 $Cs_2CuCl_{4-x}Br_x$ の磁化プラトー	小野　俊雄	大阪府立大学	大学院理学系研究科	Magnetization plateaux in triangular antiferromagnet mixture system $Cs_2CuCl_{4-x}Br_x$	Toshio Ono	Osaka Prefecture University
184	〃	富永　紘基	大阪府立大学	大学院理学系研究科	〃	Hiroki Tominaga	Osaka Prefecture University
185	新しい有機ポリラジカル磁性体の強磁場磁化測定	細越　裕子	大阪府立大学	大学院理学系研究科	High-field magnetization measurements of new organic polyradical magnets	Yuko Hosokoshi	Osaka Prefecture University
186	〃	天谷　直樹	大阪府立大学	大学院理学系研究科	〃	Naoki Amaya	Osaka Prefecture University
187	〃	菊地　健太郎	大阪府立大学	大学院理学系研究科	〃	Kentaro Kikuchi	Osaka Prefecture University
188	単結晶 $LaCo_{1-x}Rh_xO_3$ の強磁場磁化	佐藤　桂輔	茨城工業高等専門学校	自然科学	Field induced spin-state transition in $LaCo_{1-x}Rh_xO_3$	Keisuke Sato	Ibaraki National College of Technology
189	頂点及び辺共有した四面体の低次元性と幾何学的競合効果	浅野　貴行	九州大学	大学院理学研究院	Low-dimensionality and geometrically frustrated effect in corner- and edge-sharing tetrahedra	Takayuki Asano	Kyushu University
190	〃	川見　洋一郎	九州大学	大学院理学府	〃	Yoichiro Kawami	Kyushu University
191	ボラサイト型磁性強誘電体における方向複屈折	有馬　孝尚	東京大学	大学院新領域創成科学研究科	Directional birefringence in boracite-type magnetic ferroelectrics	Taka-hisa Arima	The University of Tokyo
192	〃	阿部　伸行	東京大学	大学院新領域創成科学研究科	〃	Nobuyuki Abe	The University of Tokyo
193	〃	豊田　新悟	東京大学	大学院新領域創成科学研究科	〃	Shingo Toyoda	The University of Tokyo
194	近藤半導体 (Yb,R)B_{12} のワンターンコイル 120T パルス磁場下での強磁場磁化過程	伊賀　文俊	茨城大学	理学部	High field magnetization of Kondo insulator (Yb,R)B_{12} by using one-turn coil in a 120 T pulse magnet	Fumitoshi Iga	Ibaraki University

No.	課題名	氏名	所属		Title	Name	Organization
195	近藤半導体 $(Yb,R)B_{12}$ のワンターンコイル 120T パルス磁場下での強磁場磁化過程	石井　克弥	茨城大学	大学院理工学研究科	High field magnetization of Kondo insulator $(Yb,R)B_{12}$ by using one-turn coil in a 120 T pulse magnet	Katsuya Ishii	Ibaraki University
196	$BiCo_{1-x}(Fe,Ni)_xO_3$ のパルス強磁場中磁気電気効果の観察	岡　研吾	東京工業大学	応用セラミックス研究所	Investigation of the electro-magnetic effect in $BiCo_{1-x}(Fe,Ni)_xO_3$ under pulsed magnetic field	Kengo Oka	Tokyo Institute of Technology
197	カルコパイライト型カルコゲン化合物の強磁場物性の探索	小林　夏野	青山学院大学	理工学部	Investigation of novel properties on chalcopyrite type chalcogenides in high magnetic fields	Kaya Kobayashi	Aoyama Gakuin University
198	コバルトヒ素伝導面を有する化合物の磁化過程	太田　寛人	東京農工大学	大学院工学研究院	Magnetic behavior of compounds with cobalt pnictide conducting planes	Hiroto Ohta	Tokyo University of Agriculture and Technology
199	〃	赤羽　栄介	東京農工大学	大学院工学府	〃	Eisuke Akabane	Tokyo University of Agriculture and Technology
200	コバルト酸化物の磁気形状記憶効果	佐藤　桂輔	茨城工業高等専門学校	自然科学	Magnetic shape memory effect in cobalt oxide	Keisuke Sato	Ibaraki National College of Technology
201	パルス磁場による磁場誘起クロミズムの直接観測	浅野　貴行	九州大学	大学院理学研究院	Direct observation of field-induced chromism in high pulsed magnetic fields	Takayuki Asano	Kyushu University
202	〃	福井　博章	九州大学	大学院理学府	〃	Hiroaki Fukui	Kyushu University
203	フラストレーションを有する磁性体の強磁場下での振舞い	香取　浩子	東京農工大学	大学院工学研究院	Properties of frustrated magnets in high magnetic fields	Hiroko Katori	Tokyo University of Agriculture and Technology
204	〃	斉藤　大地	東京農工大学	大学院工学府	〃	Daichi Saito	Tokyo University of Agriculture and Technology
205	強磁場による中間価数状態を示す準結晶の研究	出口　和彦	名古屋大学	大学院理学研究科	High magnetic field experiments of mixed-valence quasicrystal	Kazuhiko Deguchi	Nagoya University
206	〃	松川　周矢	名古屋大学	大学院理学研究科	〃	Shuya Matsukawa	Nagoya University
207	導電性パイロクロア型酸化物の強磁場下の物性研究	松平　和之	九州工業大学	大学院工学研究院	Transport and magnetic properties of conductive pyrochlore oxides under high field magnetic field	Kazuyuki Matsuhira	Kyushu Institute of Technology
208	〃	坂本　健	九州工業大学	大学院工学府	〃	Takeru Sakamoto	Kyushu Institute of Technology
209	Cu(111) 上に作製した BDTDA ラジカル単層膜における LEED I-V 実験	山本　真幸	山梨大学	医学工学総合研究部	LEED I-V experiment on BDTDA radical monolayer formed on Cu(111)	Masayuki Yamamoto	University of Yamanashi
210	歪半導体の表面近傍の歪み量の精密測定	武田　さくら	奈良先端科学技術大学院大学	物質創成科学研究科	Precise measurement of strain in the subsurface region of strained semiconductors	Sakura Takeda	Nara Institute of Science and Technology
211	マイクロリボン化によるグラフェンの超高速キャリアダイナミクスの変調	吹留　博一	東北大学	電気通信研究所	Modulated ultrafast carrier dynamics of graphene micro-ribbon	Hirokazu Fukidome	Tohoku University

No.	課題名	氏名	所属		Title	Name	Organization
212	強いスピン軌道相互作用を有する空間反転対称性の破れた物質の電子状態	坂野　昌人	東京大学	大学院工学系研究科	Electronic structures of strongly spin-orbit coupled noncentrosymmetric materials	Masato Sakano	The University of Tokyo
213	極低温超高分解能レーザー光電子分光装置による超伝導ギャップ測定	岡崎　浩三	東京大学	大学院理学系研究科	Superconducting-gap measurements by low-temperature high-resolution laser photoemission spectroscopy	Kozo Okazaki	The University of Tokyo
214	〃	堀尾　眞史	東京大学	大学院理学系研究科	〃	Masafumi Horio	The University of Tokyo
215	角度分解光電子分光による鉄系超伝導体における擬ギャップの研究	園部　竜也	東京大学	大学院工学系研究科	APRES study on pseudogap in Iron-pnictides	Tatsuya Sonobe	The University of Tokyo
216	高温超伝導体 Bi2212 におけるラマン散乱スペクトルと角度光電子分光スペクトルの定量的比較	宮坂　茂樹	大阪大学	大学院理学研究科	Quantitative comparison between electronic Raman spectra and angle-resolved photoemission spectra on high-T_c superconductor Bi2212	Shigeki Miyasaka	Osaka University
217	希土類磁性体の異方的磁気体積効果	大橋　政司	金沢大学	理工研究域	Anisotropic magnetovolume effect of rare earth compounds	Masashi Ohashi	Kanazawa University
218	テラヘルツ分光装置を用いた酸化物磁性材料の研究	大越　慎一	東京大学	大学院理学系研究科	Study of magnetic oxide using terahertz spectroscopy	Shin-ichi Ohkoshi	The University of Tokyo
219	〃	生井　飛鳥	東京大学	大学院理学系研究科	〃	Asuka Namai	The University of Tokyo
220	〃	吉清　まりえ	東京大学	大学院理学系研究科	〃	Marie Yoshikiyo	The University of Tokyo
221	Fe-$MgSiO_3$-H_2 系の高温高圧下におけるふるまいの解明	飯塚　理子	愛媛大学	地球深部ダイナミクス研究センター	Behavior of Fe-$MgSiO_3$-H_2 system under high pressure and temperature condition	Riko Iizuka	Ehime University
222	強相関型セリウム化合物および合金の量子相転移と磁性	村山　茂幸	室蘭工業大学	大学院工学研究科	Quantum phase transition and magnetism in the strongly correlated Ce compounds and alloys	Shigeyuki Murayama	Muroran Institute of Technology
223	〃	雨海　有佑	室蘭工業大学	大学院工学研究科	〃	Yusuke Amakai	Muroran Institute of Technology
224	〃	水野　博貴	室蘭工業大学	大学院工学研究科	〃	Hiroki Mizuno	Muroran Institute of Technology
225	HREELS によるグラファイトにおける電子格子散乱の直接測定	田中　慎一郎	大阪大学	産業科学研究所	Direct measurement of the electron-phonon scattering in graphite by using HREELS	Shin-ichiro Tanaka	Osaka University
226	強相関電子系化合物の秩序相に対する結晶対称性および軌道縮退の効果	横山　淳	茨城大学	理学部	Effects of crystal symmetry and orbital degeneracy in ordered states of strongly correlated electron systems	Makoto Yokoyama	Ibaraki University
227	〃	藤村　健司	茨城大学	大学院理工学研究科	〃	Kenji Fujimura	Ibaraki University
228	Pr 内包カゴ状化合物 $PrIr_2Zn_{20}$ の超伝導転移と四極子秩序に対する圧力効果	梅尾　和則	広島大学	自然科学研究支援開発センター	Pressure effect on the superconducting and antiferroquadrupolar transitions in a caged compound $PrIr_2Zn_{20}$	Kazunori Umeo	Hiroshima University

No.	課題名	氏名	所属		Title	Name	Organization
229	Pr 内包カゴ状化合物 $PrIr_2Zn_{20}$ の超伝導転移と四極子秩序に対する圧力効果	菅野　雄介	広島大学	大学院先端物質科学研究科	Pressure effect on the superconducting and antiferroquadrupolar transitions in a caged compound $PrIr_2Zn_{20}$	Yusuke Sugano	Hiroshima University
230	スピン正四面体を内包する希土類磁性体の極低温磁化測定	木村　健太	大阪大学	大学院基礎工学研究科	Magnetization measurements of the spin tetrahedral rare-earth magnet at very low temperatures	Kenta Kimura	Osaka University
231	顕微分光による Er ドープ GaAs の発光特性に関する研究	矢口　裕之	埼玉大学	大学院理工学研究科	Micro photoluminescence study of Er doped GaAs	Hiroyuki Yaguchi	Saitama University
232	〃	高宮　健吾	埼玉大学	大学院理工学研究科	〃	Kengo Takamiya	Saitama University
233	〃	山崎　泰由	埼玉大学	大学院理工学研究科	〃	Yasuyuki Yamazaki	Saitama University
234	MoS_2 電界誘起超伝導の上部臨界磁場	笠原　裕一	東京大学	大学院工学系研究科	Upper critical field of electric-field-induced superconductivity in MoS_2	Yuichi Kasahara	The University of Tokyo
235	NMR による有機三角格子物質の基底状態の研究	清水　康弘	名古屋大学	大学院理学研究科	NMR study for the ground state of organic triangular lattice materials	Yasuhiro Shimizu	Nagoya University
236	マルチフェロイックな CuO における強磁場中の電気磁気相図に関する研究	木村　剛	大阪大学	大学院基礎工学研究科	Investigation of magnetoelectric phase diagram in multiferroic CuO	Tsuyoshi Kimura	Osaka University
237	三角格子磁性体 $NaM(Acac)_3benzen(M=Ni,Mn,Fe)$ の低温磁性	柄木　良友	琉球大学	教育学部	Low temperature magnetism of triangular lattice antiferromagnet $NaM(Acac)_3benzene$ (M=Ni,Mn,Fe)	Yoshitomo Karaki	University of the Ryukyus
238	超強磁場を利用した NiMn 基低温異常現象の起源解明	キョ　キョウ	東北大学	大学院工学研究科	Clarification of the origin of anomalous behaviors at low temperature under strong magnetic field in NiMn based alloys	Xiao XU	Tohoku University
239	新奇トポロジカル絶縁体の 2 光子光電子分光	朱　思源	広島大学	大学院理学研究科	Two photon photoemission spectroscopy of exotic topological insulators	Zhu Siyuan	Hiroshima University
240	水素結合型分子性機能物質における重水素効果の理論的解析	立川　仁典	横浜市立大学	大学院生命ナノシステム科学研究科	Theoretical analysis of deuterated effect on hydrogen-bonded molecular materials	Masanori Tachikawa	Yokohama City University
241	〃	兼松　佑典	横浜市立大学	大学院生命ナノシステム科学研究科	〃	Yusuke Kanematsu	Yokohama City University
242	〃	緒方　勇大	横浜市立大学	大学院生命ナノシステム科学研究科	〃	Yudai Ogata	Yokohama City University
243	高温超伝導体 Bi2212 におけるラマン散乱スペクトルと角度光電子分光スペクトルの定量的比較	ゾビレイ ティルマン レナルト	大阪大学	大学院理学研究科	Quantitative comparison between electronic Raman spectra and angle-resolved photoemission spectra on high-T_c superconductor Bi2212	Sobirey Tilman Lennart	Osaka University

物質合成・評価設備 P クラス（Materials Synthesis and Characterization P Class Researcher）

No.	課題名	氏名	所属		Title	Name	Organization
1	ReO_3・VF_3 型化合物の構造転移に関するアニオン操作の影響	小林　洋治	京都大学	大学院工学研究科	The effect of anion manipulation on structural transitions in ReO_3/VF_3 type compounds	Yoji Kobayashi	Kyoto University
2	〃	淺井　啓	京都大学	大学院工学研究科	〃	Kei Asai	Kyoto University
3	〃	増田　直也	京都大学	大学院工学研究科	〃	Naoya Masuda	Kyoto University
4	遷移金属酸窒化物、金属間化合物における構造物性研究	山浦　淳一	東京工業大学	元素戦略研究センター	Structural physics on the transition metal oxynitrides and intermetallic compounds	Junichi Yamaura	Tokyo Institute of Technology
5	コンドライト母天体における含揮発性元素鉱物の形成環境の推定	瀬戸　雄介	神戸大学	大学院理学研究科	Formation environment of volatile element rich minerals on chondrite's parent bodies	Yusuke Seto	Kobe University
6	〃	松本　恵	神戸大学	研究基盤センター	〃	Megumi Matsumoto	Kobe University
7	〃	森家　智嗣	神戸大学	大学院理学研究科	〃	Satoshi Moriya	Kobe University
8	〃	酒井　碧	神戸大学	大学院理学研究科	〃	Midori Sakai	Kobe University
9	超臨界流体中レーザーアブレーションによるダイヤモンドイド合成の分光学的診断による反応機構の探索	シュタウス スヴェン	東京大学	大学院新領域創成科学研究科	Investigation of the reaction mechanisms of diamondoid synthesis by laser ablation in supercritical fluids by spectroscopic diagnostics	Sven Stauss	The University of Tokyo
10	〃	姫野　翔平	東京大学	大学院新領域創成科学研究科	〃	Shohei Himeno	The University of Tokyo
11	パイロクロア型希土類酸化物の単結晶育成と磁気フラストレーションの研究	松平　和之	九州工業大学	大学院工学研究院	Single crystal growth and study of frustrated magnetism in pyrochlore rare-earth oxides	Kazuyuki Matsuhira	Kyushu Institute of Technology

物質合成・評価設備 G クラス（Materials Synthesis and Characterization G Class Researcher）

No.	課題名	氏名	所属		Title	Name	Organization
1	高温高圧水を用いた医療廃棄物の小型オンサイト処理システムの開発	大友　順一郎	東京大学	大学院新領域創成科学研究科	Development of small size on-site disposal system in sub- and supercritical water for medical waste.	Junichiro Otomo	The University of Tokyo
2	〃	長澤　祐介	東京大学	大学院新領域創成科学研究科	〃	Yusuke Nagasawa	The University of Tokyo
3	超臨界水を用いた有機・無機複合廃棄物からのマテリアルリサイクル	大友　順一郎	東京大学	大学院新領域創成科学研究科	Material recycling from organic-inorganic composite waste using supercritical water	Junichiro Otomo	The University of Tokyo

No.	課題名	氏名	所属		Title	Name	Organization
4	超臨界水を用いた有機・無機複合廃棄物からのマテリアルリサイクル	松本　祐太	東京大学	大学院新領域創成科学研究科	Material recycling from organic-inorganic composite waste using supercritical water	Yuta Matsumoto	The University of Tokyo
5	ペロブスカイト型酸化物を用いたケミカルルーピングシステムの開発	大友　順一郎	東京大学	大学院新領域創成科学研究科	Study on perovskite based oxygen carrier materials for CLC/CLR applications	Junichiro Otomo	The University of Tokyo
6	〃	オーチェン　ジェームズ　オーチェン	東京大学	大学院新領域創成科学研究科	〃	Ochieng James Ochieng	The University of Tokyo
7	金属酸化物の酸化還元反応における担体効果の検討	大友　順一郎	東京大学	大学院新領域創成科学研究科	Effect of support material on redox reaction of metal oxide	Junichiro Otomo	The University of Tokyo
8	〃	高坂　文彦	東京大学	大学院新領域創成科学研究科	〃	Fumihiko Kosaka	The University of Tokyo
9	高温高圧水中における固体酸・塩基触媒反応の速度論的解析	大友　順一郎	東京大学	大学院新領域創成科学研究科	Kinetic analysis of solid acid and base catalyzed reactions in sub- and supercritical water	Junichiro Otomo	The University of Tokyo
10	〃	秋月　信	東京大学	大学院新領域創成科学研究科	〃	Makoto Akizuki	The University of Tokyo
11	酸化セリウム - 金属微粒子系のキャラクタリゼーション	佐々木　岳彦	東京大学	大学院新領域創成科学研究科	Characterization of cerium oxide with metal nanoparticles	Takehiko Sasaki	The University of Tokyo
12	〃	梶　智大	東京大学	大学院新領域創成科学研究科	〃	Tomohiro Kaji	The University of Tokyo
13	〃	原田　慧	東京大学	大学院新領域創成科学研究科	〃	Kei Harada	The University of Tokyo
14	〃	板子　健太郎	東京大学	大学院新領域創成科学研究科	〃	Kentaro Itako	The University of Tokyo
15	フラストレート磁性とスピン軌道相互作用の協調・競合効果	有馬　孝尚	東京大学	大学院新領域創成科学研究科	Interplay between frustrated magnetism and spin-orbit interaction	Taka-hisa Arima	The University of Tokyo
16	〃	阿部　伸行	東京大学	大学院新領域創成科学研究科	〃	Nobuyuki Abe	The University of Tokyo
17	〃	佐賀山　基	東京大学	大学院新領域創成科学研究科	〃	Hajime Sagayama	The University of Tokyo
18	〃	松浦　慧介	東京大学	大学院新領域創成科学研究科	〃	Keisuke Matsuura	The University of Tokyo
19	〃	豊田　新悟	東京大学	大学院新領域創成科学研究科	〃	Shingo Toyoda	The University of Tokyo
20	〃	植松　大介	東京大学	大学院新領域創成科学研究科	〃	Daisuke Uematsu	The University of Tokyo

No.	課題名	氏名	所属		Title	Name	Organization
21	3d 遷移金属の三角格子をもつ新規層状化合物の物性評価	植田　浩明	京都大学	大学院理学研究科	Characterization of novel layered compounds with a triangular lattice of 3d transition metals	Hiroaki Ueda	Kyoto University
22	〃	小林　慎太郎	京都大学	大学院理学研究科	〃	Shintaro Kobayashi	Kyoto University
23	〃	森下　翔	京都大学	大学院理学研究科	〃	Haruka Morishita	Kyoto University
24	高温高圧水中における層状固体酸触媒反応の基礎研究	大友　順一郎	東京大学	大学院新領域創成科学研究科	Fundamental research of layered solid acid catalyzed reaction in sub- and supercritical water.	Junichiro Otomo	The University of Tokyo
25	〃	名越　詩織	東京大学	大学院新領域創成科学研究科	〃	Shiori Nagoya	The University of Tokyo
26	酸化物イオン伝導体とプロトン伝導体を用いた新規二次電池の開発	大友　順一郎	東京大学	大学院新領域創成科学研究科	Development of novel rechargeable battery using oxide ion and proton conductors	Otomo Junichiro	The University of Tokyo
27	〃	櫻井　健一朗	東京大学	大学院新領域創成科学研究科	〃	Kenichiro Sakurai	The University of Tokyo
28	SOFC 空気極性能に対する製造プロセス由来微量成分の影響評価	大友　順一郎	東京大学	大学院新領域創成科学研究科	Evaluation of the effects of minor components derived from production processes on SOFC cathode performance	Junichiro Otomo	The University of Tokyo
29	〃	大石　淳矢	東京大学	大学院新領域創成科学研究科	〃	Junya Oishi	The University of Tokyo
30	アンモニア分解及び合成反応における電気化学特性と速度論解析	大友　順一郎	東京大学	大学院新領域創成科学研究科	Electrochemical properties and kinetic analysis in ammonia decomposition and synthesis	Junichiro Otomo	The University of Tokyo
31	〃	野田　直人	東京大学	大学院新領域創成科学研究科	〃	Naoto Noda	The University of Tokyo
32	ケミカルループ燃焼における酸化物イオン伝導体を用いた酸素キャリア材料の還元反応特性	大友　順一郎	東京大学	大学院新領域創成科学研究科	Reduction kinetics of oxygen carrier using oxide ion conductor in chemical-looping combustion	Junichiro Otomo	The University of Tokyo
33	〃	磯貝　俊介	東京大学	大学院新領域創成科学研究科	〃	Shunsuke Isogai	The University of Tokyo
34	タングステン酸ランタンにおけるプロトン伝導率に与える影響因子の評価	大友　順一郎	東京大学	大学院新領域創成科学研究科	Study on physicochemical properties for proton conductivity in lanthanum tungstate	Junichiro Otomo	The University of Tokyo
35	〃	庄野　洋平	東京大学	大学院新領域創成科学研究科	〃	Yohei Shono	The University of Tokyo
36	プロトン伝導性リン酸ガラス - セラミックスの微構造観察とイオン伝導特性	大友　順一郎	東京大学	大学院新領域創成科学研究科	Evaluation of microstructure and proton conductivity in phosphate glass-ceramics	Junichiro Otomo	The University of Tokyo
37	〃	門田　稔	東京大学	大学院新領域創成科学研究科	〃	Minoru Kadota	The University of Tokyo

No.	課題名	氏名	所属		Title	Name	Organization
38	結晶界面における無機複合型プロトン電解質の合成とイオン伝導度の評価	大友　順一郎	東京大学	大学院新領域創成科学研究科	Synthesis of proton conducting electrolyte and evaluation of ion conductivity of grain boundary	Otomo Junichiro	The University of Tokyo
39	〃	岩永　愛季	東京大学	大学院新領域創成科学研究科	〃	Aki Iwanaga	The University of Tokyo
40	固体酸化物形燃料電池の電極 - 電解質界面におけるカチオンの拡散挙動	大友　順一郎	東京大学	大学院新領域創成科学研究科	Diffusion mechanism at interface between electrode and electrolyte in solid oxide fuel cells	Junichiro Otomo	The University of Tokyo
41	〃	伊原　冬樹	東京大学	大学院新領域創成科学研究科	〃	Fuyuki Ihara	The University of Tokyo
42	高温高圧水を利用した有機修飾微粒子の連続式合成技術の開発	大友　順一郎	東京大学	大学院新領域創成科学研究科	Development of continuous synthesis of organic-modified particles in high temperature and pressure water	Junichiro Otomo	The University of Tokyo
43	〃	生駒　健太郎	東京大学	大学院新領域創成科学研究科	〃	Kentaro Ikoma	The University of Tokyo
44	酸化物イオン伝導体を担体に用いた金属酸化物の還元反応機構の解明	大友　順一郎	東京大学	大学院新領域創成科学研究科	Reduction mechanism of metal oxide supported by oxide ion conductor	Junichiro Otomo	The University of Tokyo
45	〃	菊池　典晃	東京大学	大学院新領域創成科学研究科	〃	Noriaki Kikuchi	The University of Tokyo
46	新規エネルギー変換デバイスに用いる複合セラミックス電解質材料のイオン輸送現象の研究	大友　順一郎	東京大学	大学院新領域創成科学研究科	Study on ionic transport in ceramics composites for new energy conversion devices	Junichiro Otomo	The University of Tokyo
47	〃	宮崎　顕也	東京大学	大学院新領域創成科学研究科	〃	Kenya Miyazaki	The University of Tokyo
48	超臨界水熱合成における複合酸化物ナノ粒子生成機構の解明	大友　順一郎	東京大学	大学院新領域創成科学研究科	Elucidation of formation mechanism for mixed oxide nanoparticles under supercritical hydrothermal synthesis	Junichiro Otomo	The University of Tokyo
49	〃	横　哲	東京大学	大学院新領域創成科学研究科	〃	Akira Yoko	The University of Tokyo
50	多重安定性を示す光誘起分子磁性体のサイズ効果の研究	糸井　充穂	日本大学	医学部	Size effect on photo-switchable molecular magnet $K_{0.3}Co[Fe(CN)_6]_{0.77}\cdot 3.4H_2O$	Miho Itoi	Nihon University
51	超臨界二酸化炭素中パルスレーザーアブレーションの分光診断法開発	占部　継一郎	東京大学	大学院新領域創成科学研究科	Development of spectroscopic diagnostic methods for pulsed laser ablation plasma in supercritical carbon-dioxide	Keiichiro Urabe	The University of Tokyo
52	太陽電池級シリコンの新規製造法の開発	坪内　賢太	東京大学	大学院新領域創成科学研究科	Development of new method to produce solar grade silicon	Kenta Tsubouchi	The University of Tokyo
53	ナノ構造制御に基づく蓄電池材料開発	細野　英司	産業技術総合研究所	エネルギー技術研究部門	Development of the battery materials based on the nanostructure control	Eiji Hosono	National Institute of Advanced Industrial Science and Technology
54	高温高圧下における水素によるエンスタタイトの安定性、相関係への影響	篠崎　彩子	東京大学	大学院理学系研究科	Influence of H_2 fluid on the stability and phase relation of enstatite under high pressure and high temperature	Ayako Shinozaki	The University of Tokyo

No.	課題名	氏名	所属		Title	Name	Organization
55	新規磁石材料の微細構造解析	齋藤　哲治	千葉工業大学	工学部	Microstructural studies of newly developed permanent magnet materials	Tetsuji Saito	Chiba Institute of Technology
56	天然鉱物の微細組織と結晶性の実態	永嶌　真理子	山口大学	大学院理工学研究科	Evaluation of micro-texture and crystallinity of natural minerals	Mariko Nagashima	Yamaguchi University
57	超臨界二酸化炭素中パルスレーザープラズマによる新規炭素ナノ材料の合成法の確立	シュタウス　スヴェン	東京大学	大学院新領域創成科学研究科	Development of synthesis method of carbon nanomaterials by pulsed-laser plasmas in supercritical CO_2	Sven Stauss	The University of Tokyo
58	〃	加藤　智嗣	東京大学	大学院新領域創成科学研究科	〃	Satoshi Kato	The University of Tokyo
59	ハーフメタル型ホイスラー合金の磁性と輸送特性に関する研究	重田　出	鹿児島大学	大学院理工学研究科	Study on the magnetic and transport properties of half-metallic Heusler alloys	Iduru Shigeta	Kagoshima University
60	〃	西迫　裕也	鹿児島大学	大学院理工学研究科	〃	Yuya Nishisako	Kagoshima University
61	ホイスラー型化合物の磁性と伝導の研究	廣井　政彦	鹿児島大学	大学院理工学研究科	Study on the magnetic and electrical properties of Heusler compounds	Hiroi Masahiko	Kagoshima University
62	〃	佐野　紘晃	鹿児島大学	大学院理工学研究科	〃	Hiroaki Sano	Kagoshima University
63	新規ペロブスカイト型酸化物の磁気物性	長谷川　正	名古屋大学	大学院工学研究科	Magnetism of novel perovskite-type oxides	Masashi Hasegawa	Nagoya University
64	〃	志村　元	名古屋大学	大学院工学研究科	〃	Gen Shimura	Nagoya University
65	新規遷移金属硫化物固溶体の磁気物性	長谷川　正	名古屋大学	大学院工学研究科	Magnetism of novel transition metal sulfide solid solutions	Masashi Hasegawa	Nagoya University
66	〃	岩崎　純也	名古屋大学	大学院工学研究科	〃	Junya Iwasaki	Nagoya University
67	クラスター固体の熱電物性に関する研究	木村　薫	東京大学	大学院新領域創成科学研究科	Thermoelectric properties of cluster compounds	Kaoru Kimura	The University of Tokyo
68	〃	高際　良樹	東京大学	大学院新領域創成科学研究科	〃	Yoshiki Takagiwa	The University of Tokyo
69	〃	北原　功一	東京大学	大学院新領域創成科学研究科	〃	Kouichi Kitahara	The University of Tokyo
70	〃	柳原　大輔	東京大学	大学院新領域創成科学研究科	〃	Daisuke Yanagihara	The University of Tokyo
71	〃	星野　建	東京大学	大学院新領域創成科学研究科	〃	Takeru Hoshino	The University of Tokyo

No.	課題名	氏名	所属		Title	Name	Organization
72	クラスター固体の熱電物性に関する研究	佐藤　直大	東京大学	大学院新領域創成科学研究科	Thermoelectric properties of cluster compounds	Naoki Sato	The University of Tokyo

物質合成・評価設備 U クラス（Materials Synthesis and Characterization U Class Researcher）

No.	課題名	氏名	所属		Title	Name	Organization
1	シリサイド系半導体単結晶の光学特性評価	鵜殿　治彦	茨城大学	工学部	Characterizations of optical properties single crystalline semiconducting silicides	Haruhiko Udono	Ibaraki University
2	Cu – Ni-X（X=Co,Fe）系単結晶性合金中の磁性微粒子析出過程と磁気特性の関係	竹田　真帆人	横浜国立大学	大学院工学研究院	Precipitation behavior and magnetic properties of fine magnetic particles in Cu-Ni base alloys single crystal	Mahoto Takeda	Yokohama National University
3	〃	李　東海	横浜国立大学	大学院工学府	〃	Lee donghae	Yokohama National University
4	〃	金　俊燮	横浜国立大学	大学院工学府	〃	Kim Junseop	Yokohama National University
5	Si 基ナノ複合熱電材料の TEM による微細組織評価	宮崎　吉宣	大阪大学	大学院工学研究科	Microstructural characterization of Si-based nanocomposite thermoelectric materials by TEM	Yoshinobu Miyazaki	Osaka University
6	Au 基正 20 面体近似結晶の磁気構造の解明	廣戸　孝信	東京理科大学	大学院基礎工学研究科	Magnetic structure of Au based icosahedral approximant to the quasicrystal	Takanobu Hiroto	Tokyo University of Science
7	異常マイクロ波応答の観測に向けた空間反転対称性が破れた磁性体の X 線試料評価	小野瀬　佳文	東京大学	大学院総合文化研究科	X-ray characterization of noncentrosymmetic magnetic samples for the observation of anomalous microwave response	Yoshinori Onose	The University of Tokyo
8	〃	井口　雄介	東京大学	大学院総合文化研究科	〃	Yusuke Iguchi	The University of Tokyo
9	〃	南川　晴紀	東京大学	大学院総合文化研究科	〃	Haruki Namikawa	The University of Tokyo

長期留学研究員（Long Term Young Researcher）

No.	課題名	氏名	所属		Title	Name	Organization
1	トポロジカル絶縁体 $Cu_{0.17}Bi_2Se_3$ の極紫外レーザー時間分解光電子分光	山本　貴士	東京理科大学	大学院理学研究科	Time resolved ARPES of topological insulator $Cu_{0.17}Bi_2Se_3$	Takashi Yamamoto	Tokyo University of Science
2	窒素ドープ炭素材料の酸素還元反応メカニズムの解明	木内　久雄	東京大学	大学院工学系研究科	Study on the oxygen reduction reaction of nitrogen-doped carbon material	Hisao Kiuchi	The University of Tokyo
3	超流動ヘリウム 3-A 相の半整数量子渦の研究	木村　豊	大阪市立大学	大学院理学研究科	Study of the half quantized vortex in superfluid ^{3}He-A phase	Yutaka Kimura	Osaka City University

短期留学研究員（Short Term Young Researcher）

No.	課題名	氏名	所属		Title	Name	Organization
1	カゴメ格子反強磁性体 volborthite における極低温熱励起の研究	渡邊　大樹	京都大学	大学院理学研究科	Study of thermal excitations of kagome lattice material vorborthite in very low temperature	Daiki Watanabe	Kyoto University
2	熱輸送測定を用いたスピン液体の研究	渡邊　大樹	京都大学	大学院理学研究科	Study of spin liquids by thermal transport measurement	Daiki Watanabe	Kyoto University

Publications

Division of New Materials Science

Takigawa group

We have been performing nuclear magnetic resonance experiments on various quantum spin systems and strongly correlated electron systems to explore novel quantum phases with exotic ordering and fluctuation phenomena. The major achievements in the year 2013 include: (1) Investigation by ^{7}Li-NMR of the magnetic phase transition in the frustrated antiferromagnets $LiInCr_4O_8$ and $LiGaCr_4O_8$ with the novel breathing pyrochlore structure, (2) Microscopic examination of the quantum critical and non-fermi liquid behavior in the valence fluctuating Yb compound alpha- and beta- $YbAlB_4$, (3) Continued investigation of the magnetic and structural transition in single crystals of volborthite with the distorted Kagome lattice aimed at the full understanding of the phase diagram in magnetic field.

1. †Anisotropic spin fluctuations in the quasi one-dimensional frustrated magnet $LiCuVO_4$: K. Nawa, M. Takigawa, M. Yoshida and K. Yoshimura, J. Phys. Soc. Jpn. **86** (2013) 094709(1-13).
2. *Magnetic Order in the Spin-1/2 Kagome Antiferromagnet Vesignieite: M. Yoshida, Y. Okamoto, M. Takigawa and Z. Hiroi, J. Phys. Soc. Jpn. **82** (2013) 013702(1-5).
3. *Incomplete Devil`s Staircase in the Magnetization Curve of $SrCu_2(BO_3)_2$: M. Takigawa, M. Horvatic, T. Waki, S. Kramer, C. Berthier, F. L. Bertrand, I. Sheikin, H. Kageyama, Y. Ueda and F. Mila, Phys. Rev. Lett. **110** (2013) 067210(1-5).
4. Iterative deconvolution of quadrupole split NMR spectra: F. Mila and M. Takigawa, Eur. Phys. J. B **86** (2013) 354(1-4).
5. †*Field-induced incommensurate phase in the strong-rung spin ladder with ferromagnetic legs: H. Yamaguchi, H. Miyagai, M. Yoshida, M. Takigawa, K. Iwase, T. Ono, N. Kase, K. Araki, S. Kittaka, T. Sakakibara, T. Shimokawa, T. Okubo, K. Okunishi, A. Matsuo and Y. Hosokoshi, Phys. Rev. B **89** (2014) 220402.

Sakakibara group

We study magnetism and superconductivity of materials having low characteristic temperatures. These include heavy-electron systems, quantum spin systems and frustrated spin systems. The followings are some selected achievements in the fiscal year 2013. (1) Field and temperature variations of the specific heat C(H,T) of the iron pnictide superconductor KFe_2As_2 (Tc=3.4 K) were examined at temperatures down to 100 mK. Thermodynamic evidence for the presence of line nodes is obtained from the square-root H dependence of C/T in the low-T and low-H regime. Under a magnetic field rotated within the tetragonal ab plane, a fourfold oscillation is observed in Ce and its sign changes at 0.08 Tc. The results indicate that line nodes exist on the superconducting gap where the Fermi velocity is parallel to [100] directions. (2) We measured the temperature dependence of the magnetization M(T) of a S=1/2 one dimensional Heisenberg antiferromagnet CuPzN (interaction parameter J~10 K) near the saturation field Hs~14 T where a quantum phase transition from a Luttinger liquid ground state to a fully polarized state occurs. It is found that M(T) at Hs exhibits a square-root T dependence below ~1 K down to 80 mK, in good agreement with a prediction of the exact solutions.

1. Anomalous Field-Angle Dependence of the Specific Heat of Heavy-Fermion Superconductor UPt_3: S. Kittaka, K. An, T. Sakakibara, Y. Haga, E. Yamamoto, N. Kimura, Y. Onuki and K. Machida, J. Phys. Soc. Jpn. **82** (2013) 024707(1-5).
2. †Coexistence of Ising and XY Spin Systems on a Single Tb Atom in $TbCoGa_5$: N. Sanada, Y. Amou, R. Watanuki, K. Suzuki, I. Yamamoto, H. Mitamura, T. Sakakibara, M. Akatsu, Y. Nemoto and T. Goto, J. Phys. Soc. Jpn. **82** (2013) 044713(1-7).
3. *Evidence of a High-Field Phase in PrV_2Al_{20} in a [100] Magnetic Field: Y. Shimura, Y. Ohta, T. Sakakibara, A. Sakai and S. Nakatsuji, J. Phys. Soc. Jpn. **82** (2013) 043705(1-4).
4. †*High-Field Phase Diagram of $SmRu_4P_{12}$ Determined by Ultrasonic Measurements in Pulsed Magnetic Field up to 55 T: M. Yoshizawa, H. Mitamura, F. Shichinomiya, S. Fukuda, Y. Nakanishi, H. Sugawara, T. Sakakibara and K. Kindo, J. Phys. Soc. Jpn. **82** (2013) 033602(1-5).

---

* Joint research among groups within ISSP.

5. Verification of Anisotropic *s*-Wave Superconducting Gap Structure in $CeRu_2$ from Low-Temperature Field-Angle-Resolved Specific Heat Measurements: S. Kittaka, T. Sakakibara, M. Hedo, Y. Onuki and K. Machida, J. Phys. Soc. Jpn. **82** (2013) 123706(1-4).

6. †*Long-range order and spin-liquid states of polycrystalline $Tb_{2+x}Ti_{2-x}O_{7+y}$: T. Taniguchi, H. Kadowaki, H. Takatsu, B. Fåk, J. Ollivier, T. Yamazaki, T. J. Sato, H. Yoshizawa, Y. Shimura, T. Sakakibara, T. Hong, K. Goto, L. R. Yaraskavitch and J. B. Kycia, Phys. Rev. B **87** (2013) 060408R(1-5).

7. †*Quasi-one-dimensional S=1/2 Heisenberg antiferromagnetic chain consisting of the organic radical p-Br-V: K. Iwase, H. Yamaguchi, T. Ono, Y. Hosokoshi, T. Shimokawa, Y. Kono, S. Kittaka, T. Sakakibara, A. Matsuo and K. Kindo, Phys. Rev. B **88** (2013) 184431(1-5).

8. †*Various regimes of quantum behavior in an S=1/2 Heisenberg antiferromagnetic chain with fourfold periodicity: H. Yamaguchi, T. Okubo, K. Iwase, T. Ono, Y. Kono, S. Kittaka, T. Sakakibara, A. Matsuo, K. Kindo and Y. Hosokoshi, Phys. Rev. B **88** (2013) 174410(1-5).

9. Determining the Surface-To-Bulk Progression in the Normal-State Electronic Structure of Sr_2RuO_4 by Angle-Resolved Photoemission and Density Functional Theory: C. N. Veenstra, Z. -H. Zhu, B. Ludbrook, M. Capsoni, G. Levy, A. Nicolaou, J. A. Rosen, R. Comin, S. Kittaka, Y. Maeno, I. S. Elfimov and A. Damascelli, Phys. Rev. Lett. **110** (2013) 097004(1-5).

10. †Unconventional Magnetic and Thermodynamic Properties of S=1/2 Spin Ladder with Ferromagnetic Legs: H. Yamaguchi, K. Iwase, T. Ono, T. Shimokawa, H. Nakano, Y. Shimura, N. Kase, S. Kittaka, T. Sakakibara, T. Kawakami and Y. Hosokoshi, Phys. Rev. Lett. **110** (2013) 157205(1-5).

11. 高次多極子がもたらす磁場誘起相：志村 恭通 , 榊原 俊郎 , 大貫 惇睦 , 固体物理 **48** (2013) 721-727.

12. Magnetization steps in Yb_2Pt_2Pb with the Shastry-Sutherland lattice: Y. Shimura, T. Sakakibara, K. Iwakawa, Y. Onuki and K. Sugiyama, J. Kor. Phys. Soc. **63** (2013) 551-554.

13. Singlet-triplet crossover in the two-dimensional dimer spin system $YbAl_3C_3$: S. Kittaka, T. Sugiyama, Y. Shimura, T. Sakakibara, S. Matsuda and A. Ochiai, J. Kor. Phys. Soc. **62** (2013) 2088-2092.

14. †Fine-Tuning of Magnetic Interactions in Organic Spin Ladders: H. Yamaguchi, H. Miyagai, T. Shimokawa, K. Iwase, T. Ono, Y. Kono, N. Kase, K. Araki, S. Kittaka, T. Sakakibara, T. Kawakami, K. Okunishi and Y. Hosokoshi, J. Phys. Soc. Jpn. **83** (2014) 033707(1-4).

15. Novel Electronic States of Heavy Fermion Compound $YbCo_2Zn_{20}$: F. Honda, Y. Taga, Y. Hirose, S. Yoshiuchi, Y. Tomooka, M. Ohya, J. Sakaguchi, T. Takeuchi, R. Settai, Y. Shimura, T. Sakakibara, I. Sheikin, T. Tanaka, Y. Kubo and Y. Onuki, J. Phys. Soc. Jpn. **83** (2014) 044703(1-9).

16. †Possible Evolution of Antiferromagnetism in Zn-Doped Heavy-Fermion Superconductor $CeCoIn_5$: M. Yokoyama, K. Fujimura, S. Ishikawa, M. Kimura, T. Hasegawa, I. Kawasaki, K. Tenya, Y. Kono and T. Sakakibara, J. Phys. Soc. Jpn. **83** (2014) 033706(1-5).

17. Thermodynamic Study of Nodal Structure and Multiband Superconductivity of KFe_2As_2: S. Kittaka, Y. Aoki, N. Kase, T. Sakakibara, T. Saito, H. Fukazawa, Y. Kohori, K. Kihou, C. Ho Lee, A. Iyo, H. Eisaki, K. Deguchi, N. K. Sato, Y. Tsutsumi and K. Machida, J. Phys. Soc. Jpn. **83** (2014) 013704(1-4).

18. †*Field-induced incommensurate phase in the strong-rung spin ladder with ferromagnetic legs: H. Yamaguchi, H. Miyagai, M. Yoshida, M. Takigawa, K. Iwase, T. Ono, N. Kase, K. Araki, S. Kittaka, T. Sakakibara, T. Shimokawa, T. Okubo, K. Okunishi, A. Matsuo and Y. Hosokoshi, Phys. Rev. B **89** (2014) 220402.

19. Measurement of the spin-orbit coupling in superconducting Sr_2RuO_4 using polarized light and spin-resolved photoemission spectroscopy: Evidence for a breakdown in the singlets and triplets pairing mechanisms: C. N. Veenstra, Z. -H. Zhu, M. Raichle, B. M. Ludbrook, A. Nicolaou, B. Slomski, G. Landolt, S. Kittaka, Y. Maeno, J. H. Dil, I. S. Elfimov, M. W. Haverkort and A. Damascelli, Phys. Rev. Lett. **112** (2014) 127002(1-4).

20. Multiband superconductivity with unexpected deficiency of nodal quasiparticles in $CeCu_2Si_2$: S. Kittaka, Y. Aoki, Y. Shimura, T. Sakakibara, S. Seiro, C. Geibel, F. Steglich, H. Ikeda and K. Machida, Phys. Rev. Lett. **112** (2014) 067002(1-5).

21. *Magnetization and Specific Heat of the Caged Compound PrV_2Al_{20}: K. Araki, Y. Shimura, N. Kase, T. Sakakibara, A. Sakai and S. Nakatsuji, J. Phys. Soc. Jpn. (2014), in print.

† Joint research with outside partners.

Mori group

We have successfully developed and characterized the functional molecular materials. The major achievements in 2013 are (1) to discover the novel spin liquid state of purely organic single-component crystal κ-H_3(Cat-EDT-TTF)$_2$, (2) to develop the proton-electron coupled molecular conductor with tuning π-electron bandwidth and hydrogen bond, and (3) to clarify the electronic state between 3/4-filled and effective 1/2-filled band structure by optical measurement for pressure-induced superconductor β-(*meso*-DMBEDT-TTF)$_2$$PF_6$.

1. Optical Conductivity Measurement of a Dimer Mott-Insulator to Charge-Order Phase Transition in a Two-Dimensional Quarter-Filled Organic Salt Compound: R. Okazaki, Y. Ikemoto, T. Moriwaki, T. Shikama, K. Takahashi, H. Mori, H. Nakaya, T. Sasaki, Y. Yasui and I. Terasaki, Phys. Rev. Lett. **111** (2013) 217801.
2. †Fabrication of a field effect transistor structure using charge-ordered organic materials α-(BEDT-TTF)$_2I_3$ and α′-(BEDT-TTF)$_2$$IBr_2$: M. Kimata, T. Ishihara, A. Ueda, H. Mori and H. Tajima, Synth. Met. **173** (2013) 43-45.
3. Pyridone derivatives carrying radical moieties: Hydrogen-bonded structures, magnetic properties, and metal coordination: M. Ueda, T. Mochida and H. Mori, Polyhedron **52** (2013) 755-760.
4. Crystal Architectures and Magnetic Properties of Alkylferrocenium Salts with F_nTCNQ(n = 0, 2, 4): Effect of Substituents on the Self-Assembled Structures: T. Mochida, T. Akasaka, Y. Funasako, Y. Nishio and H. Mori, Crystal Growth & Design **13** (2013) 4460.
5. Hydrogen bond-promoted metallic state in a purely organic single-component conductor under pressure: T. Isono, H. Kamo, A. Ueda, K. Takahashi, A. Nakao, R. Kumai, H. Nakao, K. Kobayashi, Y. Murakami and H. Mori, Nat. Commun. **4** (2013) 1344-1349.
6. Gapless Quantum Spin Liquid in an Organic Spin-1/2 Triangular-Lattice κ-H_3(Cat-EDT-TTF)$_2$: T. Isono, H. Kamo, A. Ueda, K. Takahashi, M. Kimata, H. Tajima, S. Tsuchiya, T. Terashima, S. Uji and H. Mori, Phys. Rev. Lett. **112** (2014) 177201.
7. Biferrocenium salts with magnetite-like mixed-valence iron: coexistence of Fe^{3+} and $Fe^{2.5+}$ in the crystal: T. Mochida, E. Nagabuchi, M. Takahashi and H. Mori, Chem. Commun. **50** (2014) 2481.
8. Protonation of Pyridyl-Substituted TTF Derivatives: Substituent Effects in Solution and in the Proton-Electron Correlated Charge-Transfer Complexes: S. C. Lee, A. Ueda, A. Nakao, R. Kumai, H. Nakao, Y. Murakami and H. Mori, Chem. Eur. J. **20** (2014) 1909.
9. Charge-Transfer Salts of Biferrocene Derivatives with F_2- and F_4-Tetracyanoquinodimethane: Correlation Between Donor–Acceptor Ratios and Cation Valence States: T. Mochida, Y. Funasako, E. Nagabuchi and H. Mori, Crystal Growth & Design **14** (2014) 1459.
10. Synergistic Spin Transition between Spin Crossover and Spin-Peierls-like Singlet Formation in the Halogen-Bonded Molecular Hybrid System: [Fe(Iqsal)$_2$][Ni(dmit)$_2$]·CH_3CN·H_2O: K. Fukuroi, K. Takahashi, T. Mochida, T. Sakurai, H. Ohta, T. Yamamoto, Y. Einaga and H. Mori, Angew. Chem. Int. Ed. **53** (2014) 1983.
11. 単成分純有機金属材料で金属伝導は可能か？: 森 初果 , 上田 顕 , 化学 **68** (2013) 64-65.
12. 磁性と伝導性が相関した多重機能性分子性物質の開発 : 森 初果 , 高橋 一志 , まぐね **8** (2013) 148-154.
13. はたらくこと　生きること理工系女性の想い : 森 初果 , 日刊工業新聞 (2013).
14. 化学の力を生かした新しい分子性機能材料の開発 : 森 初果 , 化学 **69**, **No1** (2014) 20-21.
15. 金属状態を示す純有機単成分導体 : 森 初果 , 工業材料 **62**　**No1** (2014) 26-27.

Nakatsuji group

Our group explores novel quantum phases and phase transitions in rare-earth and transition metal based compounds. The followings are some relevant results obtained in 2013. (1) We have found that the metallic spin ice compound $Pr_2Ir_2O_7$ exhibits quantum criticality in a nontrivial semimetallic state. (2) The Fe doping at the Al site in α-$YbAlB_4$ induces an antiferromagnetic ordering whose ordering temperature goes up to 10 K, which is the highest among the Yb based heavy fermion materials. The large enhancement of the magnetic ordering indicates that the mixed valence plays an important role. (3) Finally, our success in synthesizing high quality single crystals of $PrTr_2Al_{20}$ allows us to reveal that the superconductivity in $PrTi_2Al_{20}$ and the antiferro-quadrupolar transition in PrV_2Al_{20} can be easily suppressed by disorder. This highlights the importance of high quality crystals for the study of strong hybridization effects in quadrupolar Kondo systems.

* Joint research among groups within ISSP.

1. Conduction electron spin resonance in AlB_2: L. M. Holanda, L. Mendonça-Ferreira, R. A. Ribeiro, J. M. Osorio-Guillén, G. M. Dalpian, K. Kuga, S. Nakatsuji, Z. Fisk, R. R. Urbano, P. G. Pagliuso and C. Rettori, J. Phys.: Condens. Matter **25** (2013) 216001.

2. [*]Evidence of a High-Field Phase in PrV_2Al_{20} in a [100] Magnetic Field: Y. Shimura, Y. Ohta, T. Sakakibara, A. Sakai and S. Nakatsuji, J. Phys. Soc. Jpn. **82** (2013) 043705(1-4).

3. Determination of long-range all-in-all-out ordering of Ir^{4+} moments in a pyrochlore iridate $Eu_2Ir_2O_7$ by resonant x-ray diffraction: H. Sagayama, D. Uematsu, T. Arima, K. Sugimoto, J. J. Ishikawa, E. O'Farrell and S. Nakatsuji, Phys. Rev. B **87** (2013) 100403(4 pages).

4. Magnetic excitations and c-f hybridization effect in $PrTi_2Al_{20}$and PrV_2Al_{20}: Y. Tokunaga, H. Sakai, S. Kambe, A. Sakai, S. Nakatsuji and H. Harima, Phys. Rev. B **88** (2013) 085124.

5. Dynamical spin–orbital correlation in the frustrated magnet $Ba_3CuSb_2O_9$: Y. Ishiguro, K. Kimura, S. Nakatsuji, S. Tsutsui, A. Q. R. Baron, T. Kimura and Y. Wakabayashi, Nat. Commun. **4** (2013) 2022(1-6).

6. Quantum fluctuations in spin-ice-like $Pr_2Zr_2O_7$: K. Kimura, S. Nakatsuji, J.-J. Wen, C. Broholm, M. B. Stone, E. Nishibori and H. Sawa, Nat. Commun. **4** (2013) 1934(1-6).

7. [*]Chemical effects of high-resolution Yb $L\gamma_4$ emission spectra: a possible probe for chemical analysis: H. Hayashi, N. Kanai, N. Kawamura, Y. H. Matsuda, K. Kuga, S. Nakatsuji, T. Yamashita and S. Ohara, X-Ray Spectrom. **42** (2013) 450-455.

8. Low temperature transport properties of the quadrupolar Kondo lattice system $PrTi_2Al_{20}$: A. Sakai and S. Nakatsuji, J. Kor. Phys. Soc. **63** (2013) 398-400.

9. Magnetic order induced by Fe doping in the intermediate valence system β-$YbAlB_4$: K. Kuga and S. Nakatsuji, J. Kor. Phys. Soc. **63** (2013) 549-550.

10. Mössbauer spectroscopy of Fe-doped valence-fluctuating α-$YbAlB_4$: Y. Sakaguchi, S. Ikeda, H. Kobayashi, K. Kuga, K. Sone and S. Nakatsuji, J. Kor. Phys. Soc. **62** (2013) 2146-2149.

11. Single-crystal study on the low-temperature magnetism of the pyrochlore magnet $Pr_2Zr_2O_7$: K. Kimura, S. Nakatsuji and A. A. Nugroho, J. Kor. Phys. Soc. **63** (2013) 719-721.

12. [*]Synchrotron X-ray spectroscopy study on the valence state in α- and β-$YbAlB_4$ at low temperatures and high magnetic fields: Y. H. Matsuda, T. Nakamura, K. Kuga, S. Nakatsuji, S. Michimura, T. Inami, N. Kawamura and M. Mizumaki, J. Kor. Phys. Soc. **62** (2013) 1778-1781.

13. Quantum criticality in a metallic spin liquid: Y. Tokiwa, J. J. Ishikawa, S. Nakatsuji and P. Gegenwart, Nature Mater. **13** (2014) 356.

14. X-ray Photoemission and X-ray Absorption Spectroscopy of Hexagonal $Ba_3CuSb_2O_9$: T. Sugimoto, T. Mizokawa, H. Wadati, K. Takubo, A. Damascelli, T. Z. Regier, G. A. Sawatzky, N. Katayama, H. Sawa, K. Kimura and S. Nakatsuji, J. Kor. Phys. Soc. **63** (2014) 549-550.

15. [*]Heavy fermion superconductivity under pressure in the quadrupole system $PrTi_2Al_{20}$: K. Matsubayashi, T. Tanaka, J. Suzuki, A. Sakai, S. Nakatsuji, K. Kitagawa, Y. Kubo and Y. Uwatoko, J. Phys. Soc. Jpn. (2014), in print.

16. Magnetic and Thermal Properties of the Single Crystalline $Pr_2Zr_2O_7$ in a [111] field: K. Kimura and S. Nakatsuji, J. Phys. Soc. Jpn. (2014), in print.

17. [*]Magnetization and Specific Heat of the Caged Compound PrV_2Al_{20}: K. Araki, Y. Shimura, N. Kase, T. Sakakibara, A. Sakai and S. Nakatsuji, J. Phys. Soc. Jpn. (2014), in print.

18. [*]Magnetization of Yb-based mixed-valent compounds at megagauss fields: T. Terashima, Y. H. Matsuda, K. Kuga, Y. Matsumoto and S. Nakatsuji, J. Phys. Soc. Jpn. (2014), in print.

19. Sample Dependence of the Quadrupolar Transition in the Nonmagnetic cubic Γ_3 Compound PrV_2Al_{20}: M. Tsujimoto, A. Sakai and S. Nakatsuji, J. Phys. Soc. Jpn. (2014), in print.

20. Structural and Magnetic Properties of α-$Yb(Al_{1-x}Fe_x)B_4$ under Hydtostatic Pressure: Y. Sakaguchi, S. Ikeda, K. Kuga, S. Nakatsuji, N. Hirao, Y. Ohishi and H. Kobayashi, J. Phys. Soc. Jpn. (2014), in print.

21. Superconducting properties of the ferroquadrupolar cubic Γ_3 compound $PrTi_2Al_{20}$: A. Sakai, K. Kuga and S. Nakatsuji, J. Phys. Soc. Jpn. (2014), in print.

[†] Joint research with outside partners.

22. Suppression of the Heavy Fermion State in Magnetic Fields in the Mixed Valent α-$YbAlB_4$: Y. Matsumoto, K. Kentaro and S. Nakatsuji, J. Phys. Soc. Jpn. (2014), in print.

23. Two magnetic phases in α-$YbAl_{1-x}Fe_xB_4$: K. Kuga, S. Suzuki and S. Nakatsuji, J. Phys. Soc. Jpn. (2014), in print.

24. 銅酸化物における乱れに強い量子液体状態：中辻 知，澤 博，「超伝導現象と高温超伝導体」，新日本編集企画，(NTS 出版社, 2013), 475-481.

Ohgushi group

Our group is focused on an exploratory synthesis and characterization of oxides, chalcogenides, and intermetallics. The major achievements in the fiscal year 2013 are (1) finding of new superconductivity in anti-post-perovskite compounds, and (2) elucidation of orbital states of iridium oxides by means of resonant x-ray diffraction.

1. *Observation of Phonon-Assisted Magnon Absorption in Spin–Orbit Coupling Induced Mott Insulator Sr_2IrO_4: Y. Hirata, H. Tajima and K. Ohgushi, J. Phys. Soc. Jpn. **82** (2013) 035002(1-2).

2. Complex orbital state stabilized by strong spin-orbit coupling in a metallic iridium oxide IrO_2: Y. Hirata, K. Ohgushi, J.-I. Yamaura, H. Ohsumi, S. Takeshita, M. Takata and T. Arima, Phys. Rev. B **87** (2013) 161111(1-5).

3. Magnetoelasticity in ACr_2O_4 spinel oxides (A = Mn, Fe, Co, Ni, and Cu): V. Kocsis, S. Bordács, D. Varjas, K. Penc, A. Abouelsayed, C. A. Kuntscher, K. Ohgushi, Y. Tokura and I. Kézsmárki, Phys. Rev. B **87** (2013) 064416(1-9).

4. *Mechanism of Enhanced Optical Second-Harmonic Generation in the Conducting Pyrochlore-Type $Pb_2Ir_2O_{7-x}$ Oxide Compound: Y. Hirata, M. Nakajima, Y. Nomura, H. Tajima, Y. Matsushita, K. Asoh, Y. Kiuchi, A. G. Eguiluz, R. Arita, T. Suemoto and K. Ohgushi, Phys. Rev. Lett. **110** (2013) 187402(1-5).

5. Resonant X-ray Diffraction Study of the Strongly Spin-Orbit-Coupled Mott Insulator $CaIrO_3$: K. Ohgushi, J.-I. Yamaura, H. Ohsumi, K. Sugimoto, S. Takeshita, A. Tokuda, H. Takagi, M. Takata and T.-H. Arima, Phys. Rev. Lett. **110** (2013) 217212(1-5).

6. *Hydrostatic pressure (8GPa) dependence of electrical resistivity of $BaCo_2As_2$ single crystal: C. Ganguli, K. Matsubayashi, K. Ohgushi, Y. Uwatoko, M. Kanagaraj and S. Arumugam, Mat. Res. Bull. **48** (2013) 4329-4331.

7. †Suppression of Intersite Charge Transfer in Charge-Disproportionated Perovskite $YCu_3Fe_4O_{12}$: H. Etani, I. Yamada, K. Ohgushi, N. Hayashi, Y. Kusano, M. Mizumaki, J. Kim, N. Tsuji, R. Takahashi, N. Nishiyama, T. Inoue, T. Irifune and M. Takano, J. Am. Chem. Soc. **135** (2013) 6100-6106.

8. *5d 遷移金属パイロクロア酸化物における低温磁気構造の研究：山浦 淳一，大串 研也，広井 善二，日本結晶学会誌 **55** (2013) 116-120.

9. †Control of Bond-Strain-Induced Electronic Phase Transitions in Iron Perovskites: I. Yamada, H. Etani, K. Tsuchida, S. Marukawa, N. Hayashi, T. Kawakami, M. Mizumaki, K. Ohgushi, Y. Kusano, J. Kim, N. Tsuji, R. Takahashi, N. Nishiyama, T. Inoue, T. Irifune and M. Takano, Inorg. Chem. **52** (2013) 13751-13761.

10. †*B*-Site Deficiencies in *A*-site-Ordered Perovskite $LaCu_3Pt_{3.75}O_{12}$: M. Ochi, I. Yamada, K. Ohgushi, Y. Kusano, M. Mizumaki, R. Takahashi, S. Yagi, N. Nishiyama, T. Inoue and T. Irifune, Inorg. Chem. **52** (2013) 3985-3989.

11. †Pd^{2+}-Incorporated Perovskite $CaPd_3B_4O_{12}$(B = Ti, V): K. Shiro, I. Yamada, N. Ikeda, K. Ohgushi, M. Mizumaki, R. Takahashi, N. Nishiyama, T. Inoue and T. Irifune, Inorg. Chem. **52** (2013) 1604-1609.

12. Superconductivity in anti-post-perovskite vanadium compounds: B. Wang and K. Ohgushi, Sci. Rep. **3** (2013) 3381.

13. †NMR study of successive magnetic transitions in the A-site ordered perovskite $LaMn_3Cr_4O_{12}$: Y. Kawasaki, S. Takase, Y. Kishimoto, T. Ohno, I. Yamada, K. Shiro, R. Takahashi, K. Ohgushi, N. Nishiyama, T. Inoue and T. Irifune, J. Kor. Phys. Soc. **63** (2013) 640-643.

14. *High-pressure effects in anti-post-perovskite superconductors V_3PnN_x (Pn = P, As): B. S. Wang, J. -G. Cheng, K. Matsubayashi, Y. Uwatoko and K. Ohgushi, Phys. Rev. B **89** (2014) 144510 (1-4).

15. Magnetoelectric responses from the respective magnetic R and Fe subsystems in the noncentrosymmetric antiferromagnets $RFe_3(BO_3)_4$ (R = Eu, Gd, and Tb): T. Kurumaji, K. Ohgushi and Y. Tokura, Phys. Rev. B **89** (2014) 195126 (1-13).

* Joint research among groups within ISSP.

16. *Pseudogap formation above the superconducting dome in iron pnictides: T. Shimojima, T. Sonobe, W. Malaeb, K. Shinada, A. Chainani, S. Shin, T. Yoshida, S. Ideta, A. Fujimori, H. Kumigashira, K. Ono, Y. Nakashima, H. Anzai, M. Arita, A. Ino, H. Namatame, M. Taniguchi, M. Nakajima, S. Uchida, Y. Tomioka, T. Ito, K. Kihou, C. H. Lee, A. Iyo, H. Eisaki, K. Ohgushi, S. Kasahara, T. Terashima, H. Ikeda, T. Shibauchi, Y. Matsuda and K. Ishizaka, Phys. Rev. B **89** (2014) 045101(1-10).

17. $CaIrO_3$: a Spin-Orbit Mott Insulator Beyond the j_{eff} = 1/2 Ground State: M. Moretti Sala, K. Ohgushi, A. Al-Zein, Y. Hirata, G. Monaco and M. Krisch, Phys. Rev. Lett. **112** (2014) 176402.

18. ポストペロブスカイト型化合物 $CaIrO_3$ の磁気構造 : 大串 研也 , 大隅 寛幸 , 山浦 淳一 , 有馬 孝尚 , 日本結晶学会誌 **56** (2014) 36.

Division of Condensed Matter Theory

K. Ueda group

When a simple lattice is depleted in a periodic manner, electronic states of a tight binding model on such a depleted lattice sometimes shows a peculiar feature like a flat band or a Dirac cone. A typical example is the triangular lattice: the honeycomb lattice is obtained by the one third depletion and the kagome lattice by the one quarter depletion. In 2013, we concentrated on the quantum phase transitions of the Hubbard model on the one fifth depleted square lattice. This structure exists in nature in CaV4O9 and in some iron pnictide compound. At quarter filling the Dirac cone at the gamma point coincides with the Fermi energy and furthermore the Dirac cone touches with an almost flat band forming an SU(3) multiplet. We have shown that quantum phase transitions around the symmetric point is controlled by the SU(3) Dirac electrons. At half filling the effective theory in the strong coupling limit is a Heisenberg model which shows quantum phase transitions from the dimer singlet to the antiferromagnetic phase and further onto the plaquette singlet phase. Quantum phase transitions of the Hubbard model on this lattice have been investigated by using the cluster dynamical mean field theory.

1. SU(3) Dirac Electrons in the 1/5-Depleted Square-Lattice Hubbard Model at 1/4-Filling: Y. Yamashita, M. Tomura, Y. Yanagi and K. Ueda, Phys. Rev. B **88** (2013) 195104(1-7).

Takada group

Employing several techniques including the Green's-function approach, the density-matrix renormalization group, quantum Monte Carlo simulations, band-structure calculations, and several types of variational approaches, we are studying various aspects of quantum many-body problems in condensed matter physics, based mainly on the first-principles Hamiltonian. This year we have studied the following issues: (1) In order to better reproduce the electron-density profile obtained by the diffusion Monte Carlo method for the system of a single atom embedded in the electron gas with arbitrary densities, we have improved on the GGA-PBE version of the exchange-correlation energy functional in the density functional theory. In making this improvement, we have paid special attention to fulfilling the cusp theorem at the atom site. The improved functional will be applied to a wide range of topics in the future, including the phase diagram of the solid hydrogen under high pressures. (2) A further analysis is made for an electron-like elementally excitation (pseudoelectron) in the Luttinger liquid in competition with the spinon and holon excitations by using the powerful self-consistent numerical GWΓ scheme. (3) Mechanisms of superconductivity are considered in the low-density system in the framework of the ***kp*** perturbation theory with application to the n-type doped $SrTiO_3$. We have considered the effects of various issues such as the ferroelectric soft-phonon exchange, the plasmon contribution, the band multiplicity and the spin-orbit interaction.

1. 第 1 原理からの超伝導理論 : 高田 康民 , 物性研究 電子版 **Vol.3, No.1** (2013) 031203(1-29).

2. Structural evolution of the one-dimensional spectral function from the low- to the high-energy limit: H. Maebashi and Y. Takada, Phys. Rev. B **89** (2014) 201109(R) (1-5).

3. Theory for Reliable First-Principles Prediction of the Superconducting Transition Temperature: Y. Takada, in: *Carbon-based New Superconductors: Toward high-Tc superconductivity (ISBN 978-981-4303-30-9 (Hardcover), 978-981-4303-31-6 (eBook))*, Ch 8, edited by J. Haruyama, (Pan Stanford Publishing Pte. Ltd., 2014), 38page.

Oshikawa group

We studied a wide range of fundamental problems in condensed matter theory and statistical mechanics. In particular, we investigated the effects of quantum particle statistics on the ground-state energy. In the case of free particles, a ground state of bosons is given by a Bose-Einstein Condensation of all the particles into the lowest-energy single-particle state. In contrast, the ground

† Joint research with outside partners.

state of fermions is given by putting the particles to lowest-energy single-particle state, but with the restriction that no more than one particle can occupy an identical state (Pauli exclusion principle). Thus the ground-state energy for the identical Hamiltonian would be higher in the case of fermions, compared to the case of bosons. However, the comparison becomes not trivial when the particles are interacting. In fact, we established several examples in which the hard-core bosons have a higher ground-state energy than the corresponding fermions. We have also provided a novel understanding how the particle statistics affects the ground-state energy: Fermi statistics introduces a sort of frustration among hoppings of many particles. When there is no other frustration among hoppings, we proved that the bosons have a lower ground-state energy than the corresponding fermions, even in the presence of interactions. On the other hand, when frustration is introduced through phases of hopping amplitudes, the effects may partially cancel with each other, resulting in a reversal of the ground-state energy.

1. †Dimensional crossover in layered f-electron superlattices: Y. Tada, R. Peters and M. Oshikawa, Phys. Rev. B **88** (2013) 235121 (1-7).

2. †Electron spin resonance shifts in S=1 antiferromagnetic chains: S. C. Furuya, Y. Maeda and M. Oshikawa, Phys. Rev. B **87** (2013) 125122 (1-10).

3. †Entanglement spectra between coupled Tomonaga-Luttinger liquids: Applications to ladder systems and topological phases: R. Lundgren, Y. Fuji, S. Furukawa and M. Oshikawa, Phys. Rev. B **88** (2013) 245137 (1-14).

4. †Hole statistics and superfluid phases in quantum dimer models: C. A. Lamas, A. Ralko, M. Oshikawa, D. Poilblanc and P. Pujol, Phys. Rev. B **87** (2013) 104512(1-20).

5. †Response to a twist in systems with Z_p symmetry: The two-dimensional p-state clock model: Y. Kumano, K. Hukushima, Y. Tomita and M. Oshikawa, Phys. Rev. B **88** (2013) 104427 (1-6).

6. †Ground-State Energies of Spinless Free Fermions and Hard-Core Bosons: W. Nie, H. Katsura and M. Oshikawa, Phys. Rev. Lett. **111** (2013) 100402 (1-5).

7. †Quantum criticality in an asymmetric three-leg spin tube: A strong rung-coupling perspective: Y. Fuji, S. Nishimoto, H. Nakada and M. Oshikawa, Phys. Rev. B **89** (2014) 054425 (1-13).

8. †Valence bond distribution and correlation in bipartite Heisenberg antiferromagnets: D. Schwandt, F. Alet and M. Oshikawa, Phys. Rev. B **89** (2014) 104416 (1-14).

Tsunetsugu group

We have investigated novel phases of non-Kramers doublets realized in the heavy fermion compound $PrIr_2Zn_{20}$ and related materials. Non-Kramers doublet is a ground state of f^2 electron configuration protected by cubic symmetry of the crystalline field. Based on a microscopic model and an effective field theory, we have used symmetry arguments and mean-field approach to study possible symmetry breaking at low temperatures with and without magnetic field. We have found various antiferro quadrupole ordered phases depending on the magnetic field direction. The most important ingredient is the presence of a unique Z_3 anisotropy in the order parameter space, and in particular, the zero-field order corresponds to the spontaneous breaking of $Z_3 \times Z_2$ symmetry. This also results in unusual divergence of quadrupole susceptibility in several channels near the critical point. This may be related to observed singularity in ultrasound measurements. We have also numerically studied doublon dynamics near the Mott metal-insulator transition. It has been long believed that the Mott transition is a binding-unbinding transition of doublons and holons, but this point has been directly examined only by equal-time correlations. We have performed large-scale computations of cluster dynamical mean-field theory for the half-filled Hubbard model on the triangular lattice, and calculated dynamical correlations of doublons and holons on the same site and also between nearest-neighbor sites. The results show drastic changes in their dynamics between the metallic and insulating phases. In particular, the doublon-holon pair correlation shows fluctuations up to a very long time in the metallic phase, while the correlation decays very quickly in the insulating phase. This supports the binding-unbinding transition picture of the Mott transition. (Reference: Toshihiro Sato and Hirokazu Tsunetsugu, arXiv:1404.6598) Quantum impurities coupled to Tomonaga-Luttinger liquids are interesting physical systems including an impurity in quantum wire, a spin coupled to a two-dimensional topological insulator etc. We have developed a new method of quantum Monte Carlo simulation with continuous time formulation. This is base on the duality between electrons and bosons, and this results in the advantage of negative sign free nature. The new method is applied to various problems and scaling properties of correlation functions are examined. (Reference: K. Hattori and A. Rosch, arXiv: 1405.3300)

1. Continuous-Time Quantum Monte Carlo Approach for Impurity Anderson Models with Phonon-Assisted Hybridizations: K. Hattori, J. Phys. Soc. Jpn. **82** (2013) 064709 (5 pages).

2. Exotic disordered phases in the quantum J1-J2 model on the honeycomb lattice: H. Zhang and C. A. Lamas, Phys. Rev. B **87** (2013) 024415 (10 pages).

3. p-wave superconductivity near a transverse saturation field: K. Hattori and H. Tsunetsugu, Phys. Rev. B **87** (2013) 064501 (5 pages).

---

* Joint research among groups within ISSP.

4. Antiferro Quadrupole Orders in Non-Kramers Doublet Systems: K. Hattori and H. Tsunetsugu, J. Phys. Soc. Jpn. **83** (2014) 034709 (19 pages).

Kohmoto group

Energy versus magnetic field (Hofstadter butterfly diagram) in twisted bilayer graphene is studied theoretically. If we take the usual Landau gauge, we cannot take a finite periodicity even when the magnetic flux through a supercell is a rational number. We show that the periodic Landau gauge, which has the periodicity in one direction, makes it possible to obtain the Hofstadter butterfly diagram. Since a supercell can be large, magnetic flux through a supercell normalized by the flux quantum can be a fractional number with a small denominator, even when a magnetic field is not extremely strong. As a result, quantized Hall conductance can be a solution of the Diophantine equation which cannot be obtained by the approximation of the linearized energy dispersion near the Dirac points.

1. †Periodic Landau gauge and quantum Hall effect in twisted bilayer graphene: Y. Hasegawa and M. Kohmoto, Phys. Rev. B **88** (2013) 125426(1-8).

2. †The Spectral Shift Function and the Friedel Sum Rule: M. Kohmoto, T. Koma and S. Nakamura, Ann. Henri Poincaré **14** (2013) 1413-1424.

Sugino group

We have advanced the first-principles molecular dynamics approach to the electrochemical interfaces. This was done by improving the effective screening medium (ESM) method. With the method, new results was obtained regarding the planar and particle catalysts and the mechanism of the reactions. We have continued to develop a many-body Green's function approach to the spectroscopy and began to obtain promising results. Progress has been made on the tensor network approach to obtain accurate density matrix of molecules.

1. Improved modeling of electrified interfaces using the effective screening medium method: I. Hamada, O. Sugino, N. Bonnet and M. Otani, Phys. Rev. B **88** (2013) 155427.

2. Nonadiabatic couplings from time-dependent density functional theory: Formulation by the Kohn-Sham derivative matrix within density functional perturbation theory: C. Hu, T. Tsukagoshi, O. Sugino and K. Watanabe, Phys. Rev. B **87** (2013) 035421(1-7).

3. Reply to “Comment on ‘Nonadiabatic couplings from the Kohn-Sham derivative matrix: Formulation by time-dependent density-functional theory and evaluation in the pseudopotential framework’”: C. Hu, O. Sugino, H. Hirai and Y. Tateyama, Phys. Rev. A **88** (2013) 056502.

4. First-Principles Investigation on Structural and Optical Properties of $M^+@C_{60}$ (Where M = H, Li, Na, and K): Y. Noguchi, O. Sugino, H. Okada and Y. Matsuo, J. Phys. Chem. C **117** (2013) 15362.

5. 白金電極上における水素発生反応の第一原理的理解に向けて : I. Hamada and O. Sugino, J. Surf. Sci. Soc. Jpn. **34** (2013) 638.

6. Microscopic understanding of the electrochemical interfaces: O. Sugino, AIP Conf. Proc. **1568** (2013) 43.

7. Electronic structures of oxygen-deficient Ta_2O_5: Y. Yang, H.-H. Nahm, O. Sugino and T. Ohno, AIP Advances **3** (2013) 042101(1-8).

8. Effect of thermal motion on catalytic activity of nanoparticles in polar solvent: N. Bonnet, O. Sugino and M. Otani, J. Chem. Phys. **140** (2014) 044703.

9. Performance of Tamm-Dancoff approximation on nonadiabatic couplings by time-dependent density functional theory: C. Hu, O. Sugino and K. Watanabe, J. Chem. Phys. **140** (2014) 054106.

10. First-principles thermodynamic description of hydrogen electroadsorption on the Pt(111) surface: T. T. T. Hanh, Y. Takimoto and O. Sugino, Surf. Sci. **625** (2014) 104.

Kato group

The main research subject in our laboratory is theory of nonequilibrium properties in nanoscale devices. We have performed (1) evaluation of coherence in single-photon and single-electron generation quantum, (2) exact calculation of transport properties in the Anderson impurity at high bias voltages, and (3) Kondo-like phenomena in heat transport through a local two-state system.

† Joint research with outside partners.

1. Properties of a Single Photon Generated by a Solid-State Emitter: Effects of Pure Dephasing: E. Iyoda, T. Kato, T. Aoki, K. Edamatsu and K. Koshino, J. Phys. Soc. Jpn. **82** (2013) 014301(1-10).

2. Relaxor Behavior and Morphotropic Phase Boundary in a Simple Model: Y. Tomita and T. Kato, J. Phys. Soc. Jpn. **82** (2013) 063002(1-5).

3. Exact interacting Green's function for the Anderson impurity at high bias voltages: A. Oguri and R. Sakano, Phys. Rev. B **88** (2013) 155424(1-12).

4. *Experimental Verification of Comparability between Spin-Orbit and Spin-Diffusion Lengths: Y. Niimi, D. Wei, H. Idzuchi, T. Wakamura, T. Kato and Y. Otani, Phys. Rev. Lett. **110** (2013) 016805.

5. Kondo Signature in Heat Transfer via a Local Two-State System: K. Saito and T. Kato, Phys. Rev. Lett. **111** (2013) 214301(1-5).

6. 1/(N − 1) expansion approach to full-counting statistics for the SU(N) Anderson model: A. Oguri and R. Sakano, J. Kor. Phys. Soc. **63** (2013) 423-427.

7. Dephasing in single-electron generation due to environmental noise probed by Hong-Ou-Mandel interferometry: E. Iyoda, T. Kato, K. Koshino and T. Martin, Phys. Rev. B **89** (2014) 205318(1-8).

8. メゾスコピック系の物理―基礎から最近の話題まで―（第 58 回物性若手夏の学校 : 講義）: 加藤 岳生 , 物性研究・電子版 **3** (2014) 031201(1-26).

Division of Nanoscale Science

Iye group

Thermoelectric effect and high frequency conduction in GaAs/AlGaAs 2DEG subjected to periodic potential modulation (lateral superlattice) has been investigated. Commensurability oscillation in thermoelectric power is observed in one-dimensional lateral superlattice sample. AC conductivity in the quantum Hall plateau region of a hexagonal lateral superlattice sample exhibits a few characteristic resonance peaks.

1. *Control of magnetic anisotropy in (Ga,Mn)As with etching depth of specimen boundaries: Y. Hashimoto, Y. Iye and S. Katsumoto, J. Cryst. Growth **378** (2013) 381.

2. *Suppression of Andreev current due to transverse current flow in an InAs two-dimensional electrons: Y. Takahashi, Y. Hashimoto, Y. Iye and S. Katsumoto, J. Cryst. Growth **378** (2013) 400.

3. *Spin Hall reduction of Josephson effect in InAs two-dimensional electrons: T. Nakamura, Y. Takahashi, Y. Hashimoto, D. H. Yun, S. W. Kim, Y. Iye and S. Katsumoto, Phys. Status Solidi C **10** (2013) 1473.

4. Commensurability oscillations in the rf conductivity of unidirectional lateral superlattices: measurement of anisotropic conductivity by coplanar waveguide: A. Endo, T. Kajioka and Y. Iye, J. Phys. Soc. Jpn **82** (2013) 054710(1-7).

5. Diffusion Thermopower of Quantum Hall States Measured in Corbino Geometry: S. Kobayakawa, A. Endo and Y. Iye, J. Phys. Soc. Jpn **82** (2013) 053702(1-4).

6. *Mechanical modification of magnetic anisotropy in (Ga,Mn)As: Y. Hashimoto, Y. Iye and S. Katsumoto, in: *AIP Conference Proceedings "International Conference on Physics of Semiconductors"*, edited by T. Ihn (AIP, 2013), 347.

Katsumoto group

The two-electron tunneling process to a side-coupled quantum dot has been applied to detect spin polarization in the target device. The method is most powerful among so far developed and the device voltage dependence can be measured. We have revealed that the polarization mechanism at so called 0.5 plateau is the Stern-Gelach type spin-filter while that at 1.0 plateau is the spin rotation predicted a decade ago.

1. Robustness of spin filtering against current leakage in a Rashba-Dresselhaus-Aharonov-Bohm interferometer: S. Matityahu, A. Aharony, O. Entin-Wohlman and S. Katsumoto, Phys. Rev. B **87** (2013) 205438(1-8).

2. †*Adiabatic measurements of magneto-caloric effects in pulsed high magnetic fields up to 55 T: T. Kihara, Y. Kohama, Y. Hashimoto, S. Katsumoto and M. Tokunaga, Rev. Sci. Instrum. **84** (2013) 074901(1-7).

* Joint research among groups within ISSP.

3. *Control of magnetic anisotropy in (Ga,Mn)As with etching depth of specimen boundaries: Y. Hashimoto, Y. Iye and S. Katsumoto, J. Cryst. Growth **378** (2013) 381.

4. *Suppression of Andreev current due to transverse current flow in an InAs two-dimensional electrons: Y. Takahashi, Y. Hashimoto, Y. Iye and S. Katsumoto, J. Cryst. Growth **378** (2013) 400.

5. *Spin Hall reduction of Josephson effect in InAs two-dimensional electrons: T. Nakamura, Y. Takahashi, Y. Hashimoto, D. H. Yun, S. W. Kim, Y. Iye and S. Katsumoto, Phys. Status Solidi C **10** (2013) 1473.

6. *Heat-pulse measurements of specific heat in 36 ms pulsed magnetic fields: Y. Kohama, Y. Hashimoto, S. Katsumoto, M. Tokunaga and K. Kindo, Meas. Sci. Technol. **24** (2013) 115005(1-9).

7. Effect of transverse current on Andreev bound state: Y. Takahashi, Y. Hashimoto, D. H. Yun, S. W. Kim, T. Nakamura, Y. Iye and S. Katsumoto, in: *AIP Conference Proceedings, "International Conference on Physics of Semiconductors"*, edited by T. Ihn (AIP, 2013), 345.

8. *Mechanical modification of magnetic anisotropy in (Ga,Mn)As: Y. Hashimoto, Y. Iye and S. Katsumoto, in: *AIP Conference Proceedings "International Conference on Physics of Semiconductors"*, edited by T. Ihn (AIP, 2013), 347.

9. 量子の匠 : 勝本 信吾 , (丸善 , 東京 , 2014).

Otani group

We have studied on three topics including spin Hall effect, spin diffusion length, and magnonic crystals. Firstly we have applied our non-local spin injection technique to 5d iridium oxide, and succeeded in detecting a very large inverse spin Hall resistivity at room temperature which guarantees this material as a good spin current detector. Secondly we experimentally confirmed that weak antilocalization measurements can be employed as a complementary method for determining the spin diffusion lengths of noble metals. Thirdly in collaboration with Indian group lead by Prof. Barman in Bose Center Kolkata, we have performed all-optical time-resolved magneto-optical Kerr microscope measurements and found that the anisotropic propagation of spin waves are tunable by arranging different symmetries in the form of artificial ferromagnetic nanodot lattices. The observations are important for further development in magnonic crystal based devices.

1. *Experimental Verification of Comparability between Spin-Orbit and Spin-Diffusion Lengths: Y. Niimi, D. Wei, H. Idzuchi, T. Wakamura, T. Kato and Y. Otani, Phys. Rev. Lett. **110** (2013) 016805.

2. Configurational anisotropic spin waves in cross-shaped $Ni_{80}Fe_{20}$ nanoelements: B. K. Mahato, B. Rana, R. Mandal, D. Kumar, S. Barman, Y. Fukuma, Y. Otani and A. Barman, Appl. Phys. Lett. **102** (2013) 192402.

3. Impact of interface properties on spin accumulation in dual-injection lateral spin valves: H. Idzuchi, S. Karube, Y. Fukuma, T. Aoki and Y. Otani, Appl. Phys. Lett. **103** (2013) 162403.

4. Spin injection properties in trilayer graphene lateral spin valves: Y. P. Liu, H. Idzuchi, Y. Fukuma, O. Rousseau, Y. Otani and W. S. Lew, Appl. Phys. Lett. **102** (2013) 033105.

5. Tunable Magnonic Spectra in Two-Dimensional Magnonic Crystals with Variable Lattice Symmetry: S. Saha, R. Mandal, S. Barman, D. Kumar, B. Rana, Y. Fukuma, S. Sugimoto, Y. Otani and A. Barman, Adv. Funct. Mater. **23** (2013) 2378.

6. 5d iridium oxide as a material for spin-current detection: K. Fujiwara, Y. Fukuma, J. Matsuno, H. Idzuchi, Y. Niimi, Y. Otani and H. Takagi, Nat. Commun. **4** (2013) 3893.

7. Propagation of nonlinearly generated harmonic spin waves in microscopic stripes: O. Rousseau, M. Yamada, K. Miura, S. Ogawa and Y. Otani, J. Appl. Phys. **115** (2014) 053914.

8. Effect of anisotropic spin absorption on the Hanle effect in lateral spin valves: H. Idzuchi, Y. Fukuma, S. Takahashi, S. Maekawa and Y. Otani, Phys. Rev. B **89** (2014) 081308(R).

9. Extrinsic spin Hall effects measured with lateral spin valve structures: Y. Niimi, H. Suzuki, Y. Kawanishi, Y. Omori, T. Valet, A. Fert and Y. Otani, Phys. Rev. B **89** (2014) 054401.

10. Spin Injection into a Superconductor with Strong Spin-Orbit Coupling: T. Wakamura, N. Hasegawa, K. Ohnishi, Y. Niimi and Y. Otani, Phys. Rev. Lett. **112** (2014) 036602.

† Joint research with outside partners.

Komori group

Electronic structures of Pt-induced nanowires on the Ge(001) surface were studied by ARPES. Two one-dimensional (1D) metallic surface bands are clearly identified at temperatures much lower than its structural transition temperature. This 1D system exhibits neither Peierls instability nor Luttinger liquid behaviors. The elastic-scattering vectors within the topological surface state (TSS) of a topological insulator $Bi_{1.5}Sb_{0.5}Te_{1.7}Se_{1.3}$ were studied using quasiparticle interference patterns measured by STM. The results are compared by the surface band obtained using time-resolved ARPES. The scattering in the TSS is effectively prohibited in a wide angular range of 100-180°.

1. Selective doping in a surface band and atomic structures of the Ge(111) ($\sqrt{3} \times \sqrt{3}$) R30°–Au surface: K. Nakatsuji, Y. Motomura, R. Niikura and F. Komori, J. Phys.: Condens. Matter **25** (2013) 045007 (9).

2. Fabrication and characterization of strain-driven self-assembled CrN nanoislands on Cu(001): P. Krukowski, T. Iimori, K. Nakatsuji, M. Yamada and F. Komori, J. Appl. Phys. **113** (2013) 174309 (5).

3. *Fermi gas behavior of a one-dimensional metallic band of Pt-induced nanowires on Ge(001): K. Yaji, I. Mochizuki, S. Kim, Y. Takeichi, A. Harasawa, Y. Ohtsubo, P. Le Fevre, F. Bertran, A. Taleb-Ibrahimi, A. Kakizaki and F. Komori, Phys. Rev. B **87** (2013) 241413R (5).

4. †Graphene nanoribbons on vicinal SiC surfaces by molecular beam epitaxy: T. Kajiwara, Y. Nakamori, A. Visikovskiy, T. Iimori, F. Komori, K. Nakatsuji, K. Mase and S. Tanaka, Phys. Rev. B **87** (2013) 121407R (1-4).

5. Growth and structure of CrN nanoislands on Cu(001) studied by scanning tunneling microscopy and X-ray photoemission spectroscopy: P. Krukowski, T. Iimori, K. Nakatsuji, M. Yamada and F. Komori, Thin Solid Films **531** (2013) 251-254.

6. †Systematic study of surface magnetism in Si(111)-Fe system grown by solid phase epitaxy: In situ schematic magnetic phase diagram of Si(111)-Fe: A. N. Hattori, K. Hattori, K. Kataoka, E. Takematsu, A. Ishii, F. Komori and H. Daimon, J. Magn. Magn. Mater. **363** (2014) 158-165.

7. *Robust Protection from Backscattering in the Topological Insulator $Bi_{1.5}Sb_{0.5}Te_{1.7}Se_{1.3}$: S. Kim, S. Yoshizawa, Y. Ishida, K. Eto, K. Segawa, Y. Ando, S. Shin and F. Komori, Phys. Rev. Lett. **112** (2014) 136802(1-5).

8. *Observing hot carrier distribution in an n-type epitaxial graphene on a SiC substrate: T. Someya, H. Fukidome, Y. Ishida, R. Yoshida, T. Iimori, R. Yukawa, K. Akikubo, Sh. Yamamoto, S. Yamamoto, T. Yamamoto, T. Kanai, K. Funakubo, M. Suemitsu, J. Itatani, F. Komori, S. Shin and I. Matsuda, Appl. Phys. Lett. **104** (2014) 161103(1-4).

9. †*Scanning tunneling microscopic and spectroscopic studies on a crystalline silica monolayer epitaxially formed on hexagonal SiC(000-1) surfaces: H. Tochihara, T. Shirasawa, T. Suzuki, T. Miyamachi, T. Kajiwara, K. Yagyu, S. Yoshizawa, T. Takahashi, S. Tanaka and F. Komori, Appl. Phys. Lett. **104** (2014) 051601(1-4).

10. エピタキシャルグラフェンの電子状態：中辻 寛，小森 文夫，「ポストシリコン半導体 - ナノ成膜ダイナミクスと基板・界面効果 -」，６章２．２，財満　鎮明，(NTS, 東京都文京区湯島 2-16-16, 2013), 334-345.

Yoshinobu group

We conducted several research projects in the fiscal year 2013. (1) The adsorption and activation of CO_2 on Cu(997) studied by SR-PES and IRAS. (2) The adsorption and decomposition of formic acid on Cu(111) studied by SR-PES and IRAS. (3) Spectroscopic characterization and transport properties of the Si(111) native oxide surface with tetrafluorotetracyanoquinodimethane. (4) Electronic structure of alufa-sexithiophene ultra thin films grown on passivated Si(001) surfaces.

1. Energy level alignment of cyclohexane on Rh(111): the importance of interfacial dipole and final-state screening: T. Koitaya, K. Mukai, S. Yoshimoto and J. Yoshinobu, J. Chem. Phys. **138** (2013) 044702 (9 pages).

2. 巻頭言「君たちは何のために研究するのか？」：吉信 淳，表面科学 **34** (2013) 403.

3. Site-specific chemical states of adsorbed CO on Pt(997): a high resolution XPS study: S. Shimizu, H. Noritake, T. Koitaya, K. Mukai, S. Yoshimoto and J. Yoshinobu, Surf. Sci. **608** (2013) 220-225.

4. Spectroscopic Characterization and Transport Properties of Aromatic Monolayers Covalently Attached to Si(111) Surfaces: Y. Harada, T. Koitaya, K. Mukai, S. Yoshimoto and J. Yoshinobu, J. Phys. Chem. C **117** (2013) 7497-7505.

5. Quantitative analysis of chemical interaction and doping of the Si(111) native oxide surface with tetrafluorotetracyanoquinodimethane: S. Yoshimoto, M. Furuhashi, T. Koitaya, Y. Shiozawa, K. Fujimaki, Y. Harada, K. Mukai and J. Yoshinobu, J. Appl. Phys. **115** (2014) 143709.

---

* Joint research among groups within ISSP.

6. †Electronic structure of α-sexithiophene ultrathin films grown on passivated Si(001) surfaces: K. Hiraga, H. Toyoshima, H. Tanaka, K. Inoue, S. Ohno, K. Mukai, J. Yoshinobu and M. Tanaka, Appl. Surf. Sci. **307** (2014) 520.

7. Aqueous-Phase Oxidation of Epitaxial Graphene on the Silicon Face of SiC(0001): Md. Zakir Hossain, M. B. A. Razak, S. Yoshimoto, K. Mukai, T. Koitaya, J. Yoshinobu, H. Sone, S. Hosaka and M. C. Hersam, J. Phys. Chem. C **118** (2014) 1014.

8. Structure and Photo-Induced Charge Transfer of Pyridine Molecules Adsorbed on TiO_2(110): A NEXAFS and Core-Hole-Clock Study: H. Kondoh, Y. Higashi, M. Yoshida, Y. Monya, R. Toyoshima, K. Mase, K. Amemiya, F. Tsukioka, M. Nagasaka, Y. Iwasawa, H. Orita, K. Mukai and J. Yoshinobu, Electrochemistry **82** (2014) 341.

9. Interface state and energy level alignment of F_4-TCNQ sandwiched between a pentacene film and the ethylene-terminated Si(100) surface: S. Yoshimoto, K. Kameshima, T. Koitaya, Y. Harada, K. Mukai and J. Yoshinobu, Organic Electronics **15** (2014) 356.

10. 淡青評論「東京大学憲章を読んでみませんか」：吉信 淳 , 学内広報 **1450** (2014) 12.

11. 「現代ケイ素化学 - 体系的な基礎概念と応用に向けて」のうち第 24 章「ケイ素単結晶表面の修飾」(p.377-p.388)．：吉良 満夫 , 玉尾皓平 (編集), 吉信淳（部分執筆）, (化学同人 , 京都市 , 2013).

12. 絶対微小　日常生活を量子論で理解する： マイケ ル・D・フェイヤー著 , 丑田 公規 , 吉信淳 訳 , (化学同人 , Kyoto, 2013).

13. 「水素の事典」のうち 5 章 1-a（p.86-p.89）を分担執筆．：水素エ ネルギー協会編 , (朝倉書店 , 東京 , 2014).

Hasegawa group

We studied the superconducting proximity effect in real space by using low-temperature scanning tunneling microscopy and spectroscopy aiming at the observation of peculiar superconducting states, such as Fulde–Ferrell–Larkin–Ovchinnikov (FFLO) states and odd-frequency superconductivity. So far, we observed the spatial distribution of superconductivity around an interface between Pb islands and a two-dimensional (2D) diffusive normal metal, and found that the surface steps in the 2D normal metal working as a potential barrier exhibit a significant role on the proximity effect; through the real-space mapping of superconductivity in nano-meter spatial resolution, we observed the steps blocking the propagation of the proximity and enhancing it in confined area between the steps and the super/normal interface. The enhancement is explained with reflectionless tunneling, quantum interference phenomenon between the incident electrons and retro-reflected holes formed by the Andreev reflection at the interface. On a 2D surface superconductor, which can be formed by depositing 1 monolayer In or Pb on Si(111) substrate, we also observed Josephson vortices at the step edges, indicating weakened superconductivity there.

1. Trapping and squeezing of vortices in voids directly observed by scanning tunneling microscopy and spectroscopy: T. Tominaga, T. Sakamoto, H. Kim, T. Nishio, T. Eguchi and Y. Hasegawa, Phys. Rev. B **87** (2013) 195434.

2. †Microscopic origin of the π states in epitaxial silicene: A. Fleurence, Y. Yoshida, C. -C. Lee, T. Ozaki, Y. Yamada-Takamura and Y. Hasegawa, Appl. Phys. Lett. **104** (2014) 021605 (4 pages).

Lippmaa group

High-temperature growth studies of magnetite Fe_3O_4 showed that it is possible to fabricate self-organized arrays of strain-free and uniformly oriented nanoscale pyramids. We hope to use such nanopyramid arrays for studying the multiferroic coupling in magnetite. Nanoscale composite materials based on a ferromagnetic spinel, $CoFe_2O_4$ and a ferroelectric perovskite, $Bi_5Ti_3FeO_{15}$ were characterized in collaboration with our joint-use partners. Saturation magnetism and spin dilution was studied in $Pr_{0.8}Ca_{0.2}MnO_3$ to develop a suitably weak ferromagnet for use in superconductor - ferromagnet tunnel junctions. Work proceeded on the development of light-element oxide films with the mapping of the growth mechanisms of BeO.

1. Nonmagnetic Sc Substitution in a Perovskite Ferromagnetic Insulator $Pr_{0.8}Ca_{0.2}MnO_3$: T. Harada, R. Takahashi and M. Lippmaa, J. Phys. Soc. Jpn. **82** (2013) 014801(1-5).

2. Spectroscopic studies on the electronic and magnetic states of Co-doped perovskite manganite $Pr_{0.8}Ca_{0.2}Mn_{1-y}Co_yO_3$ thin films: K. Yoshimatsu, H. Wadati, E. Sakai, T. Harada, Y. Takahashi, T. Harano, G. Shibata, K. Ishigami, T. Kadono, T. Koide, T. Sugiyama, E. Ikenaga, H. Kumigashira, M. Lippmaa, M. Oshima and A. Fujimori, Phys. Rev. B **88** (2013) 174423.

3. Epitaxial $Bi_5Ti_3FeO_{15}$–$CoFe_2O_4$ Pillar–Matrix Multiferroic Nanostructures: A. Imai, X. Cheng, H. L. Xin, E. A. Eliseev, A. N. Morozovska, S. V. Kalinin, R. Takahashi, M. Lippmaa, Y. Matsumoto and V. Nagarajan, ACS Nano **7** (2013) 11079-11086.

† Joint research with outside partners.

4. Pulsed laser deposition of epitaxial BeO thin films on sapphire and $SrTiO_3$: T. Peltier, R. Takahashi and M. Lippmaa, Appl. Phys. Lett. **104** (2014) 231608(1-4).

5. Spontaneous Growth of Strain-Free Magnetite Nanocrystals via Temperature-Driven Dewetting: R. Takahashi, H. Misumi, T. Yamamoto and M. Lippmaa, Crystal Growth & Design **14** (2014) 1264-1271.

6. Combinatorial Nanoscience and Technology for Solid-state Materials: H. Koinuma, R. Takahashi, M. Lippmaa, S.-Y. Jeong, Y. Matsumoto, T. Chikyo and S. Suzuki, in: *Handbook of Advanced Ceramics*, Ch 11.1.11, edited by S. Somiya, (Academic Press, Amsterdam, 2013), 1103-1124.

Division of Physics in Extreme Conditions

Uwatoko group

The present antiferromagnetic state T_N=7.5 K of $EuBi_3$ with the $AuCu_3$-type cubic structure is found to be stable under pressures up to 8 GPa, where the Neel temperature increases with increasing pressure, being T_N=16.5 K at 8 GPa. We have studied the effect of pressure on the superconducting transition temperature of YFe_4P_{12} and $LaFe_4P_{12}$ up to 8 GPa through electrical resistivity measurements in a cubic anvil apparatus. T_{SC} of both compounds increase to 9.3 K and 8.0 K with increasing pressure, but the slopes decreases gradually with increasing pressure, respectivily. In contrast, the T_{SC} of YRu_4P_{12} and $LaRu_4P_{12}$ monotonically decreases with pressure. The distinct pressure dependences of both T_{SC} cannot be explained solely from a structural point of view. The pressure dependence of the electrical resistivity of $BaCo_2As_2$ single crystal as a function of temperature was measured up to 8 GPa. A hybrid-type piston-cylinder pressure cell for the electron spin resonance (ESR) measurement has been developed that the pressure reaches 2.1 GPa. The cylinder of this pressure cell consists of a NiCrAl inner cylinder and a CuBe outer sleeve, and all inner parts are made of zirconium oxide which has good transmittance to the millimeter and submillimeter waves. We have also developed a transmission-type high-field ESR system having two different modulation methods for this pressure cell.

1. †AC Susceptibility of the Dipolar Spin Ice $Dy_2Ti_2O_7$: Experiments and Monte Carlo Simulations: H. Takatsu, K. Goto, H. Otsuka, R. Higashinaka, K. Matsubayashi, Y. Uwaoko and H. Kadowaki, J. Phys. Soc. Jpn. **82** (2013) 104710(1-5).

2. Change in Unusual Magnetic Properties by Rh Substitution in $CeRu_2Al_{10}$: R. Kobayashi, Y. Ogane, D. Hirai, T. Nishioka, M. Matsumura, Y. Kawamura, K. Matsubayashi, Y. Uwatoko, H. Tanida and M. Sera, J. Phys. Soc. Jpn. **82** (2013) 093702(1-5).

3. †Fermi Surface and Magnetic Properties of Antiferromagnet $EuBi_3$: A. Nakamura, Y. Hiranaka, M. Hedo, T. Nakama, Y. Tatetsu, T. Maehira, Y. Miura, A. Mori, H. Tsutsumi, Y. Hirose, K. Mitamura, K. Sugiyama, M. Hagiwara, F. Honda, T. Takeuchi, Y. Haga, K. Matsubayashi, Y. Uwatoko and Y. Onuki, J. Phys. Soc. Jpn. **82** (2013) 124708(1-6).

4. †Magnetic and Fermi Surface Properties of $EuGa_4$: A. Nakamura, Y. Hiranaka, M. Hedo, T. Nakama, Y. Miura, H. Tsutsumi, A. Mori, K. Ishida, K. Mitamura, Y. Hirose, K. Sugiyama, F. Homda, R. Settai, T. Takeuchi, M. Hagiwara, T. D. Matsuda, E. Yamamoto, Y. Haga, K. Matsubayashi, Y. Uwatoko, H. Harima and Y. Onuki, J. Phys. Soc. Jpn. **82** (2013) 104703 (1-10).

5. Microscopic Evidence of a Crossover to a Low-Temperature Intermediate Valence State in $YbCo_2Zn_{20}$: T. Mito, H. Hara, T. Ishida, K. Nakagawara, T. Koyama, K. Ueda, T. Kohara, K. Ishida, K. Matsubayashi, Y. Saiga and Y. Uwatoko, J. Phys. Soc. Jpn. **82** (2013) 103704 (1-4).

6. †Pressure and Substitution Effects on Transport and Magnetic Properties of $Y_{1-x}R_xCo_2$ Systems with Static Magnetic Disorder: M. Takeda, A. Teruya, S. Watanabe, S. Hirakawa, Y. Hiranaka, A. Nakamura, Y. Takaesu, K. Uchima, M. Hedo, T. Nakama, K. Yagasaki, K. Matsubayashi, Y. Uwatoko and A. T. Burkov, J. Phys. Soc. Jpn. **82** (2013) 014708 (1-6).

7. †Two-Dimensional Monopole Dynamics in the Dipolar Spin Ice $Dy_2Ti_2O_7$: H. Takatau, K. Goto, H. Otsuka, R. Higashinaka, K. Matsubayashi, Y. Uwatoko and H. Kadowaki, J. Phys. Soc. Jpn. **82** (2013) 073707(1-5).

8. †Magnetic properties of spinel $CuCrZrS_4$ under pressure: M. Ito, N. Kado, K. Matsubayashi, Y. Uwatoko, N. Terada, S. Ebisu and S. Nagata, J. Magn. Magn. Mater. **331** (2013) 98-101.

9. Dielectric properties of single crystal spinels in the series FeV_2O_4, MnV_2O_4, and CoV_2O_4 in high magnetic fields: A. Kismarahadja, J. S. Brooks, H. D. Zhou, E. S. Choi, K. Matsubayashi and Y. Uwatoko, Phys. Rev. B **87** (2013) 054432 (1-10).

* Joint research among groups within ISSP.

10. High-pressure synthesis of the $BaIrO_3$ perovskite: A Pauli paramagnetic metal with a Fermi liquid ground state: J. G. Cheng, T. Ishii, H. Kojitani, K. Matsubayashi, A. Matsuo, X. Li, Y. Shirako, J. S. Zhou, J. B. Goodenough, C. Q. Jin, M. Akaogi and Y. Uwatoko, Phys. Rev. B **88** (2013) 205114(1-7).

11. Pressure dependence of the superconducting transition temperature of the filled skutterudite YFe_4P_{12}: J. G. Cheng, J. S. Jhou, K. Matsubayashi, P. P. Kong, Y. Kubo, Y. Kawamura, C. Sekine, C. Q. Jin, J. B. Goodenough and Y. Uwatoko, Phys. Rev. B **88** (2013) 024514(1-8).

12. [†]Development of a Low-Temperature Insert for Precise Magnetization Measurement below T = 2 K with a Superconducting Quantum Interference Device Magnetometer: Y. Sato, S. Makiyama, Y. Sakamoto, T. Hasuo, Y. Inagaki, T. Fujiwara, H. S. Suzuki, K. Matsubayashi, Y. Uwatoko and T. Kawae, Jpn. J. Appl. Phys. **52** (2013) 106702 (1-6).

13. Possible Kondo Physics near a Metal-Insulator Crossover in the A-Site Ordered Perovskite $CaCu_3Ir_4O_{12}$: J. G. Cheng, J. S. Zhou, Y. F. Yang, H. D. Zhou, K. Matsubayashi, Y. Uwatoko, A. MacDonald and J. B. Goodnough, Phys. Rev. Lett. **111** (2013) 176403(1-5).

14. [†*]High Field Magnetization of $TbPd_2Ge_2$ Single Crystal: T. Shigeoka, T. Hasegawa, T. Fujiwara, A. Kondo, K. Kindo and Y. Uwatoko, J. Low Temp. Phys. **170** (2013) 248-254.

15. [†]Magnetic penetration depth and flux-flow resistivity measurements on $NaFe_{0.97}Co_{0.03}As$ single crystals: T. Okada, H. Takahashi, Y. Imai, K. Kitagawa, K. Matsubayashi, Y. Uwatoko and A. Maeda, Physica C **494** (2013) 109-112.

16. [*]Hydrostatic pressure (8GPa) dependence of electrical resistivity of $BaCo_2As_2$ single crystal: C. Ganguli, K. Matsubayashi, K. Ohgushi, Y. Uwatoko, M. Kanagaraj and S. Arumugam, Mat. Res. Bull. **48** (2013) 4329-4331.

17. [†]Magnetic and Structural Properties of $Mn_{1.8}Co_{0.2}Sb$ under High Magnetic Fields: H. Orihashi, M. Hiroi, Y. Mitsui, K. Takahashi, K. Watanabe, K. Matsubayashi, Y. Uwatoko and K. Koyama, Mater. Trans. **54** (2013) 969-973.

18. [†]Low energy excitations inside the vortex core of LiFe(As, P) single crystals investigated by microwave-surface impedance: T. Okada, H. Takahashi, Y. Imai, K. Kitagawa, K. Matsubayashi, Y. Uwatoko and A. Maeda, Physica C: Superconductivity **484** (2013) 27.

19. [†]Development of Hybrid-Type Pressure Cell for High-Pressure and High-Field ESR Measurement: K. Fujimoto, T. Sakurai, S. Okubo, H. Ohta, K. Matsubayashi, Y. Uwatoko and Y. Koike, Applied Magnetic Resonance **44** (2013) 893-898.

20. [†]Magnetic properties of $Mn_2Sb_{1-x}Ge_x(0.05 \leq \ \leq 0.2)$ in high magnetic fields: D. Shimada, H. Orihashi, D. Mitsunaga, M. Ito, M. Hiroi, K. Koyama, R. Onodera, K. Takahashi, K. Matsubayashi and Y. Uwatoko, J. Kor. Phys. Soc. **63** (2013) 743-746.

21. [†]Phase diagram and transport properties of $Y_{1-x}Nd_xCo_2$ pseudo-binary alloys: A. T. Burkov, M. Takeda, A. Teruya, S. Watanabe, S. Hirakawa, Y. Hiranaka, A. Nakamura, M. Hedo, T. Nakama, K. Yagasaki, Y. Takaesu, K. Uchima and Y. Uwatoko, J. Kor. Phys. Soc. **62** (2013) 2080-2083.

22. [†]Successive magnetic transitions of $PrRh_2$ single crystals: Y. Okawara, J. W. Cui, T. Fujiwara, T. Shigeoka, K. Matsubayashi, Y. Uwatoko, S. Kimura and K. Watanabe, J. Kor. Phys. Soc. **63** (2013) 743-746.

23. Pressure Effect on the Structure and Superconducting Transition Temperature of Filled Skutterudites LaT_4P_{12} (T=Fe, Ru): Y. Kawamura, T. Kawaai, J. Hayashi, C. Sekine, H. Gotou, J. Cheng, K. Matsubayashi and Y. Uwatoko, J. Phys. Soc. jpn. **82** (2013) 114702(1-4).

24. [†]Development of High-Field ESR System Using SQUID Magnetometer and its Application to Measurement under High Pressure: T. Sakurai, K. Fujimoto, S. Okubo, H. Ohata and Y. Uwatoko, Journal of Magnetics **18** (2013) 168-172.

25. [*]High-pressure effects in anti-post-perovskite superconductors V_3PnN_x (Pn = P, As): B. S. Wang, J. -G. Cheng, K. Matsubayashi, Y. Uwatoko and K. Ohgushi, Phys. Rev. B **89** (2014) 144510 (1-4).

26. Long-range antiferromagnetic order in the frustrated XY pyrochlore antiferromagnet $Er_2Ge_2O_7$: X. Li, W. M. Li, K. Matsubayashi, Y. Sato, C. Q. Jin, Y. Uwatoko, T. Kawae, A. M. Hallas, C. R. Wiebe, A. M. Arevalo-Lopez, J. P. Attfield, J. S. Gardner, R. S. Freitas, H. D. Zhou and J. -G. Cheng, Phys. Rev. B **89** (2014) 064409 (1-7).

27. [†]Magnetic Field Effect on Magnetic and Electrical Properties of$Mn_{2-x}Cu_xSb$: Y. Matsumoto, H. Orihashi, K. Matsubayashi, Y. Uwatoko, M. Hiroi and K. Koyama, IEEE Transactions on Magnetics **50** (2014) 1000704(1-4).

28. [*]Heavy fermion superconductivity under pressure in the quadrupole system $PrTi_2Al_{20}$: K. Matsubayashi, T. Tanaka, J. Suzuki, A. Sakai, S. Nakatsuji, K. Kitagawa, Y. Kubo and Y. Uwatoko, J. Phys. Soc. Jpn. (2014), in print.

† Joint research with outside partners.

Osada group

In an organic Dirac fermion system α-(BEDT-TTF)$_2$I$_3$, the ν=0 quantum Hall state is realized under magnetic fields resulting from the breaking of four-fold (spin and valley) degeneracy of the singular n=0 Landau level.. The recent NMR measurement has suggested the possible transition from the quantum Hall ferromagnetic (QHF) phase to the quantum Hall insulator (QHI) phase around 15 T. To check this possibility, we have performed high-field transport measurement up to 31T using the NHMFL at Tallahassee, USA. The interlayer resistance shows the saturating behavior up to high fields, which reflects the surface transport via helical edge state of the QHF phase. We can see no anomaly in the saturating region, especially around 15T. This result means that the QHF state survives up to 31T with no QHF-QHI transition.

1. Angle-Dependent Magnetoresistance Oscillations and Charge Density Wave in the Organic Conductor α-(BEDT-TTF)$_2$KHg(SCN)$_4$: K. Uchida, R. Yamaguchi, T. Konoike, T. Osada and W. Kang, J. Phys. Soc. Jpn. **82** (2013) 043714(1-4).

2. Anomalous Thermoelectric Transport and Giant Nernst Effect in Multilayered Massless Dirac Fermion System: T. Konoike, M. Sato, K. Uchida and T. Osada, J. Phys. Soc. Jpn. **82** (2013) 073601(1-4).

3. [†]Stereoscopic study of the angle-dependent magnetoresistance oscillations across the charge-density-wave transition of the organic conductor α-(BEDT-TTF)$_2$KHg(SCN)$_4$: W. Kang, T. Osada, T. Konoike and K. Uchida, Phys. Rev. B **88** (2013) 195105(1-9).

4. 強磁場下電気伝導に現れるサイクロトロン共鳴 : 長田 俊人 , 熊谷 篤 , 内田 和人 , 鴻池 貴子 , 固体物理 **48** (2013) 65-73.

5. 角度依存シュタルクサイクロトロン共鳴とその応用 : 鴻池 貴子 , パリティ **28(4)** (2013) 42-45.

6. 角度依存シュタルクサイクロトロン共鳴法の開発 : 長田 俊人 , パリティ **28(1)** (2013) 20-23.

7. 有機ディラック電子系における量子ホール状態 : 田嶋 尚也 , 佐藤 光幸 , 鴻池 貴子 , 長田 俊人 , 固体物理 **49** (2014) 229-240.

Yamashita group

As the first year of Yamashita group, we developed a new probe for thermal-Hall measurement which can be used in VTI system with 16 T magnet. With this probe, we successfully started the study of thermal-transport measurement of a kagomé material, Volborthite, to find if there is a thermal-Hall effect due to spinons. Developments of the measurement systems for studies under ultra-low temperatures, on the other hand, did not work out due to malfunctions of dilution refrigerators inherited from Ishimoto and Tajima groups.

Materials Design and Characterization Laboratory

Hiroi group

Spinodal decomposition is a ubiquitous phenomenon leading to phase separation from a uniform solution. We show that a spinodal decomposition occurs in a unique combination of two rutile compounds of TiO_2 and VO_2, which are chemically and physically distinguished from each other: TiO_2 is a wide-gap insulator with photo catalytic activities and VO_2 is assumed to be a strongly correlated electron system which exhibits a dramatic metal-insulator transition at 342 K. The spinodal decomposition takes place below 830 K at a critical composition of 34 mol% Ti, generates a unidirectional composition modulation along the c axis with a wavelength of approximately 6 nm, and finally results in the formation of self-assembled lamella structures made up of Ti-rich and V-rich layers stacked alternately with 30-50 nm wavelengths. A metal-insulator transition is not observed in quenched solid solutions with intermediate compositions but emerges in the thin V-rich layers as the result of phase separation. Interestingly, the metal-insulator transition remains as sharp as in pure VO_2 even in such thin layers and takes place at significantly reduced temperatures of 310-340 K, which is probably due to a large misfit strain induced by lattice matching at the coherent interface.

1. [*]Magnetic Order in the Spin-1/2 Kagome Antiferromagnet Vesignieite: M. Yoshida, Y. Okamoto, M. Takigawa and Z. Hiroi, J. Phys. Soc. Jpn. **82** (2013) 013702(1-5).

2. Magnetic Properties of the Spin-1/2 Deformed Kagome Antiferromagnet Edwardsite: H. Ishikawa, Y. Okamoto and Z. Hiroi, J. Phys. Soc. Jpn. **82** (2013) 063710.

* Joint research among groups within ISSP.

3. Pressure Effects on Rattling and Superconductivity in the Einstein Solids: Y. Ikeda, Y. Kawasaki, T. Shinohara, S. Araki, T. C. Kobayashi, A. Onosaka, Y. Okamoto, J.-I. Yamaura and Z. Hiroi, J. Phys. Soc. Jpn. **82** (2013) 063707.

4. Understanding of the Temperature–Pressure Phase Diagram of β-Pyrochlore Oxides: A Role of Anhamonicity on Superconductivity: T. Isono, D. Iguchi, T. Matsubara, Y. Machida, B. Salce, J. Flouquet, H. Ogusu, J.-I. Yamaura, Z. Hiroi and K. Izawa, J. Phys. Soc. Jpn. **82** (2013) 114708.

5. YCr_6Ge_6 as a Candidate Compound for a Kagome Metal: Y. Ishii, H. Harima, Y. Okamoto, J.-I. Yamaura and Z. Hiroi, J. Phys. Soc. Jpn. **82** (2013) 023705(1-4).

6. Breathing Pyrochlore Lattice Realized in A-Site Ordered Spinel Oxides $LiGaCr_4O_8$ and $LiInCr_4O_8$: Y. Okamoto, G. J. Nilsen, J. Paul Attfield and Z. Hiroi, Phys. Rev. Lett. **110** (2013) 097203(1-5).

7. *5d 遷移金属パイロクロア酸化物における低温磁気構造の研究：山浦 淳一，大串 研也，広井 善二，日本結晶学会誌 **55** (2013) 116-120.

8. *Spinodal Decomposition in the TiO_2–VO_2 System: Z. Hiroi, H. Hayamizu, T. Yoshida, Y. Muraoka, Y. Okamoto, J.-I. Yamaura and Y. Ueda, Chem. Mater. **25** (2013) 2202.

9. †*Iseite, $Mn_2Mo_3O_8$, a new mineral from Ise, Mie Prefecture, Japan: D. Nishio-Hamane, N. Tomita, T. Minakawa and S. Inaba, Journal of Mineralogical and Petrological Sciences **108** (2013) 37-41.

10. †*Synthesis of $LiNi_{0.5}Mn_{1.5}O_4$ and $0.5Li_2MnO_3$–$0.5LiNi_{1/3}Co_{1/3}Mn_{1/3}O_2$ hollow nanowires by electrospinning: E. Hosono, T. Saito, J. Hoshino, Y. Mizuno, M. Okubo, D. Asakura, K. Kagesawa, D. Nishio-Hamane, T. Kudo and H. Zhou, CrystEngComm **15** (2013) 2592-2597.

11. *Electronic State of $CeFe_4As_{12}$ Investigated by Using Single Crystals Grown under High Pressure of 4 GPa: Y. Ogawa, H. Sato, M. Watanabe, T. Namiki, S. Tatsuoka, R. Higashinaka, Y. Aoki, K. Kuwahara, J.-I. Yamaura and Z. Hiroi, J. Phys. Soc. Jpn. **83** (2014) 034710.

12. *Kagome–Triangular Lattice Antiferromagnet $NaBa_2Mn_3F_{11}$: H. Ishikawa, T. Okubo, Y. Okamoto and Z. Hiroi, J. Phys. Soc. Jpn. **83** (2014) 043703(1-5).

Kawashima group

We have been investigating quantum spin/boson systems and frustrated systems by means of large-scale numerical simulation. We also develop new numerical techniques. Our group's achievements of 2013 include: (1) clarifying the apparent deconfined critical behavior of the SU(N) J-Q Heisenberg model with a strong corrections to scaling, (2) lattice rotational symmetry breaking in flustrated spin systems, and (3) highly parallelized code for the molecular dynamics simulation of mixed-phase fluid dynamics.

1. Mott Transition of Bose–Fermi Mixtures in Optical Lattices Induced by Attractive Interactions: A. Masaki and H. Mori, J. Phys. Soc. Jpn. **82** (2013) 074002(1-4).

2. *Possibility of deconfined criticality in SU(N) Heisenberg models at small N: K. Harada, T. Suzuki, T. Okubo, H. Matsuo, J. Lou, H. Watanabe, S. Todo and N. Kawashima, Phys. Rev. B **88** (2013) 220408(1-4).

3. Second-order phase transition in the Heisenberg model on a triangular lattice with competing interactions: R. Tamura, S. Tanaka and N. Kawashima, Phys. Rev. B **87** (2013) 214401(1-5).

4. †*Various regimes of quantum behavior in an S=1/2 Heisenberg antiferromagnetic chain with fourfold periodicity: H. Yamaguchi, T. Okubo, K. Iwase, T. Ono, Y. Kono, S. Kittaka, T. Sakakibara, A. Matsuo, K. Kindo and Y. Hosokoshi, Phys. Rev. B **88** (2013) 174410(1-5).

5. Visibility pattern of Bose–Fermi mixtures in one-dimensional incommensurate lattices: A. Masaki and H. Mori, Philosophical Magazine Letters **93** (2013) 422(9pages).

6. Fermion-induced decoherence of bosons in optical lattices: A. Masaki and H. Mori, J. Phys.: Conf. Ser. **454** (2013) 012048(1-4).

7. Huge-scale molecular dynamics simulation of multibubble nuclei: H. Watanabe, M. Suzuki and N. Ito, Computer Physics Communications **184** (2013) 2775(8pages).

8. *Kagome–Triangular Lattice Antiferromagnet $NaBa_2Mn_3F_{11}$: H. Ishikawa, T. Okubo, Y. Okamoto and Z. Hiroi, J. Phys. Soc. Jpn. **83** (2014) 043703(1-5).

† Joint research with outside partners.

9. Parallelized Quantum Monte Carlo Algorithm with Nonlocal Worm Updates: A. Masaki-Kato, T. Suzuki, K. Harada, S. Todo and N. Kawashima, Phys. Rev. Lett. **112** (2014) 140603(1-5).

10. Phase Transitions with Discrete Symmetry Breaking in Antiferromagnetic Heisenberg Models on a Triangular Lattice: R. Tamura, S. Tanaka and N. Kawashima, JPS Conf. Proc. --- Proceedings of the 12th Asia Pacific Physics Conference (APPC12) **1** (2014) 012125(1-5).

Noguchi group

We have studied the structure formation of surfactant membranes under shear flow. We found that shear can induce a rolled lamellae structure, which structure factor agrees with those of intermediate states during lamellar-to-onion transition measured by time-resolved scatting experiments. We revealed that entropy reduction of membrane fluctuations can induce aggregation of binding proteins in multilamellar membranes. We also studied the effects of anchored polymers on membranes and dynamics of deformable active particles.

1. Dynamics of a deformable active particle under shear flow: M. Tarama, A. M. Menzel, B. T. Hagen, R. Wittkowski, T. Ohta and H. Loewen, J. Chem. Phys. **139** (2013) 104906.

2. Spatiotemporal heterogeneity of local free volumes in highly supercooled liquid: H. Shiba and T. Kawasaki, J. Chem. Phys. **139** (2013) 184502.

3. Structure formation in binary mixtures of lipids and detergents: Self-assembly and vesicle division: H. Noguchi, J. Chem. Phys. **138** (2013) 024907(1-9).

4. Structure formation of surfactant membranes under shear flow: H. Shiba, H. Noguchi and G. Gompper, J. Chem. Phys. **139** (2013) 014702.

5. Oscillatory motions of an active deformable particle: M. Tarama and T. Ohta, Phys. Rev. E **87** (2013) 062912.

6. Mechanical properties and microdomain separation of fluid membranes with anchored polymers: H. Wu, H. Shiba and H. Noguchi, Soft Matter **9** (2013) 9907.

7. Effects of anchored flexible polymers on mechanical properties of model biomembranes: H. Wu and H. Noguchi, AIP Conf. Proc. **1518** (2013) 649-653.

8. Hierarchical heterogeneous glassy dynamics of configuration changes and vibration modes: T. Kawasaki, H. Shiba and A. Onuk, AIP Conf. Proc. **1518** (2013) 784-791.

9. Structure formation of lipid membranes: Membrane self-assembly and vesicle opening-up to octopus-like micelles: H. Noguchi, AIP Conf. Proc. **1518** (2013) 566-570.

10. 脂質膜の構造形成の粗視化シミュレーション : 野口 博司 , 生物物理 **53** (2013) 11-14.

11. Entropy-driven aggregation in multilamellar membranes: H. Noguchi, EPL **102** (2013) 68001.

12. 粒子描像の流体力学計算手法 I: 野口 博司 , 分子シミュレーション研究会会誌 “アンサンブル ” **15** (2013) 265-268.

13. Morphological variation of a lipid vesicle confined in a spherical vesicle: A. Sakashita, M. Imai and H. Noguchi, Phys. Rev. E **89** (2014) 040701.

14. Multiscale modeling of blood flow: from single cells to blood rheology: D. A. Fedosov, H. Noguchi and G. Gompper, Biomech. Model. Mechanobiol. **13** (2014) 239-258.

15. 界面活性剤系の構造形成の粗視化分子シミュレーション : 芝隼 人 , 野口 博司 , 分子シミュレーション研究会会誌 “アンサンブル ” **16** (2014) 59-65.

16. 粒子描像の流体力学計算手法 II: 野口 博司 , 分子シミュレーション研究会会誌 “アンサンブル ” **16(2)** (2014) 118-121.

Materials Synthesis and Characterization group

1. [†*]Iseite, $Mn_2Mo_3O_8$, a new mineral from Ise, Mie Prefecture, Japan: D. Nishio-Hamane, N. Tomita, T. Minakawa and S. Inaba, Journal of Mineralogical and Petrological Sciences **108** (2013) 37-41.

* Joint research among groups within ISSP.

2. †Takanawaite-(Y), a new mineral of the M-type polymorph with $Y(Ta,Nb)O_4$ from Takanawa Mountain, Ehime Prefecture, Japan: D. Nishio-Hamane, T. Minakawa and Y. Ohgoshi, Journal of Mineralogical and Petrological Sciences **108** (2013) 335.

3. †*Synthesis of $LiNi_{0.5}Mn_{1.5}O_4$ and $0.5Li_2MnO_3$–$0.5LiNi_{1/3}Co_{1/3}Mn_{1/3}O_2$ hollow nanowires by electrospinning: E. Hosono, T. Saito, J. Hoshino, Y. Mizuno, M. Okubo, D. Asakura, K. Kagesawa, D. Nishio-Hamane, T. Kudo and H. Zhou, CrystEngComm **15** (2013) 2592-2597.

4. †VGCF-core@$LiMn_{0.4}Fe_{0.6}PO_4$-sheath heterostructure nanowire for high rate Li-ion batteries: K. Kagesawa, E. Hosono, M. Okubo, J. Kikkawa, D. Nishio-Hamane, T. Kudo and H. Zhou, CrystEngComm **15** (2013) 6638.

5. †Spin transition and substitution of Fe^{3+} in Al-bearing post-Mg-perovskite: K. Fujino, D. Nishio-Hamane, Y. Kuwayama, N. Sata, S. Murakami, M. Whitaker, A. Shinozaki, H. Ohfuji, Y. Kojima, T. Irifune, N. Hiraoka, H. Ishii and K.-D. Tsuei, Physics of the Earth and Planetary Interiors **217** (2013) 31.

6. Minohlite, a new copper-zinc sulfate mineral from Minoh, Osaka, Japan: M. Ohnishi, N. Shimobayashi, D. Nishio-Hamane, K. Shinoda, K. Momma and T. Ikeda, Mineral. Mag. **77** (2013) 335.

7. †Vanadoallanite-(La): a new epidote-supergroup mineral from Ise, Mie Prefecture, Japan: M. Nagashima, D. Nishio-Hamane, N. Tomita, T. Minakawa and S. Inaba, Mineral. Mag. **77** (2013) 2739.

8. *Electronic State of $CeFe_4As_{12}$ Investigated by Using Single Crystals Grown under High Pressure of 4 GPa: Y. Ogawa, H. Sato, M. Watanabe, T. Namiki, S. Tatsuoka, R. Higashinaka, Y. Aoki, K. Kuwahara, J.-I. Yamaura and Z. Hiroi, J. Phys. Soc. Jpn. **83** (2014) 034710.

9. †Magnetic properties of Mn–Bi melt-spun ribbons: T. Saito, R. Nishimura and D. Nishio-Hamane, J. Magn. Magn. Mater. **349** (2014) 9.

10. †Successive phase transitions driven by orbital ordering and electron transfer in quasi-two-dimensional $CrSe_2$ with a triangular lattice: S. Kobayashi, H. Ueda, D. Nishio-Hamane, C. Michioka and K. Yoshimura, Phys. Rev. B **89** (2014) 054413.

11. Iwateite, $Na_2BaMn(PO_4)_2$, a new mineral from the Tanohata mine, Iwate Prefecture, Japan: D. Nishio-Hamane, T. Minakawa and H. Okada, Journal of Mineralogical and Petrological Sciences **109** (2014) 34.

12. †Magnetic properties of $SmCo_{5-x}Fe_x$ (x=0–4) melt-spun ribbon: T. Saito and D. Nishio-Hamane, J. Alloys Compd. **585** (2014) 423.

13. †Electrochemical properties of $LiMn_xFe_{1-x}PO_4$ (x = 0, 0.2, 0.4, 0.6, 0.8 and 1.0)/vapor grown carbon fiber core–sheath composite nanowire synthesized by electrospinning method: K. Kagesawa, E. Hosono, M. Okubo, D. Nishio-Hamane, T. Kudo and H. Zhou, Journal of Power Sources **248** (2014) 615.

14. †Electrically Conductive and Mechanically Elastic Titanium Nitride Ceramic Microsprings: S. Yang, X. Chen, K. Yamamoto, M. Iitake, D. Nishio-Hamane, H. Sakai and M. Abe, J. Nanosci. Nanotech. **14** (2014) 4292.

15. †Ultrafast hydrothermal synthesis of Pr-doped $Ca_{0.6}Sr_{0.4}TiO_3$ red phosphor nanoparticles using corrosion resistant microfluidic devices with Ti-lined structure under high-temperature and high-pressure condition: K. Sue, T. Ono, Y. Hakuta, H. Takashima, D. Nishio-Hamane, T. Sato, M. Ohara, M. Aoki, Y. Takebayashi, S. Yoda, T. Hiaki and T. Furuya, Chemical Engineering Journal **239** (2014) 360.

Neutron Science Laboratory

Shibayama group

Shibayama group has been exploring the structure and dynamics of soft matter, especially polymer gels, micelles, and phenolic resin, utilizing a combination of small-angle neutron scattering (SANS), neutron spin echo (NSE), and dynamic light scattering (DLS). The objectives are to elucidate the mysterious relationship between the structure and variety of novel properties/ functions of polymer gels/resins. The highlights of 2012 include (1) structural analysis of high performance ion-gel comprising tetra-PEG networks, (2) atomistic molecular dynamics study of cross-linked phenolic resins, (3) rubber elasticity for incomplete polymer networks, (4) kinetic study for AB-type coupling reaction of tetra-arm polymers, (5) optimization of the thickness of a ZnS/(LiF)-Li-6 scintillator for a high-resolution detector installed on a focusing small-angle neutron scattering spectrometer (SANS-U), and so on.

1. Self-oscillating micelles: T. Ueki, M. Shibayama and R. Yoshida, Chem. Commun. **49** (2013) 6947.

† Joint research with outside partners.

2. Gelation process of Tetra-PEG ion-gel investigated by time-resolved dynamic light scattering: H. Asai, K. Nishi, T. Hiroi, K. Fujii, T. Sakai and M. Shibayama, Polymer **54** (2013) 1160.

3. Communication: Collective dynamics of room-temperature ionic liquids and their Li ion solutions studied by high-resolution inelastic X-ray scattering: K. Fujii, M. Shibayama, T. Yamaguchi, K. Yoshida, T. Yamaguchi, S. Seki, H. Uchiyama, A. Q. R. Baron and Y. Umebayashi, J. Chem. Phys. **138** (2013) 151101.

4. Correlation between Local and Global Inhomogeneities of Chemical Gels: M. Asai, T. Katashima, U.-I. Chung, T. Sakai and M. Shibayama, Macromolecules **46** (2013) 9772.

5. SANS and DLS Study of Tacticity Effects on Hydrophobicity and Phase Separation of Poly(*N* -isopropylacrylamide): K. Nishi, T. Hiroi, K. Hashimoto, K. Fujii, Y.-S. Han, T.-H. Kim, Y. Katsumoto and M. Shibayama, Macromolecules **46** (2013) 6225.

6. Solvation Structure of Poly(ethylene glycol) in Ionic Liquids Studied by High-energy X-ray Diffraction and Molecular Dynamics Simulations: H. Asai, K. Fujii, K. Nishi, T. Sakai, K. Ohara, Y. Umebayashi and M. Shibayama, Macromolecules **46** (2013) 2369.

7. Structural Study on the UCST-Type Phase Separation of Poly(*N* -isopropylacrylamide) in Ionic Liquid: H. Asai, K. Fujii, T. Ueki, S. Sawamura, Y. Nakamura, Y. Kitazawa, M. Watanabe, Y.-S. Han, T.-H. Kim and M. Shibayama, Macromolecules **46** (2013) 1101.

8. Br nsted Basicity of Solute Butylamine in an Aprotic Ionic Liquid Investigated by Potentiometric Titration: K. Fujii, K. Hashimoto, T. Sakai, Y. Umebayashi and M. Shibayama, Chem. Lett. **42** (2013) 1250.

9. Dynamic light scattering microscope: Accessing opaque samples with high spatial resolution: T. Hiroi and M. Shibayama, Opt. Express **21** (2013) 20260.

10. Gelation and cross-link inhomogeneity of phenolic resins studied by ^{13}C-NMR spectroscopy and small-angle X-ray scattering: A. Izumi, T. Nakao and M. Shibayama, Soft Matter **9** (2013) 4188.

11. Specific Solvation of Benzyl Methacrylate in 1-Ethyl-3-methylimidazolium Bis(trifluoromethanesulfonyl)amide Ionic Liquid: M. Matsugami, K. Fujii, T. Ueki, Y. Kitazawa, Y. Umebayashi, M. Watanabe and M. Shibayama, Anal. Sci. **29** (2013) 311.

12. Acid–base property of protic ionic liquid, 1-alkylimidazolium bis(trifluoromethanesulfonyl)amide studied by potentiometric titration: K. Hashimoto, K. Fujii and M. Shibayama, Journal of Molecular Liquids **188** (2013) 143.

13. Small-Angle Neutron Scattering Study on Aggregation of 1-Alkyl-3-methylimidazolium Based Ionic Liquids in Aqueous Solution: T. Kusano, K. Fujii, M. Tabata and M. Shibayama, J Solution Chem **42** (2013) 1888.

14. Multiscale Dynamics of Inhomogeneity-Free Polymer Gels: T. Hiroi, M. Ohl, T. Sakai and M. Shibayama, Macromolecules **47** (2014) 763.

15. Small-Angle Neutron Scattering Study on Defect-Controlled Polymer Networks: K. Nishi, H. Asai, K. Fujii, Y.-S. Han, T.-H. Kim, T. Sakai and M. Shibayama, Macromolecules **47** (2014) 1801.

16. SANS および SAXS によるフェノール樹脂硬化物の構造解析 : 和泉 篤士 , 中尾 俊夫 , 岩瀬 裕希 , 柴山 充弘 , 波紋 **24** (2014) 11-14.

17. 中性子散乱を用いた構造解析手法　概説とエラストマー・高分子ゲル解析への応用 : 柴山　充弘 , ゴム協会編 (2014) 1-10.

18. SANS studies on catalyst ink of fuel cell: M. Shibayama, T. Matsunaga, T. Kusano, K. Amemiya, N. Kobayashi and T. Yoshida, J. Appl. Polym. Sci. **131** (2014) 1-7.

19. 中性子による材料評価・構造解析 : 柴山 充弘 , 表面科学 **33** (2013) 258-263.

20. 小角 X 線散乱法によるフェノール樹脂ゲル化メカニズムの解析 : 和泉 篤士 , 中尾 俊夫 , 柴山 充弘 , ネットワークポリマー **34** (2013) 330-335.

21. 溶液中での重水素化ノボラックのコンフォメーション : 和泉 篤士 , 中尾 俊夫 , 柴山 充弘 , ネットワークポリマー **33** (2013) 204-208.

22. 水面をかけ抜けるには? : 東 昭 , 柴山 充弘 , 増淵 雄一 , ニュートンプレス　(2013) 90-95.

23. 中性子小角散乱を用いた分子集合体の解析 : 草野 巧巳 , 柴山 充弘 , Colloid & Interface Communication **39** (2014) 16-18.

* Joint research among groups within ISSP.

24. Fabrication, Structure, Mechanical Properties, and Application of Tetra-PEG Hydrogels Oren Scherman and Xian Jun Loh, Eds.: M. Shibayama and T. Sakai, in: *Polymeric and Self Assembled Hydrogels: Fundamentals to Applications, Chapt. 2*, edited by RSC Publishing, (RSC Publishing, 2013), 2-38.

25. Computer simulation of network formation in natural rubber (NR): T. Nakao and S. Kohjiya, in: *Chemistry, Manufacture and Applications of Natural Rubber, Kohjiya S. and Ikeda, Y. Eds.*, edited by S. Kohjiya and Y. Ikeda, (Woodhead, Cambridge, UK, 2014), 216-246.

Yoshizawa group

A systematic study on spin dynamics in two-dimensional transition-metal oxides has been carried out with use of the high resolution chopper spectrometer installed at BL12 in the Material and Life Science Facility, J-PARC. In the highly hole-doped region in the layered nickelate, it shows a checkerboard-type spin-charge ordering, and the nature of the excitation spectra changes its character and approaches to the metal-like behavior. Spin fluctuations in several quantum spin systems were also studied.

1. [†*]Long-range order and spin-liquid states of polycrystalline $Tb_{2+x}Ti_{2-x}O_{7+y}$: T. Taniguchi, H. Kadowaki, H. Takatsu, B. Fåk, J. Ollivier, T. Yamazaki, T. J. Sato, H. Yoshizawa, Y. Shimura, T. Sakakibara, T. Hong, K. Goto, L. R. Yaraskavitch and J. B. Kycia, Phys. Rev. B **87** (2013) 060408R(1-5).

2. Structural and magnetic properties in the quantum S=1/2 dimer system $Ba_3(Cr_{1-x}V_x)_2O_8$ with site disorder: T. Hong, L. Y. Zhu, X. Ke, V. O. Garlea, Y. Qiu, Y. Nambu, H. Yoshizawa, M. Zhu, G. E. Granroth, A. T. Savici, Z. Gai and H. D. Zhou, Phys. Rev. B **87** (2013) 144427(1-9).

3. Magnetic structure of the conductive triangular-lattice antiferromagnet $PdCrO_2$: H. Takatsu, G. Nénert, H. Kadowaki, H. Yoshizawa, M. Enderle, S. Yonezawa, Y. Maeno, J. Kim, N. Tsuji, M. Takata, Y. Zhao, M. Green and C. Broholm, Phys. Rev. B **89** (2014) 104408.

Yamamuro group

Our laboratory is studying chemical physics of complex condensed matters by using neutron scattering, X-ray diffraction, calorimetric, dielectric, and viscoelastic techniques. Our target materials are glasses, liquids, and various disordered systems. This year, there were two important outcomes in the study of ionic liquids. The first one, which was found in the quasielastic neutron scattering (QENS) and viscoelastic measurements, is that the inter-ionic motion is directly associated with the glass transitions in imidazolium-bases ionic liquids. The second one is that the origin of the low-*Q* diffraction peak, which is a typical property of the ionic liquids, is a local structure similar to that of a liquid-crystalline (SmA) phase. This was obtained from differential scanning calorimetry (DSC) and X-ray diffraction experiments. In the QENS study of a porous coordination polymer MIL-53, we have found that protons are carried by both water and ammonia molecules which are more mobile than those in bulk states. Other than these topics, we have made some progresses in the studies on palladium hydrides and vapor-deposited simple molecular glasses.

1. Phase Transition and Dynamics of Water Confined in Hydroxyethyl Copper Rubeanate Hydrate: T. Yamada, T. Yamada, M. Tyagi, M. Nagao, H. Kitagawa and O. Yamamuro, J. Phys. Soc. Jpn. **82** (2013) SA010 (8 pages).

2. Hyperfine structure of magnetic excitations in a novel Tb based single molecule magnet studied by high-resolution neutron spectroscopy: M. Kofu, T. Kajiwara, M. Nakano, K. Nakajima, S. Ohira-Kawamura, T. Kikuchi, Y. Inamura and O. Yamamuro, Phys. Rev. B **88** (2013) 064405 (7 pages).

3. Heterogeneous Slow Dynamics of Imidazolium Based Ionic Liquids Studied by Neutron Spin Echo: M. Kofu, M. Nagao, T. Ueki, Y. Kitazawa, Y. Nakamura, S. Sawamura, M. Watanabe and O. Yamamuro, J. Phys. Chem. B **117** (2013) 2773-2781.

4. Mode distribution analysis of quasi-elastic neutron scattering and application to liquid water: T. Kikuchi, K. Nakajima, S. Ohira-Kawamura, Y. Inamura, O. Yamamuro, M. Kofu, Y. Kawakita, K. Suzuya, M. Nakamura and M. Arai, Phys. Rev. E **87** (2013) 062314 (8 pages).

5. Magnetic relaxations in a Tb-based single molecule magnet studied by quasielastic neutron scattering: M. Kofu, T. Kajiwara, J. S. Gardner, G. G. Simeoni, M. Tyagi, K. Nakajima, S. Ohira-Kawamura, M. Nakano and O. Yamamuro, Chem. Phys. **427** (2013) 147-152.

6. Linear trinuclear Zn(II)–Ce(III)–Zn(II) complex which behaves as a single-molecule magnet: S. Hino, M. Maeda, K. Yamashita, Y. Kataoka, M. Nakano, T. Yamamura, H. Nojiri, M. Kofu, O. Yamamuro and T. Kajiwara, Dalton Trans. **42** (2013) 2683-2686.

[†] Joint research with outside partners.

7. Thermal behaviour, structure and dynamics of low-temperature water confined in mesoporous organosilica by differential scanning calorimetry, X-ray diffraction and quasi-elastic neutron scattering: M. Aso, K. Ito, H. Sugino, K. Yoshida, T. Yamada, O. Yamamuro, S. Inagaki and T. Yamaguchi, Pure and Appl. Chem. **85** (2013) 289-305.

8. Relationship between the local dynamics and gas permeability of polyacetylenes containing polymethylated indan/tetrahydronaphtalene moieties: R. Inoue, T. Kanaya, Y. Hu, T. Masuda, K. Nishida and O. Yamamuro, Polymer **55** (2014) 182-186.

9. Proton Dynamics of Two Dimensional Oxalate-Bridged Coordination Polymers: S. Miyatsu, M. Kofu, A. Nagoe, T. Yamada, M. Sadakiyo, T. Yamada, H. Kitagawa, M. Tyagi, V. Garcia Sakai and O. Yamamuro, Phys. Chem. Chem. Phys. (2014), accepted for publication.

10. 連載講座「中性子散乱による原子・分子のダイナミクスの観測」III 原子・分子のダイナミクス「液体・非晶質・表面／界面」: 山室 修 , RADIOISOTOPES **62** (2013) 691-701.

Masuda group

Recently the discovery of the multiferroics, i.e., enhanced simultaneous orders in magnetism and dielectricity,revived the study of the magnetoelectric effect. A number of studies had revealed its mechanism and clarified the relationships between dielectric and magnetic structures in homogeneous systems. Next challenge would be to find and study a new magnetoelectric effect in inhomogeneous system. A remarkable example in an inhomogeneous system is a magnet having relaxor property, relaxor magnet. In 2013 our group studied a new relaxor magnet, $LuFeCoO_4$, by combination of bulk properties measurements and neutron diffraction technique. Our study reveals a novel relationship between PNRs and magnetic correlation, and establishes the magnetic and dielectric phase diagrams of the relaxor magnet.

1. Quantum-Phase-Transition-Induced Multiferroics and Higgs Mode in Integer Spin Systems in Noncentrosymmetric Lattice with Strong Single-Ion Anisotropy: M. Matsumoto, M. Soda and T. Masuda, J. Phys. Soc. Jpn. **82** (2013) 093703.

2. ^{63,65}Cu Nuclear Resonance Study of the Coupled Spin Dimers and Chains Compound $Cu_2Fe_2Ge_4O_{13}$: J. Kikuchi, S. Nagura, K. Murakami, T. Masuda and G. J. Redhammer, J. Phys. Soc. Jpn. **82** (2013) 034710(1-10).

3. 三軸分光器入門 : 益田 隆嗣 , 波紋 **23** (2013) 223-229.

4. Spin-Nematic Interaction in the Multiferroic Compound $Ba_2CoGe_2O_7$: M. Soda, M. Matsumoto, M. Mansson, S. Ohira-Kawamura, K. Nakajima, R. Shiina and T. Masuda, Phys. Rev. Lett. **112** (2014) 127205.

5. 1 次元フラストレート強磁性鎖のスピン密度波と Bond Nematic 相関 : 萩原 雅人 , 益田 隆嗣 , 波紋 **23** (2013) 14-18.

International MegaGauss Science Laboratory

Takeyama group

The electro-magnetic flux compression techniques have been established to generate magnetic fields over 700 T by employing a new type of primary coil (a copper lined iron coil). In such a high magnetic field, a measurement of the magnetic field should be reconsidered. In pulse magnet operation, the magnetic field has been determined by a pick-up coil, wound around a thin rod, converted from the detected induced voltage from $d\varphi/dt$ (φ, a magnetic flux), followed by a certain process of calibration. We have found recently that the pick-up coil is not a reliable method anymore in such an extremely high magnetic fields. A Faraday rotation angle of quartz and the other glasses was measured up to a peak field and is calibrated with the signals from the pick-up coil. The present study revealed that the conventional pick-up coil method underestimated the values of the peak fields at least 10 %, so that 730 T ever reported could possibly reach 800 T.

1. Band-edge exciton states in a single-walled carbon nanotube revealed by magneto-optical spectroscopy in ultrahigh magnetic fields: W. Zhou, T. Sasaki, D. Nakamura, H. Liu, H. Kataura and S. Takeyama, Phys. Rev. B **87** (2013) 241406(1-4).

2. *Cyclotron resonance in ferromagnetic InMnAs and InMnSb: G. Khodaparast, Y. H. Matsuda, D. Saha, G. Sanders, C. Stanton, H. Saito, S. Takeyama, T. Merritt, C. Feeser, B. Wessels, X. Liu and J. Furdyna, Phys. Rev. B **88** (2013) 235204(11pages).

* Joint research among groups within ISSP.

3. Magnetic superfluid state in the frustrated spinel oxide $CdCr_2O_4$ revealed by ultrahigh magnetic fields: A. Miyata, S. Takeyama and H. Ueda, Phys. Rev. B **87** (2013) 214424(1-6).

4. Magneto-photoluminescence of charged excitons from $Mg_xZn_{1-x}O/ZnO$ heterojunctions: T. Makino, Y. Segawa, A. Tsukazaki, H. Saito, S. Takeyama, S. Akasaka, K. Nakahara and M. Kawasaki, Phys. Rev. B **87** (2013) 085312(1-7).

5. *Precise measurement of a magnetic field generated by the electromagnetic flux compression technique: D. Nakamura, H. Sawabe, Y. H. Matsuda and S. Takeyama, Rev. Sci. Instrum. **84** (2013) 044702 (10 pages).

6. *Magnetization of $SrCu_2(BO_3)_2$ in Ultrahigh Magnetic Fields up to 118 T: Y. H. Matsuda, N. Abe, S. Takeyama, H. Kageyama, P. Corboz, A. Honecker, S. R. Manmana, G. R. Foltin, K. P. Schmidt and F. Mila, Phys. Rev. Lett. **111** (2013) 137204 (5 pages).

7. *Magnetization Studies of Field-Induced Transitions by Using a Single-Turn Coil Technique: N. Abe, Y. H. Matsuda, S. Takeyama, K. Sato, H. Kageyama and Y. Nishiwaki, J. Low Temp. Phys. **170** (2013) 452-456.

8. †*Magneto-Absorption in the Phase of Solid Oxygen at Megagauss Magnetic Fields: T. Nomura, Y. H. Matsuda, J. L. Her, S. Takeyama, A. Matsuo, K. Kindo and T. C. Kobayashi, J. Low Temp. Phys. **170** (2013) 372-376.

9. *Precision of an Ultra-high Magnetic Field Generated by the Electro-magnetic Flux Compression: D. Nakamura, Y. H. Matsuda and S. Takeyama, J. Low Temp. Phys. **170** (2013) 457-462.

10. Exciton-phonon bound complex in single-walled carbon nanotubes revealed by high-field magneto-optical spectroscopy: W. Zhou, T. Sasaki, D. Nakamura, H. Saito, H. Liu, H. Kataura and S. Takeyama, Appl. Phys. Lett. **103** (2013) 233101.

11. Survey of exciton-phonon sidebands by magneto-optical spectroscopy using highly specified (6,5) single-walled carbon nanotubes: W. Zhou, T. Sasaki, D. Nakamura, H. Saito, H. Liu, H. Kataura and S. Takeyama, Appl. Phys. Lett. **103** (2013) 021117(1-4).

12. Infrared cyclotron resonances of Dirac electrons in SiC epitaxial graphene in ultra-high magnetic fields: H. Saito, D. Nakamura, S. Takeyama and H. Hibino, AIP Conf. Proc. **1566** (2013) 145.

13. *Magneto-optical study of Dirac fermion in quartz CVD-grown graphene above 100 T: D. Nakamura, H. Saito, W. Zhou, Y. H. Matsuda, S. Takeyama, K. Yagi, K. Hayashi and S. Sato, AIP Conf. Proc. **1566** (2013) 169-170.

14. Magneto-optical survey of 1st and 2nd sub-bands in chirality specific (6, 5) single-walled carbon nanotube up to 190 T: T. Sasaki, W. Zhou, D. Nakamura, H. Liu, H. Kataura and S. Takeyama, AIP Conf. Proc. **1566** (2013) 171.

15. Canted 2:1:1 Magnetic Supersolid Phase in a Frustrated Magnet $MgCr_2O_4$ as a Small Limit of the Biquadratic Spin Interaction: A. Miyata, H. Ueda and S. Takeyama, J. Phys. Soc. Jpn. **83** (2014) 063702(1-4).

16. Note: Experimental evidence of three-dimensional dynamics of an electromagnetically imploded liner: D. Nakamura, H. Sawabe and S. Takeyama, Rev. Sci. Instrum. **85** (2014) 036102.

Kindo group

A new user coil has been installed. The coil can generate a short pulsed field with duration of 4 ms. 75 T field can be used every half hour. A new long-pulse magnet has been installed. The magnet can generate a long pulsed field with duration of about 1 sec. The maximum field of 36 T can be generated. Heat capacity measurement under the long pulsed field can be carried out.

1. †Antiferromagnetic ordering in Sr_2CrO_4: M. Rani, H. Sakurai, S. Okubo, K. Takamoto, R. Nakata, T. Sakurai, H. Ohta, A. Matsuo, Y. Kohama, K. Kindo and J. Ahmad, J. Phys.: Condens. Matter **25** (2013) 226001(1-5).

2. Collapse of Magnetic Order of the Quasi One-Dimensional Ising-Like Antiferromagnet $BaCo_2V_2O_8$ in Transverse Fields: S. Kimura, K. Okunishi, M. Hagiwara, K. Kindo, Z. He, T. Taniyama, M. Itoh, K. Koyama and K. Watanabe, J. Phys. Soc. Jpn. **82** (2013) 033706(1-4).

3. †Crystal Structure and Magnetic Properties of the Verdazyl Biradical *m*-Ph-V_2 Forming a Ferromagnetic Alternating Double Chain: K. Iwase, H. Yamaguchi, T. Ono, T. Shimokawa, H. Nakano, A. Matsuo, K. Kindo, H. Nojiri and Y. Hosokoshi, J. Phys. Soc. Jpn. **82** (2013) 074719(1-6).

4. †*High-Field Phase Diagram of $SmRu_4P_{12}$ Determined by Ultrasonic Measurements in Pulsed Magnetic Field up to 55 T: M. Yoshizawa, H. Mitamura, F. Shichinomiya, S. Fukuda, Y. Nakanishi, H. Sugawara, T. Sakakibara and K. Kindo, J. Phys. Soc. Jpn. **82** (2013) 033602(1-5).

† Joint research with outside partners.

5. †Marked Change in the Ground State of $CeRu_2Al_{10}$ Induced by Small Amount of Rh Substitution: A. Kondo, K. Kindo, K. Kunimori, H. Nohara, H. Tanida, M. Sera, R. Kobayashi, T. Nishioka and M. Matsumura, J. Phys. Soc. Jpn. **82** (2013) 054709(1-5).

6. Metamagnetic Behavior and Effect of Pressure on the Electronic State in Heavy-Fermion Compound $YbRh_2Zn_{20}$: F. Honda, T. Takeuchi, S. Yasui, Y. Taga, S. Yoshiuchi, Y. Hirose, Y. Tomooka, K. Sugiyama, M. Hagiwara, K. Kindo, R. Settai and Y. Onuki, J. Phys. Soc. Jpn. **82** (2013) 084705(1-10).

7. †Spin-Dependent Molecular Orientation of O_2–O_2 Dimer Formed in the Nanoporous Coordination Polymer: A. Hori, T. C. Kobayashi, Y. Kubota, A. Matsuo, K. Kindo, J. Kim, K. Kato, M. Takata, H. Sakamoto, R. Matsuda and S. Kitagawa, J. Phys. Soc. Jpn. **82** (2013) 084703(6).

8. *Temperature and Magnetic Field Dependent Yb Valence in $YbRh_2Si_2$ Observed by X-ray Absorption Spectroscopy: H. Nakai, T. Ebihara, S. Tsutsui, M. Mizumaki, N. Kawamura, S. Michimura, T. Inami, T. Nakamura, A. Kondo, K. Kindo and Y. H. Matsuda, J. Phys. Soc. Jpn. **82** (2013) 124712 (5pages).

9. †Crystal structure and magnetic properties of honeycomb-like lattice antiferromagnet p-BIP-V_2: H. Yamaguchi, S. Nagata, M. Tada, K. Iwase, T. Ono, S. Nishihara, Y. Hosokoshi, T. Shimokawa, H. Nakano, H. Nojiri, A. Matsuo, K. Kindo and T. Kawakami, Phys. Rev. B **87** (2013) 125120(1-8).

10. †High magnetic field study of the Tm_2Fe_{17} and $Tm_2Fe_{17}D_{3.2}$ compounds: O. Isnard, A. V. Andreev, M. D. Kuz'min, Y. Skourski, D. I. Gorbunov, J. Wosnitza, N. V. Kudrevatykh, A. Iwasa, A. Kondo, A. Matsuo and K. Kindo, Phys. Rev. B **88** (2013) 174406(1-10).

11. †*Quasi-one-dimensional S=1/2 Heisenberg antiferromagnetic chain consisting of the organic radical p-Br-V: K. Iwase, H. Yamaguchi, T. Ono, Y. Hosokoshi, T. Shimokawa, Y. Kono, S. Kittaka, T. Sakakibara, A. Matsuo and K. Kindo, Phys. Rev. B **88** (2013) 184431(1-5).

12. †*Various regimes of quantum behavior in an S=1/2 Heisenberg antiferromagnetic chain with fourfold periodicity: H. Yamaguchi, T. Okubo, K. Iwase, T. Ono, Y. Kono, S. Kittaka, T. Sakakibara, A. Matsuo, K. Kindo and Y. Hosokoshi, Phys. Rev. B **88** (2013) 174410(1-5).

13. †Magnetization Process and Collective Excitations in the S=1/2 Triangular-Lattice Heisenberg Antiferromagnet $Ba_3CoSb_2O_9$: T. Susuki, N. Kurita, T. Tanaka, H. Nojiri, A. Matsuo, K. Kindo and H. Tanaka, Phys. Rev. Lett. **110** (2013) 267201(5).

14. †*High Field Magnetization of $TbPd_2Ge_2$ Single Crystal: T. Shigeoka, T. Hasegawa, T. Fujiwara, A. Kondo, K. Kindo and Y. Uwatoko, J. Low Temp. Phys. **170** (2013) 248-254.

15. †*Magneto-Absorption in the α Phase of Solid Oxygen at Megagauss Magnetic Fields: T. Nomura, Y. H. Matsuda, J. L. Her, S. Takeyama, A. Matsuo, K. Kindo and T. C. Kobayashi, J. Low Temp. Phys. **170** (2013) 372-376.

16. *Observation of Field-induced Anomaly in High-field Magnetization on a Complex Spin-Driven Multiferroic Compound, $LiCu_{2-z}Zn_zO_2$: J. L. Her, H. C. Hsu, Y. H. Matsuda, K. Kindo and F. C. Chou, J. Low Temp. Phys. **170** (2013) 285-290.

17. †Present Status and Future Plan at High Magnetic Field Laboratory in Osaka University: M. Hagiwara, T. Kida, K. Taniguchi and K. Kindo, J. Low Temp. Phys. **170** (2013) 531-540.

18. †*Magnetic field hysteresis under various sweeping rates for Ni-Co-Mn-In metamagnetic shape memory alloys: X. Xu, T. Kihara, M. Tokunaga, A. Matsuo, W. Ito, R. Y. Umetsu, K. Kindo and R. Kainuma, Appl. Phys. Lett. **103** (2013) 122406(1-4).

19. †Itinerant electron magnetism of η-carbides Co_6M_6C and Ni_6M_6C (M=Mo and W): T. Waki, D. Furusawa, Y. Tabata, C. Michioka, K. Yoshimura, A. Kondo, K. Kindo and H. Nakamura, J. Alloys Compd. **554** (2013) 21-24.

20. †*Optical imaging and magnetocaloric effect measurements in pulsed high magnetic fields and their application to Ni–Co–Mn–In Heusler alloy: T. Kihara, I. Katakura, M. Tokunaga, A. Matsuo, K. Kawaguchi, A. Kondo, K. Kindo, W. Ito, X. Xu and R. Kainuma, J. Alloys Compd. **577** (2013) S722-S725.

21. †Magnetoresistance and Transformation Hysteresis in the $Ni_{50}Mn_{34.4}In_{15.6}$ Metamagnetic Shape Memory Alloy: R. Y. Umetsu, K. Endo, A. Kondo, K. Kindo, W. Ito, X. Xu, T. Kanomata and R. Kainuma, Mater. Trans. **54** (2013) 291.

22. †Magnetic properties of the frustrated magnet $Cu_5(PO_4)_3(OH)_4$ on a peculiar spin network composed of pentagons and triangles: H. Kikuchi, Y. Nguyen Thi Tinh, Y. Fujii, A. Matsuo and K. Kindo, J. Kor. Phys. Soc. **62** (2013) 2037-2040.

---

* Joint research among groups within ISSP.

23. [*]Heat-pulse measurements of specific heat in 36 ms pulsed magnetic fields: Y. Kohama, Y. Hashimoto, S. Katsumoto, M. Tokunaga and K. Kindo, Meas. Sci. Technol. **24** (2013) 115005(1-9).

24. [†]Spin Frustration and Field-Induced Transitions of Modified Pyrochlore Fluorides ACr_2F_6 (A = Rb and Cs): H. Ueda, A. Matsuo, K. Kindo and K. Yoshimura, J. Phys. Soc. Jpn. **83** (2014) 014701(1-6)

25. [†]Unconventional spin freezing in the highly two-dimensional spin-1/2 kagome antiferromagnet $Cd_2Cu_3(OH)6(SO_4)24H_2O$: Evidence of partial order and coexisting spin singlet state on a distorted kagome lattice: M. Fujihala, X.-G. Zheng, H. Morodomi, T. Kawae, A. Matsuo, K. Kindo and I. Watanabe, Phys. Rev. B **89** (2014) 100401(1-5).

Tokunaga group

By measuring the resistance of thin-film thermometers deposited on the sample surface, we succeeded in rapid temperature monitoring of the sample with the response time shorter than 0.1 ms. With using this technique, we developed a measurement system of magneto-caloric effects in pulsed high magnetic fields up to 55 T. This technique provides us of novel thermodynamic information of various kind of phase transitions induced in high magnetic fields and also direct information of the entropy in frustrated magnets.

1. Giant Magnetoresistance Effect in the Metal–Insulator Transition of Pyrochlore Oxide $Nd_2Ir_2O_7$: K. Matsuhira, M. Tokunaga, M. Wakeshima, Y. Hinatsu and S. Takagi, J. Phys. Soc. Jpn. **82** (2013) 023706(1-4).

2. High-Field Magnetization of Quasi-One-Dimensional Ising-Like Antiferromagnet $TlCoCl_3$: Y. Nishiwaki, M. Tokunaga, N. Todoroki and T. Kato, J. Phys. Soc. Jpn. **82** (2013) 104717(1-5).

3. Metamagnetic Transition and Its Related Magnetocapacitance Effect in Phthalocyanine-Molecular Conductor Exhibiting Giant Magnetoresistance: N. Hanasaki, T. Tateishi, H. Tajima, M. Kimata, M. Tokunaga, M. Matsuda, A. Kanda, H. Murakawa, T. Naito and T. Inabe, J. Phys. Soc. Jpn. **82** (2013) 094713(1-5).

4. Thermal Transport and Magnetotransport Properties of $CuCr_{1-x}Mg_xO_2$ with a Spin-3/2 Antiferromagnetic Triangular Lattice: T. Okuda, S. Oozono, T. Kihara and M. Tokunaga, J. Phys. Soc. Jpn. **82** (2013) 014706(1-7).

5. Magnetic control of electric polarization in the noncentrosymmetric compound $(Cu,Ni)B_2O_4$: N. D. Khanh, N. Abe, K. Kubo, M. Akaki, M. Tokunaga, T. Sasaki and T. Arima, Phys. Rev. B **87** (2013) 184416(1-5).

6. Shubnikov–de Haas oscillations in the bulk Rashba semiconductor BiTeI: C. Bell, M. S. Bahramy, H. Murakawa, J. G. Checkelsky, R. Arita, Y. Kaneko, Y. Onose, M. Tokunaga, Y. Kohama, N. Nagaosa, Y. Tokura and H. Y. Hwang, Phys. Rev. B **87** (2013) 081109(R)(1-5).

7. [†*]Adiabatic measurements of magneto-caloric effects in pulsed high magnetic fields up to 55 T: T. Kihara, Y. Kohama, Y. Hashimoto, S. Katsumoto and M. Tokunaga, Rev. Sci. Instrum. **84** (2013) 074901(1-7).

8. Field-Induced Magnetostructural Transitions in Antiferromagnetic $Fe_{1+y}Te_{1-x}S_x$: M. Tokunaga, T. Kihara, Y. Mizuguchi and Y. Takano, J. Low Temp. Phys. **170** (2013) 340-345.

9. High Magnetic Field Dependence of Magnetodielectric Properties in $Sr_2CoSi_2O_7$ Crystal: M. Akaki, T. Tadokoro, T. Kihara, M. Tokunaga and H. Kuwahara, J. Low Temp. Phys. **170** (2013) 291-295.

10. [†*]Magnetic field hysteresis under various sweeping rates for Ni-Co-Mn-In metamagnetic shape memory alloys: X. Xu, T. Kihara, M. Tokunaga, A. Matsuo, W. Ito, R. Y. Umetsu, K. Kindo and R. Kainuma, Appl. Phys. Lett. **103** (2013) 122406(1-4).

11. Detection of Berry's Phase in a Bulk Rashba Semiconductor: H. Murakawa, M. S. Bahramy, M. Tokunaga, Y. Kohama, C. Bell, Y. Kaneko, N. Nagaosa, H. Y. Hwang and Y. Tokura, Science **342** (2013) 1490-1493.

12. Spin Frustration from *cis* -Edge or -Corner Sharing Metal-Centered Octahedra: R. Gautier, K. Oka, T. Kihara, N. Kumar, A. Sundaresan, M. Tokunaga, M. Azuma and K. R. Poeppelmeier, J. Am. Chem. Soc. **135** (2013) 19268-19274.

13. [†*]Optical imaging and magnetocaloric effect measurements in pulsed high magnetic fields and their application to Ni–Co–Mn–In Heusler alloy: T. Kihara, I. Katakura, M. Tokunaga, A. Matsuo, K. Kawaguchi, A. Kondo, K. Kindo, W. Ito, X. Xu and R. Kainuma, J. Alloys Compd. **577** (2013) S722-S725.

14. Optical Microscopic Study on NiCoMnAl Metamagnetic Shape Memory Alloy by In Situ Observation under a Pulsed High Magnetic Field: X. Xu, I. Katakura, T. Kihara, M. Tokunaga, W. Ito, R. Y. Umetsu and R. Kainuma, Mater. Trans. **54** (2013) 357-362.

[†] Joint research with outside partners.

15. Anisotropic magnetic properties in Åkermanite $Sr_2MSi_2O_7$ (M=Co, Mn) crystals: M. Akaki, T. Tadokoro, H. Kuwahara, T. Kihara and M. Tokunaga, J. Kor. Phys. Soc. **62** (2013) 1812-1814.

16. Magnetotransport property of the hole-doped delafossite $CuCr_{0.97}Mg_{0.03}O_2$ with a Spin-3/2 antiferromagnetic triangular sublattice: T. Okuda, S. Oozono, T. Kihara and M. Tokunaga, J. Kor. Phys. Soc. **62** (2013) 2168-2172.

17. *Heat-pulse measurements of specific heat in 36 ms pulsed magnetic fields: Y. Kohama, Y. Hashimoto, S. Katsumoto, M. Tokunaga and K. Kindo, Meas. Sci. Technol. **24** (2013) 115005(1-9).

Y. Matsuda group

The magnetization process of $SrCu_2(BO_3)_2$ shows exotic multi-plateau structure, indicating the crystallization of the excited triplet dimers with the several factional fillings in the sea of the singlet dimers. We have succeeded in observing the magnetization curve of $SrCu_2(BO_3)_2$ in ultrahigh magnetic fields of up to 118 Tesla. The long predicted 1/2 plateau has been clearly observed at the field range from 84 to 108 Tesla for the first time. A destructive way of magnetic field generation, single-turn coil method (STC), was used for the experiment. In addition to the magnetization measurement, the cyclotron resonance in ferromagnetic semiconductors and magneto-absorption spectroscopy in solid oxygen have been performed at very high magnetic fields over 100 Tesla. The synchrotron x-ray spectroscopy on Yb-based heavy fermion compounds $YbRh_2Si_2$ and $YbAlB_4$ revealed that the valence instability was affected by a strong magnetic field, suggesting the importance of the charge degree of freedom for understanding their exotic properties at very low temperatures.

1. *Temperature and Magnetic Field Dependent Yb Valence in $YbRh_2Si_2$ Observed by X-ray Absorption Spectroscopy: H. Nakai, T. Ebihara, S. Tsutsui, M. Mizumaki, N. Kawamura, S. Michimura, T. Inami, T. Nakamura, A. Kondo, K. Kindo and Y. H. Matsuda, J. Phys. Soc. Jpn. **82** (2013) 124712 (5pages).

2. X-ray Diffraction and Absorption Spectroscopy in Pulsed High Magnetic Fields: Y. H. Matsuda and T. Inami, J. Phys. Soc. Jpn. **82** (2013) 021009 (17 pages).

3. *Cyclotron resonance in ferromagnetic InMnAs and InMnSb: G. Khodaparast, Y. H. Matsuda, D. Saha, G. Sanders, C. Stanton, H. Saito, S. Takeyama, T. Merritt, C. Feeser, B. Wessels, X. Liu and J. Furdyna, Phys. Rev. B **88** (2013) 235204(11pages).

4. *Precise measurement of a magnetic field generated by the electromagnetic flux compression technique: D. Nakamura, H. Sawabe, Y. H. Matsuda and S. Takeyama, Rev. Sci. Instrum. **84** (2013) 044702 (10 pages).

5. *Magnetization of $SrCu_2(BO_3)_2$ in Ultrahigh Magnetic Fields up to 118 T: Y. H. Matsuda, N. Abe, S. Takeyama, H. Kageyama, P. Corboz, A. Honecker, S. R. Manmana, G. R. Foltin, K. P. Schmidt and F. Mila, Phys. Rev. Lett. **111** (2013) 137204 (5 pages).

6. *Magnetization Studies of Field-Induced Transitions by Using a Single-Turn Coil Technique: N. Abe, Y. H. Matsuda, S. Takeyama, K. Sato, H. Kageyama and Y. Nishiwaki, J. Low Temp. Phys. **170** (2013) 452-456.

7. †*Magneto-Absorption in the Phase of Solid Oxygen at Megagauss Magnetic Fields: T. Nomura, Y. H. Matsuda, J. L. Her, S. Takeyama, A. Matsuo, K. Kindo and T. C. Kobayashi, J. Low Temp. Phys. **170** (2013) 372-376.

8. *Observation of Field-induced Anomaly in High-field Magnetization on a Complex Spin-Driven Multiferroic Compound, $LiCu_{2-z}Zn_zO_2$: J. L. Her, H. C. Hsu, Y. H. Matsuda, K. Kindo and F. C. Chou, J. Low Temp. Phys. **170** (2013) 285-290.

9. *Precision of an Ultra-high Magnetic Field Generated by the Electro-magnetic Flux Compression: D. Nakamura, Y. H. Matsuda and S. Takeyama, J. Low Temp. Phys. **170** (2013) 457-462.

10. Structural and electrical characteristics of high-κ $ErTi_xO_y$ gate dielectrics on InGaZnO thin-film transistors: F.-H. Chen, J.-L. Her, Y.-H. Shao, W.-C. Li, Y. H. Matsuda and T.-M. Pan, Thin Solid Films **539** (2013) 251-255.

11. Effect of surface roughness on electrical characteristics in amorphous InGaZnO thin-film transistors with high-κ Sm_2O_3 dielectrics: F.-H. Chen, M.-N. Hung, J.-F. Yang, S.-Y. Kuo, J.-L. Her, Y. H. Matsuda and T.-M. Pan, Journal of Physics and Chemistry of Solids **74** (2013) 570-574.

12. *Magneto-optical study of Dirac fermion in quartz CVD-grown graphene above 100 T: D. Nakamura, H. Saito, W. Zhou, Y. H. Matsuda, S. Takeyama, K. Yagi, K. Hayashi and S. Sato, AIP Conf. Proc. **1566** (2013) 169-170.

13. *Chemical effects of high-resolution Yb $L\gamma_4$ emission spectra: a possible probe for chemical analysis: H. Hayashi, N. Kanai, N. Kawamura, Y. H. Matsuda, K. Kuga, S. Nakatsuji, T. Yamashita and S. Ohara, X-Ray Spectrom. **42** (2013) 450-455.

* Joint research among groups within ISSP.

14. *Synchrotron X-ray spectroscopy study on the valence state in α- and β-$YbAlB_4$ at low temperatures and high magnetic fields: Y. H. Matsuda, T. Nakamura, K. Kuga, S. Nakatsuji, S. Michimura, T. Inami, N. Kawamura and M. Mizumaki, J. Kor. Phys. Soc. **62** (2013) 1778-1781.

15. Structural and electrical characteristics of high-κ Er_2O_3 and Er_2TiO_5 gate dielectrics for a-IGZO thin-film transistors: F.-H. Chen, J.-L. Her, Y.-H. Shao, Y. H. Matsuda and T.-M. Pan, Nanoscale Res Lett **8** (2013) 18 (5 pages).

16. *Magnetization of Yb-based mixed-valent compounds at megagauss fields: T. Terashima, Y. H. Matsuda, K. Kuga, Y. Matsumoto and S. Nakatsuji, J. Phys. Soc. Jpn. (2014), in print.

Center of Computational Materials Science

Akai group

We have developed methodologies that enable us to calculate electronic structure of wide range of systems such as strongly correlated systems and systems in non-equlibrium states. One of them is a scheme of first-principles calculation of the non-equilibrium Green's function of tunnelling junctions in the framework of the Korringa-Kohn-Rostoker (KKR) Green's function method is developed. Another is the optimized effective potential (OEP) method applied to static RPA scheme. The latter includes an elaboration that dissolves a well-known difficulty arising from the indefiniteness inherent in the theory of OEP. One of main topics we are now working on is the theory of permanent magnet. This year we have developed the theory of magnetic anisotropy of Sm-Fe-N magnet, in particular discussing the role of N that experimentally is is known to be important to realize the uni-axial magnetic anisotropy of this system.

1. Basic and applications of Moessbauer spectrometry and the electronics structure of matters: H. Akai, ISOTOPES **63** (2014) 163-174.

2. 鉄の事典 : 赤井 久純 , (朝倉書店 , 東京 , 2014) in print.

Todo group

We study novel phases and critical phenomena in strongly correlated many-body systems, such as quantum magnets and Bose-Hubbard model, by using the state-of-the-art computational physics techniques like the quantum Monte Carlo method. We also develop new computational algorithms for quantum many-body systems, such as the tensor-network method, study the parallelization technique for supercomputers, and develop open-source software for next-generation parallel simulations: (1) Analysis of quantum phases and quantum phase transitions by local Z2 Berry phase (2) Critical phenomena of long-range interacting spin model (3) Quantum phase transition of SU(N) J-Q model (4) Irreversible Markov chain Monte Carlo (5) Simulation method for systems with strong spatial anisotropy (6) Parallelization of worm algorithm quantum Monte Carlo method (7) Parallel exact diagonalization package “Rokko".

1. Long-Range Order of the Three-Sublattice Structure in the S =1 Heisenberg Antiferromagnet on a Spatially Anisotropic Triangular Lattice: H. Nakano, S. Todo and T. Sakai, J. Phys. Soc. Jpn. **82** (2013) 043715.

2. *Possibility of deconfined criticality in SU(N) Heisenberg models at small N: K. Harada, T. Suzuki, T. Okubo, H. Matsuo, J. Lou, H. Watanabe, S. Todo and N. Kawashima, Phys. Rev. B **88** (2013) 220408(1-4).

3. Monte Carlo simulation with aspect-ratio optimization: Anomalous anisotropic scaling in dimerized antiferromagnets: S. Yasuda and S. Todo, Phys. Rev. E **88** (2013) 061301.

4. Path-integral Monte Carlo method for the local Z_2 Berry phase: Y. Motoyama and S. Todo, Phys. Rev. E **87** (2013) 021301(1-5).

5. Geometric allocation approaches in Markov chain Monte Carlo: S. Todo and H. Suwa, J. Phys.: Conf. Ser. **473** (2013) 012013.

6. 詳細つりあいを満たさないマルコフ連鎖モンテカルロ法とその一般化 : 諏訪 秀麿 , 藤堂 眞治 , 数理解析研究所 講究録 **1848** (2013) 93.

7. Numerical Analysis of Quantum Phase Transitions with Dynamic Control of Anisotropy: S. Yasuda and S. Todo, JPS Conf. Proc. **1** (2014) 012127.

8. Path-Integral Monte Carlo for the Gauge-Fixed Berry Connection and the Local Z_2 Berry Phase: Y. Motoyama and S. Todo, JPS Conf. Proc. **1** (2014) 012130.

† Joint research with outside partners.

9. Loop Algorithm: S. Todo, in: *Strongly Correlated Systems: Numerical Methods (Springer Series in Solid-State Sciences)*, Ch 6, edited by A. Avella and F. Mancini, (Springer-Verlag, Berlin, 2013), 153-184.

Laser and Synchrotron Research Center

Suemoto group

To study ultrafast spin dynamics in canted ferromagnets, terahertz pump-Faraday probe experiments were performed on orthoferrites and several new aspects were revealed as follows. (1) Extremely long coherence time and beating phenomena were found in spin precession modes. (2) Dynamics of magnetic anisotropy parameters modified by optical excitation was observed. (3) Resonance enhancement of the spin precession by using a metamaterial structure (split ring resonator) was demonstrated. As for the photoinduced phase transition, femtosecond dynamics in a novel nanocrystalline titanium oxide was studied and ultrafast phase change was confirmed, which guarantees usefulness of this material for optical storage. Newtons's ring in soft x-ray region (at 13.9 nm) was firstly observed during the laser ablation process, suggesting an extremely thin and flat expansion front.

1. [†]Dynamics of pulsed laser ablation in high-density carbon dioxide including supercritical fluid state: K. Urabe, T. Kato, S. Stauss, S. Himeno, S. Kato, H. Muneoka, M. Baba, T. Suemoto and K. Terashima, J. Appl. Phys. **114** (2013) 143303.

2. [*]Access to hole dynamics in graphite by femtosecond luminescence and photoemission spectroscopy: T. Suemoto, S. Sakaki, M. Nakajima, Y. Ishida and S. Shin, Phys. Rev. B **87** (2013) 224302(1-5).

3. [*]Mechanism of Enhanced Optical Second-Harmonic Generation in the Conducting Pyrochlore-Type $Pb_2Ir_2O_{7-x}$ Oxide Compound: Y. Hirata, M. Nakajima, Y. Nomura, H. Tajima, Y. Matsushita, K. Asoh, Y. Kiuchi, A. G. Eguiluz, R. Arita, T. Suemoto and K. Ohgushi, Phys. Rev. Lett. **110** (2013) 187402(1-5).

4. Terahertz Time-Domain Observation of Spin Reorientation in Orthoferrite $ErFeO_3$ through Magnetic Free Induction Decay: K. Yamaguchi, T. Kurihara, Y. Minami, M. Nakajima and T. Suemoto, Phys. Rev. Lett. **110** (2013) 137204 1-5.

5. Dielectric probe for scattering-type terahertz scanning near-field optical microscopy: T. Kurihara, K. Yamaguchi, H. Watanabe, M. Nakajima and T. Suemoto, Appl. Phys. Lett. **103** (2013) 151105.

6. High-power THz wave generation in plasma induced by polarization adjusted two-color laser pulses: Y. Minami, T. Kurihara, K. Yamaguchi, M. Nakajima and T. Suemoto, Appl. Phys. Lett. **102** (2013) 041105(1-4).

7. Longitudinal THz wave generation from an air plasma filament induced by a femtosecond lase: Y. Minami, T. Kurihara, K. Yamaguchi, M. Nakajima and T. Suemoto, Appl. Phys. Lett. **102** (2013) 151106(1-3).

8. [†]Pulsed laser ablation plasmas generated in CO_2 under high-pressure conditions up to supercritical fluid: T. Kato, S. Stauss, S. Kato, K. Urabe, M. Baba, T. Suemoto and K. Terashima, Appl. Phys. Lett. **101** (2013) 224013(1-4).

9. [†]Probing of local structures of thermal and photoinduced phases in rubidium manganese hexacyanoferrate by resonant Raman spectroscopy: R. Fukaya, A. Asahara, S. Ishige, M. Nakajima, H. Tokoro, S.-I. Ohkoshi and T. Suemoto, J. Chem. Phys. **139** (2013) 084303(1-7).

10. [†]The synthesis of rhodium substituted ε-iron oxide exhibiting super high frequency natural resonance: A. Namai, M. Yoshikiyo, S. Umeda, T. Yoshida, T. Miyazaki, M. Nakajima, K. Yamaguchi, T. Suemoto and S. Ohkoshi, Journal of Materials Chemistry C **1** (2013) 5200-5206.

11. [*]Gain-switching dynamics in optically pumped single-mode InGaN vertical-cavity surface-emitting lasers: S. Chen, A. Asahara, T. Ito, J. Zhang, B. Zhang, T. Suemoto, M. Yoshita and H. Akiyama, Optics Express **22** (2014) 4196-4201.

12. [*]Spectral dynamics of picosecond gain-switched pulses from nitride-based vertical-cavity surface-emitting lasers: S. Chen, T. Ito, A. Asahara, M. Yoshita, W. Liu, J. Zhang, B. Zhang, T. Suemoto and H. Akiyama, Sci. Rep. **4** (2014) 4325.

Shin group

We studied high Tc Fe-pnictide superconductors using 7-eV laser. High resolution photoemission study with polarization dependence is very powerful for the study of the superconducting mechanism. Orbital fluctuation mechanism is also important in addition to the spin fluctuation mechanism.

1. Bulk-Sensitive Angle-Resolved PhotoemissionSpectroscopy on TTF-TCNQ: K. Koizumi, K. Ishizaka, T. Kiss, M. Okawa, R. Kato and S. Shin, J. Phys. Soc. Jpn. **82** (2013) 025004(1-2).

---

* Joint research among groups within ISSP.

2. [*]Access to hole dynamics in graphite by femtosecond luminescence and photoemission spectroscopy: T. Suemoto, S. Sakaki, M. Nakajima, Y. Ishida and S. Shin, Phys. Rev. B **87** (2013) 224302(1-5).

3. Quantifying covalency and metallicity in correlated compounds undergoing metal-insulator transitions: A. Chainani, A. Yamamoto, M. Matsunami, R. Eguchi, M. Taguchi, Y. Takata, S. Shin, Y. Nishino, M. Yabashi, K. Tamasaku and T. Ishikawa, Phys. Rev. B **87** (2013) 045108(1-10).

4. [†*]Anomalous Doping Variation of the Nodal Low-Energy Feature of Superconducting $(Bi,Pb)_2(Sr, La)_2CuO_{6+}$ Crystals Revealed by Laser-Based Angle-Resolved Photoemission Spectroscopy: T. Kondo, Y. Nakashima, W. Malaeb, Y. Ishida, Y. Hamaya, T. Takeuchi and S. Shin, Phys. Rev. Lett. **110** (2013) 217006(1-5).

5. [†*]Anomalous Dressing of Dirac Fermions in the Topological Surface State of Bi_2Se_3, Bi_2Te_3, and Cu-Doped Bi_2Se_3: T. Kondo, Y. Nakashima, Y. Ota, Y. Ishida, W. Malaeb, K. Okazaki, S. Shin, M. Kriener, S. Sasaki, K. Segawa and Y. Ando, Phys. Rev. Lett. **110** (2013) 217601(1-5).

6. Existence of Orbital Order and its Fluctuation in Superconducting $Ba(Fe_{1-x}Co_x)_2As_2$ Single Crystals Revealed by X-ray Absorption Spectroscopy: YK. Kim, WS. Jung, GR. Han, KY. Choi, CC. Chen, TP. Devereaux, A. Chainani, J. Miyawaki, Y. Takata, Y. Tanaka, M. Oura, S. Shin, A. P. Singh, H. G Lee, JY. Kim and C. Kim, Phys. Rev. Lett. **111** (2013) 217001(1-5).

7. [†*]Selective Probing of the OH or OD Stretch Vibration in Liquid Water Using Resonant Inelastic Soft-X-Ray Scattering: Y. Harada, T. Tokushima, Y. Horikawa, O. Takahashi, H. Niwa, M. Kobayashi, M. Oshima, Y. Senba, H. Ohashi, KT. Wikfeldt, A. Nilsson, LGM. Pettersson and S. Shin, Phys. Rev. Lett. **111** (2013) 193001(1-5).

8. Strongly Spin-Orbit Coupled Two-Dimensional Electron Gas Emerging near the Surface of Polar Semiconductors: M. Sakano, M. S. Bahramy, A. Katayama, T. Shimojima, H. Murakawa, Y. Kaneko, W. Malaeb, S. Shin, K. Ono, H. Kumigashira, R. Arita, N. Nagaosa, H. Y. Hwang, Y. Tokura and K. Ishizaka, Phys. Rev. Lett. **110** (2013) 107204(1-5).

9. [*]Resonant inelastic X-ray scattering of liquid water: A. Nilsson, T. Tokushima, Y. Horikawa, Y. Harada, M. P. Ljungberg, S. Shin and L. G. M. Pettersson, J. Electron Spectrosc. Relat. Phenom. **188** (2013) 84-100.

10. [†*]Surface electronic structure of the topological Kondo-insulator candidate correlated electron system SmB_6: M. Neupane, N. Alidoust, S. -Y. Xu, T. Kondo, Y. Ishida, D. J. Kim, C. Liu, I. Belopolski, Y. J. Jo, T. -R. Chang, H. -T. Jeng, T. Durakiewicz, L. Balicas, H. Lin, A. Bansil, S. Shin, Z. Fisk and M. Z. Hasan, Nat. Commun. **4** (2013) 2991(1-7).

11. [*] 液体水分子の内殻電子励起ダイナミクスと局所構造 : 原田 慈久 , 徳島 高 , 堀川 裕加 , 丹羽 秀治 , 木内 久雄 , 小林 正起 , 尾嶋 正治 , 辛 埴 , しょうとつ **10** (2013) 14-20.

12. Evidence for excluding the possibility of d-wave superconducting-gap symmetry in Ba-doped KFe_2As_2: Y. Ota, K. Okazaki, Y. Kotani, T. Shimojima, W. Malaeb, S. Watanabe, C. -T. Chen, K. Kihou, C. H. Lee, A. Iyo, H. Eisaki, T. Saito, H. Fukazawa, Y. Kohori and S. Shin, Phys. Rev. B **89** (2014) 081103(1-5).

13. [†*]Observation of a giant Kerr rotation in a ferromagnetic transition metal by M-edge resonant magneto-optic Kerr effect: Sh. Yamamoto, M. Taguchi, M. Fujisawa, R. Hobara, S. Yamamoto, K. Yaji, T. Nakamura, K. Fujikawa, R. Yukawa, T. Togashi, M. Yabashi, M. Tsunoda, S. Shin and I. Matsuda, Phys. Rev. B **89** (2014) 064423(1-6).

14. [*]Pseudogap formation above the superconducting dome in iron pnictides: T. Shimojima, T. Sonobe, W. Malaeb, K. Shinada, A. Chainani, S. Shin, T. Yoshida, S. Ideta, A. Fujimori, H. Kumigashira, K. Ono, Y. Nakashima, H. Anzai, M. Arita, A. Ino, H. Namatame, M. Taniguchi, M. Nakajima, S. Uchida, Y. Tomioka, T. Ito, K. Kihou, C. H. Lee, A. Iyo, H. Eisaki, K. Ohgushi, S. Kasahara, T. Terashima, H. Ikeda, T. Shibauchi, Y. Matsuda and K. Ishizaka, Phys. Rev. B **89** (2014) 045101(1-10).

15. [†*]Ultrafast photoinduced transition of an insulating VO_2 thin film into a nonrutile metallic state: R. Yoshida, T. Yamamoto, Y. Ishida, H. Nagao, T. Otsuka, K. Saeki, Y. Muraoka, R. Eguchi, K. Ishizaka, T. Kiss, S. Watanabe, T. Kanai, J. Itatani and S. Shin, Phys. Rev. B **89** (2014) 205114(1-7).

16. [*]Robust Protection from Backscattering in the Topological Insulator $Bi_{1.5}Sb_{0.5}Te_{1.7}Se_{1.3}$: S. Kim, S. Yoshizawa, Y. Ishida, K. Eto, K. Segawa, Y. Ando, S. Shin and F. Komori, Phys. Rev. Lett. **112** (2014) 136802(1-5).

17. Selective Probing of the OH or OD Stretch Vibration in Liquid Water Using Resonant Inelastic Soft-X-Ray Scattering: Y. Harada, T. Tokushima, Y. Horikawa, O. Takahashi, H. Niwa, M. Kobayashi, M. Oshima, Y. Senba, H. Ohashi, KT. Wikfeldt, A. Nilsson, LGM. Pettersson and S. Shin, Phys. Rev. Lett. **111** (2014) 193001(1-5).

18. レーザー光電子分光による分子性導体の電子構造の観測 : 石坂 香子 , 小泉 健二 , 木須 孝幸 , 辛 埴 , 固体物理 **49** (2014) 153-162.

† Joint research with outside partners.

19. *Observing hot carrier distribution in an n-type epitaxial graphene on a SiC substrate: T. Someya, H. Fukidome, Y. Ishida, R. Yoshida, T. Iimori, R. Yukawa, K. Akikubo, Sh. Yamamoto, S. Yamamoto, T. Yamamoto, T. Kanai, K. Funakubo, M. Suemitsu, J. Itatani, F. Komori, S. Shin and I. Matsuda, Appl. Phys. Lett. **104** (2014) 161103(1-4).

20. †*Solvation dependence of valence electronic states of water diluted in organic solvents probed by soft X-ray spectroscopy: T. Tokushima, Y. Horikawa, O. Takahashi, H. Arai, K. Sadakane, Y. Harada, Y. Takata and S. Shin, Phys. Chem. Chem. Phys. **16** (2014) 10753.

21. Superconductivity in an electron band just above the Fermi level: possible route to BCS-BEC superconductivity: K. Okazaki1, Y. Ito, Y. Ota, Y. Kotani, T. Shimojima, T. Kiss, S. Watanabe, C. -T. Chen, S. Niitaka, T. Hanaguri, H. Takagi, A. Chainani and S. Shin, Sci. Rep. **4** (2014) 4109(1-6).

22. Development of a single-shot CCD-based data acquisition system for time-resolved X-ray photoelectron spectroscopy at an X-ray free-electron laser facility: M. Oura, T. Wagai, A. Chainani, J. Miyawaki, H. Sato, M. Matsunami, R. Eguchi, T. Kiss, T. Yamaguchi, Y. Nakatani, T. Togashi, T. Katayama, K. Ogawa, M. Yabashi, I. Y. Tanaka, Y. Kohmura, K. Tamasaku, S. Shin and T. Ishikawa, J.Syn.Rad. **21** (2014) 183-192.

23. The electronic structure of carbonate ion in aqueous solution studied by soft X-ray emission spectroscopy: Y. Horikawa A. Yoshida, O. Takahashi, H. Araia, T. Tokushima, T. Gejo and S. Shin, J.Mol.Liq **189** (2014) 9-12.

24. †*New soft X-ray beamline BL07LSU at SPring-8: S. Yamamoto, Y. Senba, T. Tanaka, H. Ohashi, T. Hirono, H. Kimura, M. Fujisawa, J. Miyawaki, A. Harasawa, T. Seike, S. Takahashi, N. Nariyama, T. Matsushita, M. Takeuchi, T. Ohata, Y. Furukawa, K. Takeshita, S. Goto, Y. Harada, S. Shin, H. Kitamura, A. Kakizaki, M. Oshima and I. Matsuda, J Synchrotron Rad **21** (2014) 352-365.

Takahashi group

We have been studying the structure and phase transition of surfaces and interfaces with diffraction techniques. Topological insulators attract much attention due to potential applications such as spintronics and quantum computing. The structure of a Bi(001)/Bi_2Te_3(001) heteroepitaxial film grown on Si(111) was studied with atomic layer resolution by using X-ray crystal truncation rod scattering in combination with a novel structure analysis method. We revealed the Bi thin film is heavily distorted due to the interaction with the substrate Bi_2Te_3, resulting in the topological phase transition of the Bi film. We could also get quantitative information on the structural inhomogeneity at the interface between both Bi/Bi_2Te_3 and Bi_2Te_3/Si(111).

1. Structure of a Bi/Bi_2Te_3 heteroepitaxial film studied by x-ray crystal truncation rod scattering: T. Shirasawa, J. Tsunoda, T. Hirahara and T. Takahashi, Phys. Rev. B **87** (2013) 075449(1-5).

2. A method for measuring the specular X-ray reflectivity with millisecond time resolution: W. Voegeli, T. Matsushita, E. Arakawa, T. Shirasawa, T. Takahashi and Y. F. Yano, J. Phys.: Conf. Ser. **425** (2013) 092003(1-4).

3. †*Scanning tunneling microscopic and spectroscopic studies on a crystalline silica monolayer epitaxially formed on hexagonal SiC(000-1) surfaces: H. Tochihara, T. Shirasawa, T. Suzuki, T. Miyamachi, T. Kajiwara, K. Yagyu, S. Yoshizawa, T. Takahashi, S. Tanaka and F. Komori, Appl. Phys. Lett. **104** (2014) 051601(1-4).

4. Determination of atomic positions in silicene on Ag(111) by low-energy electron diffraction: K. Kawahara, T. Shirasawa, R. Arafune, C. -L. Lin, T. Takahashi, M. Kawai and N. Takagi, Surf. Sci. **623** (2014) 25-28.

5. 「グラフェン／ SiC(000-1) 界面構造の研究」角田 潤一 , 新領域物質系 (2013).

6. Structure and transport properties 1 of Cu doped Bi_2Se_3 films: T. Shirasawa, M. Sugiki, T. Hirahara, M. Aitani, T. Shirai, S. Hasegawa and T. Takahashi, Phys. Rev. B (2014), accepted for publication.

Akiyama group

In 2013, we started experimental and theoretical study on energy conversion efficiencies and sub-cell internal luminescence yields of tandem solar cells on the basis of a detailed-balance relation. We applied this key relation to the study of intrinsic radiative lifetime of one-dimensional excitons, and fluorescent radiation thermometry at cryogenic temperatures. We also started collaboration on the photoluminescence emission of photoexcited undoped GaAs quantum wells induced by an intense single-cycle terahertz pulse. We intensively studied spectral dynamics in short-pulse generation via gain switching of semiconductor lasers, such as Fabry-Perot GaAs or InGaAs lasers, InGaN VCSELs, and InGaAsP DFB lasers. We developed and characterized double-core-slab-waveguide semiconductor lasers for end optical pumping. We studied the effect of site-directed mutant luciferase on quantitative green and orange/red emission intensities in firefly bioluminescence, and firefly oxyluciferin in enzymatic environment on the basis of stability monitoring. Intensive studies were made with TD-DFT theoretical calculations on electronic states for luciferin and oxyluciferin.

---

* Joint research among groups within ISSP.

1. Transient hot-carrier optical gain in a gain-switched semiconductor laser: T. Ito, S. Chen, M. Yoshita, T. Mochizuki, C. Kim, H. Akiyama, L. N. Pfeiffer and K. W. West, Appl. Phys. Lett. **103** (2013) 082117.

2. [†]Electroluminescence of GaNAs/GaAs MQWs p–i–n junctions grown by RF-MBE using modulated nitrogen radical beam source: N. Ohta, K. Arimoto, M. Shiraga, K. Ishii, M. Inada, S. Yanai, Y. Nakai, H. Akiyama, T. Mochizuki, T. Takahashi, N. Takahashi, H. Miyagawa, N. Tsurumachi, S. Nakanishi and S. Koshiba, J. Cryst. Growth **378** (2013) 150.

3. Fluorescent Radiation Thermometry at Cryogenic Temperatures Based on Detailed Balance Relation: T. Mochizuki, T. Ihara, M. Yoshita, S. Maruyama, H. Akiyama, L. N. Pfeiffer and K. W. West, Appl. Phys. Express **6** (2013) 056602 (1-3).

4. Dynamics of short-pulse generation via spectral filtering from intensely excited gain-switched 155-μm distributed-feedback laser diodes: S. Chen, M. Yoshita, A. Sato, T. Ito, H. Akiyama and H. Yokoyama, Opt. Express **21** (2013) 10597-10605.

5. Gain-switched pulses from InGaAs ridge-quantum-well lasers limited by intrinsic dynamical gain suppression: S. Chen, M. Yoshita, T. Ito, T. Mochizuki, H. Akiyama and H. Yokoyama, Opt. Express **21** (2013) 7570-7576.

6. Double-core-slab-waveguide semiconductor lasers for end optical pumping: T. Nakamura, T. Mochizuki, C. Kim, S. Chen, M. Yoshita and H. Akiyama, Applied Physics Express **6** (2013) 062702.

7. Impact of Site-Directed Mutant Luciferase on Quantitative Green and Orange/Red Emission Intensities in Firefly Bioluminescence: Y. Wang, H. Akiyama, K. Terakado and T. Nakatsu, Sci. Rep. **3** (2013) 2490.

8. Intrinsic radiative lifetime derived via absorption cross section of one-dimensional excitons: S. Chen, M. Yoshita, A. Ishikawa, T. Mochizuki, S. Maruyama, H. Akiyama, Y. Hayamizu, L. N. Pfeiffer and K. W. West, Sci. Rep. **3** (2013) 1941.

9. Theoretical Study of Firefly Luciferin pK_a Values-Relative Absorption Intensity in Aqueous Solutions: M. Hiyama, H. Akiyama, K. Yamada and N. Koga, Photochem Photobiol **89** (2013) 571.

10. Theoretical study for absorption spectra of oxyluciferin in aqueous solutions: M. Hiyama, H. Akiyama, Y. Wang and N. Koga, Chemical Physics Letters **577** (2013) 121.

11. Large enhancement of the photoluminescence emission of photoexcited undoped GaAs quantum wells induced by an intense single-cycle terahertz pulse: K. Shinokita, H. Hirori, K. Tanaka, T. Mochizuki, C. Kim, H. Akiyama, L. N. Pfeiffer and K. W. West, Phys. Rev. Lett **111** (2013) 067401.

12. Theoretical Study of Fluorescence Spectra Utilizing the pKa Values of Acids in Their Excited States: M. Hiyama, H. Akiyama, K. Yamada and N. Koga, Photochem. Photobiol **90** (2013) 35-40.

13. Low Threshold Lasing of GaN-Based VCSELs With Sub-Nanometer Roughness Polishing: W.-J. Liu, S.-Q. Chen, X.-L. Hu, Z. Liu, J.-Y. Zhang, L.-Y. Ying, X.-Q. Lv, H. Akiyama, Z.-P. Cai and B.-P. Zhang, IEEE Photon. Technol. Lett. **25** (2013) 2014.

14. Mode imaging and loss evaluation of semiconductor waveguides: T. Mochizuki, C. Kim, M. Yoshita, T. Nakamura, H. Akiyama, L. N. Pfeiffer and K. W. West, Rev. Sci. Instrum. **85** (2014) 053109.

15. Robust red-emission spectra and yields in firefly bioluminescence against temperature changes: T. Mochizuki, Y. Wang, M. Hiyama and H. Akiyama, Appl. Phys. Lett. **104** (2014) 213704.

16. Spectroscopic Study of Firefly Oxyluciferin in an Enzymatic Environment on the Basis of Stability Monitoring: Y. Wang, Y. Hayamizu and H. Akiyama, J. Phys. Chem. B **118** (2014) 2070–2076.

17. [*]Gain-switching dynamics in optically pumped single-mode InGaN vertical-cavity surface-emitting lasers: S. Chen, A. Asahara, T. Ito, J. Zhang, B. Zhang, T. Suemoto, M. Yoshita and H. Akiyama, Optics Express **22** (2014) 4196-4201.

18. Gain switching of a double-core-waveguide semiconductor laser via traveling-wave optical pumping: H. Nakamae, T. Nakamura, T. Ito, T. Mochizuki, C. Kim, S. Chen, M. Yoshita and H. Akiyama, Appl. Phys. Express **7** (2014) 062701.

19. [*]Spectral dynamics of picosecond gain-switched pulses from nitride-based vertical-cavity surface-emitting lasers: S. Chen, T. Ito, A. Asahara, M. Yoshita, W. Liu, J. Zhang, B. Zhang, T. Suemoto and H. Akiyama, Sci. Rep. **4** (2014) 4325.

20. Impact of Sub-cell Internal Luminescence Yields on Energy Conversion Efficiencies of Tandem Solar Cells: A design principle: L. Zhu, C. Kim, M. Yoshita, S. Chen, S. Sato, T. Mochizuki, H. Akiyama and Y. Kanemitsu, Applied Physics Letters **104** (2014) 031118.

† Joint research with outside partners.

I. Matsuda group

Developments and experiments of the advanced spectroscopies have been carried out by using vacuum ultraviolet (VUV) and soft X-rays (SX). At SPring-8 BL07LSU, picosecond-time-resolved SX photoemission spectroscopy measurements have been carried out to trace relaxation of photo-excited carriers at metal oxide surfaces. Analyses of the carrier life time have directly revealed the electron-hole recombination process. At Kashiwa campus, dynamics of the Dirac Fermion in a graphene layer is studied by femtosecond-time-resolved VUV photoemission spectroscopy. The transient electron temperature has indicated generation of the cascade carrier multiplication in the femtosecond-time scale. As a part of the undulator development at SPring-8 BL07LSU, phase shifters with electromagnetic coils were mechanically adjusted and installed in the electron storage ring. The phase shifters will be used to make fast polarization switching of the beamline.

1. Time-resolved photoelectron spectroscopies using synchrotron radiation: Past, present, and future: S. Yamamoto and I. Matsuda, J. Phys. Soc. Jpn. **82** (2013) 021003(1-18).

2. Electronic structure of the hydrogen-adsorbed $SrTiO_3$(001) surface studied by polarization-dependent photoemission spectroscopy: R. Yukawa, S. Yamamoto, K. Ozawa, M. D'Angelo, M. Ogawa, M. G. Silly, F. Sirotti and I. Matsuda, Phys. Rev. B **87** (2013) 115314(1-6).

3. Oscillatory relaxation of surface photovoltage on a semiconductor surface: M. Ogawa, S. Yamamoto, R. Yukawa, R. Hobara, L. -C. Huang, R. -Y. Liu, S. -J. Tang and I. Matsuda, Phys. Rev. B **87** (2013) 235308(1-4).

4. Relaxations of the surface photovoltage effect on the atomically controlled semiconductor surfaces studied by time-resolved photoemission spectroscopy: M. Ogawa, S. Yamamoto, K. Fujikawa, R. Hobara, R. Yukawa, Sh. Yamamoto, S. Kitagawa, D. Pierucci, M. G. Silly, C. -H. Lin, R. -Y. Liu, H. Daimon, F. Sirotti, S. -J. Tang and I. Matsuda, Phys. Rev. B **88** (2013) 165313(1-9).

5. Structure of silicene on a Ag(111) surface studied by reflection high-energy positron diffraction: Y. Fukaya, I. Mochizuki, M. Maekawa, K. Wada, T. Hyodo, I. Matsuda and A. Kawasuso, Phys. Rev. B **88** (2013) 205413(1-4).

6. 金属超薄膜内に閉じ込められた電子系のフェルミ面トポロジー制御 - 量子効果で銀細工：永村 直佳，小河 愛実，松田 巌，固体物理 **48** (2013) 13-19.

7. Anisotropic electronic conduction in metal nanofilms grown on a one-dimensional surface superstructure: N. Nagamura, R. Hobara, T. Uetake, T. Hirahara, K. Kobayashi, I. Matsuda and S. Hasegawa, Phys. Rev. B **89** (2014) 125415(1-5).

8. †*Observation of a giant Kerr rotation in a ferromagnetic transition metal by M-edge resonant magneto-optic Kerr effect: Sh. Yamamoto, M. Taguchi, M. Fujisawa, R. Hobara, S. Yamamoto, K. Yaji, T. Nakamura, K. Fujikawa, R. Yukawa, T. Togashi, M. Yabashi, M. Tsunoda, S. Shin and I. Matsuda, Phys. Rev. B **89** (2014) 064423(1-6).

9. *Observing hot carrier distribution in an n-type epitaxial graphene on a SiC substrate: T. Someya, H. Fukidome, Y. Ishida, R. Yoshida, T. Iimori, R. Yukawa, K. Akikubo, Sh. Yamamoto, S. Yamamoto, T. Yamamoto, T. Kanai, K. Funakubo, M. Suemitsu, J. Itatani, F. Komori, S. Shin and I. Matsuda, Appl. Phys. Lett. **104** (2014) 161103(1-4).

10. Non-linear kinetic model for oscillatory relaxation of the photovoltage effect on a Si(111)7x7 surface: M. Ogawa, R. -Y. Liu, C. -H. Lin, S. Yamamoto, R. Yukawa, R. Hobara, S. -J. Tang and I. Matsuda, Surf. Sci. **624** (2014) 70-75.

11. 反射高速陽電子回折（RHEPD）による Ag(111) 表面上のシリセンの構造決定：深谷 有喜，望月 出海，前川 雅樹，和田 健，兵頭 俊夫，松田 巌，河裾 厚男，PF News **32** (2014) 10-14.

12. 表面電子化合物：松田 巌，深谷 有喜，PF News **31** (2014) 33-37.

13. †Electron–Hole Recombination Time at TiO_2 Single-Crystal Surfaces: Influence of Surface Band Bending: K. Ozawa, M. Emori, S. Yamamoto, R. Yukawa, S. Yamamoto, R. Hobara, K. Fujikawa, H. Sakama and I. Matsuda, J. Phys. Chem. Lett. **5** (2014) 1953.

14. Rashba effects within the space charge layer of a semiconductor: C.-H. Lin, T.-R. Chang, Ro. -Ya. Liu, C.-M. Cheng, K.-D. Tsuei, H. -T. Jeng, C.-Y. Mou, I. Matsuda and S. -J. Tang, New. J. Phys. **16** (2014) 045003(1-12).

15. †*New soft X-ray beamline BL07LSU at SPring-8: S. Yamamoto, Y. Senba, T. Tanaka, H. Ohashi, T. Hirono, H. Kimura, M. Fujisawa, J. Miyawaki, A. Harasawa, T. Seike, S. Takahashi, N. Nariyama, T. Matsushita, M. Takeuchi, T. Ohata, Y. Furukawa, K. Takeshita, S. Goto, Y. Harada, S. Shin, H. Kitamura, A. Kakizaki, M. Oshima and I. Matsuda, J Synchrotron Rad **21** (2014) 352-365.

16. 量子井戸： 松田 巌，「表面科学会教科書シリーズ 6　問題と解説で学ぶ表面科学」， 松井文彦，（共立出版，2013), 88.

* Joint research among groups within ISSP.

Kobayashi group

We have demonstrated a precision spectroscopy in VUV region by using VUV frequency comb.

1. vuv frequency-comb spectroscopy of atomic xenon: A. Ozawa and Y. Kobayashi, Phys. Rev. A **87** (2013) 022507(1-4).
2. 6-GHz, Kerr-lens mode-locked Yb:Lu_2O_3 ceramic laser for comb-resolved broadband spectroscopy: M. Endo, A. Ozawa and Y. Kobayashi, Opt. Lett. **38** (2013) 4502.
3. 10-MHz, Yb-fiber chirped-pulse amplifier system with large-scale transmission gratings: Y. Kobayashi, N. Hirayama, A. Ozawa, T. Sukegawa, T. Seki, Y. Kuramoto and S. Watanabe, Optics Express **21** (2013) 12865.
4. Static FBG strain sensor with high resolution and large dynamic range by dual-comb spectroscopy: N. Kuse, A. Ozawa and Y. Kobayashi, Optics Express **21** (2013) 11141.
5. 光源としての光コム (2)　VUV 領域および高繰り返しコム : 小林 洋平 , 分光研究 **62** (2013) 185.
6. 紫外光周波数コム発生と精密分光への応用 : 小澤 陽 , 小林 洋平 , OplusE **35** (2013) 1132.
7. デュアルコム分光 FT-IR にかわる高速広帯域精密分光 : 久世 直也 , 小澤 陽 , 小林 洋平 , 日本物理学会 **69** (2014) 29.

Itatani group

The Itatani group worked mainly on (i) the generation of soft-X-ray high harmonics using a BIBO-based optical parametric chirped pulse amplifier at 1.6 μm and (ii) the generation of intense THz pulses and their application to coherent control of small molecules. Regarding the BIBO-based source, we measured high harmonic spectra up to 330 eV with various experimental parameters such as backing pressures and carrier-envelope phases of the driver pulses. We observed clear CEP-dependences up to the backing pressure of 3 atm, which showed a potential to increase the photon flux of soft-X-ray attosecond pulses. As for the THz generation, we controlled the rotational wavepackets in jet-cooled HBr molecules to achieve molecular orientation (alignment with head-and-tail discrimination). We observed clear signature of molecular orientation by a newly-developed velocity-map imaging apparatus. This is the first clear demonstration of molecular orientation by using intense THz pulses.

1. [†]Orientation of jet-cooled polar molecules with an intense single-cycle THz pulse: K. Kitano, N. Ishii, N. Kanda, Y. Matsumoto, T. Kanai, M. Kuwata-Gonokami and J. Itatani, Phys. Rev. A **88** (2013) 061405.
2. [†*]Ultrafast photoinduced transition of an insulating VO_2 thin film into a nonrutile metallic state: R. Yoshida, T. Yamamoto, Y. Ishida, H. Nagao, T. Otsuka, K. Saeki, Y. Muraoka, R. Eguchi, K. Ishizaka, T. Kiss, S. Watanabe, T. Kanai, J. Itatani and S. Shin, Phys. Rev. B **89** (2014) 205114(1-7).
3. [*]Observing hot carrier distribution in an n-type epitaxial graphene on a SiC substrate: T. Someya, H. Fukidome, Y. Ishida, R. Yoshida, T. Iimori, R. Yukawa, K. Akikubo, Sh. Yamamoto, S. Yamamoto, T. Yamamoto, T. Kanai, K. Funakubo, M. Suemitsu, J. Itatani, F. Komori, S. Shin and I. Matsuda, Appl. Phys. Lett. **104** (2014) 161103(1-4).
4. [†]Carrier-envelope phase-dependent high harmonic generation in the water window using few-cycle infrared pulses: N. Ishii, K. Kaneshima, K. Kitano, T. Kanai, S. Watanabe and J. Itatani, Nat. Commun. **5** (2014) 3331.

Harada group

1) Operando soft X-ray RIXS spectroscopy for electronic structure analysis of catalytic reactions:: We have developed a novel electrochemical cell system for operando soft X-ray emission spectroscopy for analysis of catalytic reactions. We have applied the system to identify the active site for oxygen reduction reaction in polymer electrolyte fuel cells cathode catalysts. We have observed the electronic structure of iron in an iron phthalocyanine-based cathode catalyst under various working conditions and found that an oxidized iron site exists and is active for oxygen adsorption, which is not expected from ex situ results in which a metallic iron site dominates. 2) Development of the soft X-ray RIXS system around sample manipulation:: In order to extend the public use of the soft X-ray emission spectroscopy station we have realized precise temperature control of liquids in the range of -5 ~ 80 ^{o}C within ±1K accuracy using an originally developed thermal shielding, and surface cleaning by neutralized ion sputtering and annealing at more than 1000 K by electron bombardment. We also have implemented a liq. He sample cooling system down to 35 K. All these systems are now in operation and open to public. 3) Pioneering work on soft X-ray vibrational RIXS of liquids: Ultrahigh resolution resonant inelastic soft X-ray scattering was applied to observe multiple vibrational excitations in liquid water. By tuning X-ray excitation energy to a particular structure in the X-ray absorption spectrum we have successfully obtained vibrational frequencies well correlate with the OH stretching mode of a particular configuration of water. This enables element- and site-specific vibrational spectroscopy that is not accessible by the conventional IR or Raman spectroscopy.

† Joint research with outside partners.

1. †*Selective Probing of the OH or OD Stretch Vibration in Liquid Water Using Resonant Inelastic Soft-X-Ray Scattering: Y. Harada, T. Tokushima, Y. Horikawa, O. Takahashi, H. Niwa, M. Kobayashi, M. Oshima, Y. Senba, H. Ohashi, KT. Wikfeldt, A. Nilsson, LGM. Pettersson and S. Shin, Phys. Rev. Lett. **111** (2013) 193001(1-5).

2. *Resonant inelastic X-ray scattering of liquid water: A. Nilsson, T. Tokushima, Y. Horikawa, Y. Harada, M. P. Ljungberg, S. Shin and L. G. M. Pettersson, J. Electron Spectrosc. Relat. Phenom. **188** (2013) 84-100.

3. Probing carbon edge exposure of iron phthalocyanine-based oxygen reduction catalysts by soft X-ray absorption spectroscopy: H. Niwa, M. Saito, M. Kobayashi, Y. Harada, M. Oshima, S. Moriya, K. Matsubayashi, Y. Nabae, S. Kuroki, T. Ikeda, K. Terakura, J.-I. Ozaki and S. Miyata, Journal of Power Sources **223** (2013) 30-35.

4. * 液体水分子の内殻電子励起ダイナミクスと局所構造 : 原田 慈久 , 徳島 高 , 堀川 裕加 , 丹羽 秀治 , 木内 久雄 , 小林 正起 , 尾嶋 正治 , 辛 埴 , しょうとつ **10** (2013) 14-20.

5. Operando soft X-ray emission spectroscopy of iron phthalocyanine-based oxygen reduction catalysts: H. Niwa, H. Kiuchi, J. Miyawaki, Y. Harada, M. Oshima, Y. Nabae and T. Aoki, Electrochemistry Communications **35** (2013) 57-60.

6. †Unveiling the impurity band induced ferromagnetism in the magnetic semiconductor (Ga,Mn)As: M. Kobayashi, I. Muneta, Y. Takeda, Y. Harada, A. Fujimori, J. Krempaský, T. Schmitt, S. Ohya, M. Tanaka, M. Oshima and V. N. Strocov, Phys. Rev. B **89** (2014) 205204(1-8).

7. †Electronic Excitations of a Magnetic Impurity State in the Diluted Magnetic Semiconductor (Ga,Mn)As: M. Kobayashi, H. Niwa, Y. Takeda, A. Fujimori, Y. Senba, H. Ohashi, A. Tanaka, S. Ohya, P. N. Hai, M. Tanaka, Y. Harada and M. Oshima, Phys. Rev. Lett. **112** (2014) 107203(1-7).

8. †*Solvation dependence of valence electronic states of water diluted in organic solvents probed by soft X-ray spectroscopy: T. Tokushima, Y. Horikawa, O. Takahashi, H. Arai, K. Sadakane, Y. Harada, Y. Takata and S. Shin, Phys. Chem. Chem. Phys. **16** (2014) 10753.

9. †*New soft X-ray beamline BL07LSU at SPring-8: S. Yamamoto, Y. Senba, T. Tanaka, H. Ohashi, T. Hirono, H. Kimura, M. Fujisawa, J. Miyawaki, A. Harasawa, T. Seike, S. Takahashi, N. Nariyama, T. Matsushita, M. Takeuchi, T. Ohata, Y. Furukawa, K. Takeshita, S. Goto, Y. Harada, S. Shin, H. Kitamura, A. Kakizaki, M. Oshima and I. Matsuda, J Synchrotron Rad **21** (2014) 352-365.

10. †Iron-Nitrogen Coordination in Modified Graphene Catalyzes a Four-Electron-Transfer Oxygen Reduction Reaction: K. Kamiya, H. Koshikawa, H. Kiuchi, Y. Harada, M. Oshima, K. Hashimoto and S. Nakanishi, ChemElectroChem (2014), accepted for publication.

Wadati group

Our main experimental techniques are synchrotron-based x-ray spectroscopy and scattering. We studied the orbital and magnetic phase transitions in $Pr_{0.5}Ca_{0.5}MnO_3$ epitaxial thin films by resonant soft x-ray scattering and observed three phase transitions, one of which is absent in bulk $Pr_{0.5}Ca_{0.5}MnO_3$. We also studied the valence of Bi in Bi-based new-type superconductors by x-ray absorption spectroscopy and obtained evidence for the scenario of electron doping for the emergence of superconductivity.

1. Antiferromagnetic Order of the Co^{2+} High-Spin State with a Large Orbital Angular Momentum in $La_{1.5}Ca_{0.5}CoO_4$: J. Okamoto, H. Nakao, Y. Yamasaki, H. Wadati, A. Tanaka, M. Kubota, K. Horigane, Y. Murakami and K. Yamada, J. Phys. Soc. Jpn. **83** (2014) 044705.

2. Insulator-to-Superconductor Transition upon Electron Doping in a BiS_2 -Based Superconductor $Sr_{1-x}La_xFBiS_2$: H. Sakai, D. Kotajima, K. Saito, H. Wadati, Y. Wakisaka, M. Mizumaki, K. Nitta, Y. Tokura and S. Ishiwata, J. Phys. Soc. Jpn. **83** (2014) 014709.

3. Revealing orbital and magnetic phase transitions in $Pr_{0.5}Ca_{0.5}MnO_3$ epitaxial thin films by resonant soft x-ray scattering: H. Wadati, J. Geck, E. Schierle, R. Sutarto, F. He, D. G. Hawthorn, M. Nakamura, M. Kawasaki, Y. Tokura and G. A. Sawatzky, New J. Phys. **16** (2014) 033006.

* Joint research among groups within ISSP.

Kondo group

We use angle-resolved photoemission spectroscopy (ARPES) with ultrahigh energy resolution, achieved by using laser photon source, and study the nonconventional superconductors, heavy fermions, strongly correlated systems, topological quantum phases, and quantum well states. The main findings in 2013 are as follows: (1) Formation of Gapless Fermi Arcs and Fingerprints of Order in the Pseudogap State of Cuprate Superconductors. (2) Anomalous Dressing of Dirac Fermions in the Topological Surface State. (3) Significant doping Variation of the Nodal Low-Energy Feature of Superconducting $Bi_2Sr_2CuO_{6+\delta}$ (Bi2201) crystals.

1. †*Anomalous Doping Variation of the Nodal Low-Energy Feature of Superconducting $(Bi,Pb)_2(Sr, La)_2CuO_{6+\delta}$ Crystals Revealed by Laser-Based Angle-Resolved Photoemission Spectroscopy: T. Kondo, Y. Nakashima, W. Malaeb, Y. Ishida, Y. Hamaya, T. Takeuchi and S. Shin, Phys. Rev. Lett. **110** (2013) 217006(1-5).

2. †*Anomalous Dressing of Dirac Fermions in the Topological Surface State of Bi_2Se_3, Bi_2Te_3, and Cu-Doped Bi_2Se_3: T. Kondo, Y. Nakashima, Y. Ota, Y. Ishida, W. Malaeb, K. Okazaki, S. Shin, M. Kriener, S. Sasaki, K. Segawa and Y. Ando, Phys. Rev. Lett. **110** (2013) 217601(1-5).

3. Formation of Gapless Fermi Arcs and Fingerprints of Order in the Pseudogap State of Cuprate Superconductors.: T. Kondo, A. D. Palczewski, Y. Hamaya, T. Takeuchi, J. S. Wen, Z. J. Xu, G. Gu and A. Kaminski, Phys. Rev. Lett. **111** (2013) 157003(1-5).

4. †*Surface electronic structure of the topological Kondo-insulator candidate correlated electron system SmB_6: M. Neupane, N. Alidoust, S. -Y. Xu, T. Kondo, Y. Ishida, D. J. Kim, C. Liu, I. Belopolski, Y. J. Jo, T. -R. Chang, H. -T. Jeng, T. Durakiewicz, L. Balicas, H. Lin, A. Bansil, S. Shin, Z. Fisk and M. Z. Hasan, Nat. Commun. **4** (2013) 2991(1-7).

5. Fermi Surface and Pseudogap Evolution in a Cuprate Superconductor.: Y. He, Y. Yin, M. Zech, A. Soumyanarayanan, M. M. Yee, T. Williams, M. C. Boyer, K. Chatterjee, W. D. Wise, I. Zeljkovic, T. Kondo, T. Takeuchi, H. Ikuta, P. Mistark, R. S. Markiewicz, A. Bansil, S. Sachdev, E. W. Hudson and J. E. Hoffman, Science **344** (2014) 608-611.

† Joint research with outside partners.

The Institute for Solid State Physics
The University of Tokyo

5-1-5 Kashiwanoha, Kashiwa, Chiba 277-8581

http://www.issp.u-tokyo.ac.jp